Adaptive potential of sulfate content in *Arabidopsis thaliana*

Doctoral thesis

for

the award of the doctoral degree

of the Faculty of Mathematics and Natural Sciences

of the University of Cologne

submitted by

Varsa Shukla

April 2026

Reviewers:

Prof. Dr. Stanislav Kopriva

Prof. Dr. Tatjana Hildebrandt

TABLE OF CONTENTS

ABBREVIATIONS

A11	Chalcone Flavanone Isomerase
ABA	Abscisic Acid
ACC2	1-Amino-Cyclopropane-1-Carboxylate Synthase 2
AER	2-Alkenal Reductase
AK3	Aspartate Kinase 3
AOP2/3	Alkenyl Hydroxyalkyl Producing 2/3
APK	APS Kinase
APR	APS Reductase
APS	Adenosine 5'-Phosphosulfate
APX2	Ascorbate Peroxidase 1B
ATPHS2	Alpha-Glucan Phosphorylase 2
ATPHT1;2	Phosphate Transporter
ATPS	ATP Sulfurylases
ATTIPS2	Induced by Pi Starvation 2
BCAA	Branched-Chain Amino Acids
BCAT4	Branched-Chain Aminotransferase 4
BGAL4	Beta-Glucosidase 4
BGLU1	Beta-Glucosidase 1
BSO	L-Buthionine Sulfoximine
BXL2	Beta-Xylosidase 2
CB5-C	Cytochrome B5 Isoform C
CBP1	CCG-Binding Protein 1
CCA1	Circadian Clock Associated 1
CCL	CCR-Like
CHIL	Chalcone Isomerase Like
CHS	Chalcone Synthase
CLE6	Clavata3/Esr-Related 6
COBL2	Cobra-Like Protein 2
CSC	Cysteine Synthase Complex
CYP79B2	Cytochrome P450 Subfamily B
4CL3	4-Coumarate: CoA Ligase 3
Cys	Cysteine
DAB	3,3′-Diaminobenzidine
DEGs	Differentially Expressed Genes
DHAR2	Dehydroascorbate Reductase 2

DHNAT-2	1,4-Dihydroxy-2-Naphthoyl-Coa Thioesterases
DIN10	Dark Inducible 10
DTX9	Detoxification 9
eGWAS	Expression Genome-Wide Association Studies
EIL1	Ethylene-Insensitive3-Like 1
ELIP1	Early Light-Inducible Protein
EMB2794	Embryo Defective 2794
ENODL2	Early Nodulin-Like Protein 2
EXT4	Extensin 4
F3'H	Flavanone 3-Hydroxylase
FLS1	Flavonol Synthase 1
GABA	Gamma Amino Butyric Acid
GC-MS	Gas Chromatography–Mass Spectrometry
GGCT2;1	Gamma-Glutamyl-Cyclotransferase 2;1
GLY14	Glyoxylase 14
GO	Gene Ontology
GoLS1	Galactinol Synthase 1
GSH	Glutathione
GSLs	Glucosinolates
GSM1	Glucosinolate Metabolism 1
GSTL1	Glutathione S-Transferase Lambda 1
GSTU26	Glutathione S-Transferase Tau 26
GTE	Global Transcription Factor Group E Proteins
GWAS	Genome-Wide Association Studies
γ-ECS	Gamma-Glutamylcysteine
H_2O_2	Hydrogen Peroxide
HAI1	Highly ABA-Induced Pp2C Gene 1
HBP2	Heme (Tetrapyrrole) Binding Protein 2
HCEF1	High Cyclic Electron Flow 1
HMA3 ATPase	Molybdate Transporter
HPLC	High-Performance Liquid Chromatography
HYH	Elongated Hypocotyl 5 Homolog
IAA34	Indole-3-Acetic Acid Inducible 34
ICP-MS	Inductively Coupled Plasma Mass Spectrometry
ICS2	Isochorismate Synthase 2
IES2B	Chromatin Remodeling Factor Ino80 Subunit 2B
IGMT5	Indole Glucosinolate O-Methyltransferase 5

IMD1	Isopropylmalate Dehydrogenase 1
IMS2	2-Isopropylmalate Synthase 2
ISA3	Isoamylase 3
LEUD1	Isopropylmalate Isomerase 2
LHY	Late Eleongated Hypocotyl 1
LNK2	Night Light-Inducible and Clock-Regulated Gene,
LSMeans	Least Square Means
LSU1	Low Sulfur Induced 1
MA	Mugineic Acid
MAM1/3	Methylthioalkylmalate Synthase 1/3
MEB1	Membrane of ER Body 1
MG	Methylglyoxal
MGL	Methionine Gamma-Lyase
MIOX2	Myo-Inositol Oxygenase 2
MSA1	More Sulfur Accumulation
MSRB5	Methionine Sulfoxide Reductase B5
NA	Nicotianamine
NBT	Nitro Blue Tetrazolium
NO	Nitric Oxide
NPGR1	No Pollen Germination Related 1
NR	Nitrate Reductase
NRT2;1	Nitrate Transporter
NS2	Nicotianamine Synthase 2
OAS	O-Acetylserine
OASC	O-Acetylserine (Thiol) Lyase-C
OASTL	O-Acetylserine (Thiol) Lyase
PAP22	Purple Acid Phosphatase 22
PAPS	Phosphoadenosine-5-Phosphosulfate
PCA	Principal Component Analysis
PDE329	Pigment Defective 329
PGR5	Proton Gradient Regulation 5
PHR1	Phosphate Response 1
PIN5	Pin-Formed 5
PSI	Photosystem I
PYD4	Pyrimidine 4
qPCR	Quantitative Real-Time PCR
QTL	Quantitative Trait Loci

RAV1	Ethylene Response Dna Binding Factor 4
RHC1	Resistant to High CO_2
RILs	Recombinant Inbred Lines
ROS	Reactive Oxygen Species
RP-HPLC	Reverse Phase - High-Performance Liquid Chromatography
RVE8	Reveille 8
SAM	S-Adenosylmethionine
SAR2	Secretion-Associated Ras Super Family 2
SAT/SERAT	Serine Acetyltransferase
SBP1	Selenium Binding Protein 1
SDI1	Sulfur Deficiency-Induced 1
SDI2	Sulfur Deficiency-Induced 2
SDS	Solo Dancers
SFP1	Senescence-Associated Sugar Transporter 1
SHM7	Serine Hydroxymethyl Transferase 7
SIG5	Sigma Factor 5
SiR	Sulfite Reductase
SLIM1	Sulfur Limitation 1
SNP	Single Nucleotide Polymorphism
SOT	Sulfotransferases
SP	Short Pulse
SPA3	Suppressor of Phy-A
SPPL1	Signal Peptide Peptidase-Like 1
SQD1/2	Sulfolipid Biosynthesis Genes
SQE3	Squalene Epoxidase 3
SULTR	Sulfate Transporter
SUS3	Sucrose Synthase 3
SWEET13	Sugar Will Eventually Be Exported Transporters 13
TAT1	Tyrosine Aminotransferase 7
TET6	Tetraspanin 6
TFs	Transcription Factors
TIM13	Translocase of The Inner Mitochondrial Membrane 13
TOR	Target of Rapamycin
TPPE	Trehalose-6-Phosphate Phosphatase E
TPPF	Trehalose-6-Phosphate Phosphatase F
TT7	Transparent Testa 7
UGE5	UDP-D-Galactose 4-Epimerase 5

UGT78D2	UDP-Glucosyl Transferases
VST	Variance-Stabilizing Transformation

ABSTRACT

Sulfur (S) is an essential macronutrient required for plant growth, metabolism, redox homeostasis, and defense, and its availability strongly constrains plant performance in both natural and agricultural systems. Plants exhibit substantial natural variation in sulfur content, for instance, *Arabidopsis thaliana* accessions show up to a six-fold difference in foliar sulfur (Baxter et al., 2007; Campos et al., 2021). Several genes, such as *APR2*, *ATPS1*, and *OASC,* were found to contribute to this variation; however, they explain only part of it, suggesting additional regulatory layers. Importantly, the functional significance of this variation and adaptive responses to sulfur limitation remain poorly understood. To address this gap, we analyzed *Arabidopsis* accessions grouped into low-, mid-, and high-foliar sulfur content using an integrated multi-omics and phenotyping framework under varying sulfate supply.

Our study revealed that despite higher basal sulfate levels, high-S accessions experienced pronounced depletion of sulfur pools and incurred significant fitness costs under sulfur deficiency. The observed decline in foliar sulfate, total sulfur, and glutathione (GSH) was associated with reduced sulfate uptake and translocation to the shoots, as well as limited flux into GSH. These physiological changes were accompanied by a strong induction of sulfur-starvation marker genes and increased oxidative stress. Besides, high-S accessions also showed restricted growth, accelerated flowering, and altered sulfur–nitrogen coordination, including repression of nitrate assimilation and broad metabolic reprogramming. In contrast, low-S accessions maintained sulfur pools and reproductive fitness under sulfur deficiency through enhanced sulfate uptake and translocation. Unlike the high-S group, low-S accessions prioritized redox homeostasis by channeling sulfur into glutathione synthesis, achieved through coordinated induction of genes involved in nitrate and cysteine assimilation. Coordinated induction of nitrate and cysteine assimilation pathways in the low-S group reflects increased utilization of nitrate and cysteine under sulfur deficiency. Mid-S accessions exhibited intermediate, context-dependent responses. We further explored transgenerational effects of sulfur deficiency and found that flowering time is sensitive to parental sulfur status, alongside other metabolic and developmental traits.

Transcriptome profiling further supported these phenotypes, with high-S accessions showing substantially more differentially expressed genes under S-deficiency. Although core sulfur starvation responses were conserved, with 55 core DEGs shared across the group, most DEGs and enriched gene ontology terms were unique to groups, indicating divergent regulatory strategies. Together, these findings demonstrate that high basal sulfur content does not confer protection against sulfur limitation but instead reflects increased vulnerability under prolonged S-deficiency. Also, with our data, we can deduce that effective sulfur stress tolerance is achieved through coordinated regulation of sulfur acquisition, metabolic fluxes, redox balance, and development, as exemplified by low-S accessions.

1. INTRODUCTION

1.1 Sulfur: The fourth major nutrient in plants

Sulfur is an essential macronutrient and is considered the fourth most important nutrient for plant growth after nitrogen, phosphorus, and potassium (Kopriva, 2015). It plays an indispensable role in both primary and secondary metabolism, contributing to protein synthesis, redox regulation, stress responses, and the production of defense-related compounds, such as the phytoalexins camalexin and brassinin (Fig. 1) (Takahashi et al., 2011). Sulfur is a key constituent of the amino acids like cysteine and methionine, where methionine initiates protein translation, and cysteine enables disulfide bond formation critical for protein structure and function (Duke & Reisenauer, 1986). Cysteine also represents the metabolic convergence point of carbon, nitrogen, and sulfur assimilation and serves as the primary bioavailable source of reduced sulfur for downstream metabolism (Jobe et al., 2019; Pivato et al., 2014). Downstream of cysteine, glutathione (GSH) plays a central role in cellular redox homeostasis, detoxification of toxic metals and metalloids, scavenging of methylglyoxal, and protection against abiotic stress (Hasanuzzmann et al., 2017) (Fig. 1). Beyond its role in protein synthesis, methionine also participates in stress-associated metabolic adjustments, including osmolyte accumulation and signalling processes that support cellular stability under adverse conditions (Takahashi et al., 2011; Shah et al., 2022) (Fig. 1). In addition to its metabolic roles, sulfur functions as a regulatory signal coordinating cellular homeostasis and stress adaptation. Reduced sulfur species such as hydrogen sulfide (H_2S), derived from cysteine metabolism, have emerged as important signaling molecules that modulate stress-responsive gene expression and interact with phytohormone pathways, thereby fine-tuning plant responses to abiotic stress (Shah et al., 2022) (Fig. 1).

Beyond primary metabolism, sulfur is integral to the synthesis of chlorophyll, vitamins such as thiamine and biotin, and iron-sulfur clusters (Fe-S), required for photosynthesis, respiration, and DNA synthesis (Goodrich & Garrett, 1986; Lunde et al., 2008; Lu, 2018). Sulfur-containing secondary metabolites, including glucosinolates, camalexin, and brassinin, are central to plant defense against herbivores and pathogens (Halkier & Gershenzon, 2006; Bednarek et al., 2009; Koprivova & Kopriva, 2014). Collectively, sulfur-containing compounds such as glutathione, thioredoxins, and glutaredoxins coordinate redox balance, carbon metabolism, ROS scavenging, and post-translational regulation (Meyer et al., 2008) (Fig. 1). Altogether, sulfur acts not only as a structural and metabolic nutrient, but also as a central integrator of redox signalling, ion homeostasis, and hormonal control, ultimately contributing to enhanced stress tolerance and metabolic resilience in plants.

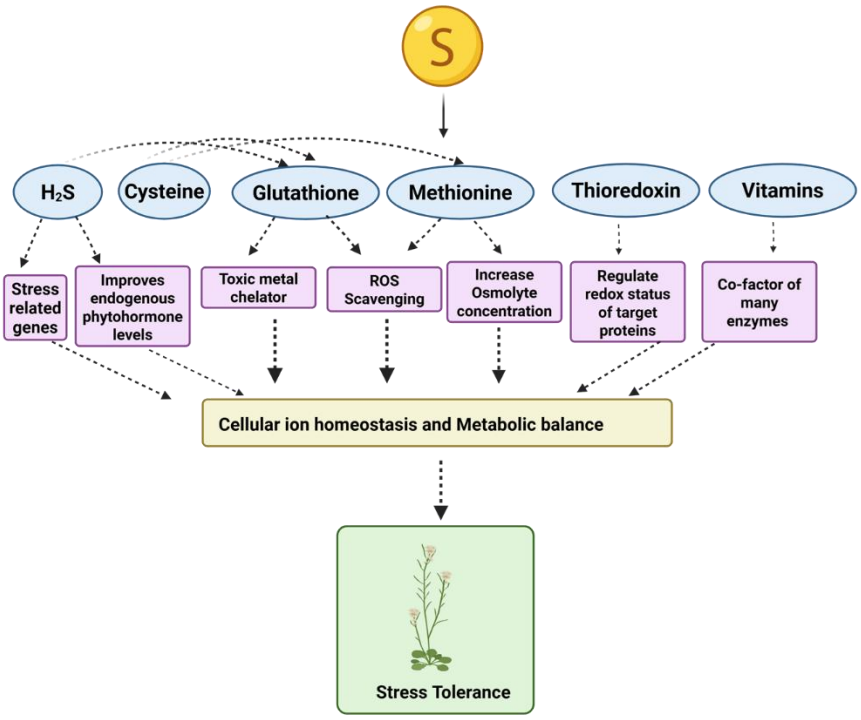

Figure 1: Overview on central role of sulfur and sulfur-derived metabolites in redox regulation, ion homeostasis, and plant stress tolerance. Figure adapted and redrawn from Shah et al. (2022) using Biorender.

1.1.1 Sulfate assimilation in plants

Plants take up S mainly in the form of sulfate (SO_4^{2-}) from the soil through roots with the help of two high-affinity sulfate transporters, i.e. SULTR1;1 and SULTR1;2 (Yoshimoto et al., 2002) (Fig. 2). These two transporters belong to group 1 sulfate transporters, which are divided into four distinct groups (SULTR1,2,3, and 4) in plants, which facilitate not only uptake but also distribution of sulfate within the plants (Maruyama-Nakashita & Ohkama-Ohtsu, 2017). Both of these high-affinity transporters are localized and expressed in root hairs, epidermis, and cortex cell layers of roots (Yoshimoto et al., 2002) and are redundant in function, but SULTR1;2 is the major component of the constitutive sulfate uptake system, while SULTR1;1 is induced mostly under S-limiting conditions (Rouached et al., 2008; Shibagaki et al., 2002; Takahashi et al., 2000; Yoshimoto et al., 2002). Low-affinity sulfate transporters belonging to subgroups 2, 3, and 4 facilitate sulfate movement through the vascular system, including xylem and phloem loading, plastidial uptake, and vacuolar export, respectively (Maruyama-Nakashita & Ohkama-Ohtsu, 2017) (Fig. 2). Through the coordinated activity of these transporters, sulfate is efficiently supplied to major assimilation sites, sink tissues, and storage compartments, while also remaining available for redistribution to support ongoing metabolic demands (Maruyama-Nakashita & Ohkama-Ohtsu, 2017). Besides root uptake of sulfate, sulfur can also enter plant shoots in the form of SO_2 and H_2S (Brunold et al., 1983; de Kok et al., 1989; Rennenberg et al., 1996). Plants can

also acquire S in S-containing amino acids, however, organic sulfates and sulfonates in the soil are not directly accessible as sulfur sources (Shah et al., 2022) (Fig. 2).

The primary assimilation of sulfate occurs in the plastids, where it is first activated by adenylation to adenosine 5'-phosphosulfate (APS) with the help of ATP sulfurylases (ATPS), and is present in four different isoforms (ATPS1, ATPS2, ATPS3, and ATPS4) in *Arabidopsis* (Fig. 2) Among these four isoforms, ATPS2 occurs in two different forms, one being cytosolic and the other in the plastids, while the remaining three isoform proteins are localized in plastids (Murillo & Leustek, 1995). APS can then follow two alternative pathways: primary assimilation or secondary assimilation (Kopriva et al., 2012). In the primary assimilation pathway, APS is first reduced to sulfite (SO_3^{2-}) by APS reductase (APR), which exists in three isoforms, all located exclusively in plastids, with APR2 accounting for 75% of total activity (Rotte & Leustek, 2000) (Fig. 2). The conversion of APS to sulfite is often considered the rate-limiting step of the primary sulfate assimilation pathway (Vauclare et al., 2002; Kopriva et al., 2012). This sulfite is then further reduced to sulfide (S^{2-}) through the transfer of six electrons, catalyzed by ferredoxin-dependent sulfite reductase (SiR) (Kopriva et al., 2012), and *Arabidopsis* contains only the SiR isoform (Fig. 2).

After reduction, sulfide is channeled into the synthesis of cysteine, the first product of the primary assimilation pathway and the first compound containing organic reduced sulfur (Hell & Wirtz, 2011) (Fig. 2). Cysteine (Cys) biosynthesis proceeds via a two-step enzymatic pathway. In the first step, serine (Ser) is acetylated by serine acetyltransferase (SAT; SERAT), which transfers an acetyl group from acetyl-CoA to form O-acetylserine (OAS) (Fig. 2). In the subsequent step, OAS (thiol) lyase (OAS-TL) catalyzes the replacement of the acetyl group with sulfide, forming cysteine (Cys) (Hell & Wirtz, 2011). Cys biosynthesis takes place in multiple cellular compartments, including plastids, mitochondria, and the cytosol (Hell & Wirtz, 2011) (Fig. 2). In *Arabidopsis thaliana*, the SERAT enzyme family is encoded by five genes with distinct subcellular localizations: SERAT2;1 and SERAT2;2 are targeted to plastids and mitochondria, respectively, whereas SERAT1;1, SERAT3;1, and SERAT3;2 are cytosolic (Krueger et al., 2009). SERAT activity can indirectly regulate Cys production by controlling the availability of OAS, which may act as a limiting precursor under certain conditions (Maruyama-Nakashita, 2017).

Cysteine represents the primary bioavailable form of reduced sulfur and serves as a precursor for the synthesis of glutathione (GSH), methionine, and other sulfur-containing metabolites (Pivato et al., 2014). GSH, a tripeptide composed of glutamate, cysteine, and glycine, functions as a major storage form of reduced sulfur and plays a central role in sulfur assimilation, redox homeostasis, stress protection, and detoxification processes (Noctor et al., 2012; Hasanuzzaman et al., 2017). Glutathione is synthesized through a two-step ATP-dependent pathway: γ-glutamylcysteine synthetase catalyzes the formation of γ-glutamylcysteine (γ-ECS) from glutamate and cysteine and is encoded by *GSH1* gene in *Arabidopsis* (Hell & Bergmann, 1990; May & Leaver, 1994), while glutathione synthetase, encoded by *GSH2*, catalyzes the subsequent addition of glycine to form GSH, with alternative splicing generating

isoforms targeted to both cytosolic and plastid compartments (Wang & Oliver, 1996; Skipsey et al., 2005b). Apart from GSH, cysteine can also react with phosphohomoserine, forming cystathionine, which is then converted to methionine via homocysteine (Calderwood & Kopriva, 2014). Methionine is an S-containing amino acid and plays a vital role in the initiation of mRNA translation and also acts as a regulatory molecule in the form of S-adenosylmethionine (SAM). SAM serves as a precursor for many metabolites, including polyamines, vitamins, nicotianamine (NA), mugineic acid (MA), ethylene, and thiamine (Astolfi et al., 2021).

In the secondary assimilation pathway, APS is phosphorylated by APS kinase (APK) to form 3-phosphoadenosine-5-phosphosulfate (PAPS), which represents the active form of sulfate and is used for the sulfation of peptides or secondary metabolites mediated by sulfotransferases (SOT) (Takahashi et al., 2011; Koprivova & Kopriva, 2014). Amino acid-derived glucosinolates act as one of the group acceptors, having a key role in plant defense against pathogens and herbivores (Halkier & Gershenzon, 2006; Bednarek et al., 2009). Similar to ATPS, there are four isoforms of APK (APK1, 2, 3, 4), of which APK3 is located in the cytosol, and the rest are localized in the plastids (Mugford et al., 2009).

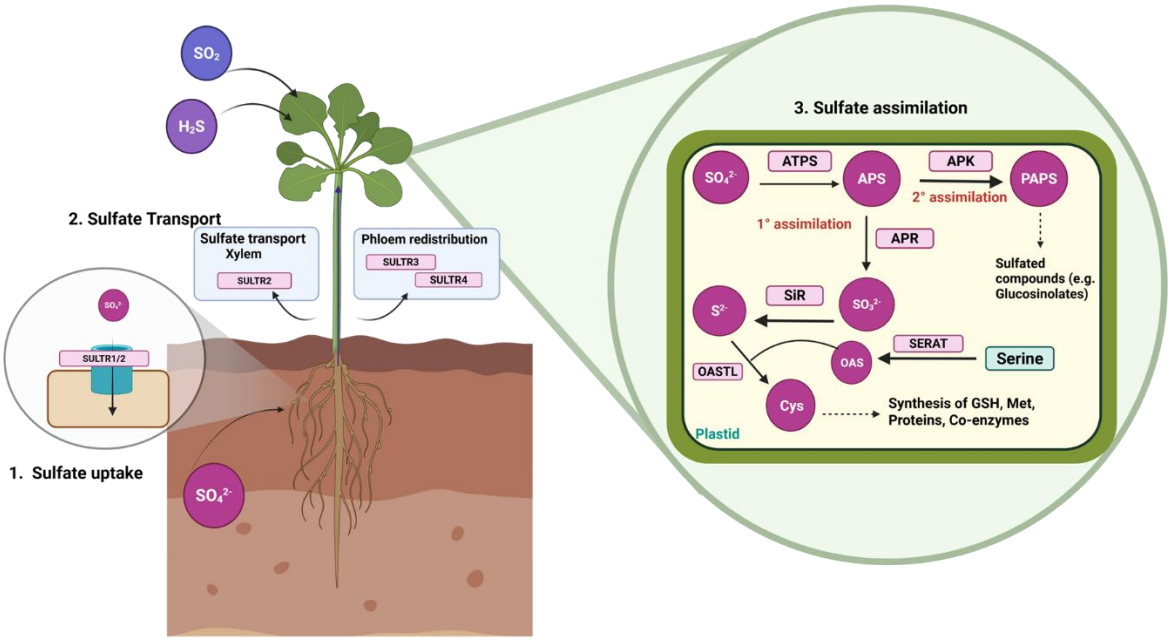

Figure 2: Schematic representation of the sulfate assimilation pathway, including sulfate uptake and transport in *Arabidopsis thaliana*. Adapted from Koprivova & Kopriva, 2014; Ristova et al., 2022, and created using Biorender.

1.1.2 Regulation of sulfate assimilation in plants

Regulation of sulfate assimilation is dependent on sulfur availability, demand for reduced sulfur, phytohormones, and distinct environmental factors (Koprivova & Kopriva, 2014). Analysis of sulfur flux through the sulfate assimilation pathway identified sulfate transport and APS reductase (APR) as the steps with the highest control (Vauclare et al., 2002). This was observed in *Arabidopsis* roots, where treatment with labeled cysteine and GSH showed that *APR*, along with sulfate transporters, accounted for 92% of control over the sulfur assimilation pathway (Vauclare et al., 2002). Several studies revealed strong transcriptional regulation of *APR* by thiols, amino compounds, carbohydrates, and hormones (Bick et al., 2001; Vauclare et al., 2002; Hartmann et al., 2004). This was further supported by analyses of plants with altered *APR* expression, where natural variation in the *APR2* isoform among *Arabidopsis* ecotypes was associated with differences in sulfate and total sulfur accumulation (Loudet et al., 2007; Chao et al., 2014). Apart from *APR,* other genes, such as *SERAT* (mitochondrial isoform) and *SiR,* also contribute significantly to the control of flux through the reductive part of sulfate assimilation (Haas et al., 2008; Khan et al., 2010). Moreover, altered expression of *ATPS1*, an ATPS isoform, has been associated with reduced flux and increased sulfate accumulation in leaves (Kawashima et al., 2011; Kopriva et al., 2013; Pilon-Smits et al., 1999; Wangeline et al., 2004). Hence, similar to *APR2*, natural variation in *ATPS1* also contributes to differences in sulfate accumulation among *Arabidopsis* accessions (Koprivova et al., 2013; Herrmann et al., 2014). However, these studies clearly indicate the presence of additional regulatory mechanisms that might target other components of the pathway, and there is no conclusive general model that connects sulfate sensing to transcriptional regulation.

Unlike other well-known nutrients like nitrogen and phosphorus, there is a gap in knowledge of sulfur sensing and its regulation, as we still don't know which molecule acts as a sensor for sulfur (Ristova and Kopriva, 2022). Only a few regulatory elements have been studied so far, SULFUR LIMITATION 1 (SLIM1), appears to be one of the key regulators of the sulfur deficiency response. SLIM1 was discovered through a mutagenesis screen in transgenic *Arabidopsis* plants expressing GFP under the control of the sulfur deficiency-inducible SULTR1;2 promoter in the Col-0 background. A single nucleotide substitution in SLIM1 resulted in mutants with a compromised sulfur deficiency response, characterized by reduced sulfate uptake, impaired growth, and altered transcriptional regulation (Maruyama-Nakashita et al., 2006). More recently, ETHYLENE-INSENSITIVE3-LIKE 1 (EIL1), a transcription factor belonging to the same family as SLIM1, was identified as an additional regulator of sulfur deficiency, acting in an additive manner (Dietzen et al., 2020). Although SLIM1 is involved in the activation of sulfate acquisition and glucosinolate degradation, the mechanism of this regulation under sulfur starvation remains poorly understood. It has previously been reported that SLIM expression was not affected under S limitation, suggesting post-transcriptional regulation (Maruyama-Nakashita et al., 2006; Aubry et al., 2014). Similarly, miRNA395, which is regulated by SLIM1, is also part of the regulatory circuit of sulfate assimilation as it targets ATPS and sulfate transporter SULTR2;1, thus controlling sulfate translocation to shoots and S-homeostasis (Jones-Rhoades & Bartel, 2004).

Apart from components of sulfate assimilation pathways, there are additional layers of regulation which controls the induction of sulfate assimilation genes, like treatment with OAS, carbohydrate, phytohormones, and heavy metals (Kopriva et al., 1999; Vauclare et al., 2002; Hesse et al., 2003; Jost et al., 2005). In contrast, the pathway can be inhibited by reduced sulfur and by limitations in available nitrogen and carbon (Koprivova et al., 2000). Target of rapamycin (TOR) kinase, which acts as a central regulator and integrator of multiple pathways, is involved in mediating sulfur signalling, adapting the metabolic network of the plant in response to sulfur supply (Yu et al., 2022). Even though the molecular regulation of sulfate assimilation has been widely studied, many open questions still remain, as it is still unclear which transcription factors (TFs) and pathways control gene regulation in response to environmental and metabolic cues. Additionally, although we know TOR is involved in S homeostasis regulation, we still lack knowledge of other cellular processes directly linked to S homeostasis. Hence, understanding these mechanisms is a prerequisite for any directed influence on this pathway, e.g., for crop engineering or enhanced stress resistance.

1.1.3 Sulfate deficiency response and its transcriptional regulation

Sulfur deficiency has emerged as a growing threat to modern agriculture due to the implementation of the 1970 Clean Air Act and 1990 amendments (Bouranis et al., 2020). This has led to a significant reduction in atmospheric S emissions, thereby posing a serious threat to modern agriculture, especially when combined with other deficiencies (Likens et al., 2001; Jobe et al., 2019). Sulfur starvation has been investigated at both the metabolic and transcriptional levels. At metabolic levels, sulfur-deficient plants show a decline in total sulfur, which is more severe under long-term S-deficiency (Nikiforova et al., 2003). Reduction in glucosinolates and sulfate is followed by a significant decline in cysteine and GSH (Hirai et al., 2003; Hirai et al., 2004; Lunde et al., 2008). The decline in GSH further leads to oxidative stress by increasing the oxidation ratio and hence more production of Reactive Oxygen Species (ROS) (Noctor & Foyer, 2016; Hasanuzzaman et al., 2017). The slowdown of sulfate reduction is further marked by accumulation of cysteine precursor OAS, and thus leading to altered metabolic composition like enrichment of tryptophan and glycine/serine and N-rich amino acids (Nikiforova et al., 2003; Nikiforova et al., 2005; Hoefgen & Nikiforova, 2008). Although methionine levels remain unchanged, a reduction in SAM levels is observed, which hinders many metabolic pathways, including photosynthesis (Nikiforova et al., 2005; Hoefgen & Nikiforova, 2008). Photosynthesis is also affected in S-starved plants due to a reduction in sulfolipids, glycolipids, and phospholipids (Lunde et al., 2008).

S-deficiency not only perturbs the metabolic levels but it also leads to transcriptional changes with high number genes differentially expressed (DEGs), for instance, around 335 DEGs were reported in *Arabidopsis thaliana* (Dietzen et al., 2020), 236 DEGs in *Oryza sativa*, and 565 DEGs in *Setaria viridis* (Zenzen et al., 2024). SLIM1 acts as key regulatory component under S-deficiency by exerting its regulatory function at the levels of S-uptake by upregulation of *SULTR1;1*, and *SULTR1;2* in roots

(Maruyama-Nakahashita et al., 2006). With the help of meta-analysis on five different sets of transcriptomic and metabolomic data, a robust set of genes were identified whose expression was tightly correlated with OAS. These six genes, *SDI1 (SULFUR DEFICIENCY-INDUCED 1), SDI2 (SULFUR DEFICIENCY-INDUCED 2), APR3 (APS REDUCTASE 3), SHM7 (SERINE HYDROXYMETHYL TRANSFERASE 7), GGCT2;1 (γ- GLUTAMYL-CYCLOTRANSFERASE 2;1)* and *LSU1 (LOW SULFUR INDUCED 1)* were termed as "OAS cluster genes" (Hubberten et al., 2012). Both SDI1 and SDI2 interact with MYB28 to repress the biosynthesis of glucosinolates during S-deficiency (Aarabi et al., 2016). *APR3* is one of 3 isoform of APS reductase although not the major one, as knockout of *APR2* reduced the enzymatic activity by 80% (Loudet al., 2007). Serine hydroxymethyltransferase (*SHM7*), also named More Sulfur Accumulation (*MSA1*) regulates S-adenosylmethionine (SAM) biosynthesis and maintains S homeostasis epigenetically via DNA methylation (Huang et al., 2016). *GGCT2;1* has a major role in glutathione degradation, especially during abiotic stress (Paulose et al., 2013). *LSU1* constitutes a network hub for proteins in response to biotic and abiotic stresses (Sirko et al., 2015). Notably, all six genes are significantly upregulated during sulfur starvation, predominantly in a SLIM1-dependent manner (except *APR3*), and are also induced by exogenous O-acetylserine (OAS) under sulfur-sufficient conditions, supporting a signalling role for OAS independent of sulfur availability (Hubberten et al., 2012). Correspondingly, all OAS cluster genes have SLIM1/EIL3 binding site in their promoter (Ran et al., 2020).

Besides transcriptional regulation, post-transcriptional mechanisms also play a crucial role in controlling the activity and stability of enzymes involved in sulfur metabolism. One well-established example is the redox regulation of APS reductase (APR), where oxidative conditions lead to an uncoupling between APR transcript levels and enzyme activity, highlighting its role in maintaining redox homeostasis under stress (Bick et al., 2001). Another key regulatory system involves O-acetylserine (OAS) and the cysteine synthase complex (CSC). OAS functions not only as a metabolic precursor but also as a signalling molecule for sulfur demand. The CSC, formed by SERAT and OASTL proteins catalyzes cysteine biosynthesis using OAS and sulfide. Under sulfur deficiency, OAS accumulates, leading to dissociation of the CSC and thereby linking sulfur availability with cysteine demand (Takahashi., 2023). In addition, miRNA395 plays a central role in post-transcriptional regulation under sulfur deficiency. It accumulates under low sulfur conditions and targets key genes such as *ATPS1, ATPS3, ATPS4*, and *SULTR2;1*, and is itself regulated by SLIM1 (Kawashima et al., 2009). Although other miRNAs have also been reported to respond to sulfur deficiency, their specific targets and functions remain largely unknown. Regulation of sulfur pools in seeds is less well understood, but available evidence suggests that seed protein synthesis under sulfur deficiency is primarily controlled at the post-transcriptional level (Higashi et al., 2006). Overall, significant progress has been made in understanding the molecular and regulatory mechanisms underlying plant responses to sulfur deficiency; however, major knowledge gaps remain. In particular, the regulation of OAS-responsive gene clusters and the mechanisms by which OAS signalling is perceived are still poorly characterized. Moreover, although sulfur deficiency is known to

suppress secondary sulfur metabolism, it remains unclear whether this results in a redirection of sulfur flux toward primary metabolic processes. A deeper understanding of these regulatory layers will be essential for elucidating how plants integrate sulfur sensing with metabolic and developmental responses, ultimately shaping adaptive strategies under sulfur limitation.

The physiological response to sulfur (S) deficiency is characterized by growth retardation, leaf chlorosis, anthocyanin accumulation, and an increased root-to-shoot ratio (Aarabi et al., 2020). Chlorosis can persist for extended periods and may eventually progress to necrosis under prolonged deficiency (Bang et al., 2020). Notably, S-deficiency symptoms typically appear first in younger leaves and spread in a basipetal direction, reflecting the relatively low mobility of sulfur within the plant (Bang et al., 2020). Although the underlying causes of these symptoms are not fully understood, they are likely influenced by interactions between sulfur, nitrogen, and iron metabolism (Forieri et al., 2017). In addition to vegetative effects, sulfur deficiency also impacts reproductive development. It can accelerate flowering while reducing flower number, altering flower development, and impairing pollen quality and quantity (Nikiforova et al., 2005; Ausma et al., 2021). In oilseed rape, for example, S-deficiency induces “white blooming,” where petals lose pigmentation due to carbohydrate accumulation and disrupted protein metabolism, leading to the formation of leuco-anthocyanins (Schnug & Haneklaus, 2005). Sulfur limitation further affects seed yield and quality. In oilseed rape, S-deficiency applied at the bolting stage reduced both seed quantity and quality, including declines in protein, oil, and glucosinolate content (Girondé et al., 2014). Similarly, reduced sulfur availability promotes the accumulation of sulfur-poor storage proteins, such as ω-gliadins and high-molecular-weight glutenin subunits, in wheat. This shift negatively impacts baking quality, as proper dough structure and loaf volume depend on disulfide bond formation within the gluten network (Liu et al., 2022). In addition, sulfur deficiency induces strong accumulation of free amino acids, particularly asparagine and glutamine, reflecting substantial metabolic reprogramming. This has important agronomic consequences, as elevated asparagine levels lead to increased acrylamide formation during food processing, as reported in wheat and potato flour (Muttucumaru et al., 2006; Elmore et al., 2010). Collectively, these findings highlight that sulfur deficiency not only constrains plant growth and development but also has far-reaching effects on reproductive success, seed composition, and food quality, underscoring the importance of efficient sulfur management in both plant adaptation and agricultural systems.

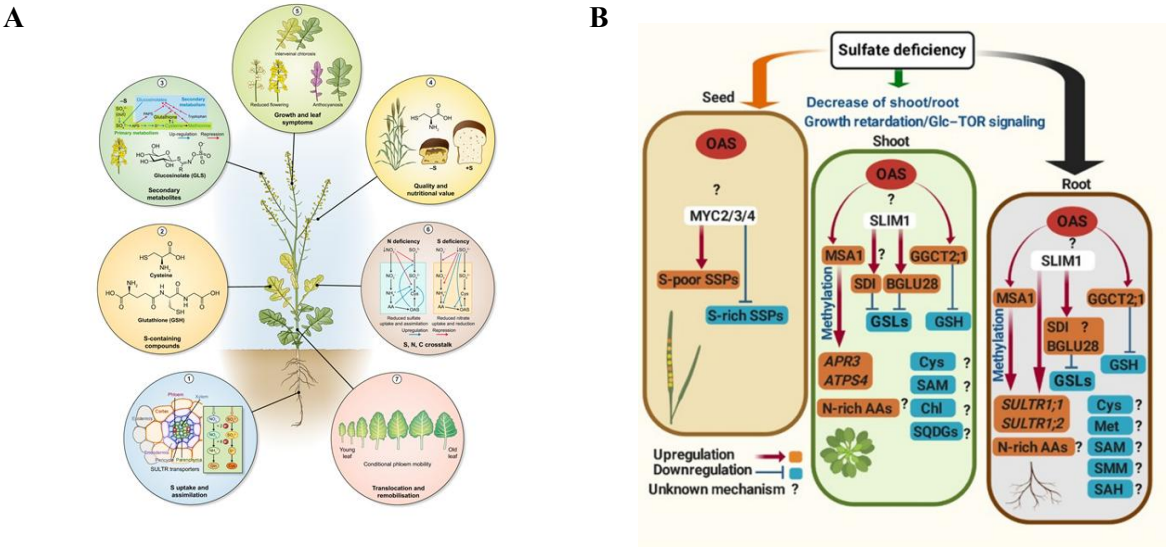

Figure 3: (A) Impact of S-deficiency on plants and (B) its transcriptional regulation in *Arabidopsis thaliana*. (A) Adapted from Bang et al., 2020; **(B)** Adapted from Aarabi et al., 2020

1.1.4 Crosstalk of Sulfur with the Nitrogen and Phosphorus metabolic pathways

The crosstalk between sulfur (S) and other nutrients has been widely studied and is considered crucial for maintaining nutrient homeostasis under fluctuating environmental conditions, including combined nutrient deficiencies. Among these interactions, the tight interconnection between sulfur and nitrogen (N) pathways is particularly important, as coordinated S-N metabolism not only supports plant growth and development but also influences the uptake and utilization of other nutrients (Shah et al., 2022). Sulfur-nitrogen interaction is essential for protein synthesis, and it has long been recognized that limitation of one nutrient can directly affect the uptake and assimilation of the other (Ahmad et al., 2007). Evidence from crop species such as *Zea mays*, *Triticum aestivum*, and *Brassica napus* demonstrates that sulfur deficiency leads to a pronounced reduction in nitrogen use efficiency, while nitrogen limitation similarly compromises sulfur use efficiency. Under sulfur deprivation, nitrogen metabolism is strongly disrupted, resulting in the accumulation of nitrate, tryptophan, serine, and O-acetylserine, alongside a marked decrease in reduced sulfur compounds such as cysteine, glutathione, and S-adenosylmethionine (Dubousset et al., 2009; Sarda et al., 2014; Lee et al., 2016). These metabolic changes highlight the close biochemical coupling of sulfur and nitrogen assimilation. At the transcriptional level, this interdependence is further reflected in the coordinated regulation of key assimilatory enzymes. Both APS reductase (APR) and nitrate reductase (NR) are induced by reduced nitrogen sources, such as ammonium and amino acids, as well as by the reduced sulfur compound cysteine (Kopriva & Rennenberg, 2004). In addition, nitrogen deficiency has been shown to regulate the expression of several sulfate transporters and genes involved in sulfate assimilation (Ristova & Kopriva, 2022). Consistent with this, increased expression of the nitrate transporter *NRT2.1* has been reported following sulfur resupply, while downregulation of the sulfate transporter *SULTR1;1* under nitrogen

starvation further supports the existence of coordinated sulfur-nitrogen signaling pathways (Bao et al., 2011). The synergistic interaction between nitrogen and sulfur has also been widely exploited in agriculture, where balanced N and S fertilization improves grain yield, protein content, and oil accumulation in crops such as rapeseed (Zhao et al., 1993; Ahmad & Abdin, 2000a). Together, these physiological, metabolic, and transcriptional responses underscore the tight interdependence of sulfur and nitrogen assimilation pathways. Despite this extensive evidence, the molecular mechanisms underlying sulfur-nitrogen crosstalk remain largely unresolved. In particular, it is still unclear how transcription factors from one signalling pathway influence the regulation of the other, and whether these interactions are activating or repressive in nature. Elucidating these mechanisms is therefore critical for improving our understanding of nutrient integration and for optimizing crop growth, physiological performance, metabolic balance, and yield.

Sulfur not only synergizes with nitrogen but also shows strong interactions with phosphorus (P), as demonstrated by Rouached et al. (2011). In this study, phosphate (Pi) deficiency resulted in reduced sulfate accumulation in shoots, while sulfate levels increased in roots. This redistribution was accompanied by upregulation of the sulfate transporter *SULTR1;3* under Pi starvation, with its induction shown to be specifically dependent on the phosphate starvation regulator PHR1 (Phosphate Response 1). In contrast, *PHR1* negatively regulates *SULTR2;1* and *SULTR3;4* in response to Pi deficiency, indicating that sulfate translocation is actively reprogrammed under altered phosphorus availability. Notably, this regulatory mechanism is evolutionarily conserved, as a similar response has been observed in *Chlamydomonas reinhardtii* via the *PHR1* homolog *PSR1*. However, Pi deficiency does not affect the expression of the high-affinity sulfate transporters *SULTR1;1* and *SULTR1;2* in *Arabidopsis* (Maruyama-Nakashita et al., 2004). Sulfur-phosphorus interactions are also evident at the metabolic level, where sulfolipids are substituted by phospholipids under sulfur deficiency, whereas under phosphorus deficiency, phospholipids are replaced by sulfolipids. This lipid remodeling is mediated by the upregulation of *SQD1* and *SQD2*, genes involved in sulfolipid biosynthesis, whose induction under Pi deficiency is impaired in the *phr1* mutant (Yu et al., 2002; Bustos et al., 2010). Additional regulatory connections are observed at the post-transcriptional level. miR395, which is regulated by SLIM1 and strongly induced under sulfur starvation, is suppressed under Pi deficiency. This repression may promote enhanced sulfur translocation from roots to shoots through targeting *SULTR2;1* (Hsieh et al., 2009). Conversely, the phosphate transporter *ATPHT1;2*, typically induced under Pi deficiency, is also upregulated under sulfur deficiency, suggesting enhanced phosphate uptake and translocation in response to sulfur limitation (Bao et al., 2011). The interaction between sulfur and phosphorus has been widely studied across crop species, where the outcome depends on nutrient availability, fertilization regime, and crop type (Shah et al., 2022). Co-fertilization with sulfur and phosphorus has been shown to improve dry matter accumulation, grain yield, straw yield, and nutrient uptake in *Oryza sativa* (Ali et al., 2004). Similar synergistic effects have been reported in *Brassica juncea* L., *Solanum melongena* L., *Zea mays* L., and *Vigna radiata* L., where combined S and P application enhanced nutrient uptake, seed

and grain yield, and overall plant growth and morphology (Teotla et al., 2000; Mishra et al., 2010; Hasan et al., 2013; Nanthakumar et al., 2014; Parashar & Tripathi, 2020). Despite substantial evidence for coordinated regulation of sulfate and phosphate homeostasis, PHR1 remains the only transcription factor currently known to directly link these nutrient signaling pathways, while additional regulatory components remain largely unidentified. Thus, understanding sulfur-phosphorus interactions will help us shape plant growth and enhance yield and crop quality, with important implications for both basic nutrient biology and agricultural management.

1.2 Natural variation of physiological traits in *Arabidopsis thaliana*

With the advent of molecular mapping markers, it became easier to study the genetic architecture of quantitative traits in the model plant *Arabidopsis thaliana* (Chang et al., 1988; Nam et al., 1989). This species belongs to a small genus with 9 members and is quite distinct for being self-compatible and having a shorter life cycle, which facilitates genetic studies. The native range of *Arabidopsis* is believed to be Eurasia and North Africa, but now it has been introduced all over the world, especially around the Northern Hemisphere (Al-Shehbaz and O'Kane et al., 2002; Weigel., 2012). *Arabidopsis* is also a good model for studying the genetic variability of plant adaptation to nutrient deficiency, since *Arabidopsis* accessions have been found in a wide range of habitats differing notably in soil richness and physiological traits (Ikram et al., 2011). This has been linked to evolutionary importance, as some traits are advantageous and add an adaptive value to a species under certain environmental conditions. Hence, there are multiple ways by which plants can respond to different stimuli to adjust their growth and yield. To study distinct adaptive strategies under nutrient stress, ionomics has emerged as a powerful and informative approach. It represents a developing functional genomics strategy that uses high-throughput elemental profiling to identify genes and gene networks involved in the acquisition, transport, and accumulation of mineral nutrients from the soil, as well as their distribution and homeostasis within the plant (Rus et al., 2006). Screening around 6,000 fast-neutron-mutagenized *Arabidopsis* plants under control conditions, Lahner et al. (2003) identified 51 mutants with altered shoot elemental profiles. From this, they estimated that approximately 2-4 % of the *Arabidopsis* genome is involved in regulating elemental composition, highlighting the complexity of ionomic control (Lahner et al., 2003; Salt et al., 2004). Additionally, two distinct ionomics datasets comprising around 350 and 1135 *A. thaliana* accessions showed large variation in the elemental composition of leaves (Baxter et al., 2007; Campos et al., 2021). For instance, leaf total sulfur content among *Arabidopsis* accessions in the Core360 panel of the Purdue Ionomics project varies widely, ranging from 2.6 g kg^{-1} DW in accession (11PNA4.101) to 18.9 g kg^{-1} DW in Hod (Baxter et al., 2007). Within the same population, foliar sulfate levels differ by nearly six-fold (Chao et al., 2014). This extensive natural variation has been widely exploited to uncover genetic regulators of nutrient accumulation, leading to key discoveries such as the identification of a molybdate transporter (Baxter et al., 2008) and the HMA3 ATPase underlying cadmium accumulation (Chao et al., 2012). Consistent with this, natural variation has been also reported for

nitrogen, phosphorus, boron, and potassium, as well as heavy metals such as zinc, and aluminium, highlighting the polygenic and environment-dependent nature of mineral nutrient regulation and adaptation (reviewed in Lefebvre et al., 2009).

1.2.1 Natural variation in sulfur content and S-containing metabolites

The two ionomics datasets also revealed large variability in foliar sulfur content among other elements (Baxter et al., 2007; Campos et al., 2021) (Fig. 4A). The S-content variation ranges up to six-fold in plants grown under control conditions and under optimal supply, indicating diverse adaptive strategies used by plants in response to different environmental stimuli (Baxter et al., 2007; Campos et al., 2021). To explain the cause of this variation, a quantitative genetic approach was employed, i.e., Quantitative Trait Loci (QTL) mapping. Through QTL mapping, genes responsible for variation in the number of traits can be identified using biparental crosses (Koornneef et al., 2004). Loudet et al. (2007) identified two major quantitative trait loci (QTLs) controlling shoot sulfate content using recombinant inbred lines (RILs) derived from the *Arabidopsis thaliana* accessions Bay-0 and Shahdara. The first QTL was mapped to *APR2*, a central enzyme in the sulfate assimilatory reduction pathway. Natural variation at this locus was shown to strongly influence sulfate accumulation, with a single amino-acid substitution (Ala399-Glu399) causing a near-complete loss of APR2 enzymatic activity and consequent sulfate accumulation in the plant (Loudet et al., 2007). Consistent with this, additional weak *APR2* alleles were independently associated with elevated sulfate or total sulfur content in the Hod and Love-1 accessions, underscoring the importance of *APR2* in sulfate homeostasis (Chao et al., 2014). Subsequent work by Koprivova et al. (2013) characterized the second major QTL, i.e., *ATPS1*, encoding the enzyme catalyzing the first committed step of sulfate assimilation. Natural variation at this locus was primarily due to differences in transcript abundance among RILs and accessions, leading to altered enzyme activity and increased sulfate accumulation in lines with lower *ATPS1* expression (Koprivova et al., 2013). Despite their importance, the QTLs harbouring *APR2* (SO10.1) and *ATPS1* (SO10.2) together accounted for only a limited proportion of the phenotypic variation in sulfate content, explaining approximately 21% and 23%, respectively (Loudet et al., 2007). Recently, another gene, mitochondrial OAS-TL, *OASC*, was linked to variation in sulfate content. Loss of *OASC* resulted in a reduction in sulfate content as sulfate uptake and translocation were significantly dropped. Genetic and transgenic complementation analyses revealed single nucleotide polymorphism (SNP) in accessions with a lysine (K) at position 81 of the OASC sequence (Col-0-like) accumulated higher sulfate than those with arginine (R) (Ha-0-like) at this position. This SNP affected the function of OASC and also sulfate accumulation. However, as the K_{81} is located in the transit peptide, it is not clear what functional impact this variation might have (Koprivova et al., 2023). Accordingly, alongside *ATPS1* and *APR2*, *OASC* emerges as an additional metabolic enzyme involved in controlling sulfate levels in *Arabidopsis*.

Also, as QTL mapping can only use variation between two genotypes, Genome-wide association studies (GWAS) was employed to cover more genes with a wide variety of genotypes in a large population (Weigel., 2012). This approach has been employed in rice, wheat, *Brassica napus,* and other plant species for analysis of traits related to sulfur metabolism (Huang & Han et al., 2014). Although GWAS has been successfully used to identify candidate genes for controlling sulfate accumulation in *B. napus* leaves, in *Arabidopsis*, this was not the case (Koprivova et al., 2014; Atwell et al., 2010). But variation in secondary S-containing metabolite i.e. glucosinolates (GSLs) were analysed using GWAS in both *B. napus* and *Arabidopsis* (Lu et al., 2014; Chan et al., 2011). GSLs are primary defense compounds against herbivores and pathogens (Burow & Halkier, 2017). However, their induction is dynamic leading to distinct changes in GSLs patterns as it is heavily dependent on biotic and environmental factors (Del Carmen Martinez-Ballesta et al., 2013; Yang et al., 2020). The extensive natural variation in GSLs in *Arabidopsis* can be due to multiple factors, such as genetics, local environment, and population history, which might play a key role in building local adaptations to biotic factors (Katz et al., 2021). Several major causal loci, such as *AOP2, AOP3, MAM1, MAM3,* and *GSL-OH,* are responsible for variation in GSLs biosynthesis and for positive selection (Chan et al., 2010; Brachi et al., 2015; Katz et al., 2021). As GSLs patterns are dynamic, understanding the control of GSLs accumulation can help in genetic variation studies such as stochastic variation, which was found to be genetically encoded as well (Jimenez-Gomez et al., 2011).

Overall, natural variation in sulfur content and sulfur-containing metabolites in *Arabidopsis thaliana* have been useful in identifying key genetic regulators of sulfur accumulation. Studies combining ionomics, quantitative genetics, and metabolic analyses have revealed that enzymes of the sulfate assimilation pathway play a central role in shaping foliar sulfur levels, while also highlighting the polygenic nature of this trait. Recent work, including that of De Jager et al. (2023), has further linked sulfur content with sulfate uptake, internal sulfate pools, and downstream sulfur metabolites across accessions. Together, these studies demonstrate that variation in sulfur content is tightly connected to sulfur metabolism and transport, providing a strong framework for exploring sulfur-related traits in *Arabidopsis*. However, whether these differences have functional consequences for plant performance under sulfur deficiency is still unclear.

A **B**

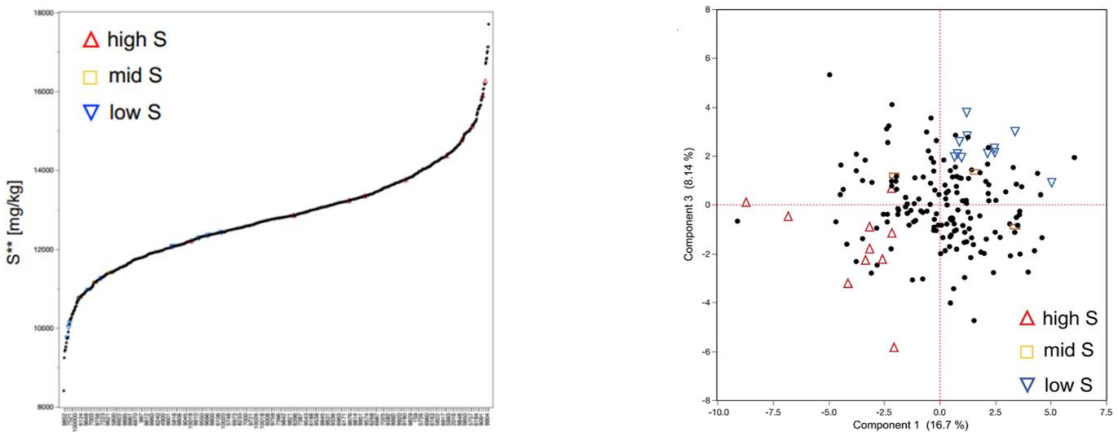

Figure 4: Natural variation in the foliar S-content of *Arabidopsis thaliana* accessions. (A) S content in leaf from Campos et al., 2021 **(B)** Principal component analysis on ionomics of 174 overlapping accessions between the two datasets (Baxter et al., 2007; Campos et al., 2021). Adapted from De Jager et al., 2023.

1.3 Aims of this thesis

Despite several genes, such as *APR2, ATPS1*, and *OASC*, having been identified for controlling foliar S- and sulfate content variation, they can only partially explain this variation, suggesting the presence of additional regulators. While the molecular mechanisms underlying sulfate accumulation in these genes are known, the broader adaptive potential arising from variation in S-content, i.e., the ecological contexts in which sulfur status influences plant performance, remains poorly understood. One reason could be that most of these studies were conducted under controlled laboratory conditions. As a result, the broader adaptive relevance of variation in sulfur content, particularly under soil-based growth conditions where nutrient availability fluctuates, remains insufficiently explored. In particular, it is unclear whether differences in sulfur content represent passive metabolic variation or distinct sulfur-use strategies that affect growth, nutrient homeostasis, and fitness. Based on this, the aims of the thesis are:

1. To assess the relevance of S-content variation on S-homeostasis under varying sulfate concentrations
2. To determine the ecological function by correlating S-related traits and fitness for *A. thaliana*
3. To evaluate transcriptional responses underlying these differences by performing global expression analysis

To address these objectives, *A. thaliana* accessions with natural variation in foliar S content were used to measure metabolic, transcriptional, and developmental traits under varying sulfate concentrations in a sand: soil experimental setup.

2. MATERIAL AND METHODS

2.1 Plant material

We selected accessions based on the previous study from Jager et al. (2024), which used the two ionomics datasets, i.e., Baxter et al. (2007) and Campos et al. (2021) to cluster *A. thaliana* accessions into three groups on the basis of their S-content, i.e., low S, mid S, and high S. Hence, depending on the availability of these accessions in our lab, a panel of 13 accessions was used for the study as mentioned in Table 1, along with their geographical information obtained from https://1001genomes.org/1135/accessions

Table 1. *A. thaliana* accessions used in the study

S. No.	Accession ID	Accession name	Group based on S-content	Latitude	Longitude
1.	5832	App1-16	Low-S	56.3130014	15.9807762
2.	7316	Rhen-1	Low-S	51.9667	5.56667
3.	6203	Tdr-18	Low-S	55.7567793	14.1225226
4.	8311	In-0	Low-S	47.5	11.5
5.	8326	Lis-1	Low-S	56.0089259	14.7427433
6.	6909	Col-0	Mid-S	38.3	-92.3
7.	7206	Kro-0	Mid-S	-	-
8.	6243	Tottarp-2	Mid-S	55.95	13.85
9.	7092	Com-1	High-S	49.416	2.823
10.	8365	Rak-2	High-S	49	16
11.	7098	Di-1	High-S	-	-
12.	7418	Zu-1	High-S	47.3667	8.55
13.	8235	Hod	High-S	48.8	17.1

2.2 Growth conditions

Seeds were surface-sterilized under a sterile hood using 125 ml sodium hypochlorite (NaOCl) and 2.5 ml of 37% (v/v) conc. HCl for 3 hours inside the dessicator. After 3 hours, sterile water was added to the seeds, which were kept at 4°C in darkness for 3 days (Stratification). These seeds were then used for subsequent experiments.

2.2.1 Growth condition: Agar plate system

The sterilized seeds were placed on Modified Long Ashton medium (Table 2) containing 0.8% agarose. The media consisted of either full nutrient (**Control;** 0.75 mM $MgSO_4x7H_2O$) or low sulfur (**Low S**; 0.75 mM $MgCl_2x6H_2O$ and 0.015 mM $MgSO_4x7H_2O$). Plates with seeds were then incubated for 18 days in Sanyo light chambers at 22ºC under long-day conditions (16 h light/8 h darkness; 150 $\mu E*m^{-2}$

*s^{-1}). After 18 days, samples from shoots and roots were collected in 1.5 mL tubes from different plates and immediately frozen in liquid nitrogen.

2.2.2 Growth condition: Hydroponic system

The seeds were placed on sterile polypropylene mesh in 12-well plates, with 1 ml of Modified Long Ashton medium in each well (components identical to those in Tables 2 & 3, except agarose), under similar conditions as in 2.2.1. The plates were then wrapped with aluminum foil and stored in the dark at 4°C for 3 days (stratification). After 3 days, the foil was removed to allow etiolation, and the plates were shifted to the Sanyo light chambers under long-day conditions (as mentioned above) to incubate for two weeks, and the media was changed every week.

2.2.3 Growth condition: Pot system

Seeds were sterilized and stratified as described before and then seeds were transferred to pots with 90% autoclaved sand/soil mixture. Plants were cultivated in a growth chamber to full maturity under long-day photoperiod (16 h light/8 h darkness; 150 µE*m-2 *s-1) with 21°C and 60% humidity. Three sulfate regimes were tested: **Control** (0.75 mM $MgSO_4^{2-}$), **Sulfur-deficient** (0.75 mM $MgCl_2$), and **Short-pulse**, where control (0.75 mM $MgSO_4^{2-}$) was supplied for four hours, and plants were washed with deionized water, and then followed by sulfur-deficient (0.75 mM $MgCl_2$) for the rest of the week. A randomized complete block design with eight biological replicates per genotype was used. Plants were watered with deionized water for the first 2 weeks after sowing, and starting in the third week, respective treatment was applied with Modified Long Ashton medium as mentioned in Table 2 & 3 (everything identical except no agar and sucrose was added). At week 5, two healthy, fully expanded leaves (the 7th and 8th) along with roots were harvested for metabolite analyses, including anions (nitrate, sulfate, phosphate), thiols (cysteine and glutathione), and gene expression studies (qPCR). A second set of plants was grown to maturity for measurement of developmental traits like rosette diameter, flowering time, plant height, number of siliques, and total seed yield per plant. For rosette diameter, plants were pictured every week starting from the 2nd week using a Canon EOS camera.

Table 2. Macroelement composition of used Long Ashton nutrient solution (Hewitt, 1952)

Macroelements	**Concentration**
$Ca(NO_3)_2$ x $4H_2O$	1.5 mM
KNO_3	1 mM
KH_2PO_4	0.75 mM
$MgSO_4$ x 7 H_2O	0.75 mM
Fe-EDTA	0.1 mM

Table 3. Microelement composition of used Long Ashton nutrient solution (Hewitt, 1952)

Microelements	Concentration
$MnCl_2$ x $4H_2O$	10 µM
H_3BO_3	50 µM
$ZnCl_2$	1.75 µM
$CuCl_2$	0.5 µM
Na_2MoO_4	0.8 µM
KI	1 µM
$CoCl_2$ x $6H_2O$	0.1 µM

Table 4. Composition of used Long Ashton Sulfur Limitation nutrient solution (Hewitt, 1952): $MgSO_4$ limitation was complemented by $MgCl_2$

Compound	Concentration (Low-S)
Ca $(NO_3)2$ x $4H_2O$	1.5 mM
KNO_3	1 mM
KH_2PO_4	0.75 mM
$MgSO_4$ x 7 H_2O	0.015 mM*
Fe-EDTA	0.1 mM
$MgCl_2$ x $6H_2O$	0.75 mM
Additives	
Sucrose	5 g/l
MES Hydrate (Sigma Aldrich)	0.8 g/l
Low EEO Agarose	8 g/l

pH adjusted to 5.7; **In case of S-deficient condition for pot system $MgSO_4$ x 7 H_2O was 0mM*

2.3 Metabolite analysis

2.3.1 Anions extraction and quantification

For the measurement of phosphate, nitrate and sulfate anions, frozen tissue material as described in section 2.2.1, around 20 mg was homogenized using a Bead Ruptor 24 3D (Omni International, USA). To this, 1 ml of sterile H_2O was added and shaken for 1 h at 4°C; then heated to 95°C for 15 min. The samples were centrifuged at maximum speed for 15 min at 4°C, and 500 µl of the supernatants was diluted with 500 µl sterile H_2O and transferred to an ion chromatography vial. Standard curves were generated using 0.5 mM, 1 mM, and 2 mM KH_2PO_4, KNO_3, and K_2SO_4. The inorganic anions were measured with the Dionex ICS-1100 chromatography system and separated using a Dionex IonPac AS22

RFIC 43 250 mm analytical column (Thermo Scientific). The running buffer was made up of 4.5 mM $NaCO_3$ and 1.4 mM $NaHCO_3$.

2.3.2 Thiols extraction and quantification

To analyze low molecular weight thiols (cysteine and GSH), approx. 20 mg of homogenized frozen shoot and root material was extracted with 0.1 M HCl at a 1:10 ratio (w/V) and subsequently centrifuged for 10 minutes at maximum speed at 4°C. In the meantime, standards, ranging from 0-100 µM, were prepared using 2 mM L-cysteine and GSH stocks and were also included in subsequent extraction steps. For the analyses, 60 µl of the supernatant was transferred to a new tube and 100 µl 0.25 M CHES-NaOH (pH 9.4) was added. Thereafter, 35 µl of 10 mM dithiothreitol (DTT) was added to reduce the thiols, the tubes were vortexed, and the mixture was incubated for 40 min at room temperature (RT). Five µl of 25 mM monobromobimane was added to the reduced extracts, the samples were vortexed and incubated in darkness for 15 min at RT. The reaction was stopped by adding 110 µl of 100 mM methansulfonic acid and vortexing. After centrifugation at 4°C for 20 min, 200 µl of supernatant was transferred into high-performance liquid chromatography (HPLC) vials. The conjugated thiols were resolved using reverse phase (RP)-HPLC (Eurospher 100-3 C18, 150 x 4 mm; Knauer) and a gradient of 90% [v/v] methanol and 0.25% [v/v] acetic acid, pH 4.1 in 10% [v/v] methanol and 0.25% [v/v] acetic acid, pH 4.1, and detected fluorimetrically with a 474 detector with an excitation wavelength at 380 nm and emission wavelength at 470 nm. The flow rate was constant at 1 mL min^{-1}.

2.3.3 Determination of elemental composition by ICP-MS

The content of total sulfur was analyzed in the leaves and seeds using an inductively coupled plasma mass spectrometry (ICP-MS). The plant material was dried at 60ºC for 48 h, and approximately 25 mg of homogenized samples were digested in metal-free polypropylene centrifuge tubes with 0.5 ml concentrated nitric acid (68%) overnight at room temperature, followed by digestion at 100 ºC for 40 min. After mineralization, the samples were diluted to approximately 5.0 ml with ultra-pure (deionized) water and centrifuged at 4 °C at 2000 g for 30 min. The elemental analysis was performed using an Agilent 7700 ICP-MS (Agilent Technologies, Santa Clara, California, USA) in the standard mode of operation.

2.3.4 Global metabolite analysis by GC-MS

For global metabolite profiling protocol described by Fiehn et al. (2000) was followed, approximately 40 mg of homogenized plant material was extracted in 1.5 ml of a precooled (-20 °C) solvent mixture consisting of H_2O: MeOH: $CHCl_3$ (1:2.5:1, v/v/v). Ribitol/DMPA was added as an internal standard to a final concentration of 5 µM. Samples were vortexed and incubated on a shaker at 4 °C for 6 min, then centrifuged at maximum speed for 5 min. The resulting supernatant was used for metabolite analysis by gas chromatography–mass spectrometry (GC-MS) using a 7200 GC-QTOF system (Agilent, Santa Clara, USA). Measurements were performed at the CEPLAS Plant Metabolism and Metabolomics

Facility, Heinrich-Heine-University Düsseldorf. Metabolite abundances were quantified by normalizing peak areas to the internal standard Ribitol/DMPA.

2.4 Gene expression analysis using qRT-PCR

2.4.1 RNA Isolation

Total RNA was extracted from the roots and shoots using standard phenol/chloroform extraction and LiCl precipitation. For isolation of RNA, samples were collected in 1.5 mL tubes, each containing three glass beads, frozen in liquid nitrogen, and homogenized using Bead Ruptor 24 3D (Omni International, USA). 500 µL of RNA extraction buffer (80 mM Tris/HCL (pH 9.0), 150 mM LiCl, 50 mM EDTA, 5% w/v SDS) was added to each sample before adding 500 µL of phenolchloroform-isoamyl alcohol (Sigma-Aldrich, Germany), samples were shaken for 5 min (RT,100 rpm) and centrifuged for 25 min (RT, maximum speed). The upper aqueous phase was transferred to new tubes containing 500 µL of phenol-chloroform-isoamyl alcohol, vortexed, and centrifuged for 20 min (RT, maximum speed). This step was repeated once more before transferring the upper aqueous phase into fresh tubes and adding 150 µL ($1/3^{rd}$) of 8 M LiCl. Samples were vortexed and kept overnight at -20°C. Samples were defrosted and centrifuged for 30 min (4°C, maximum speed) the next day. The supernatant was discarded, 300 µL of sterile H_2O was added, and the samples were incubated shaking for 10 min (65°C, 500 rpm). 100 µL of 8 M LiCl was added to each sample, and the samples were kept at -20°C overnight. On the third day, samples were defrosted and centrifuged for 30 min (4°C, maximum speed), the supernatant was discarded, 400 µL 70% EtOH was added to wash the pellet, and samples were centrifuged for 10 min (4°C, maximum speed). The supernatant was completely discarded, and pellets were left to dry for 5 min (RT) before addition. Subsequently, 15-25 µL sterile nuclease-free H_2O was added depending on the size of the pellet and incubated for 20 min (65°C, 500 rpm). RNA concentration and purity were determined using the NanoDrop 2000c Spectrophotometer (Thermo Scientific).

2.4.2 Reverse Transcription of isolated RNA

Following RNA extraction, DNase treatment was conducted prior to cDNA synthesis from 600 ng of total RNA using the QuantiTect Reverse Transcription Kit (QIAGEN), strictly adhering to the manufacturer's protocol. The resulting cDNA was subsequently diluted with nuclease-free water to a final volume of 200 µL.

2.4.3 Real-time quantitative polymerase chain-reaction (qPCR)

Quantitative real-time PCR (qPCR) analysis was carried out to assess the expression of target genes utilizing gene-specific primers listed in Table 5, which were ordered from Sigma-Aldrich**.** qPCR reactions were conducted using SYBR green as per the manufacturer's instructions and were performed on a CFX96 Touch Real-Time PCR Detection System (Bio-Rad). All quantifications were normalized to the actin and clathrin genes (Medici et al., 2015) using the $2^{-\Delta Ct}$ method. Each RT-qPCR assay was conducted in technical duplicates across six biological replicates.

Table 5. qPCR Primers used in our study

Gene name	GENE_ID (TAIR)	PRIMER
ACT2/8-F	AT3G18780	GGTAACATTGTGCTCAGRGGTGG
ACT2/8-R		AACGACCTTAATCTTCATGCTGC
CLA_F	AT2G40060	AGCATACACTGCGTGCAAAG
CLA_R		TCGCCTGTCACATATCTC
SULTR2;1_F	AT5G10180	CACAAGCTGAATCAAGCAAAGTTCG
SULTR2;1_R		CAATAACCCGTAACACAACTGGTC
BCA3_QF	AT1G23730	TGTCCTTGGGGAATCTTTTG
BCA3_QR		CAAAGGCAGGGGTAGTCTTG
PYD4_QF	AT3G08860	CCTCACAAACAGCAGCTCAG
PYD4_QR		GGGGCTGAGGAACTCTCG
LSU3_QF1	AT3G49570	GGAACGGAGAGTTGGAGAGA
LSU3_QR1		GCGCCTGATCTAAAGACTCG
SULTR1;2_F	AT1G78000	GATCAGCCTAAGTCTAAGCAGT
SULTR1;2_R		AAAGTGTAGTTACGTCCCCAAT
SBP1_QF1	AT4G14030	CATGGAGAAAGGCTCACACA
SBP1_QR1		AGGACCGTCTGGTTCATCAC
SAT3;1_F	AT1G55920	AAAAGACGTTCCTTCGCATAGT
SAT3;1_R		GGGTCTTGCTCTTCCATGAC
SAT3;2_F	AT4G35640	AGGATGTTCCTTCGCATAGC
SAT3;2_R		GCATCATGCTCCATTGTCAT
GGCT2;2_QF1	AT4G31290	ACACCGGTGAAGGAATCAAG
GGCT2;2_QR1		GGCAACAGCTTCTGGATGAT
OASTL-A _F	AT4G14880	GAACAGAACGCAAACGTCAA
OASTL-A_R		TCTTGTGAGGACCTGGCTTC
SHM7_F	AT1G36732	CAGGCATCTCATACTGCAAAGC
SHM7_R		CAATGACAACCCGAGGCTGT
MSRB5_F	AT4G04830	TGAGATCACTTGTGCTGCGT
MSRB5_R		AGAGGAAGATTTTGCCGGGT
APR2-L	AT1G62180	AAAAGAGCTCCAAGGGCTAT
APR2-R		CGACATGAGTGAATCAACATCTC
APR3-L	AT4G21990	CCAATCAAGTATCCATCAGAGAAG
APR3-R		CCGAACAAGATTCAAGAAAGATG
SDI1-L	AT5G48850	TCCCTGTGGAGACACTCCTT
SDI1-R		CCATCTCCGGGTTCTTCTCT

SDI2_F	AT1G04770	GTCCTTATGTCCGAGCGAAG
SDI2_F		TCTCGCTTTAATCGCTATCCA
LSU1_F	AT3G49580	GAGGCGGAAGAGCAACTCTG
LSU1_R		CCATGAGGAAGAGCATGCGA
LSU2_F	AT5G24660	ACGAGCTACGACGGAAGAAC
LSU2_R		GGCAGAGGCAGAGTCTGAAG
SAT2;1_F	AT1G55920	CACTGTTGGATCAGAAGCAT
SAT2;1_R		AACCAGTGTTTGATCCAGTCG
SAT2;2_F	AT3G13110	GGGAAGCTCAAGCCGAACAGTATC
SAT2;2_R		GGCCTCTCGTTTCAGGATCAAGA
SiR_F	AT5G04590	TCATTCTGTTTTCTTAGGAAGATATGG
SiR_R		GTCTCAGGCTTCGCAGGA
NIA1_F	AT1G77760	AAGCCGTACACATTAAAAGGCTA
NIA1_R		TCACCTCAACCCTCGTTACC
NIA2_F	AT1G37130	CTTTGGTAGACGCCGAACTC
NIA2_R		TTTAGCTCGTTGATTATGTACTCTGG
NiR1_F	AT2G15620	AGCGATTCCTCTTGATGC
NiR1_R		GTTCGTCGATAAGCCACA
HRS1_F	AT1G13300	TTCTTCTACCCGTAATCATTACGTC
HRS1_R		TACACTCTTTAATCCCGGCAT
NRT1;1_F	AT1G12110	GCACATTGGCATTAGGCTTT
NRT1;1_R		CTCAATCCCCACCTCAGCTA
GSH1_F	AT4G23100	ACATCGACTGTACTGGAATGACA
GSH1_R		CCAGGGAGACAGGGAAGTTT
GSH2_F	AT5G27380	CCAGGTGTTCTCGAGAGGTT
GSH2_R		CTCCAAAGCCCAGCAAAG

2.5 RNA-Sequencing

2.5.1 RNA Extraction

Total RNA was isolated with PureLink™ Plant RNA Reagent (Invitrogen, Thermo Scientific™, Waltham, Massachusetts, USA), using the small-scale isolation procedure recommended by the supplier, with minor modifications. Approximately 50 mg of shoot or root tissue samples were cryogenic-pulverized and kept frozen in liquid nitrogen before extraction. Each sample was resuspended by brief vortexing with 0.5 ml of pre-cold (4 °C) PureLink™ Plant RNA Reagent and incubated at room temperature for 5 min in a vertical rotating shaker. After centrifugation at 12,700 rpm for 2 min at room temperature, the supernatant was transferred to a new RNase-free microtube containing 0.1 ml of 5 M

NaCl, and 0.3 ml of 24:1 (v/v) chloroform-isoamyl alcohol was added, thoroughly mixed, and centrifuged at 12700 rpm for 10 min at 4 °C. The aqueous phase was recovered into a new microtube with an equal volume of 4 M LiCl-isopropyl alcohol (3:1 v/v) and incubated overnight at -20 °C. On the following day, the mixture was centrifuged at 12,700 rpm for 30 min at 4 °C, and the supernatant was decanted and replaced with 1.0 ml of 75% ethanol. Finally, the solution was centrifuged at 12,700 rpm for 5 min at room temperature, the supernatant was completely discarded, and the microtubes were left open in the fume hood for 5 min to air-dry. The isolated RNA was resuspended in 20 µl RNase-free water, and concentration was estimated spectrophotometrically using a nanodrop (NanoDrop™ 2000c Spectrophotometer, Thermo Scientific).

For RNA sequencing the RNA samples were further purified with TURBO DNA-free™ Kit (Invitrogen, Thermo Scientific), in an adapted version of the routine DNAse treatment specified by the manufacturer. In a 0.5 ml microtube, a total amount of 2 µg of RNA was resuspended in 20 µl RNase-free water and gently mixed with 2.1 µl 10X TURBO DNase™ Buffer and 1.5 µl of TURBO DNase™ Enzyme. The reaction was incubated at 37 °C, and after 30 min the enzyme activity was stopped by the addition of 4.5 µl DNase Inactivation Reagent, followed by vortexing, and incubation for 5 min at room temperature. The suspension was centrifuged at 12,700 rpm for 1.5 min at room temperature, and the supernatant containing the treated RNA was transferred to a new RNase-free microtube.

2.5.2 RNA-Sequencing by Novogene

Quality control of RNA samples was performed before sequencing using the Bioanalyzer system (2100 Bioanalyzer Instrument, Agilent Technologies, Santa Clara, California, USA), and the RNA 6000 Nano Kit (Agilent Technologies, Santa Clara, California, USA), adopting a RIN cutoff value of at least 7 (2 µg; 50–200 ng/µl; OD260/280 = 1.8–2.1; OD260/230 > 1.5). The library preparation and RNA sequencing were performed by Novogene (Novogene Co., Ltd., Cambridge, UK). After the quality control procedures, a non-strand-specific RNA library construction was carried out using poly-T mRNA enrichment. The resulting mRNA was randomly fragmented and used for the first cDNA synthesis via random hexamer priming, after which the second-strand synthesis was accomplished based on Illumina specifications, with the addition of the buffer containing dNTPs, RNase H, and DNA polymerase I (Novogene Co., Ltd., Cambridge, UK). End repair and dA-tailing were performed prior to the ligation of adapter sequences. After insert size selection and PCR amplification, the ready library was fluorometrically quantified with Qubit™ (Thermo Scientific™, Waltham, Massachusetts, USA) as well as by RT-qPCR, and re-assessed with the Bioanalyzer system for size distribution. Libraries were sequenced using Illumina NovaSeq™ 6000 Sequencing System (Illumina, Inc., San Diego, California, USA), to produce paired-end 150 bp reads and coverage of 30-40 Million reads per sample.

2.5.3 RNA-Seq: Data Processing and analysis

Output data containing the paired-end sequence data of each sample (duplicate files) and their corresponding associated FastQC quality reports were stored as FastQ (fq.gz) files. Additionally, a

quality control step was performed using MultiQC version 1.11 (Ewels et al., 2016) to check the raw data from sequenced libraries, including the total number of sequences and estimate duplicated sequence counts. When necessary, residual rRNA sequences were filtered out with SortMeRNA version 4.3.4 (Kopylova et al., 2012), and then Trimmomatic version 0.39 (Bolger et al., 2014) was used to remove the adapters employed in the sequencing. Low-quality sequences were trimmed using the 'maxinfo' method with a target length of 125 bp, and subsequently, MultiQC was used for a second quality control, and processability of over 90% was confirmed for all samples. HISAT2 version 2.1.0 (Kim et al., 2019) was used to align the sequenced fragments against the reference genome datasets *Arabidopsis* reference transcriptome (ftp://ftp.arabidopsis.org/home/tair/Genes/TAIR10_genome_release/TAIR10_gene_lists/) as transcripts per kilobase million. Read summarization was performed with featureCounts version 2.0.0 (Liao O et al., 2014) and the resulting count matrix was used for downstream analysis. The stringent differential expression analysis was performed with DESeq2 (Love et al., 2014) and limma (Ritchie et al., 2015). Here, we used log2 fold change > 1.0 or log2 fold change < -1.0, adjusted P-value < 0.05 cut off to obtain the DEGs, and then used the intersect of both analyses. Z-score was computed on a gene-by-gene basis by subtracting the mean and then dividing by the standard deviation. For functional gene ontology Gene Ontology (GO) enrichment analysis was performed using the PANTHER overrepresentation test (http://pantherdb.org) with the *Arabidopsis thaliana* genome as background. Significant GO biological process categories were identified using Fisher's Exact Test with Bonferroni correction ($P < 0.05$). For visualization, the significantly enriched terms were plotted as bubble plots using clusterprofiler package in R. The bubble size represents the number of genes in each category, and color scale corresponds to –log10(P value), indicating the significance of enrichment. Variance-stabilized counts from DESeq2 were scaled per gene (Z-score), and hierarchical clustering was performed using Euclidean distance and complete linkage. Heatmaps were generated with the pheatmap package in R.

2.6 Measurement of Sulfate uptake and flux

Sulfate uptake was assessed in *Arabidopsis* seedlings cultivated for 14 days in 12-well plates as described in section 2.2.2. For uptake assays, the growth medium was replaced with 1 mL of the modified Long-Ashton solution containing 0.2 mM sulfate and supplemented with 12 µCi of [^35S] sulfuric acid. Seedlings were incubated for 3 hours under light conditions. Following incubation, seedlings retained on the mesh support were thoroughly rinsed, blotted dry, and separated into root and shoot tissues. Tissues were individually weighed and snap-frozen in liquid nitrogen for subsequent analysis conducted on the same day. Metabolites were extracted in a 10-fold volume of 0.1 M HCl, from which 10 µL of the extract was used to determine S-uptake, and 50 ul of extract was used to measure incorporation of ^{35}S into thiols as described in Dietzen et al., 2020.

2.7 Detection of Hydrogen peroxide (H_2O_2) using DAB staining

Hydrogen peroxide (in situ) was detected via DAB (3,3′-Diaminobenzidine) staining (Sigma-Aldrich), using a modified protocol based on Daudi et al. (2012). 18-day-old *A. thaliana* shoots were grown under control (0.75 mM) and low sulfur (0.015 mM) conditions as mentioned above. These were then dipped in 5 ml of DAB solution (1 mg/mL) containing 0.05% (v/v) Tween20 along with 10 mM sodium phosphate buffer used as a control. This was followed by gentle vacuum infiltration for 5 min using dessicator. With the DAB reaction, the reaction was allowed to proceed for 4 hours at 100 rpm, after which the shoots were fixed in 3.5 ml bleaching solution (ethanol: glycerol: acetic acid, 3:1:1) by incubation at 95°C for 15 minutes in a water bath. Leaves were then incubated in fresh bleaching solution until complete chlorophyll removal. Subsequently pictures of DAB stained seedlings were acquired using a Leica DMRA microscope (Leica Microsystems) equipped with DISKUS software (Carl H. Hilgers-Technisches Büro).

2.8 Detection of Superoxide (O_2^-) using NBT Staining

NBT (Nitro Blue Tetrazolium) staining protocol by Kumar et al., 2014 was used where 18 days old *A. thaliana* seedlings grown under control (0.75 mM) and low sulfur (0.015 mM) conditions as mentioned above in section 2.2.2, were harvested and immersed in 3 ml of 0.2 % NBT staining solution prepared by dissolving 0.1 g NBT into 50 mM sodium phosphate buffer (pH 7.5). Subsequently, 35-day-old leaves from the pot system were used and dipped in the same solution. The well plates with the immersed seedlings were then wrapped with foil and kept overnight at room temperature. The next day, the staining solution was drained off, and chlorophyll was removed from the seedlings by dipping them completely in absolute ethanol and heating them in a boiling water bath for 10 minutes. These seedlings were then transferred to a paper towel saturated with 60% glycerol and were ready for photography. Pictures of NBT-stained seedlings were acquired using a Leica DMRA microscope (Leica Microsystems) equipped with DISKUS software (Carl H. Hilgers-Technisches Büro). The presence of superoxide can be confirmed using dark blue stains.

2.9 Statistical analysis

Data from metabolites and qPCR were curated, processed, and filtered in Microsoft Excel (Microsoft Office package). This processed data was then used to generate a figure using JMP software (https://www.jmp.com/en/home). To assess significant differences, a mixed model was used, in which LSMeans (Least Squares Means) were calculated for each accession/genotype, followed by a post-hoc test. In addition, for the mixed model, we kept accessions nested within groups as a random effect, as we were interested in the behavior of the three groups for most traits. Experimental values represent mean values and SE; n represents the number of independent samples with 8 replicates per accession if not specified otherwise. Heatmaps and correlation plots were created in RStudio.

3. RESULTS - Chapter 1: Ecological function of S-content variation in *Arabidopsis thaliana*

3.1 Foliar sulfur reserves and sulfate pools are strongly compromised in the high-S group under S-deficiency

Based on two independent ionomics datasets (Baxter et al., 2007; Campos et al., 2021), which reported large natural variation in elemental composition among *Arabidopsis thaliana* accessions, including leaf sulfur (S) content, we identified 175 overlapping accessions that showed significant differences in total foliar S. To further characterize this variation, Principal Component Analysis (PCA) was performed as described in Jager et al. (2023), focusing on elements contributing most strongly to the variation. The first and third principal components (PCs) together explained around 33% of the total variance, with S-content contributing most prominently to these components. Plotting these PCs against each other allowed us to classify the accessions into three distinct groups differing in their inherent leaf sulfur accumulation capacity: low-S, mid-S, and high-S accessions (Jager et al., 2023) (Fig. 4).

From these groups, a panel of 13 representative accessions with a gradient of S content was selected based on availability and previous characterization. Although the molecular mechanisms responsible for altered sulfate accumulation in certain accessions are known, where loci such as *APR2 and ATPS1* are responsible for this accumulation (Loudet et al., 2007; Koprivova et al., 2014). However, the extent to which natural variation in S-content influences plant performance under conditions of fluctuating environmental S supply remains largely unexplored. Our earlier work revealed a strong connection between total foliar S-content and the abundance of distinct S-containing metabolites under normal S-supply (Jager et al., 2023). However, how this inherent variation in S accumulation capacity impacts responses to sulfur deficiency and fluctuating S availability in soil has not yet been addressed.

To investigate this, we grew the selected accessions in a 90% sand: 10% soil mixture under three different S-regimes**: Control,** with optimal sulfate concentration (750 µM), **Sulfur-deficient (S-def)** (0µM), with no external sulfate supply, and **Short-pulse (SP)** treatment, in which sulfate was provided intermittently for a short period (4 hours) each week followed by no sulfate (S-def) for the rest of the week. Plants were fertilized twice weekly with the respective nutrient solutions, and leaves were harvested at the 5th week for biochemical analysis.

As expected, the high-S group showed significantly higher levels of total sulfur compared to the low-S group under control conditions, which were quite consistent with our previous findings in Jager et al. (2023) (Fig. 5A). A similar and even clearer trend was observed for shoot sulfate content, where high-S accessions accumulated substantially more sulfate than both mid-S and low-S groups (Fig. 5B). However, under S-deficiency, sulfate levels followed an opposite trend compared to normal S-supply. Although the sulfate levels were markedly reduced in all groups, the relative decline was most pronounced in the high-S group under S-deficiency. Interestingly, although low-S accessions displayed

early signs of S-depletion, as shoot sulfate dropped significantly under S-def conditions already at the 4th week (Supplementary Fig. 1), by the 5th week, it was the high-S group that exhibited the most dramatic response. We observed an approximately 40% reduction in shoot sulfate and a nearly 50% decrease in total foliar S content compared to their respective control values (Figs. 5A, 5B).

In contrast, for roots, there were no significant genotypic differences in sulfate levels under control conditions. Nevertheless, the impact of S-deficiency was much stronger in roots, where sulfate content declined drastically across all three groups, indicating prioritization of sulfur allocation to shoots under S-deficiency (Fig. 5C). Another interesting pattern emerged under the short-pulse (SP) treatment. In the low-S group, sulfate levels for both roots and shoots could be restored to near-control values, indicating an efficient mechanism to rapidly take up and retain sulfate even with limited temporal availability. In contrast, both mid-S and high-S groups failed to recover their sulfate pools under the same conditions, suggesting that accessions with higher baseline S content are less flexible in coping not only with S-deficient conditions but also with fluctuating S-supply (Fig. 5B & C).

In addition, to compare sulfur partitioning between inorganic sulfate and organic sulfur pools, we calculated the ratio of organic S to inorganic S for each accession (Fig. 5D). Under control conditions, low-S accessions displayed the highest organic/inorganic S ratios, indicating a greater investment in sulfur assimilation and a comparatively smaller sulfate storage pool (Fig. 5D). In contrast, high-S accessions and mid-S accessions exhibited the lowest ratios, consistent with their elevated sulfate levels. However, under S-deficiency these differences were much more pronounced. We observed that low-S accessions showed a pronounced increase in the organic/inorganic ratio by almost 26-fold, reflecting strong conservation of organic S despite experiencing decline in sulfate levels (Fig. 5D). While mid-S accessions showed rather greater variability in group with Col-0 showing much higher ratio under S-deficiency indicating stronger decline in sulfate pool (inorganic pool) with organic S pool rather conserved. High-S accessions showed stable ratios even under S-limitation, indicating their reduced capacity to maintain organic sulfur pools under S-deficiency (Fig. 5D).

Taken together, these results highlight distinct adaptive strategies among the three groups. The low-S group possesses a more robust and metabolically flexible sulfur assimilation strategy, followed by the mid-S group, which shows intermediate behavior. The high-S accessions, despite their naturally high sulfate reserves under control conditions, show the strongest depletion and least recovery capacity under deficiency. This indicates that their high-S phenotype relies predominantly on sulfate storage and lacks the metabolic plasticity needed to buffer against depletion.

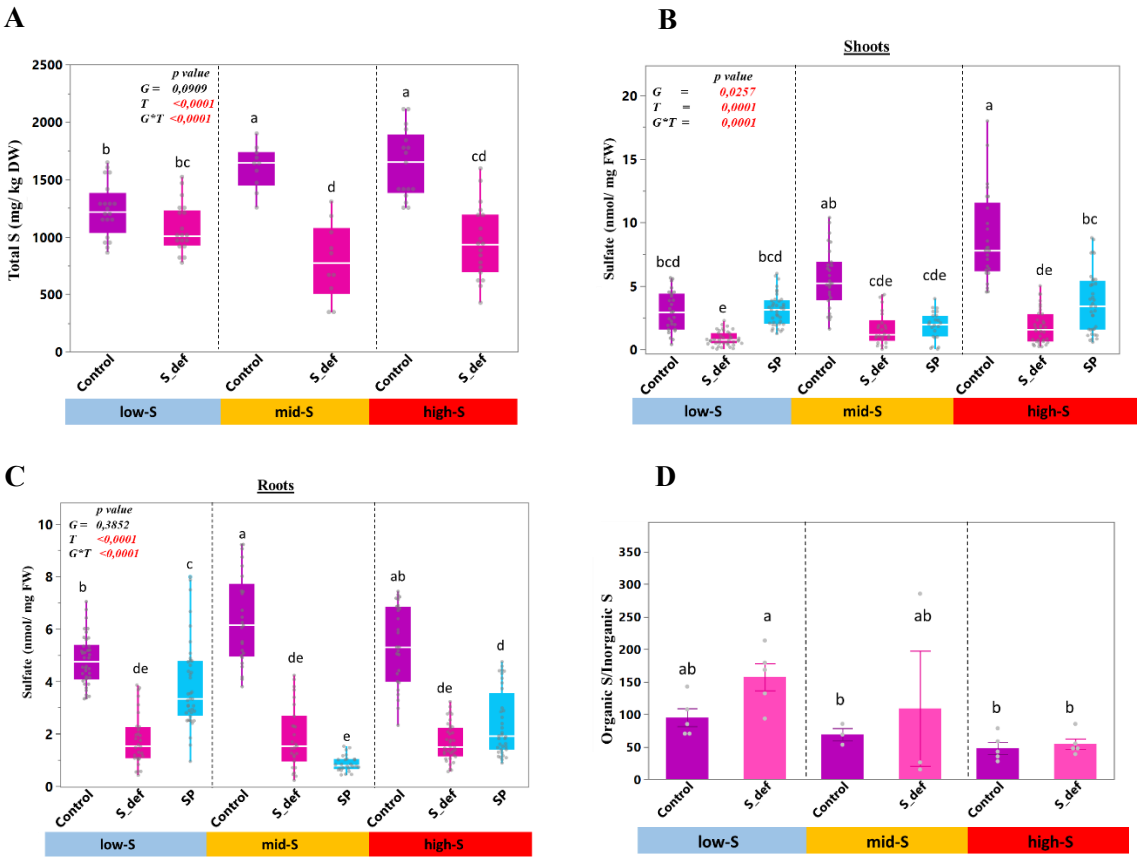

Figure 5: Sulfur deficiency reduces foliar sulfate and total sulfur, with strongest effects in high-S accessions (A) Total foliar sulfur (mg kg^{-1} DW) , **(B)** Shoot sulfate (nmol mg^{-1} FW), and **(C)** Root sulfate (nmol mg^{-1} FW) in low-S (blue), mid-S (orange), and high-S (red) accessions grown under control (750 µM sulfate), sulfur-deficient (0 µM), or short-pulse (SP; intermittent supply) conditions **(D)** Ratio of Organic S/ Inorganic S in low-S (blue), mid-S (orange), and high-S (red) accessions grown under control (750 µM sulfate), sulfur-deficient (0 µM). Plants were grown in a 9:1 sand: soil mix and fertilized twice weekly with the indicated S regimes. At week 5, the 7th–8th leaves and roots (split longitudinally) were harvested (n = 8 per accession). Data were analyzed using mixed models followed by Tukey's HSD; different letters indicate significant differences ($P < 0.05$). Boxplots show means ± SE.

Sulfur deficiency leads to extensive transcriptional reprogramming, including the upregulation of sulfate transporters and a suite of genes collectively referred to as sulfur starvation marker genes (Dietzen et al., 2020; Maruyama-Nakashita et al., 2006). Therefore, to corroborate the sulfate and total sulfur phenotypes observed across the three groups, we next evaluated the relative expression of key S-marker genes, namely *SDI1* (Sulfur Deficiency-Induced 1), *SDI2* (Sulfur Deficiency-Induced 2), *SHM7* (Serine Hydroxymethyl Transferase 7), *APR2* (Adenosine-5′-phosphosulfate reductase), *LSU2* (Low Sulfur Upregulated 2), *LSU1* (Low Sulfur Upregulated 1), and the sulfate transporters *SULTR1;1 (STR1;1)* and *SULTR1;2 (STR1;2)*. As roots are generally considered the primary site of sulfate perception and uptake

and appeared more responsive at the metabolic level under S-deficiency, we performed qPCR analysis in roots of six accessions, selecting two accessions from each group as representatives. However, because *SDI1* is known to be robustly induced by sulfur starvation in both shoots and roots, its expression was assessed in both tissues.

Consistent with its role as a canonical sulfur starvation marker, transcript levels of *SDI1* were significantly induced under S-deficiency in both shoots and roots of almost all accessions. The only notable exception was Kro-0, which showed higher relative expression in roots, albeit not significantly, while displaying no difference in relative expression of *SDI1* in shoots (Fig. 6B). Importantly, in line with the stronger relative decline in shoot sulfate content observed in high-S accessions, *SDI1* expression in shoots was significantly higher in these accessions under S-deficiency along with Col-0, indicating a more pronounced sulfur starvation response at the transcriptional level (Fig. 6B). A similar trend was observed for *SDI2*, another well-established marker of sulfur limitation. *SDI2* expression increased significantly under sulfur deficiency in multiple accessions, with the strongest induction observed in both high-S accessions i.e. Hod and Zu-1, followed by In-0 while levels remained unchanged in other genotypes (Fig. 6B).

Genes involved in sulfur metabolism and sulfur starvation signaling exhibited clear accession-specific transcriptional responses under sulfur deficiency. *APR2,* a key enzyme in the assimilatory sulfate reduction pathway, showed significant induction under S-deficiency, particularly in the high-S accessions Zu-1 and Hod, suggesting activation of sulfate reduction in response to declining sulfate availability in these genotypes (Fig. 6B). Similarly, members of the LSU gene family, which are well-established markers of sulfur-deficiency signaling, also exhibited differential induction patterns. *LSU1* was significantly upregulated in In-0 and Zu-1 under S-deficiency, whereas *LSU2* showed stronger induction in Zu-1 and Col-0, indicating considerable genotype-specific variation in sulfur starvation signaling (Fig. 6B). The gene *SHM7*, which is linked to sulfur metabolism, also responded to sulfur limitation in an accession-dependent manner. Significant upregulation of *SHM7* was observed only in In-0 and Zu-1, suggesting that activation of this pathway is restricted to specific genotypes (Fig. 6B). Expression of sulfate transporters further supported the presence of genotype-specific responses to sulfur limitation. The high-affinity sulfate transporter *SULTR1;2* showed significant increased expression in In-0 and Col-0, followed by both high-S accessions In-0 and Zu-1. In contrast, *SULTR1;1* exhibited significant upregulation only in Zu-1 and In-0 under S-deficiency (Fig. 6B).

Taken together, these results reveal substantial variation in transcriptional responses to sulfur deficiency among the accessions. Both high-S accessions showed strong induction of sulfur starvation marker genes, with Zu-1 responding to nearly all genes tested, consistent with the pronounced decline in shoot sulfate content observed under sulfur limitation. In contrast, low- and mid-S accessions exhibited more moderate or gene-specific transcriptional adjustments, suggesting that different genotypes employ distinct regulatory strategies to maintain sulfur homeostasis under limiting conditions.

A

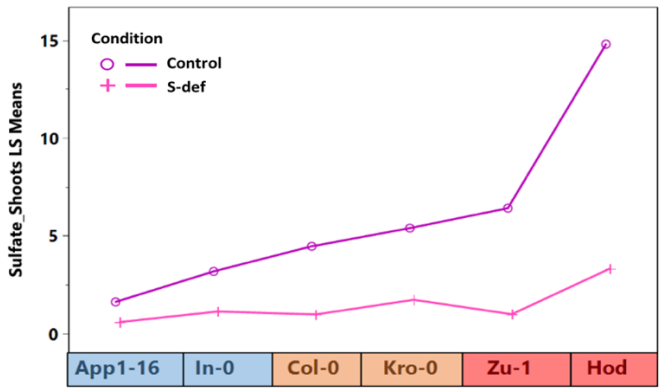

B

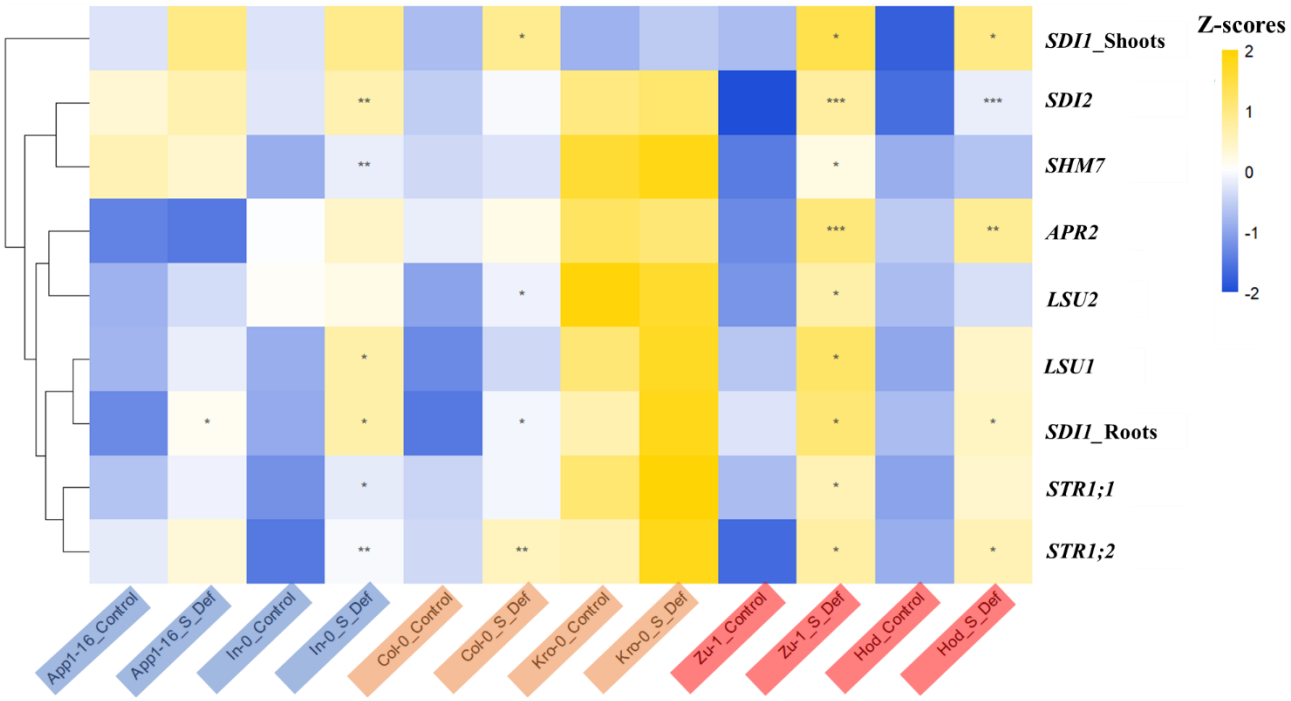

Figure 6: Relative expression of sulfur marker genes in *A. thaliana* accessions. (A) Least Square Means (LSMeans) of sulfate concentration in shoots of *A. thaliana* accessions. i.e. App1-16 (low-S), In-0 (low-S), Col-0 (mid-S), Kro-0 (mid-S), Zu-1 (high-S) and Hod (high-S) under control and S-def conditions. **(B)** Heatmap representing relative expression of S-marker genes using the $2^{-\Delta Ct}$ method and row-scaled to generate Z-scores for visualization in heatmaps under Control and S-def (S_Def) conditions. Statistical analysis was performed using two-way ANOVA followed by Tukey's post hoc test for multiple comparisons for treatment and genotype. Asterisks indicate significant differences (* $p < 0.05$, ** $p < 0.01$, *** $p < 0.001$) between the genotypes and the treatments (n=6).

3.2 Enhanced sulfate uptake and transport in low-S group during S-deficiency

Plants acquire sulfur primarily in the form of sulfate through the roots, and one of the earliest responses to sulfur limitation is an increase in sulfate uptake capacity, which is generally achieved through the induction of high-affinity sulfate transporters (Dietzen et al., 2020). In our previous study, we reported that sulfate levels under control conditions showed a positive correlation with S-uptake capacity among these accessions (Jager et al., 2023), suggesting that inherent differences in foliar sulfate accumulation are linked to differences in uptake. To determine whether this relationship persists under sulfur-deficient conditions, we grew representative accessions from each group for 14 days under either control or S-deficient conditions and quantified root sulfate uptake using [^{35}S] labeling.

Consistent with our earlier findings, we observed a significant positive correlation between foliar sulfate content and S-uptake across all accessions under control condition (Fig. 7B). This indicates that genotypes with higher steady-state sulfate levels indeed maintain higher uptake activity, under optimal supply. As expected for a typical S-deficiency response, all three groups showed an overall increase in sulfate uptake, however we observed no correlation of S-uptake and foliar sulfate content under S-def condition (Fig. 7A & B). Among the groups, high-S accessions displayed the highest absolute S-uptake rates under deficiency which is consistent with their higher sulfate accumulation capacity under non-limiting conditions (Fig. 7A).

In addition, when analyzing the relative change rather than absolute uptake rates, clear differences emerged among the groups. Low-S accessions exhibited the strongest plasticity in response to S-deficiency, with uptake increasing by approximately 27-fold compared to their control levels (Fig. 7C). Moreover, this increase in uptake was accompanied by a substantial enhancement in root-to-shoot translocation, which increased by around 37-fold (Fig. 7C). This coordinated adjustment suggests that low-S accessions actively reinforce both S-acquisition and its delivery to the shoot under limiting conditions. Such a strategy likely contributes to their ability to maintain sulfate pools and preserve foliar total sulfur levels even when external S supply is withdrawn.

In contrast, although high-S accessions showed the highest absolute uptake rates, their relative increase in uptake under S-deficiency was significantly smaller compared to the low-S group. A similar pattern was observed for translocation, where the fold change in high-S accessions was lower than that of low-S accessions. This more modest induction suggests that high-S accessions, while capable of high uptake under sufficient S, do not proportionally adjust their uptake and translocation machinery to the same extent under deficiency. These patterns are consistent with the stronger depletion of sulfate and total foliar sulfur observed in the high-S group under S-deficient conditions (Fig. 5). Together, this indicates that the high-S phenotype appears to rely on maintaining high sulfate acquisition under ample supply, but lacks the compensatory enhancement in uptake and transport that would support efficient conservation or redistribution during deficiency. Thus, their higher absolute uptake likely reflects a higher intrinsic demand rather than an adaptive strategy to cope with S limitation.

Overall, these results highlight a clear distinction in how the three groups respond to S-deficiency at the level of sulfate acquisition and movement within the plant. Low-S accessions rely on a more responsive and flexible uptake-translocation system, enabling them to stabilize foliar S more effectively, whereas high-S accessions maintain high constitutive uptake but show limited plasticity when sulfate becomes limiting. Mid-S accessions display intermediate behavior for both parameters. Also, the positive correlation between foliar sulfate content and sulfate uptake under control conditions indicates that the differences in steady-state sulfate levels among the accessions are at least partly driven by variation in their sulfate uptake capacity. However, the weakening or loss of this correlation under S-deficient conditions suggests that additional mechanisms contribute to sulfate accumulation when external supply is limited. This implies that under S-deficiency, factors beyond uptake alone, such as changes in internal redistribution, storage, or differential regulation of transport processes, may play a role in determining foliar sulfate levels.

A

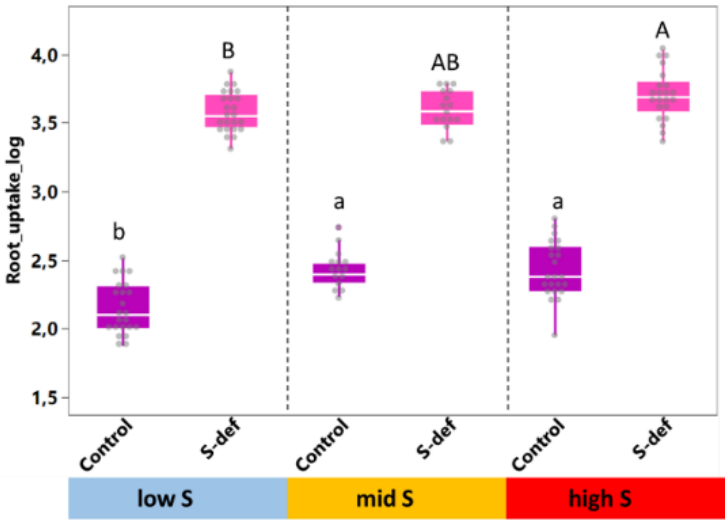

B

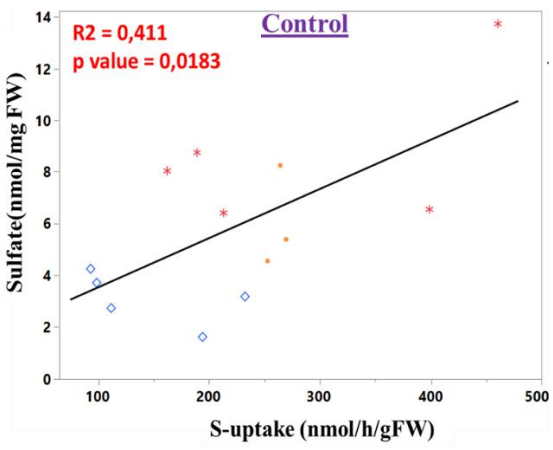

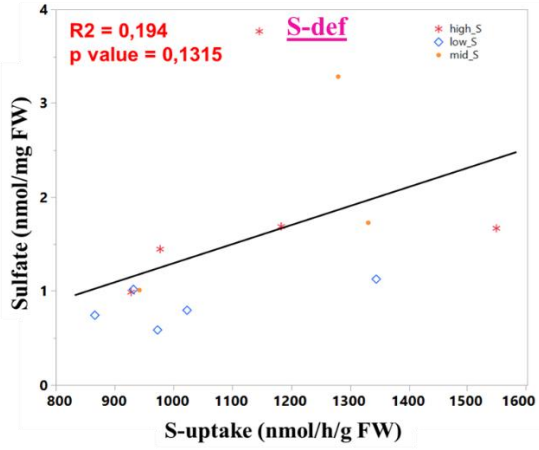

C

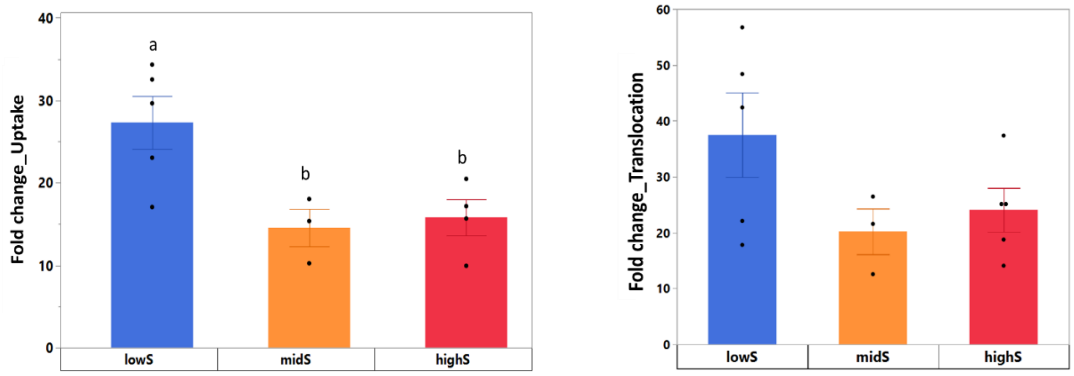

Figure 7: S-deficiency triggers stronger sulfate uptake and allocation to shoots in low-S accessions **(A)** Sulfate uptake in roots (nmol h^{-1} g^{-1} FW) **(B)** Regression analysis of Sulfate content vs S-uptake under Control and S-def conditions **(C)** Fold change uptake ($Uptake_{S\text{-}def} - Uptake_{control}$/ $Uptake_{control}$) and Root-shoot fold change translocation ($Translocation_{S\text{-}def} - Translocation_{control}$/ $Translocation_{control}$) with translocation unit measured as (nmol h^{-1} g^{-1} FW). *Arabidopsis* plants (25 seedlings) fed with either 750 µM SO_4^{2-} (Control) or 15 µM SO_4^{2-} (S-def) were grown on a nylon net in hydroculture for 14 d and, after incubation with [^{35}S] sulfate for 3 hours, shoots and roots were harvested separately and extracted with 0.1 M HCl for radioactivity quantification. Data were analyzed using mixed models followed by Tukey's HSD; different letters indicate significant differences ($P < 0.05$). Boxplots and bar plots show means ± SE (n= 6 per accession).

3.3 Reduced sulfur (thiols) pools and redox balance are differentially compromised under sulfur deficiency

Cysteine (Cys) is the first organic compound containing reduced sulfur and represents a central metabolic hub connecting three major primary metabolic pathways, namely carbon, nitrogen, and sulfate assimilation (Takahashi et al., 2011; Jobe et al., 2019). Glutathione (GSH), derived from cysteine, functions as a major storage form of reduced sulfur (Kuzuhara et al., 2000; Leustek et al., 2000). In addition, GSH is a key component of the cellular antioxidant network and is widely regarded as a major determinant of cellular redox homeostasis, thereby indirectly influencing numerous fundamental cellular processes (Ball et al., 2004). Given these central roles, we quantified both thiols in shoots and roots of the three accession groups under control, sulfur-deficient, and short sulfur pulse (SP) conditions.

As expected, in shoots, both Cys and GSH contents were significantly reduced across all groups under sulfur deficiency (Fig. 8A, C). Notably, low-S accessions accumulated significantly higher shoot Cys under control conditions (Fig. 8A), but also displayed the strongest relative reduction upon sulfur withdrawal. Under deficiency, shoot Cys levels in the low-S group declined by approximately 57-fold, corresponding to an almost three-fold decrease relative to control (Fig. 8A). In contrast, mid-S and high-S accessions exhibited more moderate reductions in shoot Cys. Importantly, Cys levels were restored in all three groups under SP treatment, with the mid-S group showing the most pronounced recovery (Fig. 8A).

A contrasting pattern was observed for shoot GSH. High-S accessions accumulated the highest GSH levels under control conditions (Fig. 8C), in agreement with previous observations (Jager et al., 2023). However, these accessions also experienced the most severe relative depletion under sulfur deficiency, with shoot GSH levels decreasing nearly three-fold. By comparison, low-S and mid-S groups exhibited smaller relative reductions in shoot GSH. Similar to cysteine, SP treatment largely restored shoot GSH levels toward control values across all groups (Fig. 8C).

In roots, thiol accumulation followed a distinct pattern compared to shoots (Fig. 8B, D). Root Cys levels showed no consistent or significant trend across the three groups under any of the treatments (Fig. 8B), indicating a relatively stable cysteine pool in roots irrespective of sulfur supply. In contrast, root GSH levels responded more dynamically: both low-S and high-S groups exhibited significant reductions in GSH under sulfur deficiency, whereas the mid-S group maintained root GSH more effectively (Fig. 8D). Following SP treatment, root GSH levels increased across all groups; however, recovery remained incomplete in low-S roots.

Taken together, these results reveal distinct thiol adjustment strategies among the three groups under sulfur limitation. Low-S accessions preferentially accumulated shoot cysteine under sulfur-sufficient conditions, but this pool was particularly sensitive to sulfur deprivation, although partial recovery was possible under intermittent sulfur supply. In contrast, high-S accessions stored larger glutathione reserves under control conditions, yet these reserves collapsed most strongly under sulfur deficiency, suggesting a heavy reliance on GSH buffering that becomes unsustainable when sulfur supply is limited. Mid-S accessions exhibited smaller and more moderate changes in both cysteine and glutathione pools, consistent with their overall intermediate and less dynamic responses to fluctuating sulfur availability.

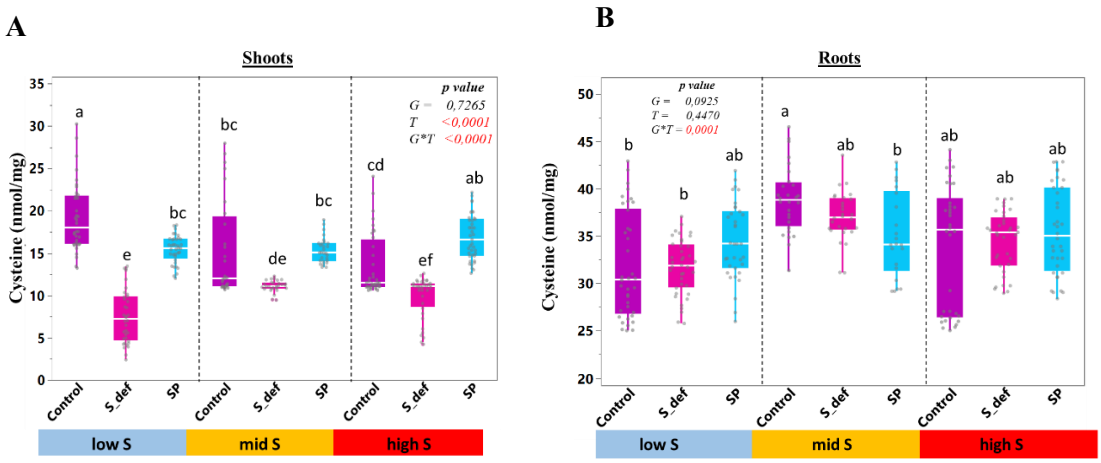

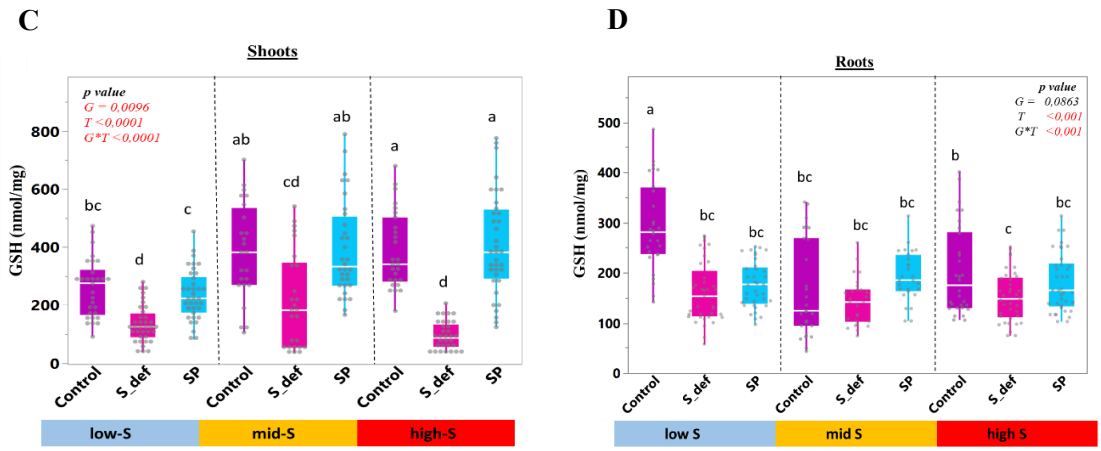

Figure 8: Distinct thiol adjustment strategies across low-, mid-, and high-S accessions (A) Shoot cysteine (nmol g^{-1} FW), **(B)** Root cysteine (nmol g^{-1} FW), and **(C)** Shoot Glutathione (GSH) (nmol g^{-1} FW) **(D)** Root GSH (nmol g^{-1} FW) in low-S (blue), mid-S (orange), and high-S (red) accessions grown under control (750 µM sulfate), sulfur-deficient (0 µM), or short-pulse (SP; intermittent supply) conditions. Plants were grown in a 9:1 sand: soil mix and fertilized twice weekly with the indicated S regimes. At week 5, the 7th–8th leaves and roots (split longitudinally) were harvested (n = 8 per accession). Data were analyzed using mixed models followed by Tukey's HSD; different letters indicate significant differences ($P < 0.05$). Boxplots show means ± SE.

3.3.1 Sulfur flux into thiols reveals preferential allocation toward glutathione in low-S accessions under sulfur deficiency

As the low-S group displayed a stronger relative decline in shoot cysteine in response to sulfur-deficient treatment, while shoot glutathione (GSH) pools did not decrease as dramatically compared to the mid-S and high-S groups, we next investigated how sulfate assimilation into reduced sulfur pools is regulated in these accessions under sulfur limitation. To address this, we selected two representative accessions from each group based on their sulfate and total sulfur contents and grew them under control and sulfur-deficient conditions for 14 days. Subsequently, plants were supplied with radiolabelled sulfate [^{35}S] for 3 hours, and the relative incorporation of [^{35}S] into cysteine and GSH was quantified separately in shoots and roots.

Consistent with known sulfur starvation responses in *Arabidopsis*, we observed a significant increase in relative incorporation of [^{35}S] into GSH under sulfur-deficient conditions across all three groups (Fig. 9A). This response aligns with previous reports demonstrating that sulfur limitation induces high-affinity sulfate transporters and enzymes involved in sulfate assimilation, and thus promotes the preferential allocation of newly assimilated sulfur toward antioxidant pools such as GSH (Dietzen et al., 2020). Importantly, the magnitude of this response differed between groups: the relative incorporation of [^{35}S] into GSH in shoots was significantly higher in the low-S group under sulfur deficiency compared to the mid-S and high-S groups (Fig. 9A). This pattern was consistently observed at the accession level, as both low-S accessions exhibited elevated [^{35}S] GSH incorporation under sulfur-deficient conditions (Fig. 9B).

In roots, we also detected an increase in relative [^{35}S] incorporation into GSH under sulfur deficiency; however, this response did not follow a clear genotype- or group-specific trend. While individual accessions showed variable incorporation levels, no consistent differences between low-, mid-, and high-S groups were apparent in roots. In contrast, relative incorporation of [^{35}S] into cysteine did not show significant alterations between groups in either shoots or roots (Supplementary Fig. 2). However, in the shoot, we observed a significant decline in relative incorporation of cysteine under S-deficiency in all groups, indicating channeling of S-flux into active GSH biosynthesis and hence no labeled cysteine being accumulated under S-limitation (Supplementary Fig. 2A).

Together, these results demonstrate that under sulfur-deficient conditions, low-S accessions preferentially enhance the relative flux of newly assimilated sulfur into glutathione, particularly in shoots as translocation was significantly enhanced for this group under S-deficiency. This flux-level adjustment is consistent with our earlier observations that shoot GSH pools in the low-S group were comparatively better maintained under sulfur deficiency than those of high-S accessions, despite a pronounced reduction in cysteine levels. Collectively, these findings suggest that low-S accessions actively prioritize glutathione biosynthesis under sulfur limitation, likely as a strategy to preserve redox homeostasis when sulfur availability becomes restrictive.

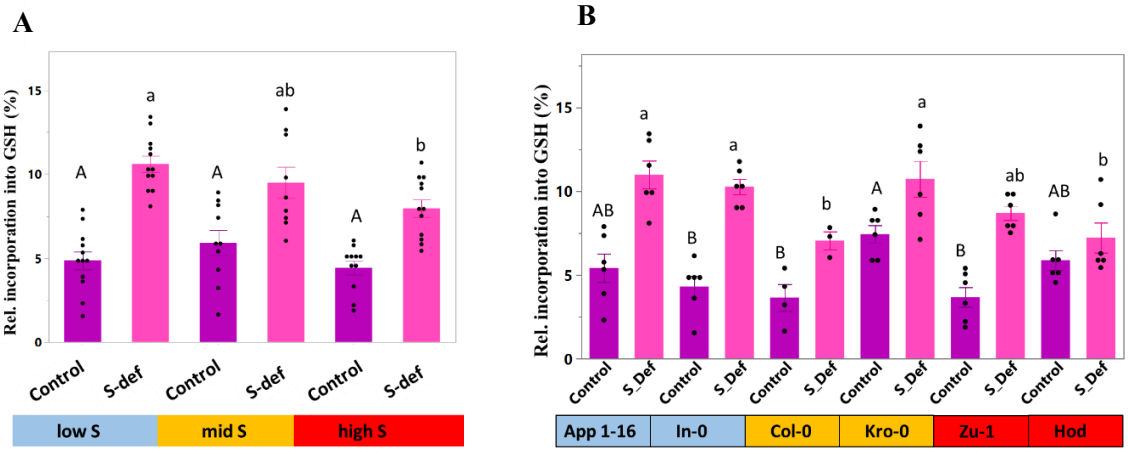

Figure 9: Low-S group depicting higher relative incorporation into GSH. (A) [^{35}S] incorporation into GSH [%] in shoots among three groups and **(B)** among individual accessions in each group under Control and S-deficient condition. *Arabidopsis* plants (25 seedlings) fed with either 750 µM SO_4^{2-} (Control) or 15 µM SO_4^{2-} (S-def) were grown on a nylon net in hydroculture for 14 d and, after incubation with [^{35}S] sulfate for 3 hours, shoots and roots were harvested separately. Thiols were separated by HPLC, and the radioactivity in Cys and GSH was measured with a radiodetector. Statistical analysis was performed using two-way ANOVA followed by Tukey's post hoc test for multiple comparisons for treatment and genotype. Different letters indicate significant differences ($p < 0.05$) between the genotypes and the treatments. Values are means ± s.e.m. (n=6).

3.3.2 Sulfur deficiency leads to a stronger oxidative imbalance in high-S accessions

Glutathione (GSH) is a central redox buffer in plant cells, functioning as a major scavenger of reactive oxygen species (ROS). Both the absolute size of the GSH pool and the ratio between reduced and oxidized glutathione (GSH: GSSG) are critical determinants of cellular redox potential and are essential for efficient detoxification of hydrogen peroxide (H_2O_2) (Hasanuzzaman et al., 2017; Madhu et al., 2023). A decline in GSH abundance, therefore, reflects a reduced buffering capacity and a shift toward a more oxidized intracellular environment. Based on our earlier observations, the pronounced reduction of GSH pools in the high-S group under sulfur deficiency likely reflects a combination of constrained biosynthetic capacity and increased oxidative demand. Furthermore, the comparatively lower relative incorporation of [^{35}S] into GSH in high-S accessions, relative to the low-S group, suggested that these genotypes may be less efficient in reinforcing their antioxidant capacity under sulfur limitation. We, therefore, hypothesized that the inability to maintain GSH pools and to sufficiently enhance sulfur flux into GSH could result in elevated oxidative stress in high-S accessions during sulfur starvation.

To test this hypothesis, we assessed ROS accumulation using 3,3′-diaminobenzidine (DAB) staining, which detects hydrogen peroxide through its oxidation by heme-containing peroxidases to form a brown precipitate (Daudi et al., 2012; Madhu et al., 2023). The presence and extent of brown staining were thus used as a direct proxy for H_2O_2 accumulation. For this analysis, we selected one representative accession from each group (App1-16, Col-0, and Hod) and stained 18-day-old seedlings grown under control and sulfur-deficient conditions. Under sulfur deficiency, all three genotypes displayed increased DAB staining, indicating elevated H_2O_2 accumulation compared to control conditions (Fig. 10A).

Quantification of shoot H_2O_2 levels was performed by calculating the percentage of stained area relative to total leaf area (Fig. 10B). Under control conditions, Hod already exhibited elevated basal staining (approximately 30–35%), whereas App1-16 and Col-0 showed comparatively lower levels (around 15-20%). Upon sulfur deficiency, DAB-stained area increased in all three genotypes; however, the response was markedly stronger in Hod, reaching approximately 60-70%. In contrast, App1-16 and Col-0 showed only a moderate increase to approximately 25-35% (Fig. 10B). The substantially higher proportion of stained area in Hod under sulfur deficiency indicates enhanced accumulation of H_2O_2 and suggests a reduced capacity to maintain redox homeostasis under sulfur-limiting conditions.

To further substantiate the elevated oxidative stress observed in high-S accessions, we next examined superoxide (O_2^-) accumulation using Nitroblue tetrazolium (NBT) staining. This experiment included two accessions per group, allowing for a broader assessment of group-level responses. Six accessions were stained at a similar developmental stage and under identical treatment conditions as described for DAB staining. NBT reacts with superoxide anions to form a blue or purple formazan precipitate, enabling visualization of O_2^- accumulation (Kumar et al., 2014). Under sulfur-deficient conditions, all accessions exhibited increased NBT staining compared to controls, confirming that sulfur limitation perturbs overall redox homeostasis (Fig. 10C). Notably, high-S accessions (Hod and Zu-1) displayed

the strongest accumulation of superoxide, followed by mid-S accessions (Col-0 and Kro-0), whereas low-S accessions showed comparatively weaker changes relative to their control conditions (Fig. 10C).

In addition, NBT staining was also performed on leaves harvested from 35-day-old plants grown under sand: soil mix. Although clear differences between control and sulfur-deficient treatments were still apparent, ROS accumulation at this later developmental stage was more spatially restricted and localized to specific leaf regions rather than distributed uniformly across the entire shoot (Supplementary Fig. 3). Low-S accessions (App1-16 and In-0) showed detectable superoxide accumulation, but staining intensity was more pronounced in mid-S and high-S accessions, with Col-0, Kro-0, and Zu-1 exhibiting particularly strong localized signals. Interestingly, Hod displayed a less dramatic overall increase compared to early vegetative stages; however, superoxide accumulation remained evident in distinct leaf regions, suggesting a shift toward localized oxidative stress rather than whole-tissue saturation (Supplementary Fig. 3). Such spatially restricted staining may reflect localized ROS production associated with stress signalling or metabolic hotspots within the leaf, as ROS bursts are often generated in specific tissues through NADPH oxidase activity and can accumulate at discrete sites of oxidative stress rather than uniformly across the entire organ (Chapman et al., 2019).

Collectively, these datasets indicate that the stronger reduction of GSH pools observed in high-S accessions under sulfur deficiency is associated with elevated ROS accumulation and a diminished ability to reinforce antioxidant defenses through enhanced sulfur flux into glutathione. In contrast, low-S accessions appear better equipped to buffer oxidative stress under sulfur limitation, likely due to their higher relative incorporation of newly assimilated sulfur into GSH. Together, these findings support a model in which differential regulation of glutathione metabolism and sulfur allocation underpins accession-specific variation in redox homeostasis during sulfur starvation.

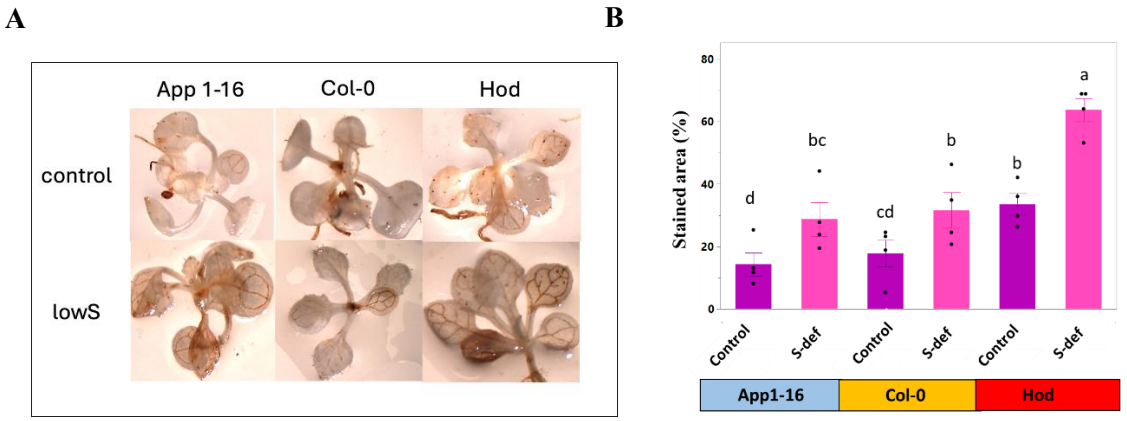

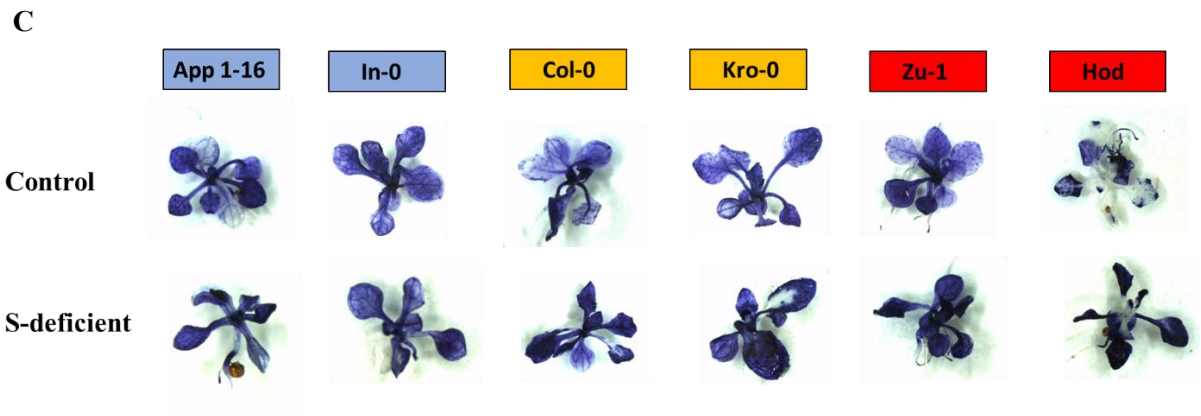

Figure 10: High-S group shows signs of oxidative damage under S-deficiency (A) Pictures of stained *A. thaliana* accessions. i.e. App1-16 (low-S group), Col-0 (mid-S group), and Hod (high-S group) under control and low-S conditions **(B)** Barplot shows stained DAB area (%) in App 1-16, Col-0, and Hod accessions, under Control and S-def conditions. **(C)** Pictures of NBT stained 18 days old seedlings of *A. thaliana* accessions. i.e. App1-16 (low-S), In-0 (low-S), Col-0 (mid-S), Kro-0 (mid-S), Zu-1 (high-S) and Hod (high-S) under Control and S-def conditions. Statistical analysis was performed using two-way ANOVA followed by Tukey's post hoc test for multiple comparisons for treatment and genotype. Lowercase letters indicate significant differences ($p < 0.05$) between the genotypes and the treatments. Values are means ± s.e.m. (n=6).

3.3.3 Transcriptional regulation of cysteine and glutathione biosynthesis genes reflects accession-specific sulfur allocation strategies under sulfur deficiency

To corroborate the phenotypes described above, we next examined whether the observed metabolic changes were reflected at the transcriptional level. As major differences in cysteine and glutathione pools were primarily detected in shoots, we focused our gene expression analyses on shoot tissue. Based on our earlier experimental design, we selected six accessions representing the low-, mid-, and high-S groups and quantified the expression of key genes involved in cysteine biosynthesis, including *SERINE ACETYLTRANSFERASE isoforms (SERAT), SULFITE REDUCTASE (SiR), and O-ACETYLSERINE(THIOL)LYASE A (OASTL-A).* SERAT enzymes catalyze the formation of O-acetylserine (OAS), the immediate precursor of cysteine, and are encoded by multiple isoforms that are localized in different cellular compartments (Watanabe et al., 2008). In this study, we focused on the major SERAT isoforms i.e. *SERAT3;1, SERAT3;2, SERAT2;1, SERAT2;2,* previously reported to contribute substantially to cellular OAS production and sulfur-responsive transcriptional regulation (Watanabe et al., 2008). Similarly, *OASTL-A*, the predominant cytosolic isoform of O-acetylserine(thiol)lyase, was selected because it catalyzes the final step of cysteine biosynthesis and represents the primary contributor to cysteine synthesis in the cytosol (Heeg et al., 2008).

Under control conditions, transcript levels of *SERAT2;2, SERAT2;1, SiR,* and *OASTL-A* were significantly higher in high-S accessions compared to low- and mid-S accessions (Fig. 11B), suggesting a higher basal sulfur assimilation capacity that may contribute to the larger sulfur pools observed in

these genotypes. However, under sulfur-deficient conditions, gene expression responses were strongly accession-specific rather than strictly group-dependent. We observed a significant upregulation of *SERAT2;2* in both mid-S accessions i.e. Col-0 and Kro-0 and also in Zu-1 under sulfur deficiency, whereas *SERAT2;2* was significantly downregulated in Hod, with no statistically significant changes detected in both low-S accessions (Fig. 11B). A similar pattern was observed for relative expression levels of *SERAT2;1*, except Hod which did showed downregulation of this gene under S-deficiency but not significant. In contrast, *SERAT3;1* showed a distinct pattern: both high-S accessions, Hod and Zu-1, exhibited significant downregulation of *SERAT3;1* under S-deficient conditions and completely opposite pattern was seen in both mid-S accession with expression being significantly enhanced. Surprisingly, Zu-1 showed upregulation for *SERAT3;2* while no change in Hod was observed under S-limitation, indicating genotype specific prioritization of different isoform under S-deficiency (Fig. 11B). Both low-S accessions did not show any significant differences for expression levels of both *SERAT3;1* and *SERAT3;2* in response to S-deprivation (Fig. 11B).

Expression of *SiR* revealed yet another layer of divergence. *SiR* was strongly induced in Zu-1 under sulfur deficiency, followed by App1-16, and both mid-S accessions also showing significant response. Notably, *SiR* expression was unchanged in another low-S accessions In-0, and the gene was downregulated in high-S accessions, Hod, when compared relative to their respective control conditions, although the change was not significant (Fig. 11B). Similarly, *OASTL-A* expression exhibited contrasting trends across accessions, with induction observed in low-S accession like App1-16 and mid-S accessions Kro-0, whereas both high-S accessions showed a reduction in transcript levels with significant differences observed for Hod under sulfur deficiency (Fig. 11B).

Taken together, these transcriptional profiles indicate that accessions employ distinct regulatory strategies to cope with sulfur deficiency at the level of cysteine biosynthesis. Low-S accessions, which exhibited the most pronounced decline in cysteine pools under sulfur deficiency, generally maintained or enhanced the expression of cysteine biosynthetic genes, suggesting an active compensatory response aimed at sustaining sulfur assimilation and downstream metabolite production. This transcriptional behavior is consistent with our metabolic and flux data, where low-S accessions preferentially increased sulfur allocation toward glutathione biosynthesis, potentially to preserve redox balance under sulfur-limiting conditions (Fig. 8C, Fig. 9A). Mid-S accessions displayed significant upregulation of most the cysteine biosynthesis genes suggesting a tendency toward compensatory regulation rather than restriction of sulfur assimilation. In contrast, high-S accessions exhibited a markedly different strategy. Despite showing strong induction of classical sulfur starvation marker genes and a robust sulfur deficiency response at the signaling level, both Hod and Zu-1 displayed downregulation of key cysteine biosynthesis genes, including *SERAT3;1* and *OASTL-A,* under sulfur-deficient conditions. This transcriptional repression, together with the pronounced decline in glutathione pools (Fig. 8C) observed earlier, suggests a restrictive strategy in which high-S accessions limit further investment into reduced sulfur biosynthesis when sulfur becomes limiting. Such restriction may reflect an inability to sustain

sulfur-intensive metabolic pathways, potentially contributing to the elevated oxidative stress phenotypes observed in these accessions. In addition, while downregulation of *SERAT2;1*, and *SERAT2;2* was observed for Hod, the opposite response in Zu-1 indicates heterogeneity in the group and distinct regulatory mechanisms in these genotypes.

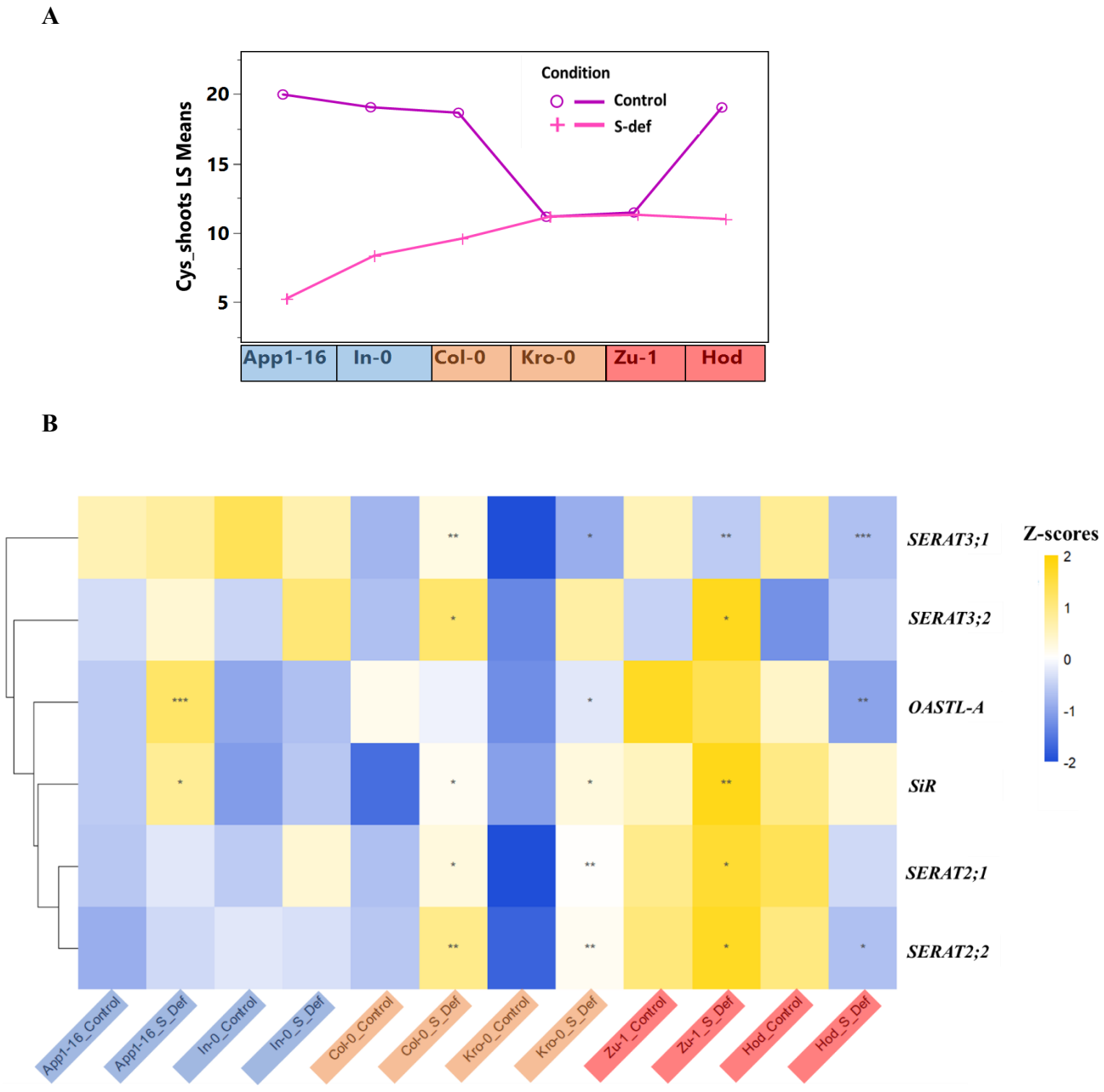

Figure 11: Relative expression of Cys synthesis genes in *A. thaliana* accessions. (A) Least Square Means (LSMeans) of shoot Cys concentration in *A. thaliana* accessions. i.e. App1-16 (low-S), In-0 (low-S), Col-0 (mid-S), Kro-0 (mid-S), Zu-1 (high-S) and Hod (high-S) under control and S_def conditions. **(B)** Heatmap representing relative expression of Cys synthesis genes in shoots using the $2^{-\Delta Ct}$ method and row-scaled to generate Z-scores for visualization in heatmaps under Control and S-def (S_Def) conditions. Statistical analysis was performed using two-way ANOVA followed by Tukey's post hoc

test for multiple comparisons for treatment and genotype. Asterisks indicate significant differences (* $p < 0.05$, ** $p < 0.01$, *** $p < 0.001$) between the genotypes and the treatments (n=6).

For the glutathione (GSH) biosynthetic pathway, we analyzed the transcript abundance of *GSH1* and *GSH2* in shoots, as the most pronounced differences in GSH pools were observed in this tissue. Under control conditions, expression levels of both *GSH1* and *GSH2* were significantly higher in the high-S accessions compared to low- and mid-S accessions, consistent with their higher steady-state GSH accumulation (Fig. 12A & B). However, under sulfur-deficient conditions, the regulation of these genes diverged markedly between groups and even among accessions within the same group.

Within the low-S group, App1-16 showed a significant upregulation of *GSH2* under sulfur deficiency, whereas In-0 displayed no significant change (Fig. 12B). This response parallels the relatively moderate decline in shoot GSH observed in these accessions under sulfur limitation (Fig. 12A), suggesting that maintenance or induction of GSH biosynthetic capacity may contribute to buffering GSH pools in low-S genotypes. In the mid-S group, contrasting behaviors were again evident: while Col-0 maintained GSH levels under sulfur deficiency, Kro-0 exhibited a significant decrease in shoot GSH (Fig. 12A). Correspondingly, only Kro-0 showed a significant induction of both *GSH1* and *GSH2* transcripts under sulfur-deficient conditions (Fig. 12B), indicating an attempted compensatory response that was nevertheless insufficient to prevent GSH depletion.

In contrast, accessions belonging to the high-S group displayed a distinct regulatory pattern. Despite experiencing the strongest relative decline in shoot GSH under sulfur deficiency (Fig. 12A), the two high-S accessions differed substantially at the transcriptional level. Hod showed a significant downregulation of both *GSH1* and *GSH2* under sulfur-deficient conditions, whereas Zu-1 maintained expression levels comparable to control conditions (Fig. 12B). This divergence suggests fundamentally different adaptive strategies within the high-S group. Genotype Hod appears to adopt a conservative strategy by actively restricting further biosynthetic investment into glutathione under sulfur limitation-thereby allowing GSH pools to decline. While Zu-1 may instead experience limitations at the level of substrate availability or flux, rather than transcriptional control, as gene expression is not induced despite strong depletion of GSH pools.

Taken together, these results indicate that accessions from the low- and mid-S groups, which generally exhibit smaller relative declines in GSH content, respond to sulfur deficiency by maintaining or enhancing the expression of GSH biosynthetic genes. In contrast, high-S accessions exhibit a decoupling between GSH pool depletion and transcriptional regulation, with accession-specific strategies ranging from transcriptional restraint (Hod) to apparent substrate-limited regulation (Zu-1). These findings further support the notion that natural variation in sulfur status is associated with fundamentally different strategies of thiol management and redox buffering under sulfur-limiting conditions.

A

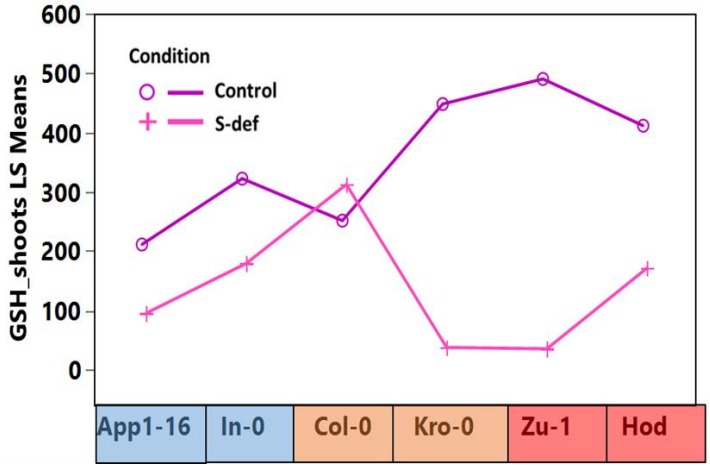

B

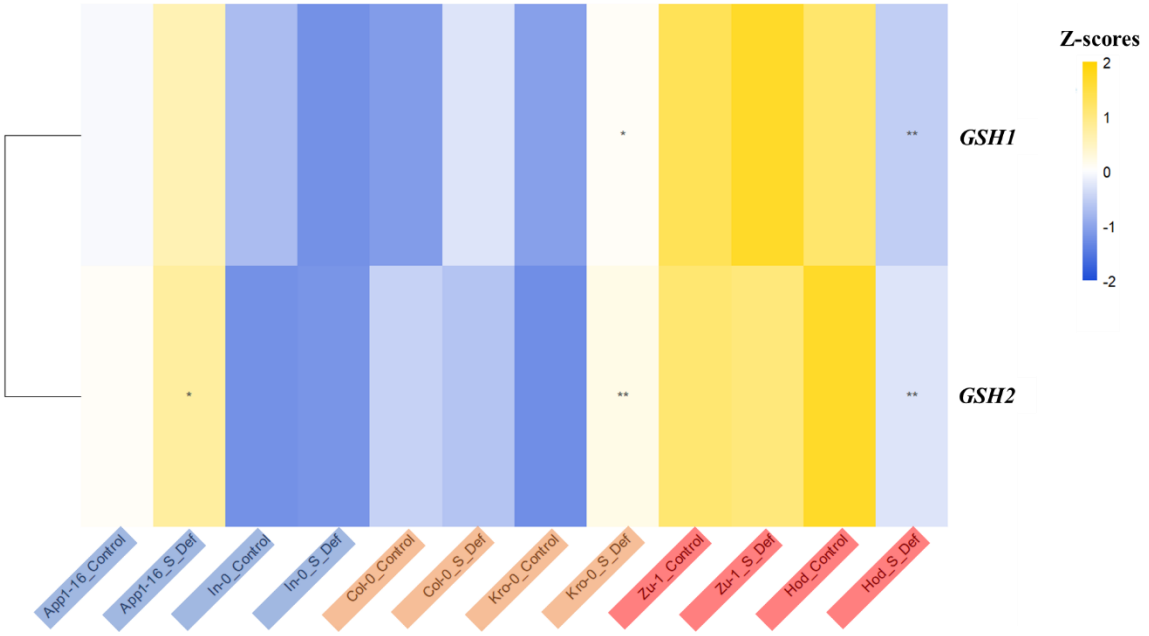

Figure 12: Relative expression of GSH synthesis genes in *A. thaliana* accessions. (A) Least Square Means (LSMeans) of shoot GSH concentration in *A. thaliana* accessions. i.e. App1-16 (low-S), In-0 (low-S), Col-0 (mid-S), Kro-0 (mid-S), Zu-1 (high-S) and Hod (high-S) under control and S_def conditions. **(B)** Heatmap representing relative expression of GSH synthesis genes in shoots using the $2^{-\Delta Ct}$ method and row-scaled to generate Z-scores for visualization in heatmaps under Control and S-def (S_Def) condition. Statistical analysis was performed using two-way ANOVA followed by Tukey's post hoc test for multiple comparisons for treatment and genotype. Asterisks indicate significant differences (* $p < 0.05$, ** $p < 0.01$, *** $p < 0.001$) between the genotypes and the treatments (n=6).

3.4 Sulfur deficiency affects accumulation of Nitrate and Phosphate in the groups differently

Distinct studies have shown strong interactions between nitrate and sulfate assimilation (Koprivova et al., 2000; Takahashi & Saito., 1996), and nitrate uptake and reduction are known to be suppressed under S deficiency (Jobe et al., 2019). Similarly, sulfur and phosphate signaling are tightly interconnected, with leaf phosphate often positively correlated with sulfate levels (Ristova et al., 2022; Soda et al., 2019; Rouached et al., 2011). Hence, we tested these accessions for the accumulation of these two anions as well and observed a strong link between these three nutrients.

We observed both shoot nitrate and phosphate decrease under S deficiency for all groups (Fig. 13A, C). The decline in shoot nitrate was particularly pronounced in the low-S group, where nitrate fell by ~ 60-fold compared to control despite higher initial levels. Notably, short-pulse (SP) supplementation restored shoot nitrate in low-S and high -S accessions to control levels, whereas mid-S groups remained comparable to their S-deficient state (Fig. 13A). In roots, the trend contrasted with shoots for low-S accessions, which contained the lowest nitrate under control, but accumulated significantly more under deficiency, suggesting altered root-to-shoot transport (Fig. 13B). However, there were no significant differences observed for mid-S and high-S accessions for root nitrate levels under S-def. With short pulse treatment, nitrate levels in roots were similar to control for all the groups except mid-S, where a significant decline was seen compared to the control condition.

For phosphate, we confirmed our previous finding (Jager et al., 2023) that low-S accessions accumulate higher shoot phosphate under control conditions with mid-S and high-S resembling each other. However, low-S group just like nitrate also exhibited the strongest relative decline under S-deficiency followed by mid-S group (Fig. 13C). Surprisingly, high-S group didn't show any significant decline in shoot phosphate levels, which could be due to already low levels of phosphate under normal condition. Root phosphate remained largely stable across treatments in all groups (Fig. 13D). Unlike nitrate, phosphate in shoots did not increase under SP conditions, indicating that short sulfate supplementation is insufficient to restore phosphate levels (Fig. 13C). Altogether, these results highlight distinct N-S and P-S interactions across accession groups and the importance of sulfur in maintaining nutrient homeostasis.

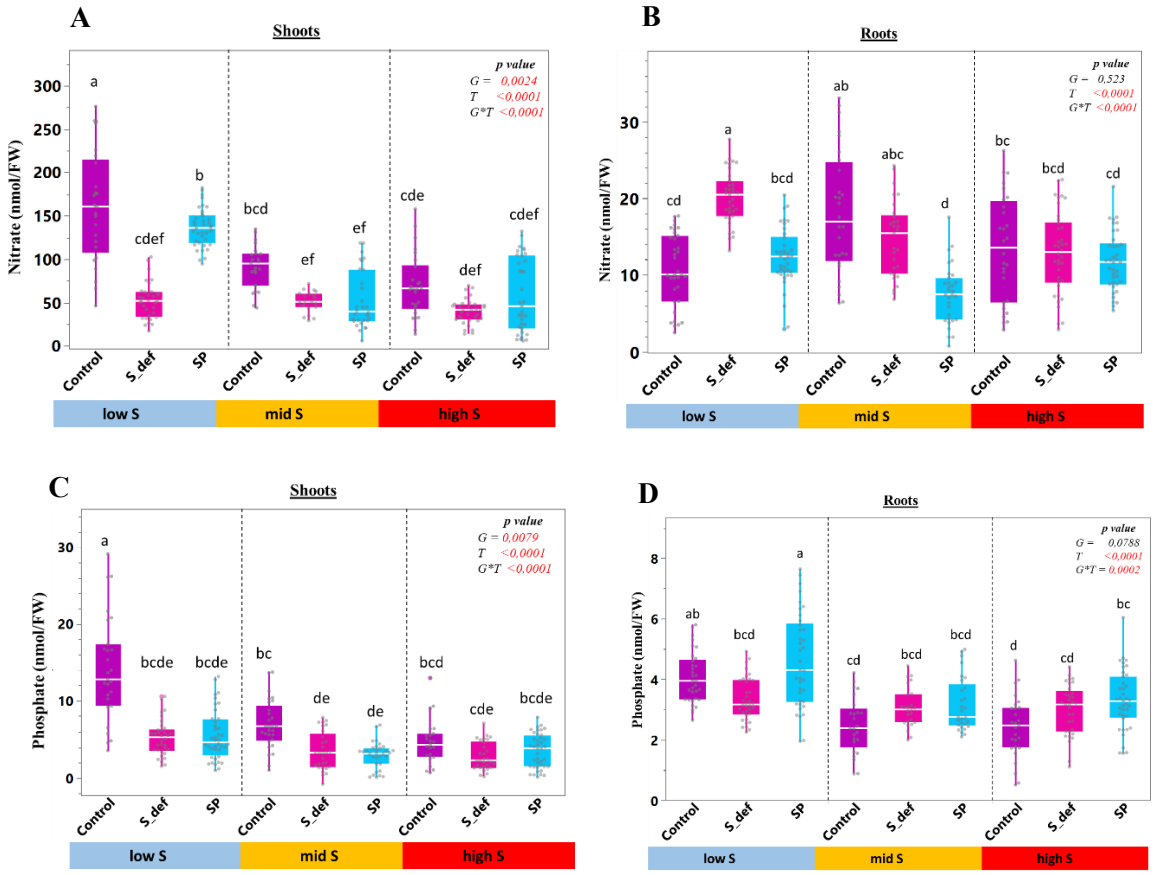

Figure 13: Sulfur deficiency alters nitrate and phosphate accumulation in a group-specific manner **(A)** Shoot nitrate (nmol g^{-1} FW), **(B)** Root nitrate (nmol g^{-1} FW), and **(C)** Shoot phosphate (nmol g^{-1} FW) **(D)** Root phosphate (nmol g^{-1} FW) in low-S (blue), mid-S (orange), and high-S (red) accessions grown under control (750 µM sulfate), sulfur-deficient (0 µM), or short-pulse (SP; intermittent supply) conditions. Plants were grown in a 9:1 sand: soil mix and fertilized twice weekly with the indicated S regimes. At week 5, the 7th–8th leaves and roots (split longitudinally) were harvested (n = 8 per accession). Data were analysed using mixed models followed by Tukey's HSD; different letters indicate significant differences ($P < 0.05$). Boxplots show means ± SE.

3.4.1 Nitrate partitioning and transcriptional responses under Sulfur deficiency differ in low-S and high-S accessions

The nitrate phenotype observed under sulfur deficiency revealed a strong group-specific response, evident in both shoots and roots, and closely resembling the cysteine phenotype previously described in shoots. Previous studies have identified cysteine biosynthesis as a major convergence point for carbon, nitrogen, and sulfur acquisition pathways (Jobe et al., 2019), indicating a strong metabolic linkage between these processes. Based on these observations, we next investigated the transcriptional regulation of nitrate uptake and assimilation genes in both tissues and examined their relationship with cysteine biosynthesis genes.

Under control conditions in shoots, Hod displayed significantly higher basal expression of most nitrate assimilation genes, including *NIA1, NIA2,* and *NRT1;1,* compared to all other accessions (Fig. 14B). This elevated basal expression is consistent with the higher nitrate levels observed in Hod relative to other genotypes (Fig. 14A), suggesting that Hod possesses an enhanced baseline capacity for nitrate acquisition and/or nitrate handling under non-stressed conditions.

Under sulfur deficiency, both low-S accessions (App1-16 and In-0) showed significant induction of *NIA1* in shoots and roots relative to their respective control conditions (Fig. 14B & C). Similar to *NIA1*, induction of *NIA2* and *NiR1* is observed in shoots of low-S accession, especially App1-16, although not significant, while In-0 showed pronounced increase in *HRS1* expression under S-deficiency (Fig. 14B). In roots, these genes did not show marked changes, with the exception of *NiR1,* which was significantly upregulated in App1-16 under sulfur deficiency (Fig. 14C). Interestingly, *HRS1* expression was significantly downregulated in roots of App1-16 under sulfur deficiency (Fig. 14C), indicating tissue-specific regulation of nitrate-responsive signaling in low-S accessions.

In mid-S accessions, consistent with their relatively homogeneous nitrate phenotype in shoots, no significant changes in nitrate assimilation gene expression were detected in shoots of Col-0 except for *NiR1* where enhanced induction was reported under sulfur deficiency (Fig. 14B). Kro-0 under S-deficiency showed significant upregulation of all nitrate assimilation genes we tested in our study, indicating active assimilation of nitrate in this genotype. In roots, although nitrate levels varied between Col-0 and Kro-0, both accessions showed a similar transcriptional response (Fig. 14C). However, in contrast to low-S accessions, Kro-0 exhibited significant downregulation of *NiR1* under sulfur deficiency (Fig. 14C).

In the high-S group, nitrate phenotypes in both shoots and roots were highly accession-specific, and this heterogeneity was reflected at the transcriptional level (Fig. 14A-C). Under sulfur deficiency, no major changes in nitrate assimilation gene expression were observed in shoots of Zu-1, except for a significant upregulation of *HRS1* and *NRT1;1* under S-deficiency. However, in Hod, transcript levels of *NiR1,* and *NRT1;1* were significantly downregulated (Fig. 14B) unlike low-S and mid-S accession where a strong induction was observed. In roots, *NIA1* was significantly upregulated in both high-S accessions and similar response was also seen in Zu-1 for *NIA2* under S-deficiency (Fig. 14C)

Correlation analysis further revealed a significant positive relationship between relative expression of nitrate assimilation genes (*NIA1, NIA2, NRT1;1,* and *HRS1*) and cysteine biosynthesis and sulfur reduction genes, including *SERAT2;2, SiR,* and *OASTL-A*, specifically in shoots (Supplementary Fig. 4A**).** This coordinated expression pattern supports a tight coupling between nitrate reduction and sulfate assimilation pathways in the shoot. In roots, expression of *APR2* correlated positively with the high-affinity nitrate transporter *NRT2.1* (Supplementary Fig. 4B**),** suggesting coordinated regulation of nitrate acquisition and sulfate reduction capacity in this tissue.

Taken together, the coordinated upregulation of nitrate assimilation genes in shoots of low-S accessions, along with induction of *NIA1* in both roots and shoots and *NiR1* in roots, indicates activation of a systemic nitrate reduction program under sulfur deficiency, consistent with the pronounced decline in shoot nitrate observed in these accessions. In contrast, downregulation of *NiR1, NRT1;1,* and *HRS1* in shoots of Hod, together with repression of *NIA2* in roots and a distinct regulation of *NIA1*, suggests that high-S accessions limit nitrate assimilation under sulfur deficiency through organ- and accession-specific transcriptional control.

A

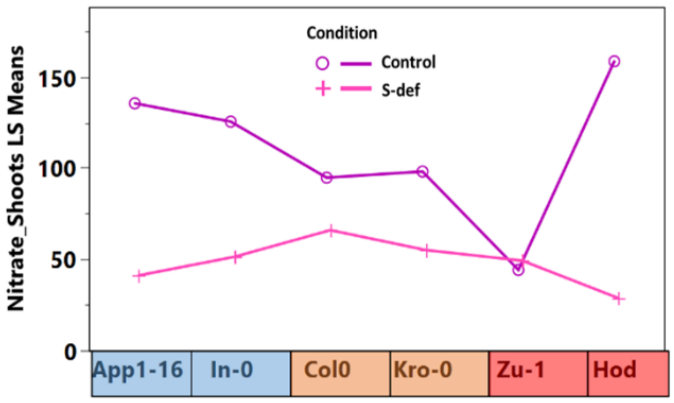

B

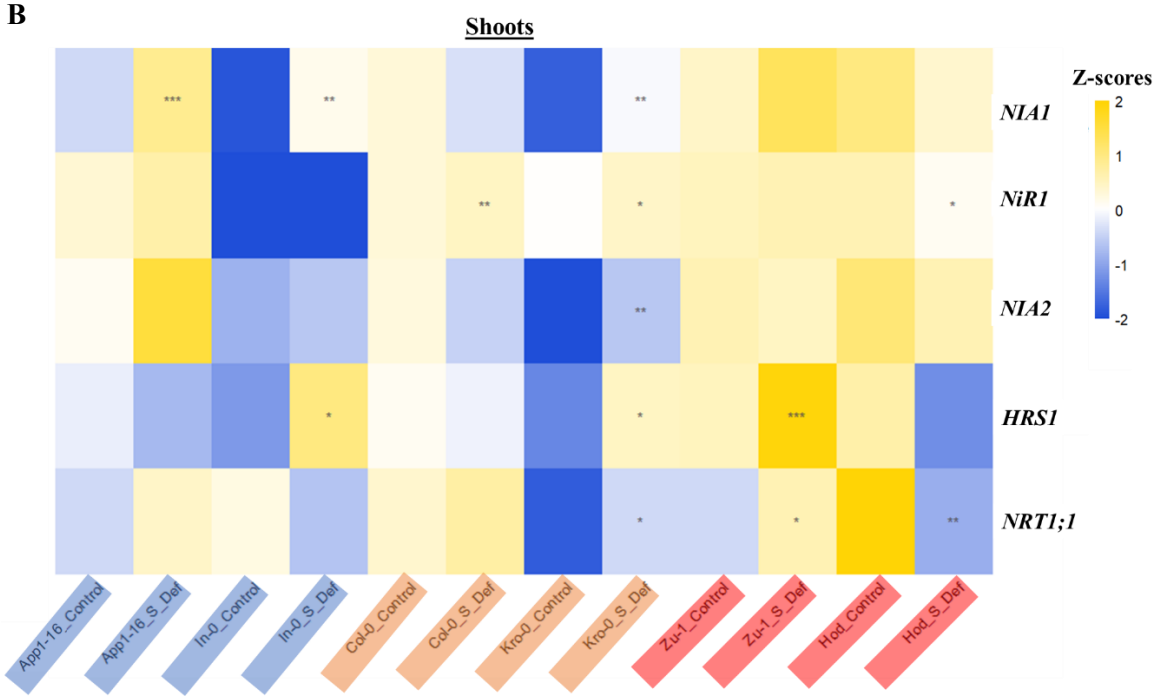

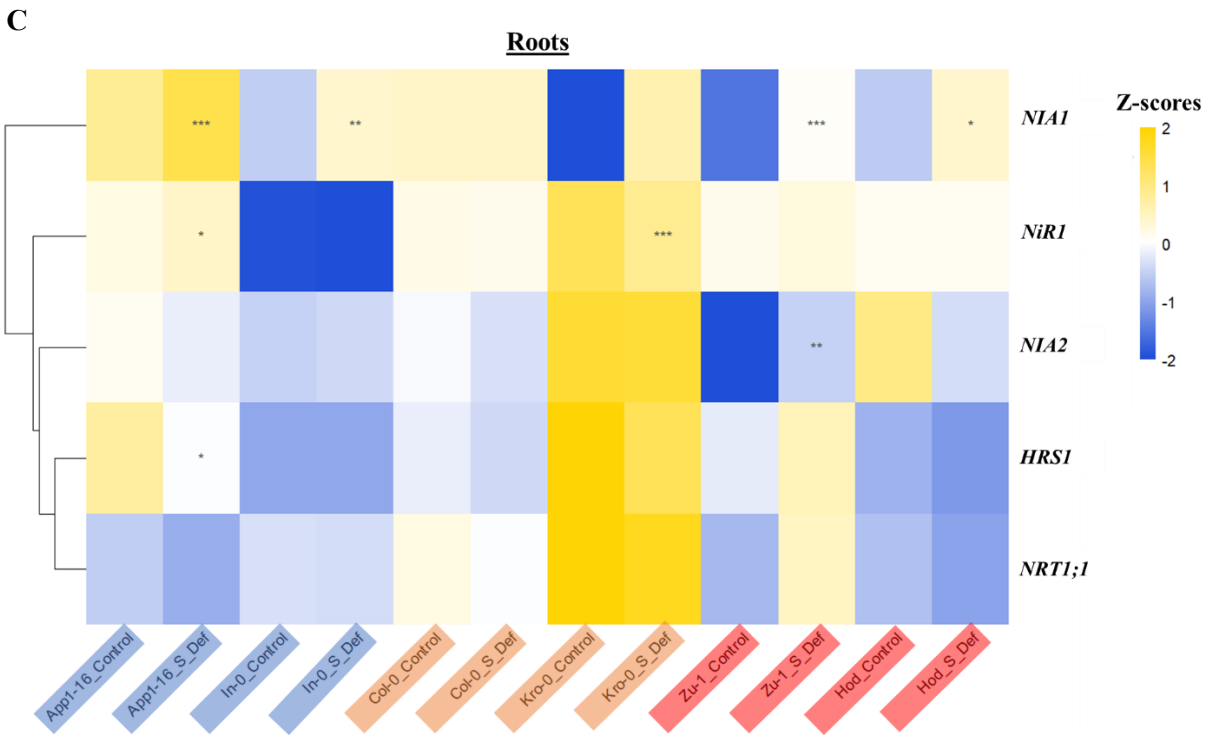

Figure 14: Relative expression ($2^{-\Delta Ct}$) of Nitrate assimilation genes *in A. thaliana* accessions. (A) Least Square means (LSMeans) of nitrate concentration in shoots of *A. thaliana* accessions. i.e. App1-16 (low-S), In-0 (low-S), Col-0 (mid-S), Kro-0 (mid-S), Zu-1 (high-S) and Hod (high-S) under control and S-def conditions. Heatmap representing relative expression of nitrate assimilation genes in **(B)** Shoots and **(C)** Roots using the $2^{-\Delta Ct}$ method and row-scaled to generate Z-scores for visualization in heatmaps under Control and S-def (S_Def) conditions. Statistical analysis was performed using two-way ANOVA followed by Tukey's post hoc test for multiple comparisons for treatment and genotype. Asterisks indicate significant differences (* $p < 0.05$, ** $p < 0.01$, *** $p < 0.001$) between the genotypes and the treatments (n=6).

3.5 Sulfur deficiency induces more extensive shoot metabolic reprogramming in high-sulfur accessions

In line with our previous observations that sulfur (S) deficiency affects not only sulfur metabolism but also the assimilation of other nutrients and gene expression, we next investigated metabolomic changes in 35-days old leaves, measured via GC-MS in these accessions. This approach was motivated by earlier studies demonstrating that S deficiency strongly impacts plant metabolism (Zenzen et al., 2024; Nikiforova et al., 2005). Overall, S deficiency induced accession-specific metabolic responses, with more pronounced changes in Kro-0 and the high-S accessions, whereas Col-0 and the low-S accessions showed comparatively modest metabolic alterations.

As expected, S deficiency led to the accumulation of several amino acids across all accessions, although the magnitude and specificity of these responses differed. Among the low-S accessions, App1-16 displayed significant increases in glutamate, glycine, serine, and threonine, whereas In-0 showed a significant increase only in threonine, accompanied by reduced levels of β-alanine, GABA (γ-Amino Butyric Acid), and methionine (Fig. 15). In the mid-S group, Col-0 exhibited increased aspartate and

threonine levels, while Kro-0 showed a much stronger response, with elevated levels of nearly all amino acids except aspartate, proline, and serine. Similarly, the high-S accession Hod showed increased concentrations of several amino acids, including asparagine, aspartate, glutamate, isoleucine, leucine, threonine, and valine. In contrast, Zu-1 exhibited a more selective response, characterized by increased glycine levels and reduced methionine content (Fig. 15).

Sugar metabolism was also differentially affected by S deficiency. Both low-S accessions accumulated raffinose, while increased disaccharide levels were observed only in App1-16 (Fig. 15). In the mid-S group, Kro-0 showed significantly higher fructose and sucrose levels, whereas no comparable changes were detected in Col-0. Both high-S accessions exhibited a significant increase in sucrose under S deficiency (Fig. 15).

Organic acid levels were largely conserved across accessions, with some notable exceptions. App1-16 showed a significant decrease in fumarate, while In-0 accumulated higher levels of glycolate (Fig. 15). Citrate/isocitrate levels showed opposite response in mid-S accessions with levels increasing in Col-0 but decreasing in Kro-0. Also, Kro-0 additionally accumulated malate and maleate under S deficiency. In the high-S group, Zu-1 showed increased pyruvate and reduced maleate levels, whereas Hod exhibited higher malate accumulation. Among other metabolites, glycerol levels were significantly elevated in App1-16, Col-0, Zu-1, and Hod under S deficiency. Both high-S accessions also showed increased levels of phosphorylated hexoses, while App1-16 and Kro-0 uniquely exhibited a significant reduction in myo-inositol (Fig. 15).

Taken together, these results indicate distinct metabolic strategies among the three groups in response to S deficiency. While the low-S accessions and Col-0 displayed relatively moderate metabolic adjustments, Kro-0 and the high-S accessions underwent extensive metabolic reprogramming, highlighting genotype-dependent differences in metabolic plasticity under sulfur-limited conditions (Fig. 15).

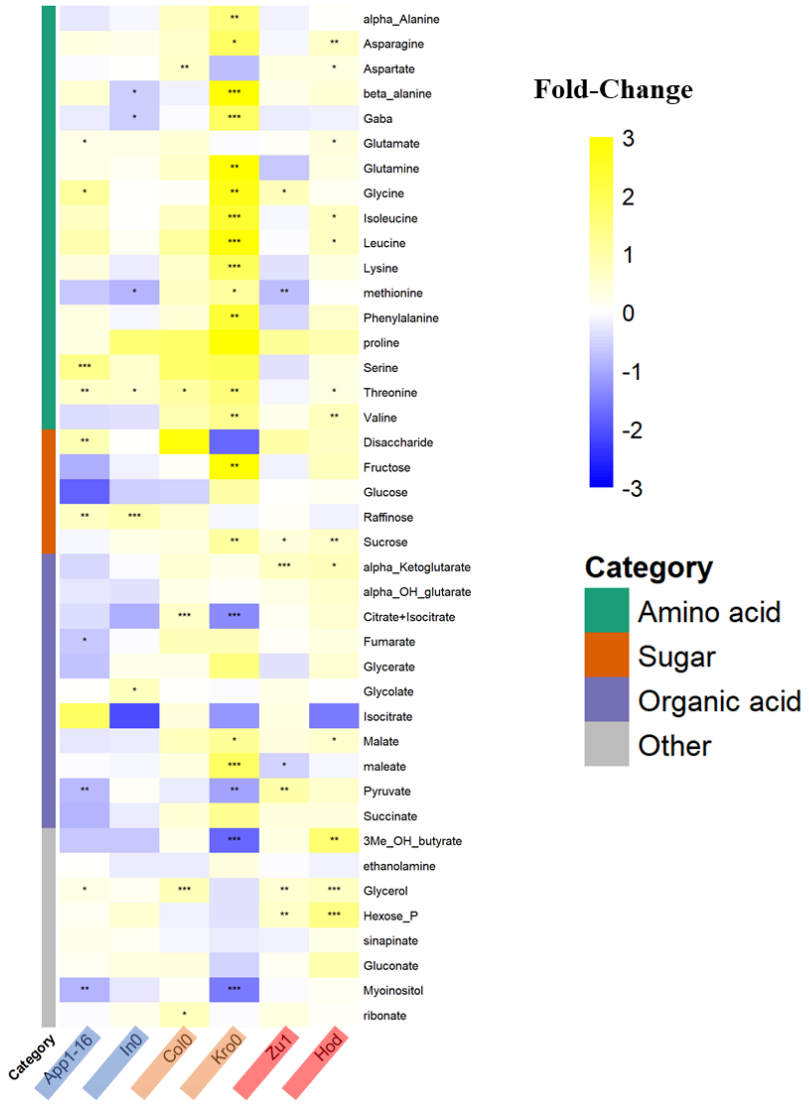

Figure 15: High-S accessions exhibit a stronger, system-wide metabolic reconfiguration under sulfur deficiency. Heatmap representing fold change (z-score) in metabolite accumulation in response to S-deficient conditions in App1-16; In-0 (low-S), Col-0; Kro-0 (mid-S), Zu-1; Hod (high-S). The blue color represents a decreasing trend, while the yellow color represents an increasing trend. Asterisks indicate statistically significant differences, according to two-way anova statistics with (n = 6) (* $p < 0.05$, ** $p < 0.01$, *** $p < 0.001$).

3.6 Fitness related trait strongly affected in high-S accessions under S-deficiency

To assess how natural variation in sulfur status affects the growth and development at normal and low S supply, we examined multiple growth- and fitness-related traits, including rosette diameter (RD), flowering time, silique number, and seed weight, across low-S, mid-S, and high-S accession groups under different sulfur regimes.

To estimate the impact of S deficiency on vegetative growth, rosette diameter was measured at four developmental time points, from day 16 to day 36, under control, sulfur-deficient, and short-pulse

conditions. Because the accessions differ substantially in flowering time, flowering time was included as a covariate in the mixed-effects model to account for intrinsic differences in developmental timing. Analysis of rosette diameter revealed clear group-specific growth trajectories (Fig. 16A-i). Low-S accessions exhibited relatively larger rosettes during early development under control conditions. The larger rosetter diameter in these accessions is consistent with their late flowering nature (Fig. 16B) where delayed bolting allows more leaf development. However, from day 28 onward, rosette growth tended to stabilize under both Control and S-deficient conditions. In contrast, under the short-pulse treatment, low-S accessions continued to increase rosette size, with significant differences observed at day 36. Notably, sulfur deficiency did not impose a strong additional penalty on rosette size in the low-S group (Fig. 16A-ii), suggesting that their growth pattern primarily reflects developmental timing rather than strong sensitivity to external sulfur limitation. Mid-S accessions, unlike the low-S group, displayed a more continuous growth pattern across all treatments. However, sulfur deficiency led to a pronounced reduction in growth, particularly between day 21 and day 28. By day 36, rosette diameter under deficiency partially recovered and approached control levels at the group mean level (Fig. 16A-i). Nevertheless, analysis at the accession level revealed that both Col-0 and Kro-0 exhibited strong growth inhibition under sulfur deficiency (Fig. 16A-ii). Under the short-pulse treatment, mid-S accessions responded differently: although rosette diameter increased significantly by day 28 relative to the control, a marked decline was observed by day 36, suggesting that transient sulfur supply was insufficient to sustain continued growth. High-S accessions showed a growth pattern broadly similar to the mid-S group, characterized by continuous rosette expansion under control conditions. However, they suffered the strongest relative decline in rosette diameter under sulfur deficiency, with significantly smaller rosettes evident from day 28 to day 36 (Fig. 16A-i). As observed for mid-S accessions, the short-pulse treatment initially stimulated growth in high-S accessions at day 28, but this was followed by a significant reduction in rosette diameter by day 36. This pattern indicates a higher and more sustained sulfur demand in high-S accessions to maintain vegetative growth, consistent with their pronounced sensitivity to sulfur limitation.

Flowering time (FT) further underscored distinct adaptive strategies among the three sulfur (S) groups (Supplementary Fig. 5A). To account for intrinsic differences in flowering behavior among accessions, flowering time responses were analyzed as fold changes relative to the control condition (Fig. 16B). This normalization revealed clear group-specific responses to sulfur availability. Low-S accessions showed flowering time ratios close to one under both S-deficient and short-pulse treatments, indicating that flowering time remained largely stable despite changes in sulfur supply (Fig. 16B). In contrast, mid-S accessions exhibited a strong delay in flowering under S-deficiency relative to control conditions with no change in flowering time under short-pulse treatment (Fig 16B). The delay in flowering in mid-S group suggests that sulfur limitation prolongs the vegetative phase rather than triggering an early reproductive transition in this group. High-S accessions displayed ratios below 1, suggesting that flowering occurred earlier under sulfur-deficient conditions compared to control plants, and showed a

similar response even under short-pulse treatment (Fig. 16B). Such accelerated flowering under nutrient limitation has previously been associated with stress-induced reproductive transitions in *Arabidopsis* (Nikiforova et al., 2005). Together, these results indicate that the three sulfur groups differ primarily in the sensitivity of their flowering responses to sulfur availability.

Reproductive performance, assessed by silique number, revealed that high-S accessions were particularly vulnerable to sulfur stress (Fig. 16C). Under S-deficiency, total seed weight declined across all groups except mid-S, but the group showed a significant decline in silique number, indicating prioritization of maintaining seed quality over seed quantity (Supplementary Fig. 5B). Reductions in silique number were also evident more strongly in high-S accessions under sulfur deficiency. Low-S accessions showed only a moderate decline in silique number, indicating relative reproductive stability (Fig. 16C). Notably, the short-pulse treatment partially restored silique numbers in low-S and mid-S accessions, whereas high-S accessions failed to recover, maintaining significantly lower silique numbers compared to control (Fig. 16C).

Besides, we also tested the seeds harvested for their total-S content by analysing elemental composition of the seeds using ICP-MS under both control and S-deficient conditions (Supplementary Fig. 6). In contrast to the pronounced differences observed in leaf sulfur levels, total sulfur content in seeds did not differ significantly among the three S-content groups under control conditions (Fig. 16D). This suggests that sulfur allocation to seeds is tightly regulated and buffered against variation in vegetative sulfur status. However, under S-deficient conditions, seed total-S decreased significantly across all groups (Fig. 16D). This indicates that while seed sulfur composition is maintained under sufficient sulfur supply, prolonged sulfur limitation reduces the overall sulfur available for reproductive allocation, resulting in a similar decline in seed sulfur content across genotypes. Together, these findings suggest that although natural variation strongly influences vegetative sulfur pools, reproductive sulfur allocation is more conserved and becomes uniformly constrained when sulfur supply is limiting.

Collectively, these results demonstrate that sulfur deficiency imposes group-specific fitness costs that reflect underlying natural variation in sulfur status. Low-S accessions adopt a conservative strategy characterized by enhanced vegetative growth and stable flowering and reproductive output. Mid-S accessions showed restricted growth with delayed flowering and moderate yield penalties under stress. High-S accessions, however, appear highly plastic in their developmental responses, displaying accelerated flowering, reduced vegetative growth, and pronounced reproductive losses. This pattern reinforces the conclusion that sulfur limitation is particularly unfavorable for high-S accessions, consistent with their stronger S-starvation responses and more oxidative stress discussed before.

A-i

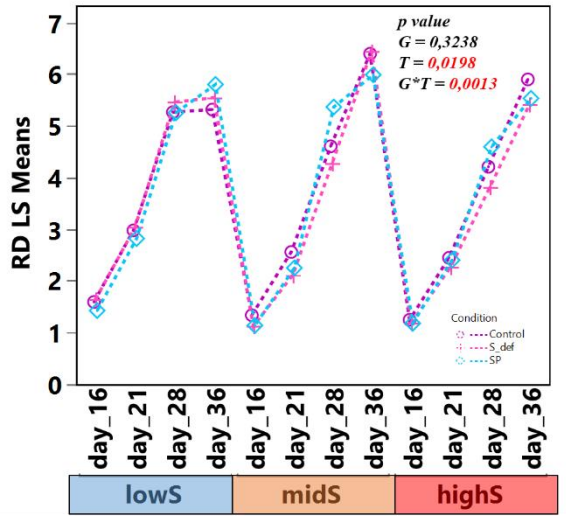
p value
G = 0,3238
T = 0,0198
G*T = 0,0013
RD LS Means
Condition
Control
S_def
SP
day_16
day_21
day_28
day_36
lowS
midS
highS

A-ii

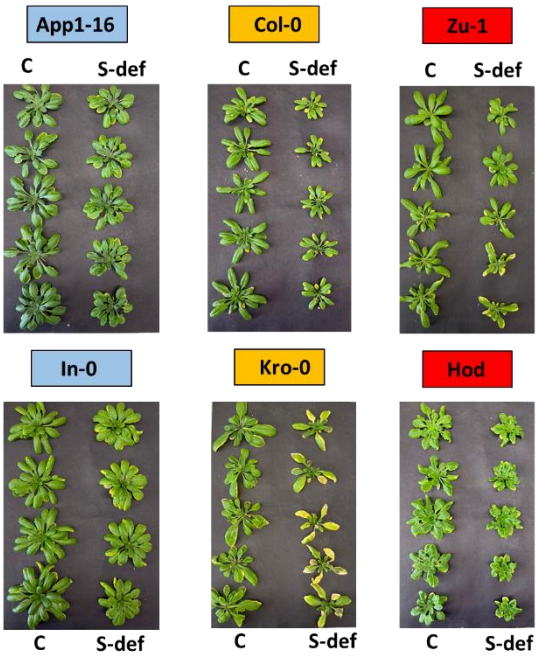
App1-16
Col-0
Zu-1
In-0
Kro-0
Hod
C
S-def

B

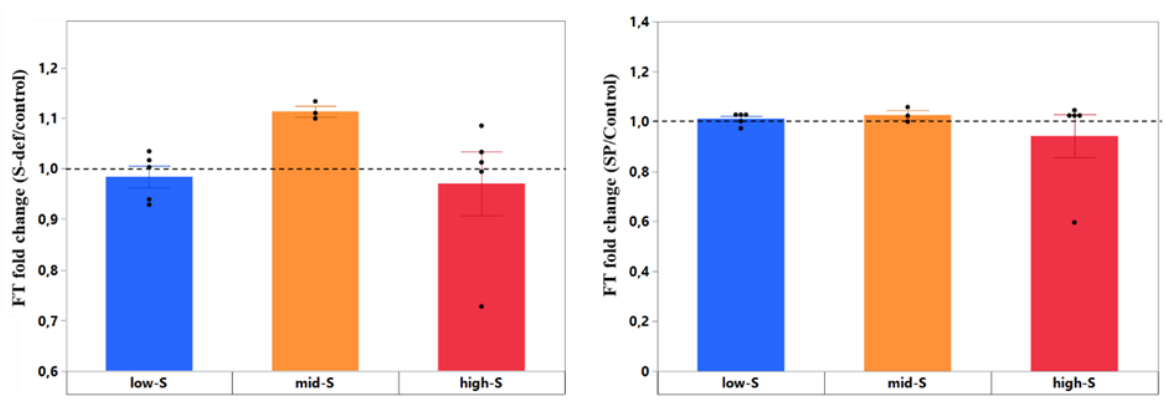
FT fold change (S-def/control)
FT fold change (SP/Control)
low-S
mid-S
high-S

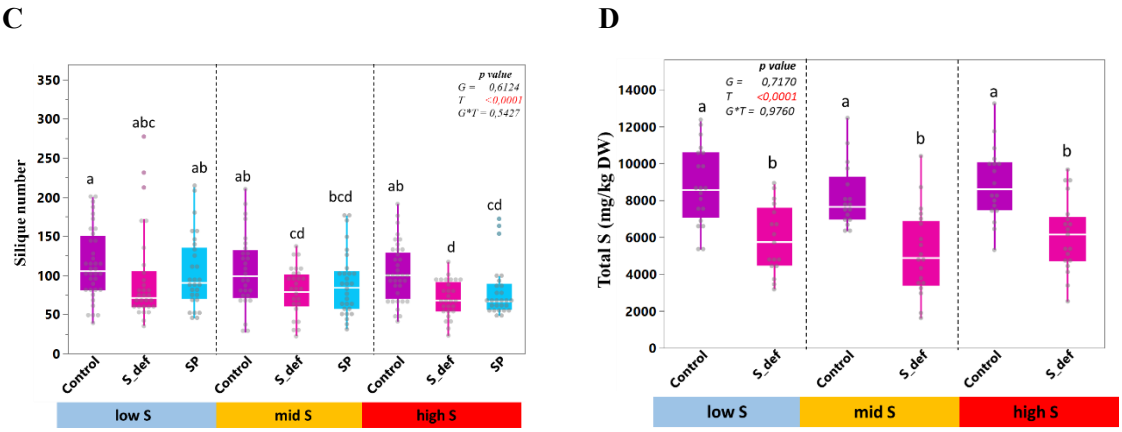

Figure 16: Growth and reproductive traits show contrasting responses to sulfur deficiency among S-content groups (A) (i) Least Square Means (LSMeans) of Rosette diameter (RD) (in cm) measured from day 16 to day 28 under Control (750 µM), S-def (0 µM) and Short pulse conditions with (ii) Pictures of plant taken at day 36 under Control and S-def condition representing App1-16, In-0 (low-S group); Kro-0, Col-0 (mid-S group); Zu-1, Hod (high-S group) **(B)** Fold change in flowering time in response to S-deficient and short-pulse treatment **(C)** Number of siliques quantified in low-S (blue), mid-S (orange), and high-S (red) accessions grown under control (750 µM sulfate), sulfur-deficient (0 µM), or short-pulse (SP; intermittent supply) conditions **(D)** Total-S (mg/ kg DW) in seeds under control (750 µM sulfate), and sulfur-deficient (0 µM). Plants were grown in a 9:1 sand: soil mix and fertilized twice weekly with the indicated S regimes. Data were analyzed using mixed models, followed by post-hoc test; different letters indicate significant differences ($P < 0.05$). Boxplots show means ± SE (n= 8 per accession).

3.7 Influence of parental sulfur availability on metabolic responses in the next generation

Previous studies have reported that epigenetic mechanisms form an integral part of the plant sulfur-deficiency response, as sulfur limitation can induce genome-wide DNA methylation in plants (Huang et al., 2016; Luo et al., 2025). We were, therefore, interested in investigating how genetically driven variation among accessions and environmentally induced variation arising from sulfur deficiency together influence metabolic and developmental responses in the next generation. In addition to the well-documented decline in total sulfur under sulfur-limiting conditions, our ionomics analysis of seeds harvested from accessions belonging to different sulfur groups revealed several group-specific elemental responses (Supplementary Fig. 6). Along with a consistent decrease in sulfur content, we observed a significant increase in molybdenum accumulation across all groups. Furthermore, cadmium levels were significantly elevated in the low-S and mid-S groups (Supplementary Fig. 6). These findings further indicated that sulfur limitation not only alters sulfur partitioning in seeds but also affects the accumulation of other elements in a group-dependent manner, potentially influencing seed quality and subsequent plant performance. Thus, we aimed to test whether seeds produced under sulfur-deficient conditions could prime the subsequent generation for improved performance or altered stress responses.

To address this, we selected five representative accessions, including two each from the low-S (App1-16, In-0) and high-S (Zu-1, Hod) groups, along with Col-0 from the mid-S group. Seeds harvested from plants grown under control (C) and sulfur-deficient (S-) conditions in the parental generation were used to generate the next generation. These seeds (App1-16_C, App1-16_S-, In-0_C, In-0_S-, Col-0_C, Col-0_S-, Zu-1_C, Zu-1_S-, Hod_C, and Hod_S-) were subsequently grown again under control and sulfur-deficient conditions in a sand: soil mixture (Fig. 17A).

The next-generation plants were analyzed for anion content (NO_3^-, PO_4^{2-}, SO_4^{2-}), thiol content (cysteine and glutathione), and key developmental traits, including flowering time and silique number. We observed that sulfate accumulation patterns in the next generation closely resembled those of the parental generation. However, in Hod, under control conditions, plants derived from S-deficient parents showed a significant decline in sulfate compared to plants from the S-sufficient condition (Fig 17B). Hod also exhibited the strongest relative decline in sulfate content under sulfur deficiency, followed by Zu-1, Col-0 (mid-S), Kro-0 (mid-S), and In-0 (low-S). In contrast, the low-S accession App1-16, similar to its parental generation, did not show a significant reduction in sulfate levels under sulfur-deficient conditions (Fig. 17B). Nitrate and phosphate contents also followed trends comparable to those observed in the parental generation, with no major differences detected between generations (Supplementary Fig. 7A & B).

In addition to anion profiles, thiol contents (cysteine and glutathione) in the next generation largely mirrored parental responses, consistent with our earlier observations that sulfur-dependent thiol regulation is strongly genotype dependent and primarily driven by current sulfur availability rather than parental sulfur status (Supplementary Fig .8). Similarly, reproductive output, as measured by silique number, did not show major deviations from parental trends (Fig. 17D). Notably, flowering time exhibited genotype-specific responses in the next generation (Supplementary Fig. 7C). Fold change analysis of flowering time revealed that low-S accessions specially App1-16, derived from sulfur-deficient parents displayed a delay in flowering under sulfur deficiency in the next generation. In addition, Col-0 maintained stable flowering time regardless of parental sulfur status, while high-S accessions, i.e., Zu-1, showed accelerated flowering in plants derived from sulfur-deficient parents. Together, these results indicate that parental sulfur limitation can influence flowering-time regulation in the subsequent generation in a genotype-dependent manner, with the clearest responses observed in App1-16 and Zu-1, although these genotypes exhibit opposite shifts in flowering behavior (Fig. 17C).

Taken together, these results indicate that, for most metabolic traits examined, sulfur availability in the parental generation does not lead to strong or fixed transgenerational inheritance effects in the immediate next generation. Instead, the majority of anion and thiol responses appear to be predominantly governed by the sulfur environment experienced by the current generation. Nevertheless, the observed flowering time shift in low-S accessions points to the possibility that parental sulfur status may modulate specific developmental responses.

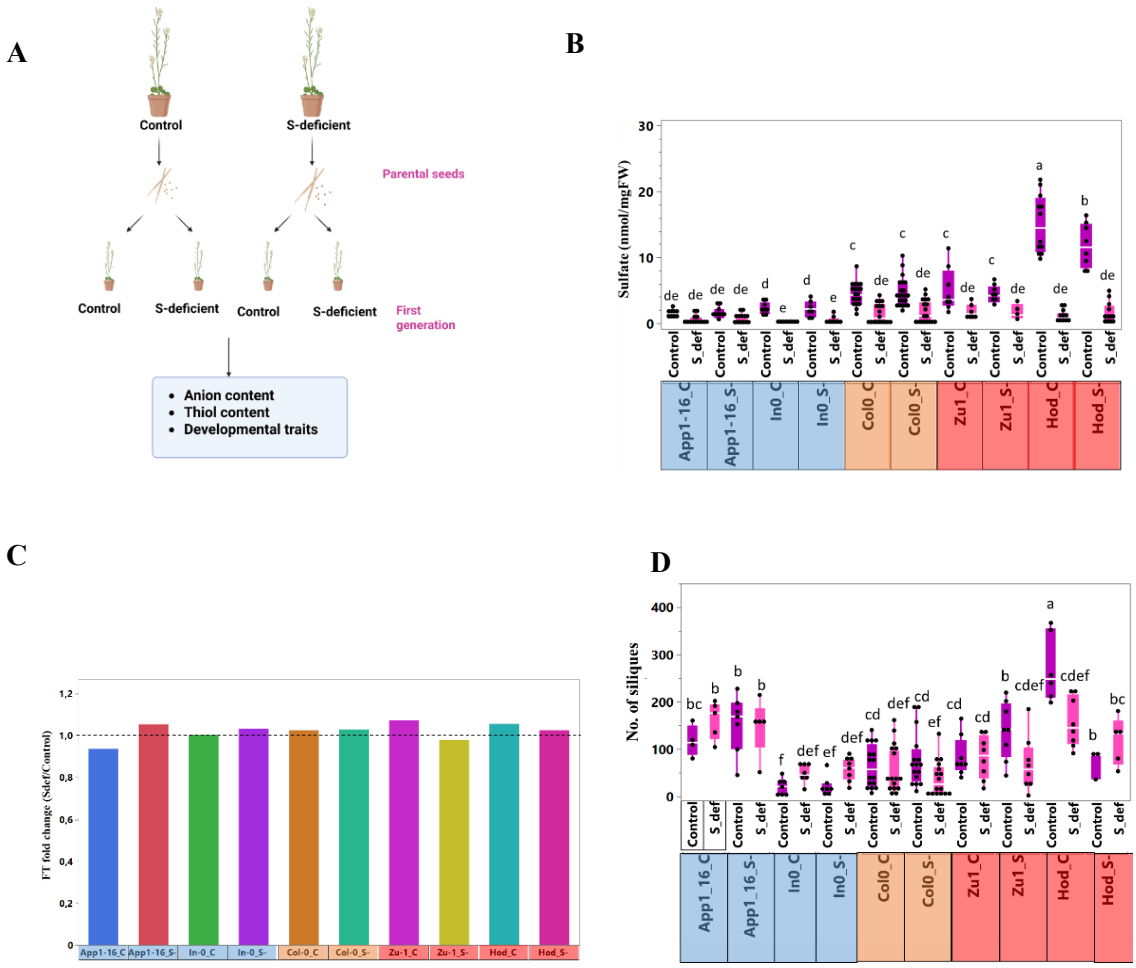

Figure 17: Parental sulfur availability influences sulfate accumulation and reproductive traits in the next generation. (A) Schematic overview of the experimental design for the parental-progeny study. Seeds harvested from plants grown under control (C) or sulfur-deficient (S-) conditions in the parental generation were used to generate the next generation, which was subsequently grown again under control or sulfur-deficient conditions. **(B)** Shoot sulfate content (nmol g^{-1} FW), **(C)** Fold change of flowering time in response to S-deficient condition compared to control **(D)** number of siliques in App1-16 and In-0 (low-S group; blue), Col-0 (mid-S group; orange), and Zu-1 and Hod (high-S group; red) accessions. Plants were grown in a 9:1 sand: soil mixture and fertilized twice weekly with either control nutrient solution containing 750 µM sulfate or sulfur-deficient solution (0 µM sulfate). For the next-generation experiment, seeds derived from parental plants grown under control (C) or sulfur-deficient (S-) conditions were germinated and cultivated under the same two sulfur regimes. At week 5, the 7th–8th rosette leaves were harvested for analysis (n = 8 per accession per treatment). Data were analyzed using two-way ANOVA followed by post hoc tests. Different letters indicate statistically significant differences among genotypes and treatments ($P < 0.05$). Boxplots represent means ± SE.

3.8 Multi-trait analysis reveals distinct sulfur response strategies both at the population and genotype levels

To investigate coordinated physiological responses to sulfur deficiency, a multi-trait principal component analysis (PCA) was performed using delta (Δ) values of a trait calculated as a difference between Least square means (LSMeans) of the trait at control and S-deficient condition which represents changes in physiological, metabolic, and growth-related traits between sulfur-deficient and control conditions. The use of Δ values or fold change differences allowed direct comparison of trait responses independent of baseline genotype differences, thereby capturing sulfur-specific physiological adjustments.

We first used the fold change differences of traits for all 14 accessions to explore adaptive strategies under S-deficiency at the population level (Fig 18A & B). We found, PCA had clear structure in the multivariate response space. The first two principal components explained 52.6% of the total variance, with PC1 accounting for 29.7% and PC2 for 22.9% of the variation. PC1 was primarily driven by traits related to nutrient uptake and transport, including fold changes in anion content in roots and shoots, ICP-based elemental accumulation in shoots, root uptake, and translocation. This axis, therefore, represents variation in nutrient acquisition and redistribution capacity under sulfur deficiency. In contrast, PC2 was dominated by sulfur metabolic and growth-related traits, including thiols in roots and shoots, ICP content in seeds, rosette diameter (RD) (day 36), and flowering time, reflecting differences in metabolic adjustment and developmental responses to sulfur limitation (Fig. 18B).

The distribution of accessions along the principal component axes revealed clear separation among sulfur-response groups. High-sulfur accessions clustered predominantly along PC1, which was strongly associated with nutrient uptake and translocation traits, indicating that variation among these accessions was largely driven by differences in acquisition and transport capacity under sulfur deficiency. In contrast, low-sulfur accessions were separated primarily along PC2, which was dominated by sulfur metabolic and growth-related traits, suggesting that although these accessions increase sulfur uptake, their response to sulfur deficiency was more strongly shaped by internal metabolic adjustment and allocation processes. Mid-sulfur accessions occupied an intermediate position between these two extremes, consistent with a more plastic or mixed response strategy. Together, these results indicate that sulfur deficiency elicits coordinated but mechanistically distinct physiological responses across accessions, with genotypes differing in the relative contribution of nutrient acquisition versus metabolic adjustment rather than in the presence or absence of these responses (Fig. 18A).

To further resolve genotype-specific behaviour, principal component analysis (PCA) was performed at the individual accession level where we utilized the phenotypic data from six accessions, used in our prior analysis. This analysis confirmed substantial genotypic variation in sulfur response strategies (Fig. 18C & D). The first principal component (PC1), explaining 33% of the total variance, was primarily driven by metabolic and growth-related traits, including fold change differences in thiol content, gene

expression, flowering time, and anion accumulation, indicating differences in internal sulfur utilization and developmental adjustments (Fig 18D). The second principal component (PC2), accounting for 30.7% of the variance, was dominated by traits associated with nutrient acquisition and allocation, such as elemental composition (ICP content), root uptake, and rosette diameter (day 35), reflecting variation in nutrient uptake efficiency and biomass investment under sulfur deficiency. Distinct positioning of individual genotypes was observed within this multivariate space. Accessions such as Hod and In-0 exhibited strong responses along either the metabolic or uptake axes, indicating contrasting sulfur response strategies. Kro-0 showed a pronounced shift along the uptake-associated axis, suggesting a strategy characterized by enhanced nutrient acquisition and allocation rather than metabolic adjustment. In contrast, App1-16 and Zu-1 displayed relatively weak responses across both principal components, indicative of a more conservative physiological adjustment to sulfur limitation. Col-0 occupied an intermediate position, reflecting balanced contributions from both metabolic and uptake-related traits (Fig. 18C).

Together, these results demonstrate that sulfur deficiency leads to coordinated yet divergent physiological responses among *Arabidopsis* accessions. Rather than exhibiting a uniform response, genotypes employ distinct combinations of nutrient acquisition, sulfur metabolic regulation, and growth adjustment, underscoring the complex and genotype-dependent nature of sulfur use efficiency.

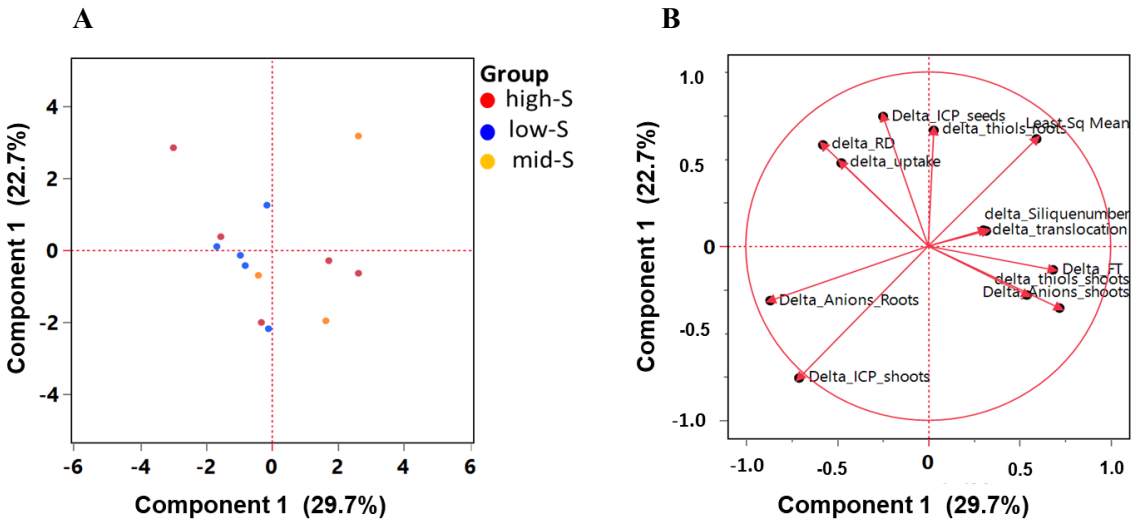

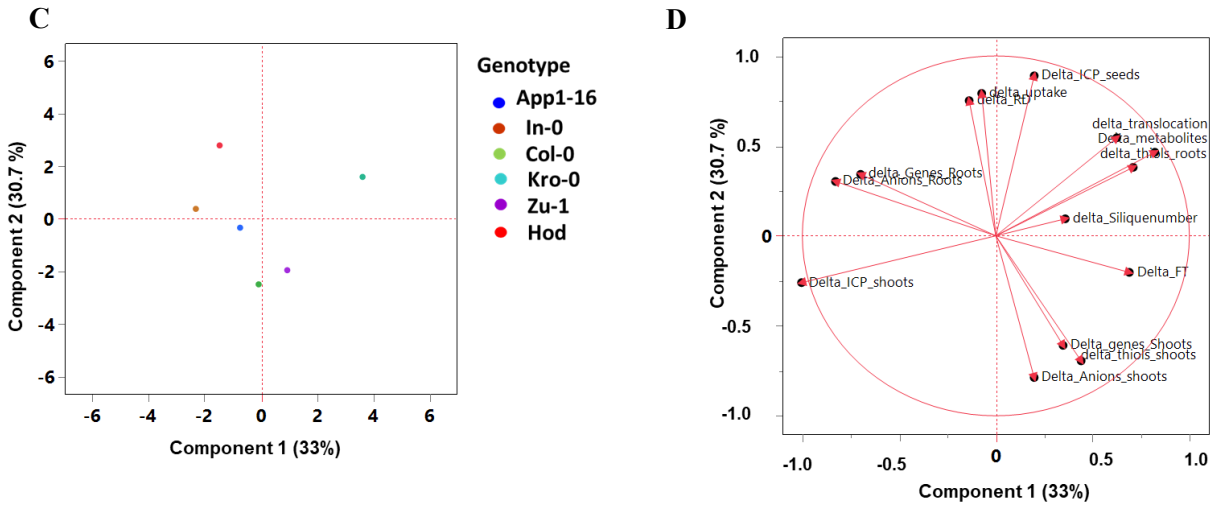

Figure 18: Principal component analysis of multi-trait responses to sulfur deficiency. (A) PCA score plot showing clustering of all 14 accessions grouped according to S-content. Red, blue, and orange symbols represent high-S, low-S, and mid-S groups, respectively. **(B)** Corresponding loading plot showing the contribution of individual traits to PC1 and PC2 across all accessions. **(C)** PCA score plot at the genotype level, including six representative accessions (App1-16; In-0; Col-0; Kro-0; Zu-1; Hod) under control and sulfur-deficient conditions. **(D)** Loading plot illustrating the contribution of individual traits to PC1 and PC2 across the six accessions. Δ (delta) values represent the change in each trait in response to sulfur deficiency, calculated as the difference between LSMeans under sulfur-deficient and control conditions (Δ = S-deficient − Control).

4. RESULTS - Chapter 2: Transcriptomic and metabolic signatures underlying sulfur-content variation during early development in *Arabidopsis thaliana*

4.1 High-S group shows more prominent transcriptional programming under S-limitation

Several studies have reported that sulfur (S) deficiency induces a coordinated reprogramming of gene expression in order to maintain cellular homeostasis under nutrient stress conditions (Yoshimoto et al., 2002; Takahashi et al., 2007; Maruyama-Nakashita et al., 2017). In addition to these previously reported responses, the contrasting physiological and metabolic behaviors observed between the high-S and low-S groups in our study, as discussed in the preceding chapters, prompted us to further investigate their transcriptional responses under S-deficient conditions.

We selected the same six *Arabidopsis* accessions used in earlier analyses, namely App1-16, In-0, Col-0, Kro-0, Zu-1, and Hod. Plants were grown for 18 days under either control (750 µM sulfate) or sulfur-deficient (15 µM sulfate) conditions, after which root tissues were harvested for transcriptomic analysis. Roots were specifically chosen for RNA extraction as they represent the primary site for sulfate uptake and sensing. For each genotype and condition, three biological replicates were used. Total RNA was isolated and sequenced using the Illumina platform at Novogene (UK). On average, at least 30 million high-quality reads per sample were generated. The reads were mapped to the *Arabidopsis thaliana* reference genome (TAIR10) using HISAT2, with more than 95% of the reads mapping uniquely. Only uniquely mapped reads were retained and quantified at the gene level using HTSeq-count.

Differential gene expression analysis was performed using DESeq2, using $q<0.05$ and $|\log_2 FC|>1$ as cut-off. To identify robust and commonly regulated genes under sulfur deficiency, an intersection analysis was subsequently applied across all six accessions, resulting in a stringent set of differentially expressed genes (DEGs). Furthermore, principal component analysis (PCA) was conducted on variance-stabilized (vst) normalized read counts to examine global transcriptional variation and sample clustering patterns (Fig. 19A). PCA analysis revealed that genotypic differences accounted for a larger proportion of the variance than treatment effects, with the exception of Hod, which exhibited a stronger separation between control and sulfur-deficient conditions (Fig. 19A). Principal component 1 (PC1) explained 17.92% of the total variance, while PC2 accounted for 12.38%. No clear clustering was observed based solely on sulfur treatment, and each accession clustered independently, indicating strong genotype-specific transcriptional signatures (Fig. 19A)

Notably, a clear trend emerged in the number of differentially expressed genes across the accessions. With increasing sulfur content, the number of significant DEGs also increased. The high-S accessions Hod exhibited the highest number of DEGs (1486 genes) in response to sulfur deficiency, followed by Zu-1 with 550 DEGs. In contrast, App1-16, belonging to the low-S group, displayed the fewest

transcriptional changes, with only 174 significant DEGs, while Kro-0 showed a similarly low response with 266 DEGs. Among the remaining accessions, Col-0, another mid-S genotype, exhibited 359 DEGs, followed closely by In-0 from low-S group with 339 induced DEGs under S-deficiency (Fig 19B).

Collectively, these results demonstrate that high-S accessions exhibit a more pronounced transcriptional response to sulfur limitation compared to low- and mid-S groups. The substantially higher number of differentially expressed genes in the high-S group suggests enhanced transcriptional reprogramming in response to sulfur deficiency, likely reflecting their increased sensitivity to sulfur stress as reported in the earlier chapter, in their metabolic and developmental traits.

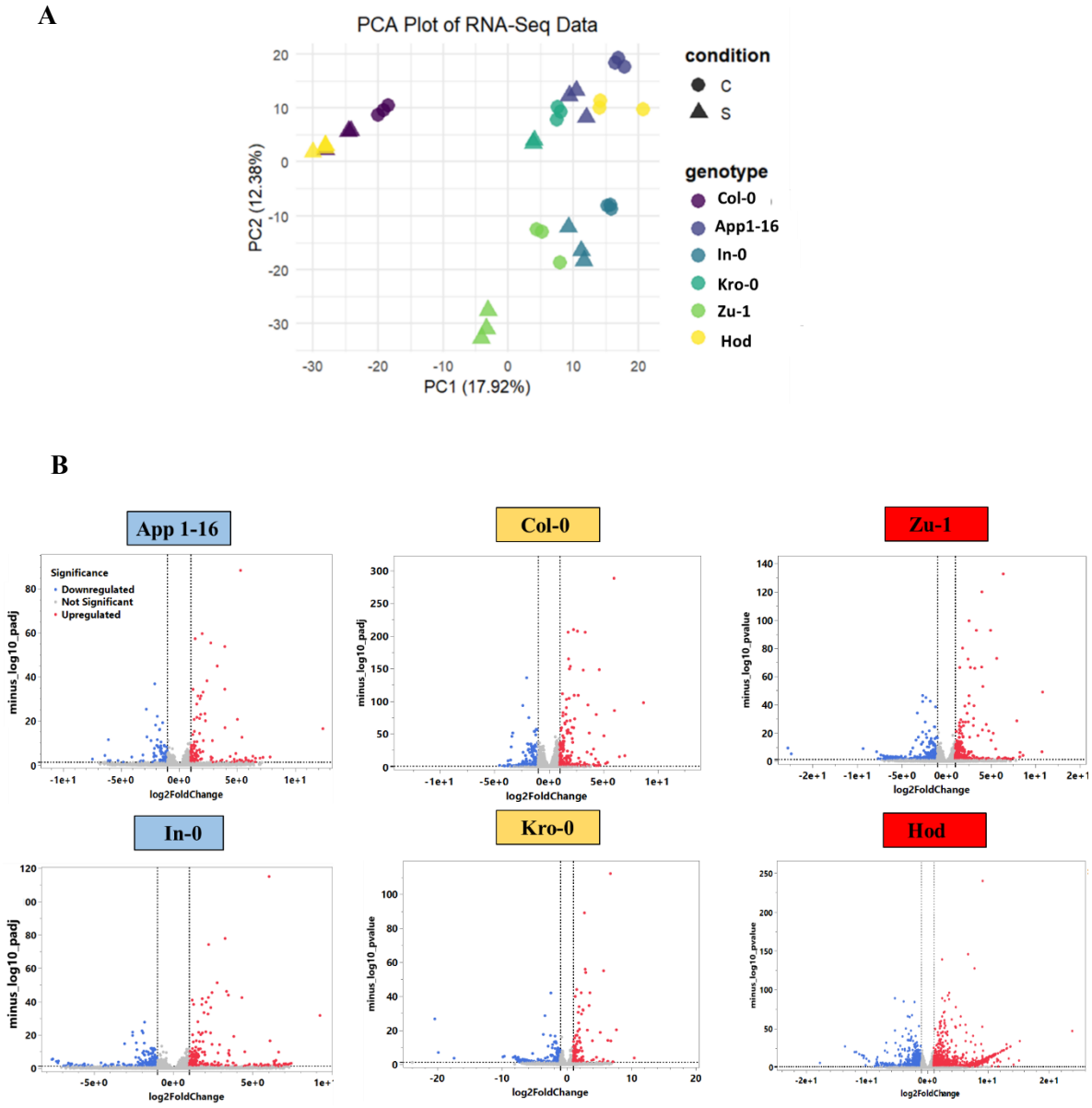

Figure 19: Transcriptomic responses to sulfur deficiency across *Arabidopsis* accessions. (A) Principal component analysis (PCA) of RNA-seq data from roots of six *Arabidopsis* accessions

belonging to low S (App1-16 and In-0), mid S (Col-0 and Kro-0), high S (Zu-1 and Hod) grown under control (750 µM sulfate) and S-deficient (15 µM sulfate) conditions. **(B)** Volcano plots of DEGs (padj < 0.05, |log2FC| > 1) under S-deficiency. Red dots indicate upregulated DEGs, and blue dots represent downregulated DEGs and gray area in the center represents not significant DEGs.

4.2 Only 55 DEGs are shared among all accessions

In order to identify a conserved transcriptional response to sulfur deficiency across all six accessions, we intersected the lists of DEGs obtained for each accession in response to S-deficiency. This analysis revealed a relatively small core set of 55 genes that were commonly regulated across all genotypes (Fig. 20A), indicating that only a limited subset of genes exhibits a uniform response to sulfur limitation irrespective of genetic background.

This conserved gene set included several well-characterized sulfur-responsive marker genes, such as *SHM7, SULTR2;1, LSU1, SDI1, APS4,* and *SERAT3;1,* all of which have been previously implicated in sulfur assimilation and sulfur starvation responses (Fig. 20B). The presence of these genes among the shared DEGs confirms the robustness of the dataset and highlights a conserved core sulfur-responsive transcriptional module across accessions. In addition, to further check the validity of the dataset obtained from RNA-Seq, we performed qPCR on ten of the S-deficiency marker genes in roots of these six accessions from an independent experiment. We then compared RNA-Seq results with qPCR by performing correlation analysis and most of the genes showed high R^2 proving our RNA-Seq results (Supplementary Fig. 9).

To further characterize the functional relevance of these shared DEGs, we performed gene ontology (GO) enrichment analysis. This revealed significant enrichment of biological processes related to sulfur metabolism, including sulfate assimilation, sulfur compound biosynthetic process, S-glycoside biosynthetic process, serine family amino acid biosynthetic process, and glucosinolate biosynthetic process (Fig. 20C). These enriched categories are consistent with known physiological adjustments that occur under sulfur limitation and underscore the central role of sulfur-related metabolic pathways in the conserved transcriptional response. Interestingly, apart from GO categories connected to the usual S-starvation response, we also observed categories that are not directly connected to S-homeostasis. These are in particular genes from the enriched GO term "regulation of circadian rhythm" *CCA1 (CIRCADIAN CLOCK ASSOCIATED 1), LCL5/ RVE8 (REVEILLE 8), LHY (LATE ELEONGATED HYPOCOTYL 1),* thus suggesting implication of S-starvation in the circadian clock (Supplementary Fig. 10). Several enriched GO terms were associated with environmental stress responses, such as response to external stimulus, and response to ultraviolet radiation, including genes *SDI1 (SULFUR DEFICIENCY-INDUCED 1), PYD4 (PYRIMIDINE 4), 4CL3 (4-COUMARATE: CoA LIGASE 3), CHS (CHALCONE SYNTHASE), HYH (ELONGATED HYPOCOTYL 5 HOMOLOGUE)* and others indicating involvement of broader stress-response pathways in addition to sulfur metabolism (Supplementary Fig. 10). Additionally, genes like *AK3 (ASPARTATE KINASE 3), IMD1 (ISOPROPYLMALATE*

DEHYDROGENASE 1), IMS2 (2-ISOPROPYLMALATE SYNTHASE 2), BCAT4 (BRANCHED-CHAIN AMINOTRANSFERASE4) were enriched in GO terms related to amino acids i.e. alpha-amino biosynthetic process and branched chain amino acid metabolic process (Supplementary Fig. 10). Furthermore, genes related to secondary metabolite biosynthesis, i.e., flavonoid biosynthesis and metabolic response, were also highly enriched, consisting of *CHIL (CHALCONE ISOMERASE LIKE), FLSI (FLAVONOL SYNTHASE 1)*, and *F3'H (FLAVANONE 3-HYDROXYLASE)* (Supplementary Fig. 10). We also observed that among the 55 shared DEGs, the majority (41 genes) were upregulated under sulfur-deficient conditions, whereas only 14 were downregulated. This bias toward upregulation suggests that sulfur deficiency primarily induces activation of transcriptional programs involved in sulfur acquisition, assimilation, and metabolic reprogramming rather than widespread transcriptional repression.

To further explore whether these conserved DEGs exhibited accession-specific expression patterns, we transformed the raw read counts using variance-stabilizing transformation (VST) in DESeq2 and calculated Δ expression values (VST_S - VST_Control) for each accession. These values were subsequently averaged within the low-S, mid-S, and high-S groups. Genes were then ranked based on the magnitude of their group-wise expression differences (defined as max − min across groups), and the top ten genes showing the strongest group-specific variation were selected for detailed analysis (Fig. 20D). This analysis successfully recovered several well-established regulators of sulfur metabolism and signalling, including *APR2, SHM7, SERAT3;1, SERAT3;2, SULTR1;2,* and *CYP79B2*, further validating the biological relevance of the approach. Importantly, it also identified several genes not previously associated with sulfur deficiency responses, such as *MSRB5 (METHIONINE SULFOXIDE REDUCTASE B5), DTX9 (DETOXIFICATION 9),* and *SFP1 (SENESCENCE-ASSOCIATED SUGAR TRANSPORTER1),* suggesting potential novel components of sulfur-responsive regulatory networks (Fig. 20D).

Interestingly, expression profiling revealed that several key sulfur-responsive genes, including *SHM7, SULTR1;2,* and *MSRB5,* were strongly induced in the high-S and mid-S accessions under sulfur deficiency, whereas their expression remained comparatively unchanged in the low-S accessions (Fig. 20D). This differential response suggests that low-S accessions employ a more restrained or fine-tuned transcriptional adjustment to sulfur limitation. Such a targeted and controlled transcriptional response may contribute to their ability to maintain sulfate levels and sustain fitness-related traits under sulfur stress, whereas high-S accessions appear to mount a more pronounced transcriptional reprogramming that is accompanied by greater physiological sensitivity to sulfur deficiency (Fig. 20D).

Collectively, these findings demonstrate that although only a small core set of sulfur-responsive genes is conserved across accessions, the magnitude and regulation of their expression are strongly genotype dependent. This highlights the importance of genetic background in shaping sulfur-responsive

transcriptional networks and supports the conclusion that sulfur adaptation strategies vary substantially among *Arabidopsis* accessions.

A

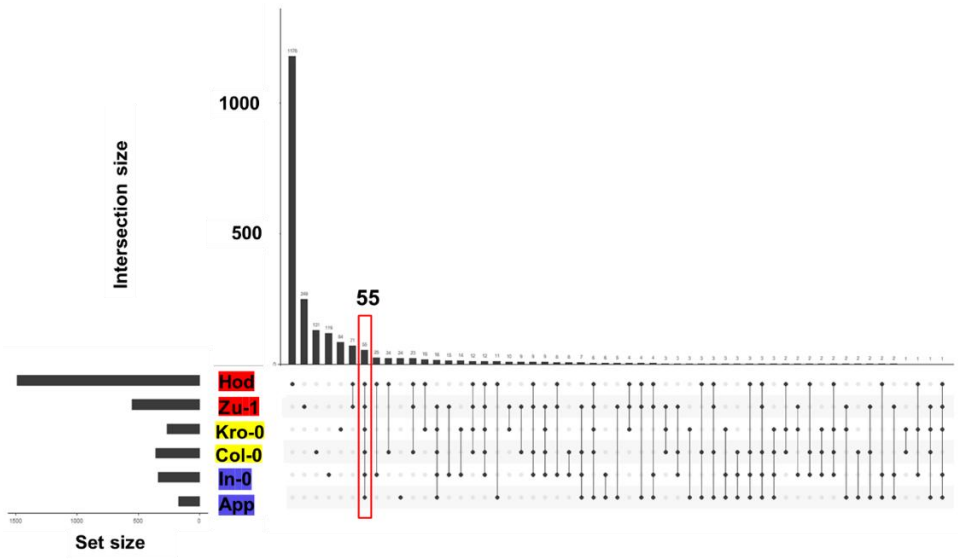

B

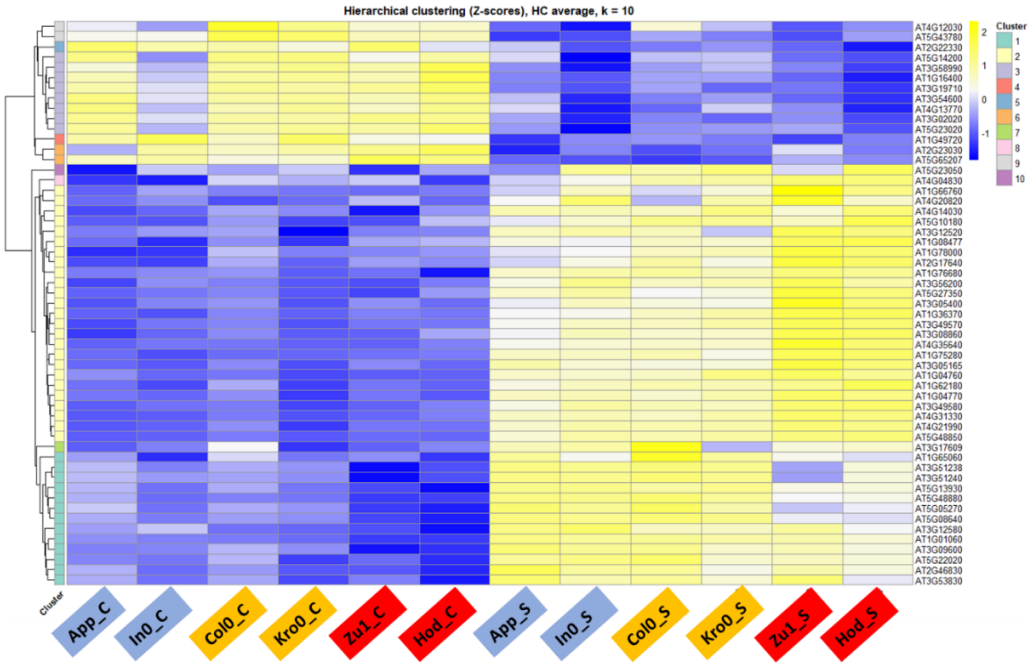

C

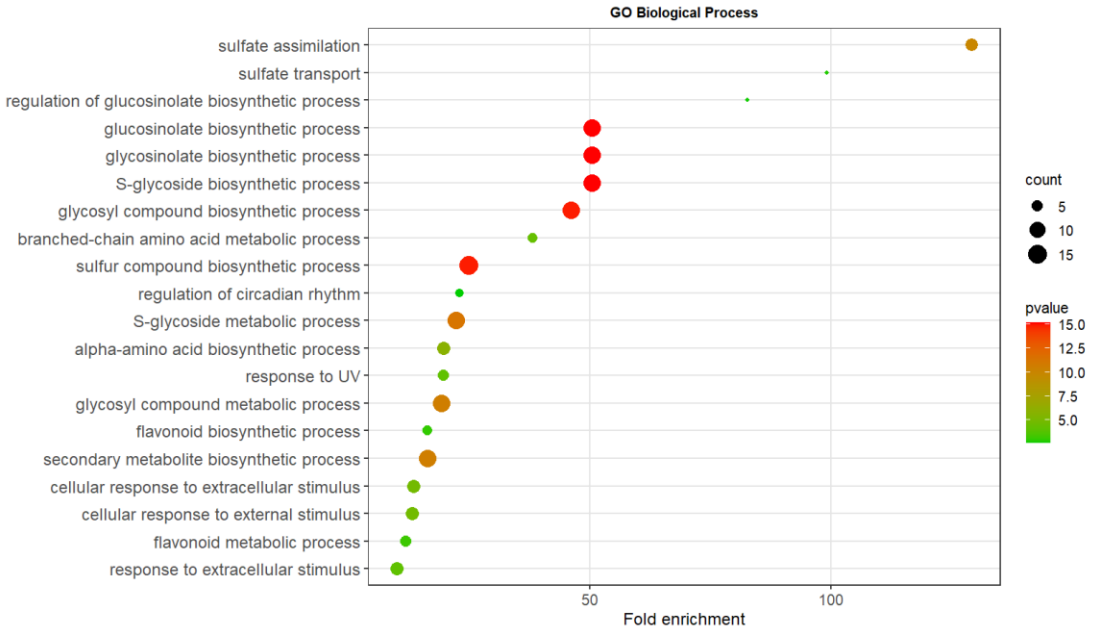

D

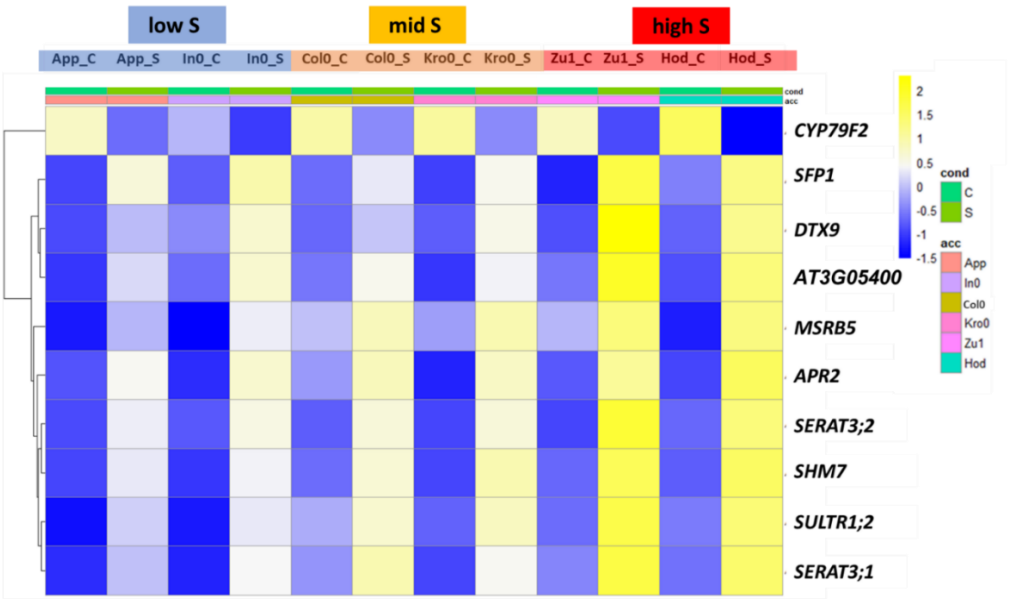

Figure 20: Core transcriptional responses and group-specific candidates under sulfur deficiency. **(A)** Upset plot showing the overlap of DEGs between six accessions belonging to low S (App1-16 and In-0), mid S (Col-0 and Kro-0), high S (Zu-1 and Hod) in response to S-deficiency, identifying 55 shared DEGs across all accessions. **(B)** Hierarchical clustering of 55 intersecting DEGs between six accessions. Different colors of the box on the extreme left correspond to different clusters (1-10). **(C)** Functional gene ontology (GO) enrichment analysis of shared DEGs. **(D)** Heatmap of the top 10 candidate genes showing group-specific variation in expression levels based on ΔVST (S - C) values. We computed per-accession expression changes as ΔVST = (VST count $_{S\text{-}def}$ - VST count $_{contol}$) (DESeq2 variance-stabilized

counts), averaged Δ VST within low-, mid-, and high-S groups, and ranked genes by the spread across groups (max–min). Candidate sets were visualized as heatmaps of z-scored VST values.

4.3 Assessing Intra-Group Similarity of Transcriptomic Responses to Sulfur Deficiency

After identifying the core set of shared DEGs across all accessions belonging to the three sulfur-content groups, we next examined the transcriptional responses within each group under sulfur deficiency. Specifically, we aimed to determine whether accessions belonging to the same sulfur-content group exhibit similar transcriptional responses to S deficiency. To address this, treatment-responsive DEGs identified for the two accessions within each group were intersected to obtain overlapping genes that were consistently regulated in both accessions. This approach allowed us to characterize the shared transcriptional response within each group and assess the degree of similarity in their regulatory responses to sulfur deficiency.

For the low-S group, comparison of App1-16 and In-0 revealed a substantial overlap in transcriptional responses to sulfur deficiency. Comparison of the two accessions revealed 108 shared DEGs, while 66 and 231 genes were uniquely regulated in App1-16 and In-0, respectively (Fig. 21A). Among the shared DEGs, 63 genes were upregulated and 45 were downregulated under sulfur deficiency (Fig. 21B). To further understand the functional relevance of these shared DEGs, we performed gene ontology (GO) enrichment analysis separately for the upregulated and downregulated gene sets.

Among the upregulated genes, as expected several enriched GO terms were associated with sulfur assimilation and sulfur compound metabolism, including sulfate assimilation, sulfate transport, and sulfur compound biosynthetic process (Fig. 21C). Representative genes associated with these categories included known regulators like *APR2, APR3, SULTR2;1* (annotated as *AST68*) which encode key enzymes involved in sulfate assimilation and translocation (Supplementary Fig 11A). In addition, classical sulfur starvation marker genes such as *SDI1/SDI2* and *LSU1/LSU3* were also induced, indicating activation of the sulfur deficiency signalling network (Supplementary Fig. 11A). Besides sulfur metabolism, several enriched GO terms were related to secondary metabolism, particularly flavonoid biosynthetic process, flavonoid metabolic process, and pigment biosynthetic process (Fig. 21C). Consistent with this enrichment, apart from genes described in previous section for flavonoid biosynthesis, some genes like *A11* (*CHALCONE FLAVANONE ISOMERASE*), *UDP-GLUCOSYL TRANSFERASE*S i.e. *UGT78D2, UGT789C1* showed increased expression under sulfur deficiency (Supplementary Fig 11B). Activation of flavonoid and pigment biosynthesis may represent a metabolic adjustment toward sulfur-independent secondary metabolites, which could help maintain protective functions under sulfur deficient condition.

Among upregulated DEGs, GO terms were also enriched for responses to external and extracellular stimuli, UV, red, and far-red light, and cellular responses to red or far-red light, indicating that sulfur deficiency in low-S accessions was accompanied by broader environmental response signalling (Fig.

21C). Several genes, such as *ELIP (EARLY LIGHT-INDUCIBLE PROTEIN), HBP2 (HEME (TETRAPYRROLE) BINDING PROTEIN 2), ATIPS2 (INDUCED BY PI STARVATION 2),* and *SIG5 (SIGMA FACTOR 5),* are induced in these categories, suggesting integration of sulfur stress with light signalling pathways (Supplementary Fig 11A). Another notable enriched category among upregulated genes was detoxification**,** indicating sulfur deficiency may trigger a protective response to limit stress-related cellular damage (Fig. 21C). In addition, enrichment of the regulation of circadian rhythm points to a connection between sulfur deficiency and temporal regulatory networks (Fig. 21C). This is particularly interesting because sulfur-responsive transcription has been linked to circadian control previously, and the induction of *LHY, LCL5, CCA1,* and *HYH* suggests that low-S accessions may coordinate sulfur stress responses with daily timing mechanisms (Supplementary Fig. 11A). Furthermore, GO terms related to amino acid metabolism, particularly L-serine metabolic process and serine family amino acid biosynthesis, were enriched (Fig. 21C). Serine is a key precursor for cysteine biosynthesis, and induction of serine-related metabolic pathways may therefore support increased sulfur assimilation under nutrient-limiting conditions.

In contrast, the downregulated shared DEGs were strongly enriched for pathways related to glucosinolate and glycosylated secondary metabolite biosynthesis, including glucosinolate biosynthetic and metabolic process, S-glycoside biosynthetic process and metabolic process, and glycosyl compound biosynthetic/metabolic process (Fig. 21C). These categories were represented by genes such as *CYP79B2 (cytochrome P450 subfamily B), CYP79B3, CYP83A1, CYP79F2, GSTU26 (GLUTATHIONE S-TRANSFERASE TAU 26)*, and *IPMI*, indicating broad repression of sulfur-rich and defense-related specialized metabolism (Supplementary Fig. 11B). Such repression of glucosinolates in *Arabidopsis* has been previously reported and connected to a resource-saving strategy in which sulfur is redirected from defense compounds toward essential primary metabolism (Hirai et al., 2003).

The downregulated genes were also enriched for processes related to indole metabolism and defense-associated secondary metabolites, including indoleacetic acid metabolism, camalexin biosynthesis, indole phytoalexin biosynthesis, and toxin biosynthetic processes (Fig. 21C). The group also showed repression of inducible defense capacity as response to insect and callose-related defense processes were also among the enriched DEGs (Fig. 21C). Together, these patterns indicate repression of pathways involved not only in glucosinolate synthesis but also in phytoalexin production, hormone-related metabolism, and defensive specialized metabolism more broadly. Both low-S accession also showed carbohydrate catabolic process to be suppressed with genes such as *BXL2 (BETA-XYLOSIDASE 2), ISA3 (ISOAMYLASE 3), ATPHS2 (ALPHA-GLUCAN PHOSPHORYLASE 2),* and *MIOX2 (MYO-INOSITOL OXYGENASE 2)* under S-deficiency indicating altered carbon use under nutrient stress (Fig. 21C and Supplementary Fig. 11B).

Overall, the shared response between App1-16 and In-0 indicates coordinated transcriptional adjustments to sulfur deficiency, characterized by activation of sulfur assimilation, secondary metabolic

and circadian-associated pathways together with repression of glucosinolate, indole, and other defense-associated metabolic processes.

A

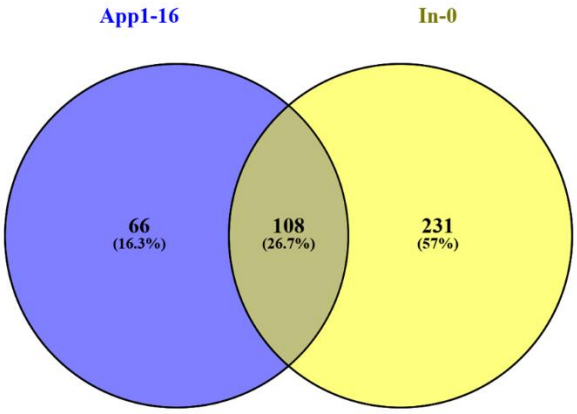

B

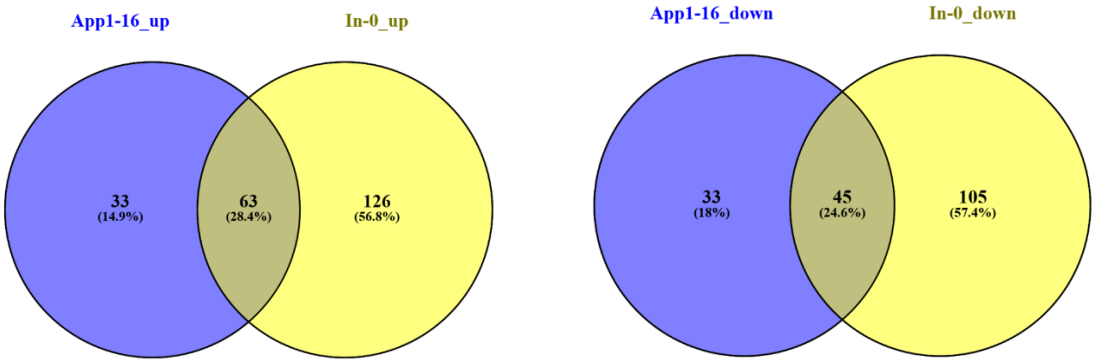

C

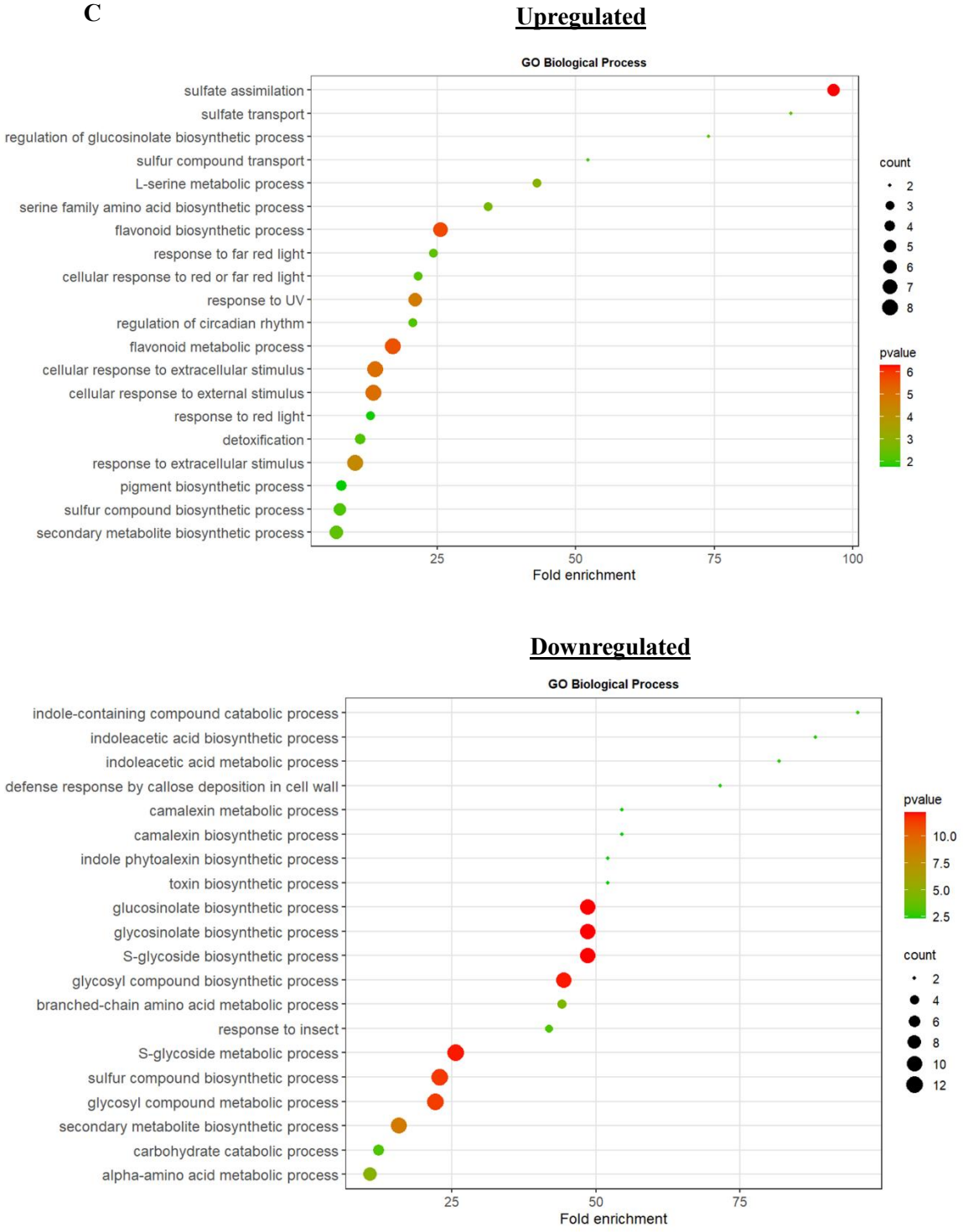

Figure 21: Within-Group Similarity of Differentially Expressed Genes under Sulfur Deficiency. **(A)** Venn diagram of DEGs for treatment effect between low-S accessions App1-16, and In-0. **(B)** Venn diagram of upregulated DEGs (up) and downregulated DEGs (down) between low-S accession App1-16 and In-0. **(C)** Functional gene ontology (GO) enrichment analysis of intersect upregulated and downregulated DEGs in low-S accessions App1-16 and In-0 where color of bubble indicates -log10 (p value) and size of bubble indicates the gene count.

For the mid-S accessions, Col-0 showed around 235 DEGs being specific to it, whereas Kro-0 exhibited only 142 uniquely regulated DEGs (Fig. 22A). In addition, we identified approximately 124 DEGs that were commonly regulated between the two accessions, hence sharing similarity percentage closely with the low-S group. Among these shared DEGs, 76 genes were upregulated and 48 genes were downregulated under sulfur deficient conditions (Fig. 22B).

GO enrichment analysis of the upregulated shared DEGs revealed several functional categories similar to low-S accessions such as sulfur metabolism and transport, flavonoid biosythesis and metabolic process, serine family amino acid biosynthesis, regulation of circadian rhythm, and response to external stimuli and UV radiation indicating the core response of S-deficiency as discussed previously in section 4.3 (Fig. 22C). However, several enriched GO categories were more pronounced or unique in the mid-S group compared with the low-S accessions. Notably, GO terms related to glutathione metabolism were enriched among the upregulated genes (Fig. 22C). Genes involved in this pathway, including GST (GLUTATHIONE S-TRANSFERASE)-related gene, i.e., *GSTU27*, *GGCT2;1*, along with the presence of *DHAR2 (DEHYDROASCORBATE REDUCTASE 2)*, indicate activation of redox buffering systems, suggesting that mid-S accessions may respond to sulfur limitation by strengthening antioxidant capacity (Supplementary Fig. 12A). Consistent with this, the group also shows the presence of an organic hydroxy compound biosynthetic process, indicating activation of hydroxylated secondary metabolites with upregulation of genes like *ICS2 (ISOCHORISMATE SYNTHASE 2), IPS2, SQE3 (SQUALENE EPOXIDASE 3)*, and *UDP-GLUCOSYL TRANSFERASE*S, i.e., *UGT78D2, UGT789C1,* that can contribute to antioxidant protection under sulfur deficiency (Fig. 22C & Supplementary Fig. 12A). In addition, apart from the detoxification process, the cellular oxidant detoxification category was uniquely enriched in the mid-S group, indicating again a stronger emphasis on redox homeostasis and oxidative stress protection, with genes like *DHAR2, LSU1, LSU2,* and *LSU3* being strongly regulated in the mid-S group (Fig. 22C & Supplementary Fig. 12A). Another notable enrichment unique to the mid-S group was response to cadmium ion, indicating activation of broader metal-stress related signaling pathways with induction of genes like *GGCT2;1, SBP1 (SELENIUM BINDING PROTEIN 1), MSA1/SHM7* (Fig. 22C & Supplementary Fig. 12A). The appearance of this GO category among upregulated DEGs was further supported by significant higher cadmium levels in the mid-S group under S-deficiency indicating enhanced Cd toxicity in this group (Supplementary Fig. 16).

The downregulated shared DEGs were enriched for several categories associated with secondary metabolism, including glucosinolate biosynthetic process, glucosinolate metabolic process, S-glycoside biosynthetic process, glycosyl compound biosynthetic process and branched chain amino acid metabolic process as also reported in low-S accessions (Fig. 22C). However, GO enrichment analysis also revealed several metabolic categories that were more characteristic for the mid-S group, including leucine biosynthetic process and leucine metabolic process with genes like *LEUD1 (ISOPROPYLMALATE ISOMERASE 2), IDM1, GSM1 (GLUCOSINOLATE METABOLISM 1), IMS2,* and *IPM1* being repressed (Fig. 22C & Supplementary Fig 12B). Additionally, several GO terms related to oxygen and hypoxia

responses, including cellular response to hypoxia, cellular response to decreased oxygen levels, and response to hypoxia, were uniquely enriched among the downregulated genes in the mid-S group (Fig. 22C). These categories involved unique sets of genes like *RAV1/EDF4 (ETHYLENE RESPONSE DNA BINDING FACTOR 4), CBP1 (CCG-BINDING PROTEIN 1), DIN10 (DARK INDUCIBLE 10)* being downregulated in mid-S accessions under S-deficiency (Fig. 22C & Supplementary Fig 12B). These categories were not prominent in the low-S accessions, suggesting that mid-S accessions may modulate oxygen-responsive signaling pathways under sulfur deficiency.

Overall, the shared response between Col-0 and Kro-0 indicates their shared transcriptional adjustments to sulfur deficiency, which, along with strong activation of sulfur assimilation pathways, includes dependency on redox-related pathways (glutathione metabolism and oxidant detoxification). At the same time, S-deficiency leads to repression of secondary metabolites, particularly glucosinolate biosynthesis; the accessions in this group show coordinated repression of oxygen-related signaling processes, being unique to the mid-S group.

A

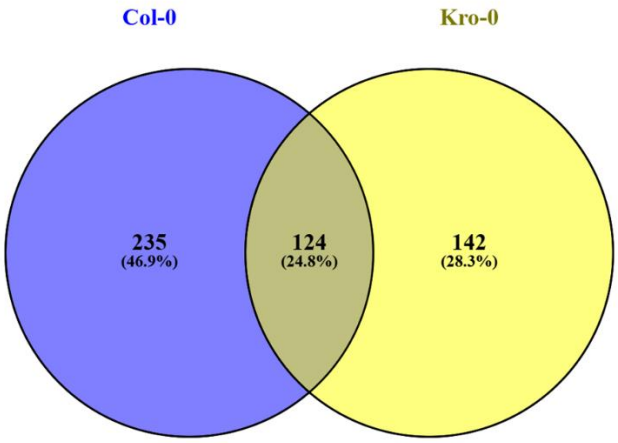

B

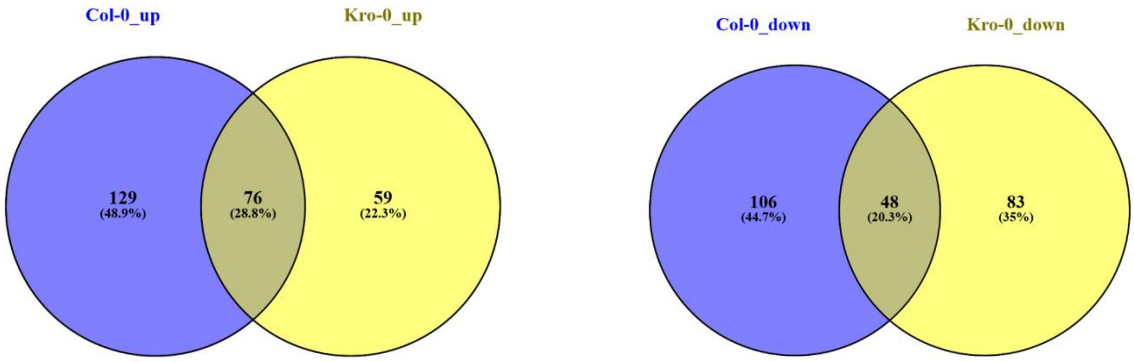

C

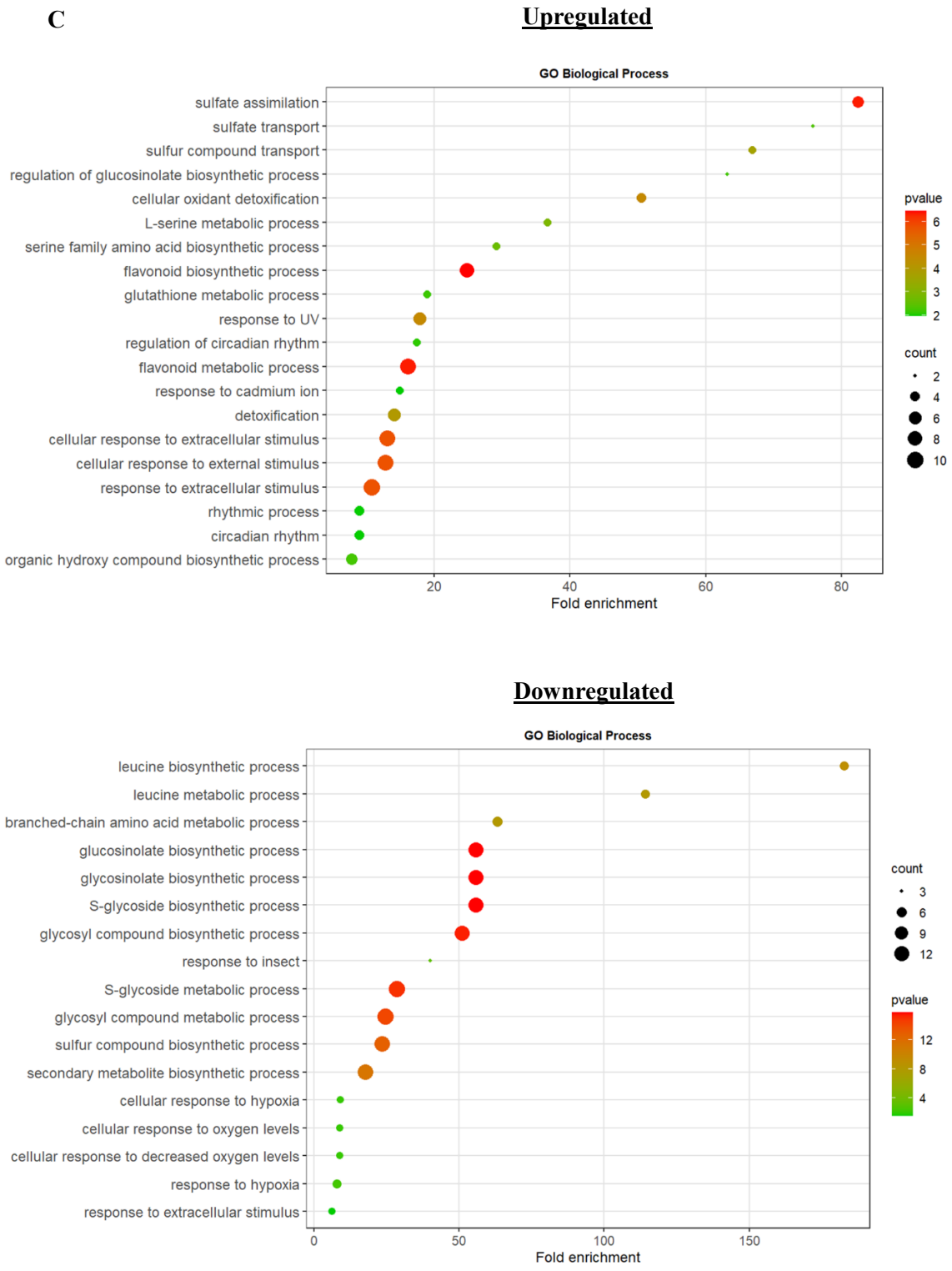

Figure 22: Within-Group Similarity of Differentially Expressed Genes under Sulfur Deficiency. **(A)** Venn diagram of DEGs for treatment effect between mid-S accessions Col-0, and Kro-0. **(B)** Venn diagram of upregulated DEGs (up) and downregulated DEGs (down) between mid-S accession Col-0 and Kro-0. **(C)** Functional gene ontology (GO) enrichment analysis of intersect upregulated and downregulated DEGs in mid-S accessions Col-0 and Kro-0 where color of bubble indicates -log10 (p value) and size of bubble indicates the gene count.

The high-S accessions, Zu-1 and Hod exhibited a relatively high number of treatment-responsive DEGs. Specifically, Zu-1 showed 335 unique DEGs, whereas Hod exhibited a substantially larger number, with 1271 DEGs unique to this accession (Fig. 23A). The large number of accession-specific genes, particularly in Hod, indicates that the transcriptional responses of high-S accessions to sulfur deficiency are considerably more divergent than those observed within the low-S and mid-S groups and also its sensitivity under S-deficient conditions. In contrast to the low-S and mid-S groups, the overlap between the two high-S accessions was relatively low with only 215 DEGs being shared between these two accesions (Fig. 23A). Among the shared DEGs, 100 genes were upregulated and 98 were downregulated under sulfur deficiency (Fig. 23B), indicating a balanced transcriptional response involving both activation and repression of metabolic pathways.

GO enrichment analysis of the upregulated shared genes revealed several biological processes that were also observed in the low-S and mid-S groups, including sulfate assimilation, sulfate transport, sulfur compound transport, flavonoid biosynthesis, detoxification, and glutathione metabolism (Fig. 23C). These enrichments were supported by induction of classical sulfur marker genes such as *SDI1, SDI2, APR2*, *APR3*, *LSU1, LSU2*, *SERAT* isoforms, and *SULTR* transporters, as described previously (Supplementary Fig. 13A). Similar to the other groups, GO categories related to circadian rhythm and rhythmic processes were also enriched (Fig. 23C). However, the genes contributing to these categories differed. In the high-S group, apart from *CCA1, LHY, HYH,* and *LCL5*, observed in the other two groups, circadian regulation was represented by additional genes such as *NIGHT LIGHT-INDUCIBLE AND CLOCK-REGULATED GENE*, i.e., *LNK2* and *LNK3* and *SPA3 (SUPPRESSOR OF PHY-A),* indicating close integration of circadian clock and light signaling (Supplementary Fig. 13A). This also suggests that although circadian regulation appears as a common theme across groups, distinct regulatory components of the circadian network may be involved in high-S accessions. Additional enriched categories included responses to extracellular stimuli, responses to UV, and flavonoid metabolism, indicating activation of environmental stress signaling and protective secondary metabolism under sulfur limitation (Fig. 23C).

The downregulated shared DEGs showed strong enrichment for pathways related to glucosinolate and sulfur-containing secondary metabolite biosynthesis, including glucosinolate biosynthetic process, S-glycoside biosynthesis, and secondary metabolite biosynthesis (Fig. 23C). While repression of glucosinolate metabolism was also observed in the other groups, several additional metabolic categories were specifically enriched in the high-S group. These included tryptophan metabolic process, amine metabolic process, and indolealkylamine metabolic process, indicating broader adjustments in indole-derived and nitrogen-containing metabolic pathways consisting of *CB5-C (CYTOCHROME B5 ISOFORM C), MSRB6, CYP79B2,* and *CYP79B3* genes (Fig. 23C & Supplementary Fig. 13B). Another distinctive feature of the high-S response was the strong repression of detoxification-related genes, particularly multiple members of the GSTU (glutathione S-transferase) family. Compared with the other groups, where detoxification pathways were often induced, the high-S accessions showed reduced

expression of several GSTU i.e *GST1, GSTF/711/14/, GSTU20* genes, suggesting differences in redox regulation and detoxification responses under sulfur deficiency (Fig. 23C & Supplementary Fig. 13B).

Overall, the transcriptional response shared between Zu-1 and Hod includes activation of sulfur assimilation, circadian regulation, and stress-related metabolic pathways, similar to those observed in the other sulfur-content groups. However, the genes contributing to these pathways differ, indicating that similar functional responses may be achieved through distinct regulatory gene networks. In addition, the high-S group showed broader repression of indole- and amine-related metabolic processes, as well as strong downregulation of *GSTU* detoxification genes, suggesting distinct adjustments in secondary metabolism and redox regulation under sulfur limitation. Finally, the relatively small overlap between Zu-1 and Hod and the large number of accession-specific DEGs, particularly in Hod, indicate that high-S accessions exhibit greater transcriptional variability in their responses to sulfur deficiency compared with the low-S and mid-S groups

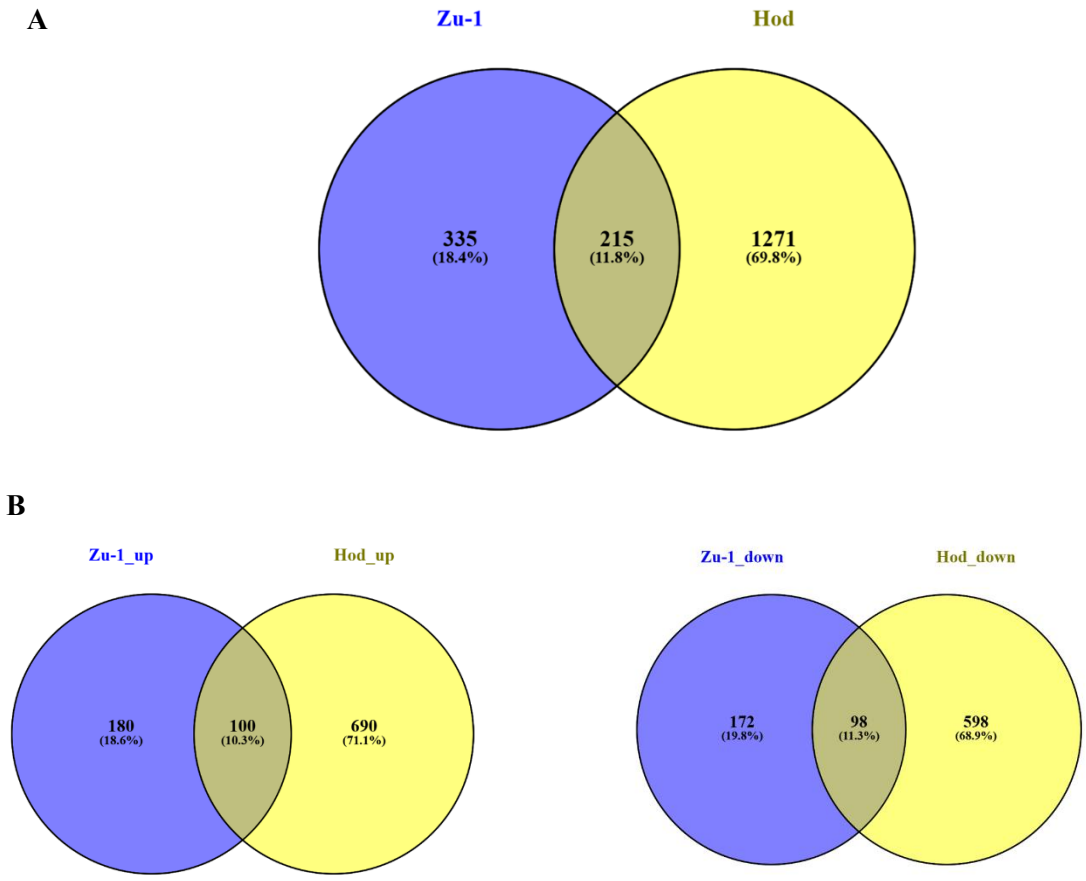

C

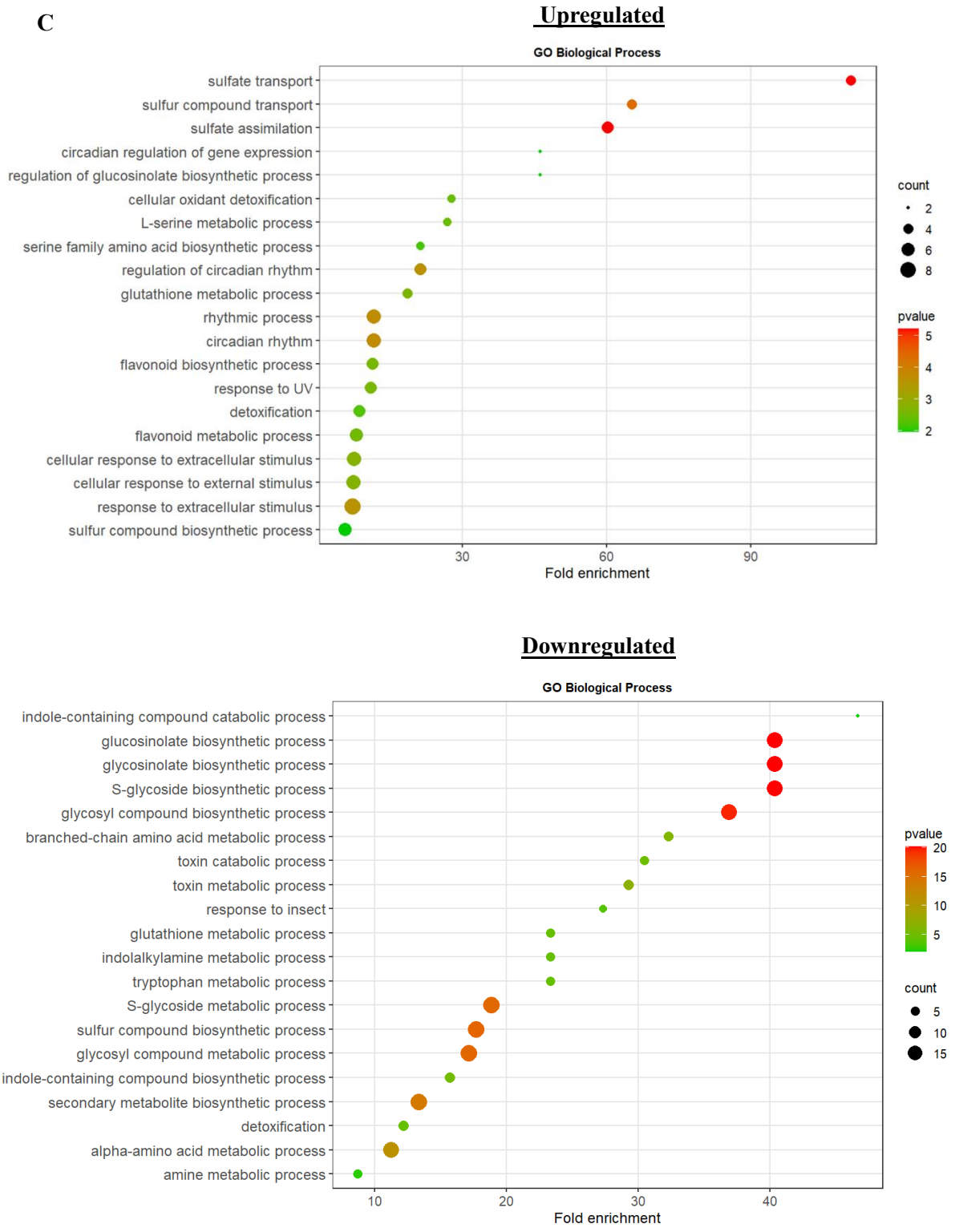

Figure 23: Within-Group Similarity of Differentially Expressed Genes under Sulfur Deficiency. **(A)** Venn diagram of DEGs for treatment effect between high-S accessions Zu-1, and Hod. **(B)** Venn diagram of upregulated DEGs (up) and downregulated DEGs (down) between high-S accession Zu-1 and Hod. **(C)** Functional gene ontology (GO) enrichment analysis of intersect upregulated and downregulated DEGs in high-S accessions Zu-1 and Hod where color of bubble indicates -log10 (p value) and size of bubble indicates the gene count.

4.4 Group-specific Transcriptional Responses to Sulfur Deficiency

After assessing the shared transcriptional responses within each sulfur-content group under sulfur deficiency, we next investigated group-specific DEGs in order to identify transcriptional responses that may contribute to distinct adaptive strategies among the sulfur-content groups under sulfur limitation. To achieve this, the sets of shared DEGs identified for each group (section 4.3) were intersected to determine genes that were unique to individual sulfur-content groups (Fig. 24A). This comparison revealed a core set of 55 DEGs shared across all three groups as discussed previously in section 4.2. In addition, we found 26 DEGs specific to the low-S group, 20 DEGs specific to the mid-S group, and a substantially larger set of 122 DEGs unique to the high-S group (Fig. 24A). The higher proportion of unique DEGs in the high-S group (43.6%) suggests a stronger transcriptional divergence of this group compared with the low-S and mid-S groups in response to sulfur deficiency. Besides, these group-specific genes, several DEGs were shared between two of the S-content groups. In particular, 30 DEGs were shared between the mid-S and high-S groups, followed by 19 DEGs shared between the low-S and mid-S groups, whereas only 8 DEGs were shared between the low-S and high-S groups (Fig. 24A). The relatively small overlap between the low-S and high-S groups indicates that these groups exhibit markedly different transcriptional acclimation strategies under sulfur deficiency, consistent with the metabolic and developmental differences observed previously.

We next examined genes that were specifically regulated in the low-S accessions (App1-16 and In-0) but not in the other sulfur-content groups. Among the 26 unique DEGs, we found 13 genes upregulated and 13 genes downregulated under sulfur deficiency, indicating that low-S accessions respond through a balanced transcriptional adjustment rather than a predominantly activating or repressive response. GO enrichment analysis of these 26 low-S-specific genes revealed biological processes mainly associated with light signaling, radiation response, and pigment biosynthesis, including cellular response to light stimulus, cellular response to radiation, cellular response to blue light, response to far-red light, and pigment biosynthetic process (Fig. 24B). Induction of genes such as *ELIP1, SIGE* and *SOUL-1 (HAEME BINDING PROTEIN 1),* in low-S accessions suggests adjustments in photosynthetic light handling, photoprotection, and chloroplast-associated metabolism under S-deficiency (Fig. 24C)

Induction of genes such as *UGT78D2* further suggest activation of flavonoid-related metabolic processes, UV protection and antioxidant buffering which might compensate for the metabolic limitations imposed by sulfur deficiency (Fig. 24C). In addition, upregulation of *SWEET13 (SUGAR WILL EVENTUALLY BE EXPORTED TRANSPORTERS 13)* might suggest increased carbon transport and allocation to facilitate pollen development under S-deficiency. These genes suggest that low-S accessions may actively coordinate plastid function with prioritizing carbon redistribution to reproductive tissue. In contrast, several genes associated with carbohydrate metabolism and sugar signaling were also downregulated in the low-S group. For example, *TPPE (TREHALOSE-6-PHOSPHATE PHOSPHATASE E)*, which participates in trehalose-6-phosphate metabolism acting as sucrose sensor, together with *ISA3 (ISOAMYLASE 3)*, a starch-degrading enzyme, and *BXL2 (BETA-*

XYLOSIDASE 2), involved in cell wall carbohydrate metabolism, were repressed under sulfur deficiency which could be strategy to repress sugar and starch breakdown during S-starvation (Fig. 24C).

Overall, the low-S group-specific transcriptional response indicates activation of photoprotective and pigment-related pathways together with adjustments in carbon allocation and repression of carbohydrate remobilization processes. These changes suggest that low-S accessions prioritize photosynthetic function and metabolic balance under sulfur deficiency through coordinated regulation of chloroplast activity and carbon metabolism.

A

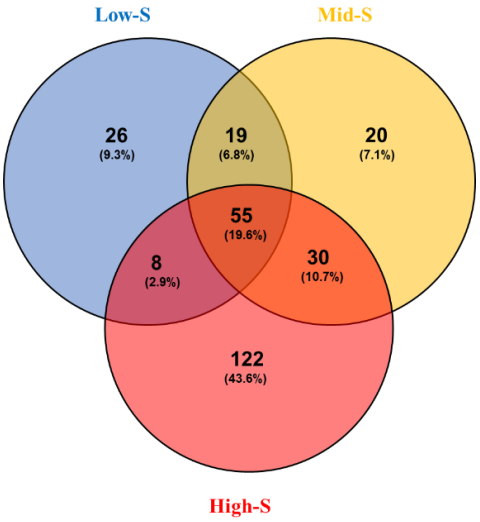

B

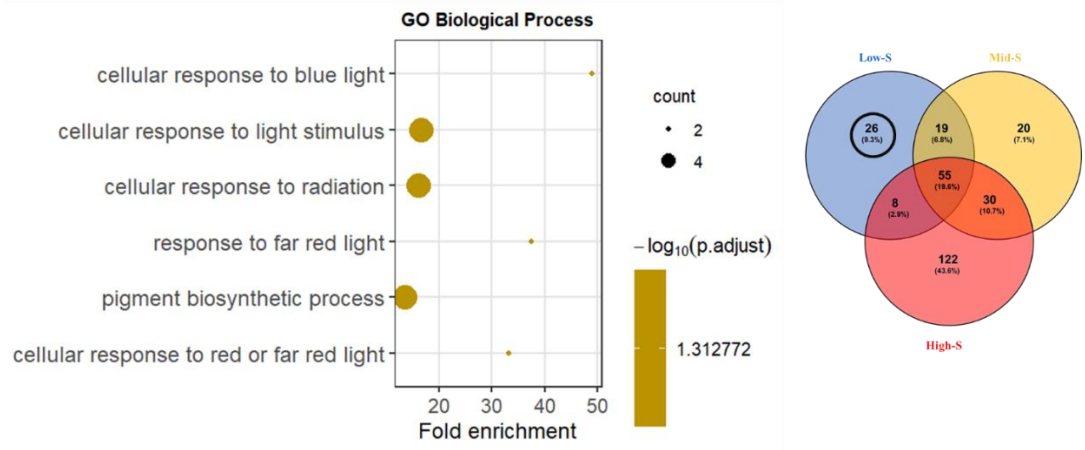

C

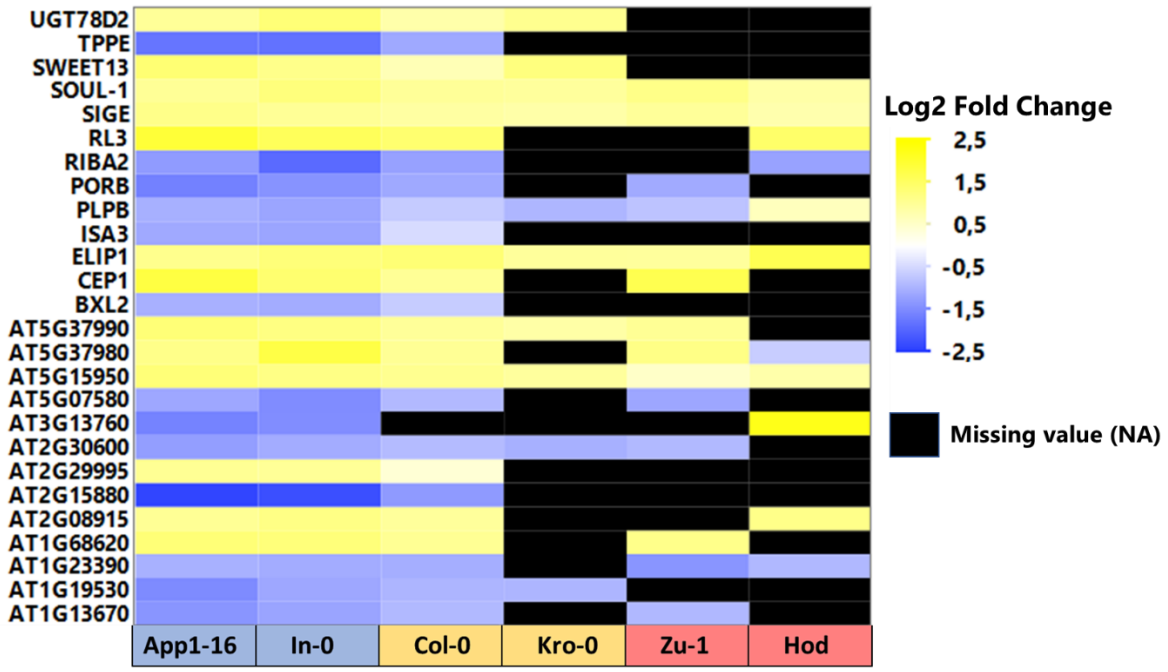

Figure 24: Group-specific transcriptional adjustments in response to S-deficiency (A) Venn diagram of shared DEGs within each group intersected to obtain group-specific DEGs **(B)** Functional gene ontology (GO) enrichment analysis of low-S group-specific DEGs, where the color of the bubble indicates -log10 (p value) and the size of the bubble indicates the gene count (**C)** Heatmap representing changes in expression levels of low-S group-specific 26 DEGs across all six accessions in response to S-deficiency

For the mid-S group, among the 20 group-specific DEGs, 14 genes were upregulated, and 6 genes were downregulated under sulfur deficiency, indicating a bias toward transcriptional activation of specific metabolic pathways rather than a balanced regulatory adjustment as observed in the low-S group. In contrast to the low-S group, GO enrichment analysis did not reveal significantly enriched biological process categories for these genes. However, KEGG pathway analysis identified enrichment of secondary metabolic pathways, particularly flavonoid biosynthesis and sesquiterpenoid and triterpenoid biosynthesis (Fig. 25A). These pathways are associated with the production of specialized metabolites that contribute to stress protection, antioxidant activity, and chemical defense, suggesting that mid-S accessions respond to sulfur limitation primarily through adjustments in secondary metabolism. Consistent with this enrichment, several genes involved in flavonoid metabolism and phenylpropanoid-related pathways were induced in the mid-S group (Fig. 25A). For example, *UGT78D1* and *TT7 (TRANSPARENT TESTA 7),* both involved in flavonoid biosynthesis and modification, were strongly upregulated under sulfur deficiency (Fig. 25B). Further, the upregulation of genes such as *GSTL1 (GLUTATHIONE S-TRANSFERASE LAMBDA 1)* and *AER (2-ALKENAL REDUCTASE)*, both associated with cellular detoxification processes, suggests activation of redox buffering and antioxidant mechanisms in the mid-S group under sulfur deficiency (Fig. 25B). *GSTL1* participates in glutathione-

dependent detoxification reactions, while *AER* reduces reactive aldehydes generated during lipid peroxidation, together indicating enhanced protection against oxidative damage (Fig. 25B). In addition to secondary metabolism and detoxification processes, genes associated with hormone signaling and developmental regulation were also differentially expressed. For example, *PIN5 (PIN-FORMED 5),* an intracellular auxin transporter involved in regulating auxin homeostasis, was induced under sulfur deficiency, suggesting potential adjustments in growth regulation and developmental plasticity in response to S limitation (Fig. 25B).

Conversely, genes involved in carbohydrate metabolism and stress-related signaling were downregulated in the mid-S group. The repression of *BGAL4 (β-GLUCOSIDASE 4)*, which participates in carbohydrate metabolism and cell wall modification, indicates reduced activity of specific carbohydrate-processing pathways and may reflect adjustments in carbon utilization and cell wall remodeling under sulfur deficiency (Fig. 25B). Additionally, *GLY14 (GLYOXYLASE 14)*, a component of the glyoxalase pathway involved in methylglyoxal detoxification, was downregulated (Fig. 25B). As the glyoxalase system plays a role in mitigating cytotoxic by-products of stress metabolism, its repression may indicate altered detoxification capacity under sulfur limitation. *GLY14* has also been implicated in crosstalk between jasmonic acid and salicylic acid signaling, suggesting potential modulation of stress-related hormonal pathways in these accessions. Finally, the downregulation of *CCL (CCR-LIKE)*, a gene associated with circadian regulation, suggests that circadian clock-associated processes may also be adjusted in the mid-S group during sulfur deficiency, indicating broader transcriptional reprogramming beyond metabolic pathways (Fig. 25B). Overall, the mid-S group-specific transcriptional response indicates a strategy characterized by activation of secondary metabolite pathways, particularly flavonoid and terpenoid biosynthesis, as well as induction of detoxification and redox-related processes. In contrast to the low-S group, which primarily activated chloroplast-associated photoprotective pathways, mid-S accessions appear to rely more strongly on secondary metabolic defenses and antioxidant systems to maintain cellular homeostasis under sulfur limitation.

A

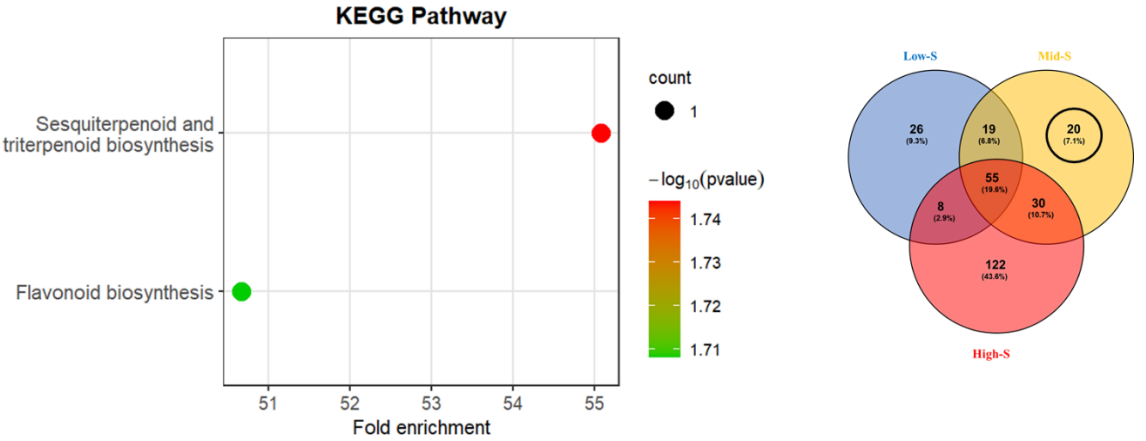

B

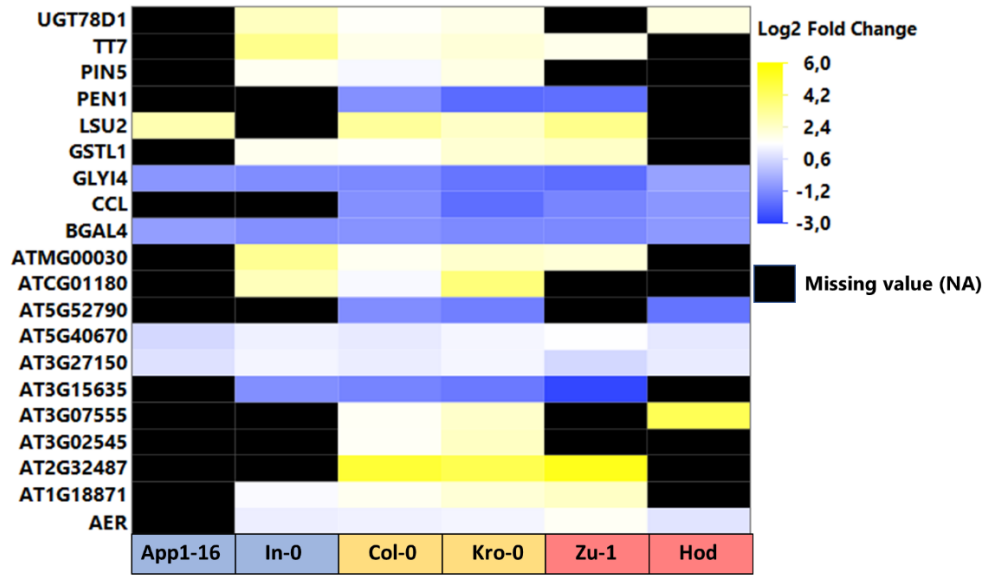

Figure 25: Mid-S group-specific transcriptional adjustments in response to S-deficiency (A) Functional gene ontology (GO) enrichment analysis of mid-S group-specific DEGs, where the color of the bubble indicates -log10 (p value) and the size of the bubble indicates the gene count **(B)** Heatmap representing changes in expression levels of mid-S group-specific 20 DEGs across all six accessions in response to S-deficiency

The high-S group showed 122 specific DEGs, of which 43 genes were upregulated, and 64 genes were downregulated, while 15 genes showed opposite regulation between the two accessions i.e. Hod and Zu-1 under sulfur deficiency. The substantially larger number of group-specific DEGs in the high-S group compared with the low-S and mid-S groups indicates that high-S accessions undergo more extensive transcriptional reprogramming under sulfur deficiency. GO enrichment analysis of the upregulated high-S-specific genes revealed biological processes associated with sulfate and sulfur compound transport (Fig. 26A). In addition, this group also showed enrichment for photosynthesis light reaction and photosynthetic electron transport in photosystem I, associated with genes such as *PGR5* (*PROTON GRADIENT REGULATION 5*), *PDE329 (PIGMENT DEFECTIVE 329)*, and *CFBP1/HCEF1* (*HIGH CYCLIC ELECTRON FLOW 1)* indicating that high-S accessions adjust photosynthetic energy generation under sulfur deficiency, likely to maintain ATP and reductant supply for stress acclimation and sulfur metabolism (Fig. 26A & Supplementary Fig. 14A). A notable feature among the upregulated genes was the enrichment of hexose, disaccharide, and oligosaccharide metabolic and biosynthetic processes. These categories were represented by genes such as *GoLS1(GALACTINOL SYNTHASE 1)*, *TPPF (TREHALOSE-6-PHOSPHATE PHOSPHATASE F)*, *SUS3 (SUCROSE SYNTHASE 3)* and *UGE5 (UDP-D-GALACTOSE 4-EPIMERASE 5)*, suggesting adjustments in soluble sugar metabolism and carbohydrate partitioning (Fig. 26A & Supplementary Fig. 14A). Such changes may reflect metabolic reorganization to support energy homeostasis and carbon supply when sulfur limitation constrains

anabolic metabolism. The upregulated gene set was also enriched for glutathione metabolic process, supported by genes such as *GGCT2;2* and *GSTU22*, indicating activation of redox buffering and glutathione-associated metabolism (Fig. 26A & Supplementary Fig. 14A). High-S accessions also showed the enrichment of circadian rhythm and regulation of circadian rhythm, represented by genes such as *LNK2* and *SPA3 (SUPPRESSOR OF PHYA-105)* indicating broader adjustments in temporal regulation under sulfur limitation (Fig. 26A & Supplementary Fig. 14A).

In contrast, the downregulated high-S-specific genes were strongly enriched for processes associated with secondary metabolism, including glucosinolate biosynthetic process and metabolic process, S-glycoside biosynthetic process and metabolic process (Fig. 26B). The group also showed enrichment for toxin metabolic process and catabolic process, and detoxification. Consistent with these enrichments, several genes associated with glutathione-dependent detoxification were repressed, including *GSTF4, GSTF7, GSTU20,* and *RHC1 (RESISTANT TO HIGH CO_2)* (Fig. 26B & Supplementary Fig. 14B). Since GST enzymes depend on glutathione for detoxification reactions, their repression suggests reduced activity of glutathione-dependent detoxification pathways, possibly reflecting restricted sulfur availability and prioritization of sulfur use apart from secondary detoxification processes. Further, repression of indole-containing compound biosynthetic and metabolic processes including genes such as *IGMT5 (INDOLE GLUCOSINOLATE O-METHYLTRANSFERASE 5),* and *MSRB6* indicates reduced investment in indole-derived defense compounds (Fig. 26B & Supplementary Fig. 14B). Similarly, downregulation of genes involved in isoprenoid biosynthesis suggests that the synthesis of other specialized metabolites may also be reduced under sulfur deficiency (Fig. 26B). In addition, the enrichment of amide transport and amino acid-related metabolic categories suggests that high-S accessions also adjust nitrogen-containing metabolite transport and amino acid metabolism under sulfur deficiency, pointing to broader reorganization of nitrogen-sulfur metabolic coordination (Fig. 26B).

A further distinctive feature of the high-S group was the presence of 15 genes showing opposite regulation between Zu-1 and Hod, indicating considerable transcriptional divergence even within this sulfur-content group (Fig. 26C). Functional gene ontology analysis revealed several GO terms related to cell wall organization and structural modification, including cell wall organization, external encapsulating structure organization, cellulose microfibril organization, and plant-type cell wall cellulose biosynthetic process being enriched (Fig. 26C). These categories were represented by genes such as *EXT4 (EXTENSIN 4), COBL2 (COBRA-LIKE PROTEIN 2), ENODL2 (EARLY NODULIN-LIKE PROTEIN 2),* and *BGLU1 (BETA-GLUCOSIDASE 1)* (Fig. 26D). These genes were upregulated in Zu-1 but downregulated in Hod, suggesting that Zu-1 may maintain or enhance cell wall remodeling and structural adjustment processes, whereas Hod may suppress these pathways under sulfur deficiency (Fig. 26D). GO enrichment also revealed the mucilage biosynthetic process involved in seed coat development, associated with genes involved in extracellular matrix formation and seed coat modification (Fig. 26C). Divergent regulation of these genes between the two accessions further suggests differences in developmental and structural responses under sulfur limitation (Fig. 26D).

Another enriched category was cellular response to sulfate starvation, represented by genes such as *MGL (METHIONINE GAMMA-LYASE)*, which participates in sulfur recycling by promoting cysteine bisynthesis through methionine degradation (Fig. 26C). In this case, *MGL* was induced in Zu-1 but repressed in Hod, suggesting that Zu-1 may activate internal sulfur recycling pathways, whereas Hod may rely on alternative strategies to cope with sulfur limitation (Fig. 26D). Processes related to protein metabolism and post-translational regulation were also enriched, including dephosphorylation, cytoplasmic translational elongation, and protein tetramerization (Fig. 26C). These categories were associated with genes such as *PAP22 (PURPLE ACID PHOSPHATASE 22)* and *NPGR1 (NO POLLEN GERMINATION RELATED 1)*, which showed opposite expression patterns between Zu-1 and Hod, indicating differences in protein modification and metabolic regulation under sulfur deficiency (Fig. 26D). Finally, genes associated with signaling and regulatory pathways, including *CLE6 (CLAVATA3/ESR-RELATED 6)* and *HAI1 (HIGHLY ABA-INDUCED PP2C GENE 1)*, also displayed opposite regulation between the two accessions (Fig. 26C & D). *CLE6* encodes a peptide ligand involved in developmental signaling, whereas *HAI1* encodes a protein phosphatase involved in abscisic acid (ABA) signaling and stress responses (Fig. 26C & D). Their divergent regulation suggests that Zu-1 and Hod may differ in hormonal and stress signaling pathways activated during sulfur deficiency.

Overall, the high-S group-specific transcriptional response indicates extensive transcriptional reprogramming characterized by activation of sulfur transport, photosynthetic processes, carbohydrate metabolism, glutathione-associated pathways, and circadian regulation, together with repression of detoxification, sulfur-rich secondary metabolism, indole-containing specialized metabolism, isoprenoid biosynthesis, and amino acid/amide-related pathways. The presence of a considerable number of oppositely regulated genes further suggests that high-S accessions do not respond uniformly to sulfur deficiency, but instead exhibit substantial intra-group divergence in developmental and metabolic adjustment mechanisms. Hence, the presence of oppositely regulated genes within the high-S accessions indicates that although Zu-1 and Hod share high sulfur content phenotypes, they may employ distinct regulatory mechanisms controlling cell wall organization, sulfur recycling, and stress-related signaling pathways in response to sulfur deficiency.

A

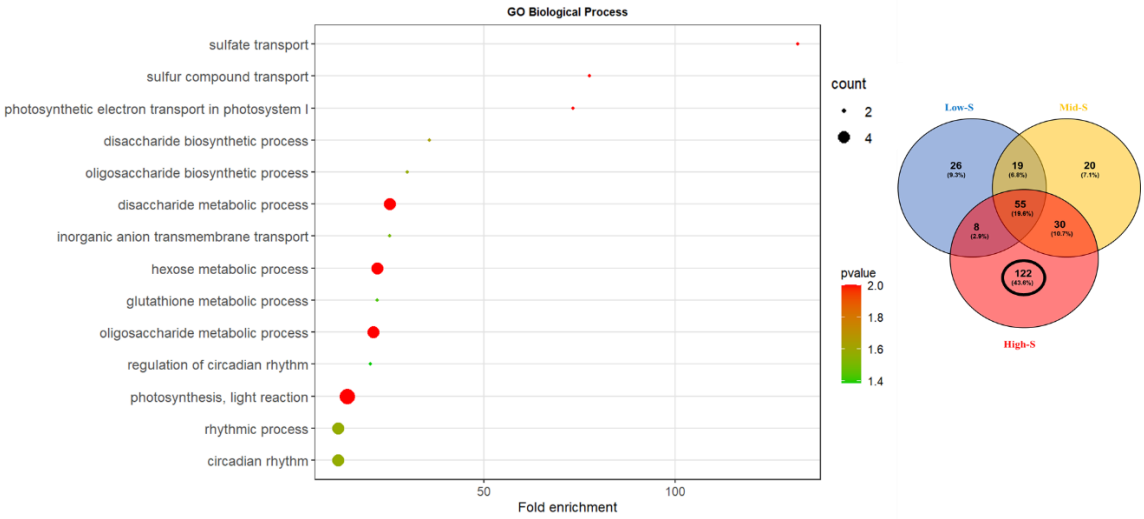
GO Biological Process
sulfate transport
sulfur compound transport
photosynthetic electron transport in photosystem I
disaccharide biosynthetic process
oligosaccharide biosynthetic process
disaccharide metabolic process
inorganic anion transmembrane transport
hexose metabolic process
glutathione metabolic process
oligosaccharide metabolic process
regulation of circadian rhythm
photosynthesis, light reaction
rhythmic process
circadian rhythm
50
100
Fold enrichment
count
2
4
pvalue
2.0
1.8
1.6
1.4
Low-S
Mid-S
High-S
26
19
20
55
8
30
122

B

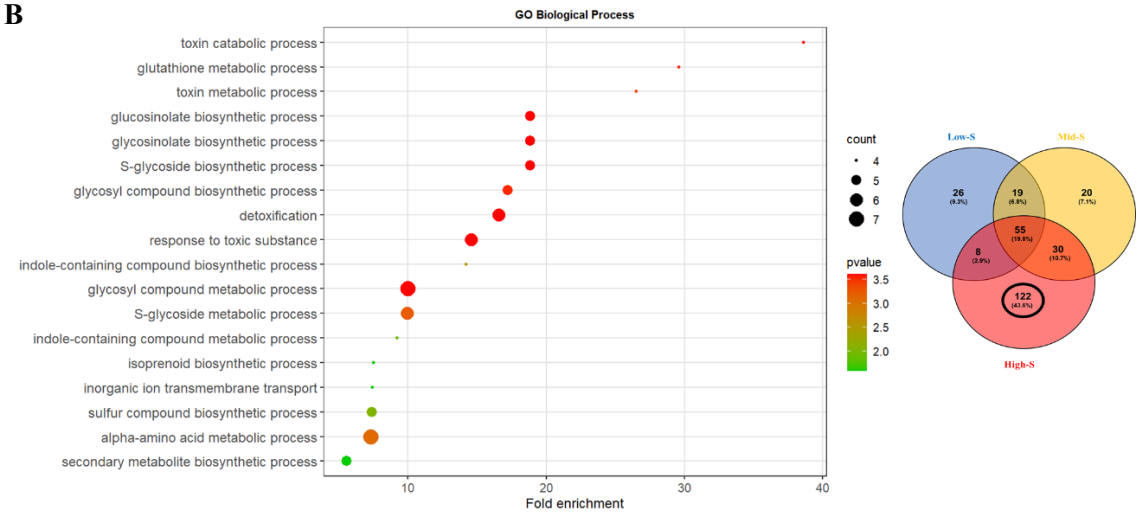
GO Biological Process
toxin catabolic process
glutathione metabolic process
toxin metabolic process
glucosinolate biosynthetic process
glycosinolate biosynthetic process
S-glycoside biosynthetic process
glycosyl compound biosynthetic process
detoxification
response to toxic substance
indole-containing compound biosynthetic process
glycosyl compound metabolic process
S-glycoside metabolic process
indole-containing compound metabolic process
isoprenoid biosynthetic process
inorganic ion transmembrane transport
sulfur compound biosynthetic process
alpha-amino acid metabolic process
secondary metabolite biosynthetic process
10
20
30
40
Fold enrichment
count
4
5
6
7
pvalue
3.5
3.0
2.5
2.0
Low-S
Mid-S
High-S
26
19
20
55
8
30
122

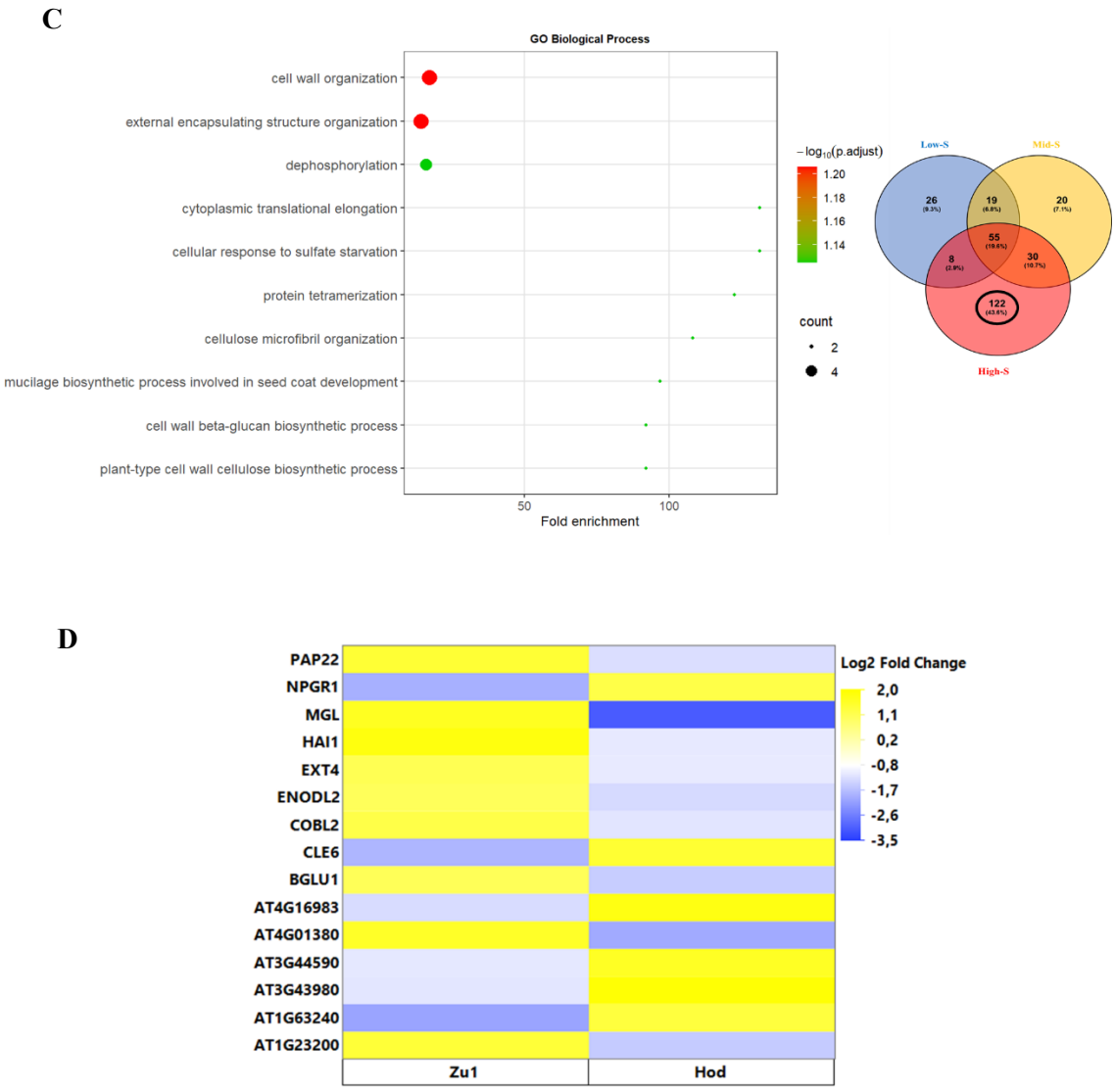

Figure 26: High-S group-specific transcriptional re-adjustments in response to S-deficiency (A) Functional gene ontology (GO) enrichment analysis of high-S group-specific upregulated DEGs **(B)** downregulated DEGs **(C)** oppositely regulated DEGs, where the color of the bubble indicates -log10 (p value) and the size of the bubble indicates the gene count **(D)** Heatmap representing changes in expression levels of high-S group-specific oppositely regulated in both accessions in response to S-deficiency

4.5 Baseline transcriptomic differences among accessions with contrasting sulfur content

The diverse transcriptional responses observed under S-deficiency for the groups led us to next examine whether these distinct sulfur-deficiency responses were associated with pre-existing transcriptional differences among the accessions. Also, we were interested in exploring what regulatory pathways or candidate genes might account for the natural variation of S-content. To achieve this, transcriptome variation among the six accessions under the control condition was analyzed. PCA revealed clear genotype-dependent clustering of samples, indicating substantial differences in transcriptional regulation among the accessions (Fig. 27A). The first two principal components explained 25% and 20% of the total variance, respectively, and separated the accessions into distinct transcriptional clusters,

suggesting that natural variation in sulfur accumulation is accompanied by differences in basal transcriptional programs.

To identify genes consistently associated with each sulfur-content group, differential expression analyses were first performed between accessions to get DEGs under the control condition. Then DEGs were intersected between two accessions within each group, using a stringent cut-off of $q<0.05$ and $|\log2FC|>2$, given the substantially higher number of DEGs obtained. This approach yielded 596 shared DEGs between the two Low-S accessions (App1-16 and In-0), 238 shared DEGs between the Mid-S accessions (Col-0 and Kro-0), and 553 shared DEGs between the High-S accessions (Zu-1 and Hod) (Fig. 27B). These shared DEGs within a group were subsequently intersected in order to identify group-specific transcriptional signatures. Intersection of the group-level DEG sets revealed distinct transcriptional patterns associated with each sulfur-content group. A total of 358 genes were uniquely associated with low-S accessions, 108 genes were specific to Mid-S accessions, and 326 genes were uniquely associated with high-S accessions, while smaller subsets of genes, i.e., 33 DEGs, were shared between the three groups (Fig. 27B). The small percentage of overlapping DEGs (3.1%) indicates each S-content group exhibits a substantial set of uniquely regulated genes, which might account for the different strategies of sulfur utilization even under non-stress conditions. Also, performing functional gene ontology on these 33 DEGs didn't yield any significant GO terms, as most of the genes have not been characterized. Similarly, no significantly enriched GO or KEGG categories were detected among the low-S group-specific genes, despite the relatively large number of genes identified (358 DEGs). The absence of clear functional enrichment, even with such a high number of DEGs, suggests that low-S accessions may not rely on a single dominant metabolic pathway but instead exhibit more distributed transcriptional adjustments across diverse biological processes.

Functional enrichment analysis of the mid-S group-specific genes identified significant enrichment only within KEGG pathway, which were metabolic pathways related to cysteine and methionine metabolism as well as ubiquinone and other terpenoid-quinone biosynthesis (Fig. 27C). These pathways are associated with sulfur-containing amino acid metabolism and redox-active cofactor biosynthesis, suggesting that mid-S accessions maintain transcriptional programs that support coordinated regulation of sulfur assimilation and redox metabolism. Network visualization of enriched pathways identified several genes contributing to these processes, including AT5G56080 *(NICOTIANAMINE SYNTHASE 2 (NS2)*, AT5G53970 *(TYROSINE AMINOTRANSFERASE 7 (TAT1))*, AT5G48950 *(1,4-DIHYDROXY-2-NAPHTHOYL-COA) THIOESTERASES (DHNAT-2)*, and AT1G01480 *(1-AMINO-CYCLOPROPANE-1-CARBOXYLATE SYNTHASE 2 (ACC 2)* (Supplementary Fig 15A). While both *NS2* and *ACC2* are involved in SAM biosynthesis and metabolic pathway, *TAT1* is responsible for amino acid tyrosine degradation and metabolism and *DHNAT-2* is involved in phylloquinone biosynthesis. Hence, the presence of these genes in the network indicates a probable connection of sulfur-containing amino acid metabolism with pathways involved in the biosynthesis of redox-active quinone cofactors.

In contrast, the high-S group-specific genes showed enrichment only for the biological process "sulfation," represented by *SULFOTRANSFERASE* genes such as *ATST4A*, *ATST4C*, and *ATST2B* (Supplementary Fig 15B). The presence of sulfotransferase genes within this category, which use PAPs as an obligate substrate for sulfation of peptides and secondary metabolites, suggests that high-S accessions may preferentially channel sulfur into secondary metabolism and regulatory modifications.

Together, these results demonstrate that *Arabidopsis* accessions differing in sulfur content already display distinct transcriptional programs under sulfur-sufficient conditions. The identification of group-specific gene sets and their associated metabolic pathways suggests that natural variation in sulfur accumulation is accompanied by different baseline regulatory strategies. While high-S accessions appear to preferentially allocate sulfur toward sulfation and specialized metabolic processes, mid-S accessions maintain balanced sulfur and redox metabolism, and low-S accessions exhibit more distributed transcriptional adjustments consistent with enhanced metabolic flexibility. These pre-existing transcriptional differences likely contribute to the distinct physiological responses observed under sulfur deficiency.

A

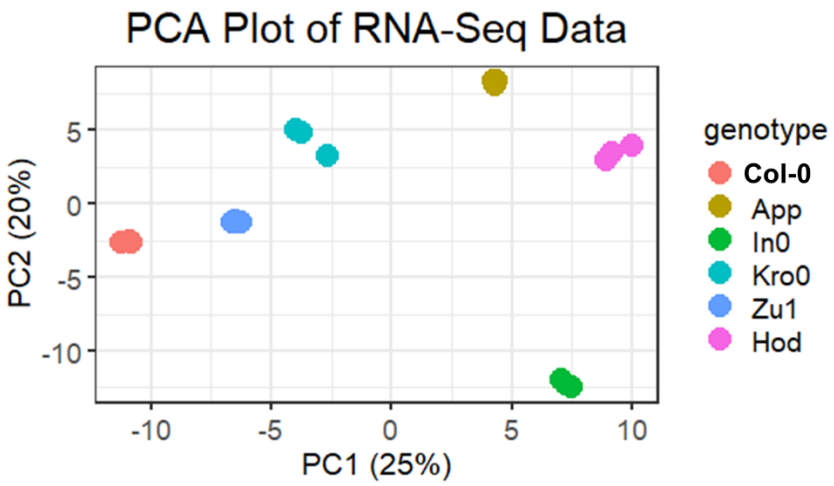

B

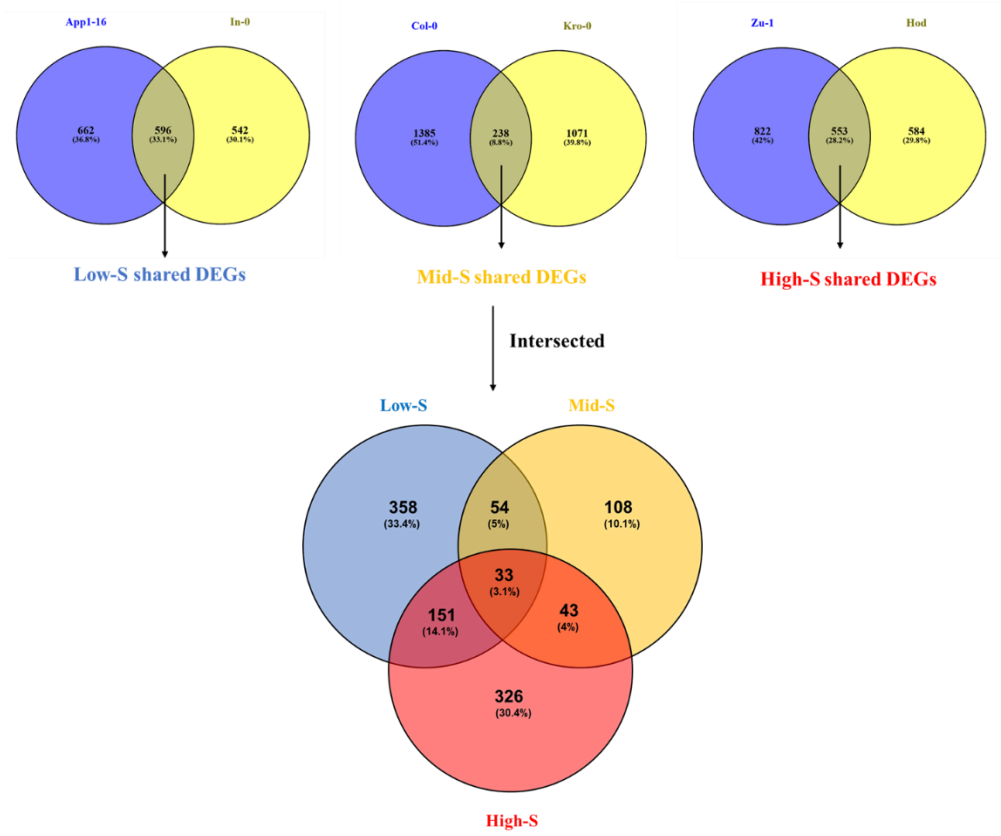

C

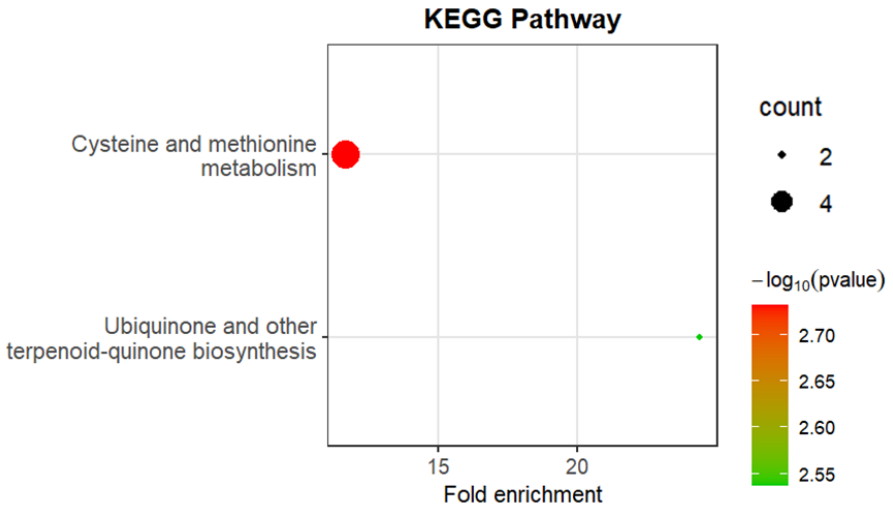

Figure 27: Comparative transcriptome analysis of *Arabidopsis* accessions under control conditions **(A)** Principal component analysis (PCA) of RNA-seq data from roots of six *Arabidopsis* accessions belonging to low S (App1-16 and In-0), mid S (Col-0 and Kro-0), high S (Zu-1 and Hod) under control (750 µM sulfate) conditions **(B)** Schematic representation used for intersection analysis to identify shared and group-specific differentially expressed genes among Low-S, Mid-S, and High-S *Arabidopsis* accessions under control conditions with cut-off of q<0.05 and |log2FC|>2 **(C)** Functional gene ontology (GO) enrichment analysis of mid-S unique DEGs under control condition.

Consistent with the observed transcriptional divergence, we next performed correlation analysis between gene expression levels and total-S content under the control condition. This analysis allowed the identification of genes whose basal transcriptional levels scale with sulfur accumulation capacity across accessions, thereby highlighting candidates potentially linked to sulfur homeostasis rather than merely accession-specific transcriptional variation.

This analysis identified several genes whose expression showed strong positive or negative correlations with sulfate levels, but, given the large list, we considered only those with Pearson correlation coefficients ≥ 0.9. From this list, we filtered around the top 20 DEGs from both positive and negative correlation lists, which showed a smooth gradient of expression from low-S to high-S accessions (Fig. 28). Genes positively correlated with sulfate content, included *TIM13 (TRANSLOCASE OF THE INNER MITOCHONDRIAL MEMBRANE 13), TET6 (TETRASPANIN6), SDS (SOLO DANCERS), SPPL1 (SIGNAL PEPTIDE PEPTIDASE-LIKE 1),* and *SAR2 (SECRETION-ASSOCIATED RAS SUPER FAMILY 2)*, etc. which displayed progressively increasing expression from Low-S to High-S accessions (Fig. 28). In contrast, genes such as *IAA34 (INDOLE-3-ACETIC ACID INDUCIBLE 34)*, *MEB1 (MEMBRANE OF ER BODY 1), EMB2794 (EMBRYO DEFECTIVE 2794), CYP705A6,* and *APX2 (ASCORBATE PEROXIDASE 1B)* and others showed strong negative correlations with sulfate levels, exhibiting higher expression in low-S accessions and progressively lower expression toward high-S accessions (Fig. 28). The presence of such expression gradients across the six accessions suggests that basal transcriptional regulation of these genes is tightly associated with natural variation in sulfur accumulation. Genes showing positive correlations with sulfate levels, including *SDS, SPPL1,* and *SAR2,* which are linked to protein turnover, membrane-associated proteolysis, and vesicular trafficking, indicate that high-S accessions may maintain elevated basal activity of pathways supporting protein processing and intracellular trafficking. In contrast, genes showing negative correlations with sulfate levels included *IAA34, MEB1, EMB2794, CYP705A6, and APX2*, which are associated with hormone signalling, defense-related structures, specialized metabolism, and reactive oxygen species detoxification, indicating that low-S accessions may maintain elevated basal activity of regulatory and stress-responsive pathways.

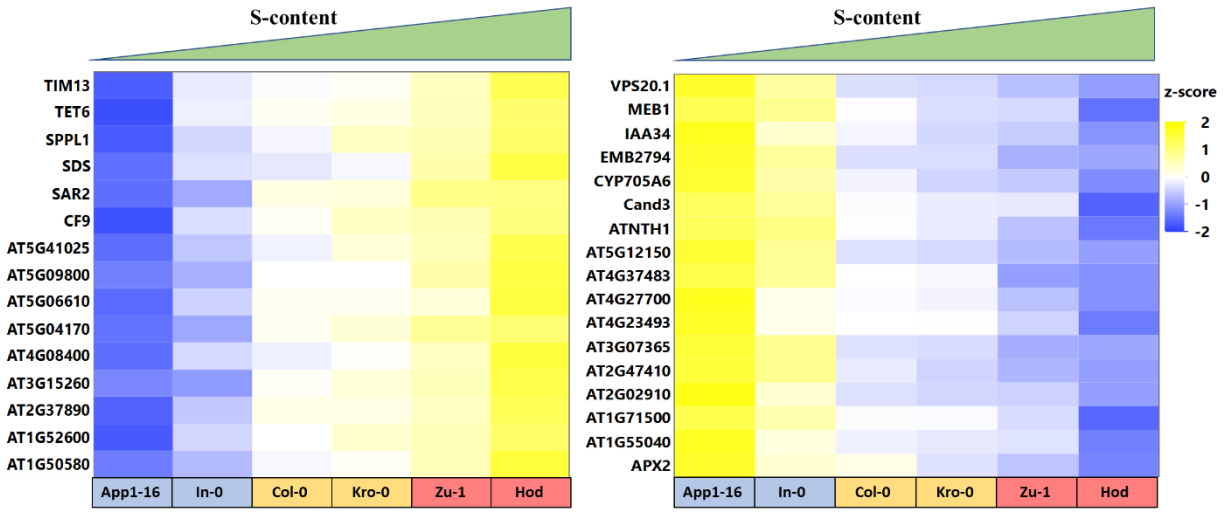

Figure 28: Expression gradients of the top 20 genes positively and negatively correlated with sulfate levels across *Arabidopsis* accessions. Expression values under the control condition were transformed using z-scores, and correlations with Pearson correlation coefficients ≥ 0.9 were considered for biological interpretation.

4.6 Differential metabolic adjustments between the groups in response to S-deficiency

Following the transcriptomic analysis, we next investigated whether the observed transcriptional responses under sulfur deficiency were also reflected at the metabolic level during early development, as we had metabolic data discussed in the previous chapter only for late development. To address this, a global metabolite profiling was performed on 18-day-old plants grown under control and sulfur-deficient conditions, using both shoot and root tissues. Log_2 fold-change analysis was applied to evaluate metabolic responses to sulfur limitation across accessions. Overall, a clear tissue-specific metabolic response was observed, with shoots exhibiting markedly stronger metabolic alterations than roots across all genotypes.

In shoots, sulfur deficiency led to pronounced changes in amino acid metabolism (Fig. 29). As expected, accumulation of branched-chain amino acids such as valine, leucine, and isoleucine were observed across all accessions; however, statistically significant increases were predominantly detected in mid-S and high-S accessions (Fig. 29). In addition, accumulation of the stress-associated amino acid proline was detected in the shoots of all accessions, although significant differences were observed only in Col-0. In contrast, root tissues exhibited an opposite trend, with a general decline in most amino acids across genotypes. An exception was observed in Hod, which showed accumulation of β-alanine, proline, and glycine under sulfur deficiency, indicating a stress-associated metabolic adjustment specific to this accession (Fig. 29).

Sugar metabolism also displayed strong accession-dependent responses under sulfur deficiency. In shoots, significant accumulation of raffinose was observed in In-0, Kro-0, Col-0, and Hod, whereas fructose accumulation was particularly evident in both low-S accessions and in Kro-0. In contrast,

glucose levels significantly declined in shoots of the accessions App1-16 and Col-0. Root tissues were comparatively less responsive with respect to sugar metabolism; however, significant sucrose accumulation was detected in low-S accessions, and raffinose accumulation was observed in Hod, indicating genotype-specific regulation of carbohydrate metabolism under sulfur stress (Fig. 29).

Organic acid metabolism was also strongly affected by sulfur deficiency. Both low-S and mid-S accessions exhibited a pronounced reduction in the levels of most organic acids in shoots, suggesting a suppression of central carbon metabolism. In high-S accessions, organic acid levels remained relatively stable, with the exception of Hod, which showed a significant decline in several tricarboxylic acid (TCA) cycle intermediates, including fumarate, malate, and succinate. In roots, metabolic responses were generally weaker; however, Col-0 and Hod again exhibited reductions in TCA cycle intermediates similar to those observed in shoots, indicating that mitochondrial respiration and carbon metabolism are particularly affected in these genotypes under sulfur deficiency (Fig. 29).

In addition to primary metabolites, several other compounds exhibited genotype-specific responses. Shoots of App1-16 and Col-0 displayed significant reductions in threonate, 2-oxo-gluconate, myo-inositol, and gluconate, accompanied by increased ribonate accumulation under sulfur-deficient conditions. Furthermore, both App1-16 and Hod showed elevated levels of 3-methyl-2-oxobutyrate, whereas Hod additionally exhibited a significant decrease in ethanolamine content. In contrast, Zu-1 displayed an opposing trend for several of these metabolites. In roots, App1-16 and Zu-1 showed significant reductions in ethanolamine, while Zu-1 also exhibited decreased gluconate levels. Hod roots, however, showed a marked accumulation of myo-inositol under sulfur deficiency (Fig. 29).

Taken together, these results reveal distinct metabolic adjustment strategies among accessions in response to sulfur deficiency. Low-S accessions primarily exhibited reductions in organic acid levels, suggesting a downregulation of central metabolism and a reallocation of sulfur toward essential processes. In contrast, mid-S and high-S accessions, particularly Hod, displayed broader metabolic remodeling, including changes in both amino acid and organic acid pools, indicative of altered protein turnover and carbon metabolism. Moreover, the comparison between tissues highlights that metabolic responses to sulfur deficiency are substantially stronger in shoots than in roots, underscoring the tissue-specific nature of sulfur-dependent metabolic regulation during early development.

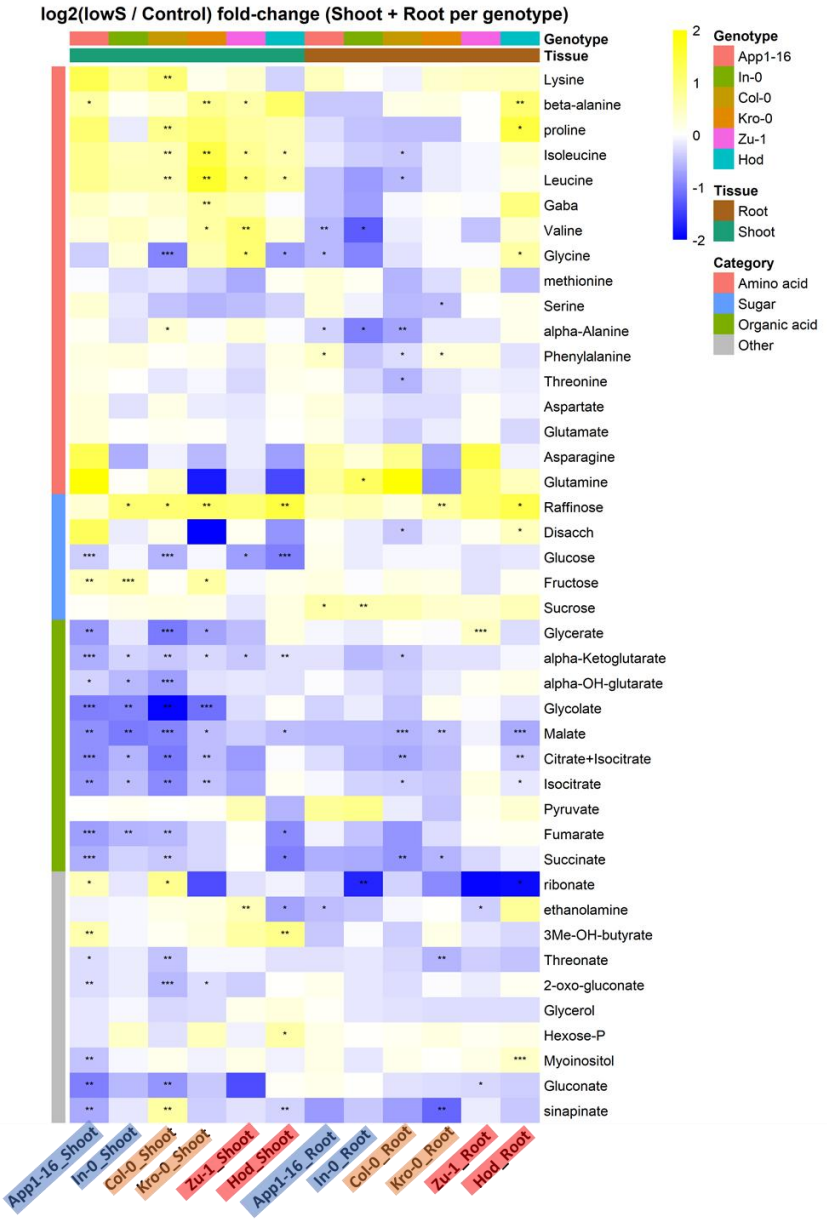

Figure 29: Metabolic reprogramming in response to sulfur deficiency during early development. Heatmap representing Log_2 fold-change of metabolite abundance under sulfur deficiency relative to control conditions in shoots and roots of six *Arabidopsis* accessions. Metabolites are grouped by biochemical class. Colors represent log_2 (low S / control) ratios, with blue indicating decreases and yellow indicating increases. Asterisks denote statistically significant differences (* $p < 0.05$, ** $p < 0.01$, *** $p < 0.001$).

4.7 Integrative correlation analysis of transcriptomic and metabolic responses to sulfur deficiency

To directly link transcriptional regulation with metabolic adjustments under sulfur deficiency, we performed a correlation analysis between core sulfur-responsive DEGs including the top 10 DEGs showing group-specific variation discussed in section 4.2 (Fig. 20D) and metabolic profile in shoots and roots. For this, we used log_2fold change of DEGs and metabolites in roots and shoots of the six

accessions. This analysis revealed distinct and tissue-specific patterns of gene-metabolite associations, indicating coordinated but differential regulation of sulfur-related metabolism at the transcriptional and metabolic levels.

In shoots, several metabolites displayed strong positive correlations with key sulfur-responsive genes. Notably, 2-oxo-gluconate showed a positive correlation with *SFP1*, suggesting that changes in organic acid metabolism are associated with sulfur-responsive transcriptional adjustments under sulfur deficiency (Fig. 30A & Supplementary Fig. 17A). The branched-chain-related metabolite 3-methyl-2-oxobutyrate (3Me-OH-butyrate) was positively correlated with *SHM7* and *SULTR1;2*, indicating a close association between sulfur uptake capacity and amino acid-related metabolic remodelling. Similarly, gluconate and glycolytic intermediates such as glucose and glycerol exhibited positive correlations with *CYP79F2* and *SHM7,* suggesting coordination between primary carbon metabolism and sulfur-responsive transcriptional programs (Fig. 30A & Supplementary Fig. 17A).

Amino acids showed particularly strong associations with sulfur-related genes in shoots as glutamine was positively correlated with *SHM7* and *SULTR1;2,* consistent with enhanced nitrogen-sulfur interaction under sulfur limitation (Fig. 30A & Supplementary Fig. 17A). In contrast, several negative correlations were also observed, particularly branched-chain amino acids exhibited strong negative associations with sulfur-deficiency markers as valine and phenylalanine were negatively correlated with *SDI1*, while isoleucine levels were negatively linked to *SDI2* expression (Fig. 30A & Supplementary Fig. 17A). Similarly, phenylalanine showed significant negative correlations with uncharacterized gene *AT3G05400* but showed opposite trend with *APR2.* Furthermore, glycine levels displayed significant negative associations with *MSRB5, APR2,* but showed positive relation with *SULTR2;1* (Fig. 30A & Supplementary Fig. 17A). Carbon metabolism in shoots also appeared tightly linked to transcriptional changes, i.e. alpha-hydroxy-glutarate showed broad negative correlation networks involving *APR2, DTX9, SERAT3;2, MSRB5, and SFP1*. Maleate exhibited a positive correlation with *DTX9* and *SFP1* (Figure 30A & Supplementary Fig. 17A).

In roots, gene-metabolite correlations showed a partially distinct pattern, reflecting tissue-specific metabolic regulation (Fig. 30B & Supplementary Fig. 17B). 2-oxo-gluconate and fumarate were negatively correlated with *CYP79F2,* suggesting repression of specific organic acid pools in association with altered secondary metabolism. Glucose displayed positive correlations with *SDI1* while glycolate showed opposite pattern (Fig. 30B & Supplementary Fig. 17B). Glutamine was negatively associated with *SULTR2;1*, indicating a tighter coupling between sulfur signaling and nitrogen metabolism in roots compared to shoots. Several amino acids exhibited strong gene-specific associations in roots. Glycine showed positive correlations with *MSRB5* while negative correlation with *CYP79F2*, whereas lysine was negatively correlated with multiple sulfur-related genes including *APR2, DTX9*, *SERAT3;2, MSRB5,* and *SFP1,* highlighting extensive transcriptional control over amino acid metabolism. Organic acids such as malate was negatively correlated with *SHM7* and *SULTR1;2,* while α-ketoglutarate showed

positive associations with *AT3G05400* and *SULTR1;2,* suggesting link between TCA cycle activity and sulfur assimilation. Additionally, proline, a stress-associated amino acid, correlated positively with *SDI1,* supporting its role in sulfur deficiency-induced stress responses (Fig. 30B & Supplementary Fig. 17B).

Overall, this integrative correlation analysis demonstrates that sulfur-responsive transcriptional programs are closely associated with coordinated metabolic reprogramming, with stronger and more diverse correlations observed in shoots, while roots exhibit more selective and gene-specific associations. These findings highlight a tight coupling between sulfur signaling, primary metabolism, and stress-related metabolic pathways, reinforcing the importance of tissue-specific regulation during early developmental responses to sulfur deficiency.

A

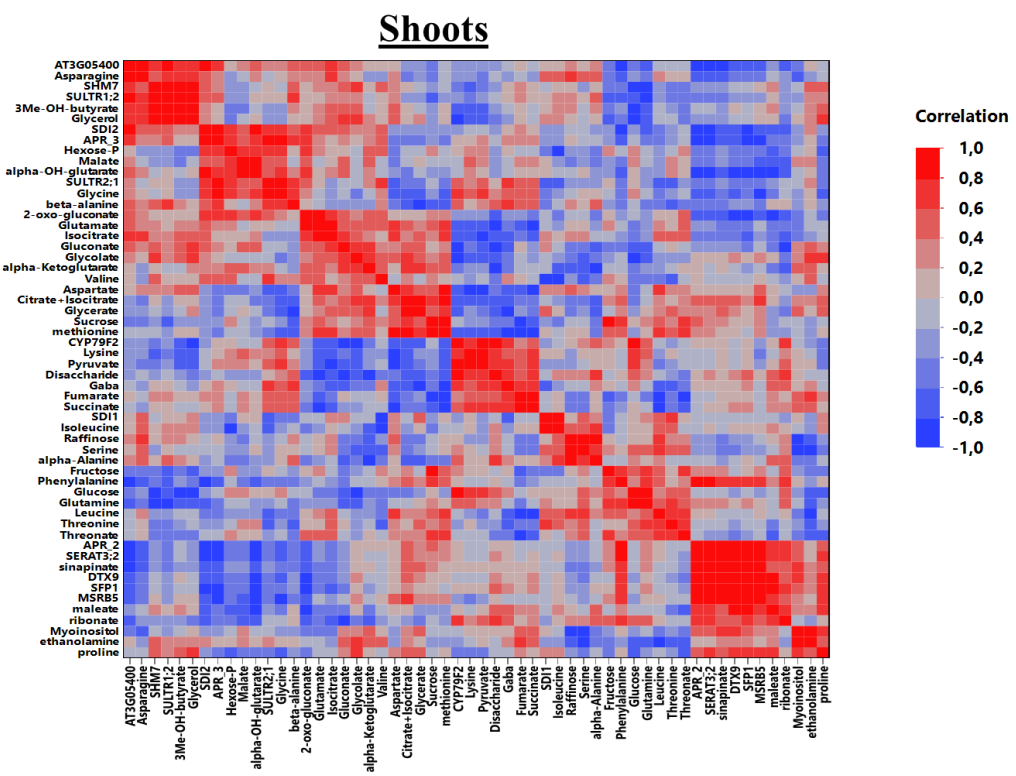

B

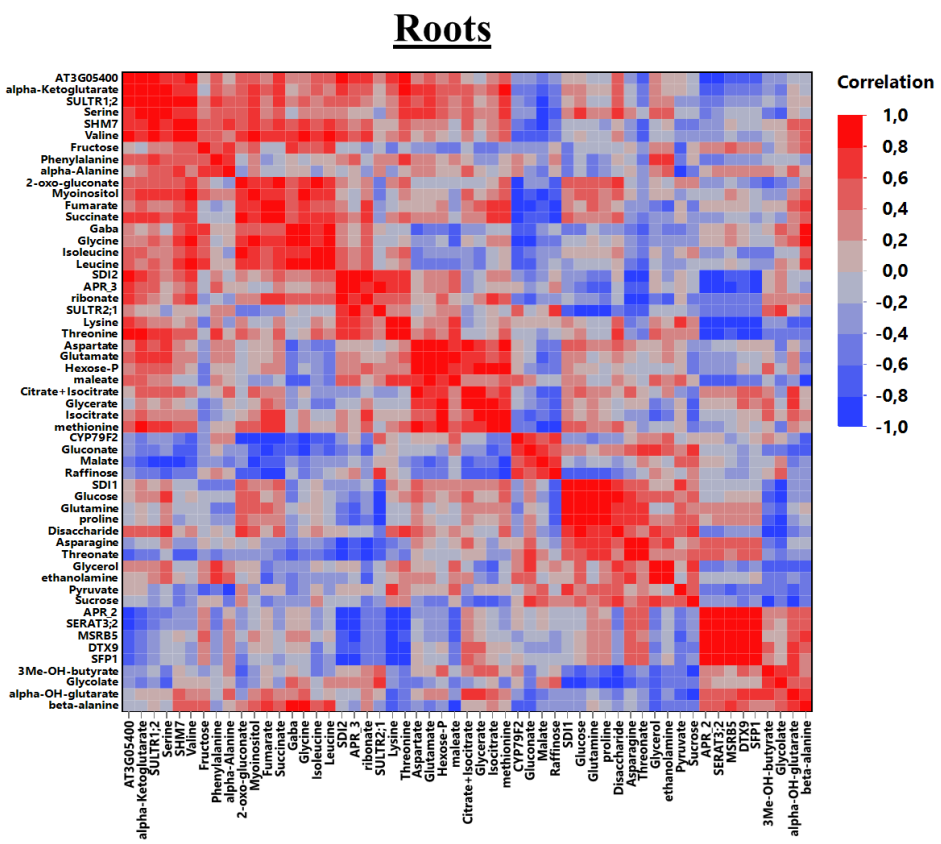

Figure 30: Correlation heatmap of sulfur-responsive genes and metabolites. Heatmaps depict Spearman correlations between $\log_2$ (low S / control) fold changes of sulfur-responsive DEGs and metabolites in **(A)** shoots and **(B)** roots. Red and blue colors indicate positive and negative correlations, respectively. Genes and metabolites are hierarchically clustered to reveal tissue-specific correlation patterns under sulfur deficiency. P-values representing significance of correlation are mentioned in Supplementary Fig. 17

5. DISCUSSION

Sulfur is considered a significant growth-limiting nutrient and ranks fourth among the major nutrient elements after nitrogen, phosphorus, and potassium (Aula et al., 2019). Various sulfur-containing metabolites, such as cysteine, glutathione, and methionine, together with sulfur-containing proteins like thioredoxins, play essential roles in maintaining ion homeostasis and regulating stress tolerance in plants (Tandon et al., 1984; Jamal et al., 2006). However, sulfur deficiency in crops has become a growing global concern and has been documented in cereals such as corn (*Zea mays*), wheat (*Triticum aestivum*), and rice (*Oryza sativa*) (Fontanetto et al., 2000; Inal et al., 2003; Randall et al., 2003). Thus, S deficiency poses a serious threat to modern agriculture, particularly when combined with other nutrient limitations (Jobe et al., 2019).

Given this agricultural importance, understanding how plants naturally vary in their sulfur content and how such variation contributes to adaptive responses under sulfur deficiency is particularly important. Natural variation in leaf S-content can span up to a 6-fold range across *Arabidopsis* accessions (Baxter et al., 2007; Campos et al., 2021), potentially leading to distinct adaptive strategies across environments. In order to explore the underlying regulatory mechanism behind this variation, quantitative genetics approaches have been employed, which identified several genes, such as *APR2* and *ATPS1*, that contribute to this variation, yet explain only a fraction (20–23%) of the observed differences (Loudet et al., 2007; Koprivova et al., 2013; Chao et al., 2014). Although loci such as *APR2* and *ATPS1* explain part of the natural variation in foliar sulfate accumulation, much less is known about the ecological consequences of this variation. Thus, the aim of the thesis is to demonstrate that differences in foliar sulfur (S) content reflect distinct adaptive strategies among *Arabidopsis* accessions, influencing how they balance metabolic adjustment, developmental timing, and transcriptional reprogramming under sulfur limitation. Furthermore, it investigates whether nutrient homeostasis covaries with functional traits such as growth, flowering, and reproductive output, thereby providing a physiological context for previously described genetic variation.

5.1 Sulfur content variation as a determinant of plant adaptive strategy

Sulfate (SO_4^{2-}) is the primary sulfur source for plants and represents the dominant sulfur pool, particularly in members of the *Brassicaceae* (Blake-Kalff et al., 1998; Narayan et al., 2022). Because sulfur deprivation elicits a coordinated systems-level response involving sulfate uptake, long-distance transport, and redistribution of internal sulfur pools (Nikiforova et al., 2005), we first examined how this pool is affected in the accessions differing in basal sulfur accumulation capacity. In natural soils, sulfate availability can fluctuate considerably due to environmental factors such as groundwater leaching (Kertesz & Mirleau, 2004; Kopriva & Rennenberg, 2004). Growth in the sand-soil system used in our study, therefore, likely reflects more closely the heterogeneous sulfur availability of natural environments than the constant nutrient and sterile conditions used in most sulfur studies. Under these

circumstances, plant genotypes may differ in their ability to buffer or respond to transient sulfur limitation. One possible expectation is that accessions with higher basal shoot sulfur content might better buffer against sulfur deficiency by relying on their larger internal sulfate reserves. However, our results rather showed that high-S accessions exhibited the most pronounced depletion of shoot sulfate and total foliar sulfur, together with poor recovery even under short-pulse sulfate supplementation (Fig. 5A, B). While the low-S accessions not only showed significantly less relative decline in shoot sulfate and total-S but also restored shoot sulfate to near-control levels under short-pulse treatment (Fig. 5A, B). These patterns indicate that sulfur starvation responses are strongly linked to the size of pre-existing sulfate pools, but in a counterintuitive manner. Such an opposite pattern can be explained by the fact that effective adaptation to sulfur limitation depends not only on the absolute size of sulfate reserves but also on the capacity to mobilize stored sulfate and dynamically reconfigure sulfur allocation (Takahashi et al., 2011). Indeed, we observed higher organic-to-inorganic sulfur ratios in shoots of low-S accessions under sulfur deficiency, while a slight or no increase in the organic-to-inorganic ratio in mid-S and high-S accessions was seen (Fig. 5D). Based on these findings, it seems that low-S accessions operate a more assimilation-oriented sulfur economy, in which sulfur flux is rapidly directed toward metabolic demand rather than long-term storage. Such a response in low-S accessions was further mediated by their enhanced sulfate uptake and increased translocation to shoots (Fig. 7) under S-deficiency, while the high-S group showed both lower relative uptake and translocation to shoots. Previous studies have established that, in *Arabidopsis*, high-affinity sulfate uptake is primarily mediated by the transporters *SULTR1;1* and *SULTR1;2*, with *SULTR1;1* typically exhibiting the strongest induction during sulfur starvation (Takahashi et al., 2000; Yoshimoto et al., 2002). Given our observation of increased uptake in low-S accessions, we then hypothesized that the group should show stronger induction of *SULTR1;1* and *SULTR1;2*. However, contrary to our hypothesis, high-S accessions showed the strongest induction of both *SULTR1;1* and *SULTR1;2* compared with control conditions. The observation that high-S accessions show higher relative expression of transporters but lower relative uptake can be explained well with the work of Yoshimoto et al. (2007), which showed that the expression of sulfate transporters does not always correlate with sulfate uptake because transporter activity is regulated post-transcriptionally, demonstrating that uptake capacity can be controlled independently of mRNA abundance. Additionally, the reduced translocation in high-S group, can also be associated with an attenuated response of miRNA395 and the SLIM1 transcription factor, both of which are important for increasing translocation to shoots under sulfur starvation by maintaining optimal levels of ATP sulfurylase transcripts, the first enzyme in sulfate assimilation, along with *SULTR2;1,* a low-affinity sulfate transporter (Kawashima et al., 2011).

Besides, our data also showed strong induction of some canonical sulfur starvation marker genes, including *SDI1, APR2, LSU1*, in roots of all accessions under sulfur deficiency (Fig. 6). This pattern is consistent with the established sulfur starvation signalling network controlled by SLIM1/EIL3 (Maruyama-Nakashita et al., 2006; Takahashi et al., 2011). However, high-S accessions again showed a

pronounced transcriptional response, whereas low-S and mid-S accessions displayed a more moderate induction (Fig. 6). These findings indicate that while high-S accessions can activate the starvation signal at the gene level, they exhibit an attenuated physiological response, suggesting a potential decoupling between starvation signaling and functional uptake capacity. On the other hand, it likely reflects severe internal sulfur limitation and cellular stress rather than effective buffering. Consistent with this, previous studies have emphasized that strong induction of sulfur starvation markers often reflects the severity of the sulfur deficit perceived by the plant rather than a successful physiological adaptation strategy (Lewandowska & Sirko, 2008; Kawashima et al., 2011). Accordingly, moderate induction of S-marker genes in low-S accessions suggests a more efficient acclimation strategy, where controlled transcriptional adjustment supports stable metabolic reorganization rather than large-scale reprogramming. Similar patterns were reported for stress-tolerant relatives of *Arabidopsis thaliana*, i.e., *Eutrema salsugineum*, which often exhibit 'stress-ready' expression programs and distinct metabolic strategies under abiotic stress, such as drought and cold (Wong et al., 2006; Kant et al., 2006). These genotypes likely achieve a new metabolic steady state through high plasticity and targeted regulation, thereby avoiding excessive transcriptional activation while sustaining sulfur homeostasis (Koprivova & Kopriva, 2014; Aarabi et al., 2020). Surprisingly, although mid-S accessions exhibited a substantial decline in sulfate pools under sulfur deficiency, their transcriptional response was similar in magnitude to that observed in low-S accessions (Fig. 6). This suggests that moderate sulfur starvation signaling did not translate into effective physiological compensation. One possible explanation is that sulfate assimilation and allocation are not controlled solely at the transcriptional level but also through post-transcriptional and post-translational mechanisms, as has been reported earlier. Key enzymes such as APS reductase are regulated by cellular redox status, while cysteine synthesis is controlled through the formation of the cysteine synthase complex (CSC) between SERAT and OASTL proteins (Bick et al., 2001; Takahashi et al., 2023).

To further assess whether these differences in sulfate uptake and translocation among the groups translate into differences in the allocation of sulfur to reduced sulfur pools, we measured shoot cysteine and GSH content in these groups. In plants, assimilated sulfate is reduced to sulfide and incorporated into cysteine, which serves as the central precursor for a wide range of sulfur-containing metabolites, including glutathione (GSH), an essential component of cellular redox homeostasis and stress protection (Noctor et al., 2012; Hasanuzzaman et al., 2017). S-deficiency causes a decline in reduced sulfur pools, in shoots as documented in *Arabidopsis thaliana, Setaria virdis,* and *Oryza sativa* (Dietzen et al., 2020; Zenzen et al., 2024). Consistent with this, we observed declines in both shoot cysteine and GSH content across all groups (Fig. 8A & C). However, based on the sulfate content and S-uptake results, we expected that the low-S group would maintain sulfur metabolism more effectively by prioritizing the synthesis and maintenance of key reduced sulfur compounds, such as cysteine and glutathione, under S-limitation. Indeed, this was the case, for the low-S group at least for shoot GSH content, although the group showed a greater relative reduction of cysteine under S-deficiency (Fig. 8A & C). One possible explanation for

the cysteine phenotype observed is that sulfur flux may be preferentially directed from cysteine toward glutathione biosynthesis under sulfur limitation, as glutathione represents a major sink for reduced sulfur and plays a central role in antioxidant defence (Noctor et al., 2012; Kopriva & Koprivova, 2014). Our results from [^{35}S] flux measurements validated this dataset (Fig. 9), as we observed that, although relative incorporation into GSH was enhanced across all groups under S-deficiency, consistent with previous findings (Dietzen et al., 2020), the low-S genotypes showed much higher sulfur allocation to GSH in shoots (Fig. 9). In contrast, we observed much greater reduction of GSH in the high-S and mid-S groups, followed by lower relative incorporation of [^{35}S] into GSH. This increased flux of cysteine to GSH in low-S accessions can also be complemented by induction of cysteine biosynthesis genes in shoots, thereby supporting continued cysteine production under sulfur limitation, even if the metabolite itself does not accumulate as it is rapidly consumed for GSH synthesis (Dietzen et al., 2020). We then assessed these accessions for relative expression of several key cysteine and GSH biosynthetic genes in shoots, including *SERATs, SiR, OASTL (OASTL-A), GSH1,* and *GSH2* (Figs. 11 and 12). Indeed, our data showed significant upregulation of *OASTL-A, SiR*, and *GSH2* in low-S accessions, as well as moderate induction of *SERAT* isoforms under S-deficiency. These genes also showed higher relative expression in both mid-S accessions, indicating these genotypes enhance their assimilatory power under S-deficiency. The induction of *OASTL-A*, *SiR*, and *SERATs* was in accordance with several studies reporting the induction of these key S assimilatory genes downstream of the SLIM1 transcription factor under sulfur starvation (Nakashita et al., 2006; Nikiforova et al., 2005). But to our surprise, high-S accessions, especially accession Hod, showed a quite distinct trend with almost all cysteine and GSH biosynthesis genes being downregulated in this genotype (Fig. 11 and 12). It also differed for its decline in shoot cysteine content with Zu-1. Such divergence in high-S accession was also reported in our RNA-Seq data, with only 11.8% of DEGs, shared among the accessions, indicate distinct regulatory network preferred by two accessions (Fig. 23A). The maintenance of cysteine levels in Zu-1 can also be linked to our root transcriptomic data showing upregulation of *MGL* under sulfur deficiency (Fig. 26D). As *MGL* participates in the trans-sulfurylation pathway, it facilitates cysteine synthesis through methionine degradation (Goyer et al., 2007). Hence, repression of cysteine biosynthesis genes along with *MGL* in Hod suggests a lower capacity to sustain cysteine biosynthesis in this genotype under sulfur deficiency, thus restricting downstream assimilatory power (Takahashi et al., 2023; Hirai et al., 2003; Nikiforova et al., 2003; Apodiakou et al., 2023; Kopriva et al., 2012). Sulfate reduction and thiol biosynthesis are energy-intensive processes, and in Hod, the loss-of-function of *APR2*, known to limit sulfate assimilation, likely reinforce this constraint (Chao et al., 2014). Therefore, the observed repression of cysteine biosynthesis genes under sulfur deficiency may reflect a protective adjustment to conserve ATP and reducing equivalents and to mitigate redox imbalance (Schnaubelt et al., 2013). The upregulation of genes related to increased electron flow to PSI, which is usually linked to maintaining ATP production, in our transcriptomic data further supports this hypothesis (Fig. 26A). Additionally, downregulation of *SERATs* and *OASTL-A* in Hod can also be linked to altered CSC dynamics as both genes are involved in

its formation. Such altered dynamic of CSC is not restricted to sulfur stress but have been associated with two highly relevant environmental stresses, i.e. drought and high-light stress. It has been reported that plastidial CSC, which requires *SERAT2;1* and *OASTL-B* for its formation, acts as an abiotic stress sensor and is important for stomatal closure induced by water limitation and high-light stress (Sun et al., 2025). Although we did not assess *OASTL-B* expression in shoots, but its unchanged expression in roots in transcriptomic dataset and the observed downregulation of *SERAT2;1* in Hod under sulfur deficiency may indicate a reduced capacity to form a functional CSC. This could contribute to increased susceptibility to additional abiotic stresses, suggesting that basal sulfur status not only influences sulfur metabolism but may also affect broader stress response mechanisms.

The restrained cysteine biosynthesis in Hod can then explain much higher relative decline in GSH content as cysteine provides the immediate sulfur donor for glutathione synthesis (Fig. 11 & 12). In contrast, despite maintaining cysteine levels, Zu-1 also exhibited a reduction in GSH under sulfur deficiency. This suggests that, in this accession, the limitation may not occur at the level of cysteine production but rather at the level of sulfur allocation toward glutathione synthesis or its subsequent turnover. Such a pattern indicates that maintaining cysteine pools alone is not sufficient to sustain glutathione levels and that additional regulatory constraints on GSH biosynthesis or utilization exist. Reduction of GSH indicates attenuated antioxidant capacity and probable oxidative damage under stress, as reported earlier by Maurizi et al. (2013), where GSH-deficient mutants showed increased oxidative stress by accumulation of more H_2O_2 and superoxide under stress conditions. Reverse is also true, as GSH has been linked to provide tolerance to several abiotic stress conditions such as drought, salinity, low temperature, and toxic metal stress (Foyer & Noctor 2005a; Hasanuzzaman et al., 2017). Hence, we further tested these groups for H_2O_2 and superoxide content under S-deficiency, and expected the high-S group to exhibit more severe oxidative damage given their greater reduction in GSH content. Our data from DAB and NBT staining were consistent with this, as high-S accessions showed higher H_2O_2 and superoxide accumulation in response to S deficiency, indicating an inability of these groups to sustain redox buffering (Fig. 10).

The distinct adaptive strategies observed for groups was also validated by multi-trait principal component analysis, which combined physiological, metabolic, transcriptional, and growth-related traits into a unified framework (Fig. 18). The PCA clearly separated accessions according to their sulfur response strategies, with high-S accessions aligning with nutrient uptake and starvation signalling traits, while low-S accessions clustered with metabolic and redox-related features. Notably, this analysis highlights that strong transcriptional activation in high-S accessions is not accompanied by effective metabolic and physiological adjustment, reinforcing the decoupling between sulfur starvation signaling and functional assimilation. In contrast, low-S accessions exhibited coordinated regulation of sulfur assimilation, glutathione allocation, and redox homeostasis, indicative of a more efficient acclimation strategy, while mid-S accessions showed intermediate behaviour. Together, these findings demonstrate that sulfur stress tolerance depends on coordinated regulation across physiological layers, and that high-

S accessions, despite strong signalling responses, are poorly suited to sustained sulfur limitation. Similar patterns have not been reported for sulfur, but for other macronutrients, where high nutrient storage (as seen in the high-S group) often reflects growth strategies adapted to nutrient-rich environments rather than improved tolerance to nutrient limitation (Chapin et al., 1990). Natural variation studies in *Arabidopsis thaliana* have similarly revealed contrasting strategies of nutrient acquisition and utilization under nitrogen limitation. Chardon et al. (2010) demonstrated that *Arabidopsis* accessions differ strongly in nitrate uptake capacity and nitrogen-use efficiency when grown under limiting nitrogen supply, indicating that some genotypes sustain growth through more efficient nitrogen utilization rather than larger nitrogen pools. In a complementary study, Ikram et al. (2012) reported substantial variation in growth and metabolic plasticity among *Arabidopsis* accessions exposed to different nitrogen regimes, highlighting that natural genetic variation can generate distinct physiological strategies for coping with nutrient scarcity. Together, these comparisons indicate that low-S accessions adopt an efficiency-driven, assimilation-based strategy; high-S accessions follow a storage-oriented but maladaptive strategy under sulfur deficiency; and mid-S accessions occupy an intermediate position, highlighting that nutrient-use efficiency rather than resource abundance determines adaptive success under sulfur deficiency. Our data also revealed that the decrease in sulfate content under S-deficiency was much stronger in roots than in shoots and showed no genotypic differences (Fig. 5C). This differential response between roots and shoots suggests a prioritization of sulfur allocation to the aerial parts under deficiency, possibly through enhanced mobilization of sulfate from roots to shoots. Such redistribution likely helps sustain essential processes in photosynthetic tissues, consistent with previous findings that sulfur is preferentially transported to shoots when external supply becomes limiting (Hawkesford, 2000; Kataoka et al., 2004; Takahashi et al., 2011).

Apart from the adaptation strategies observed across the groups, our study uncovers previously unreported features of sulfur-deficiency responses that differ from those described in earlier studies. For example, Col-0 exhibited a much stronger reduction in cysteine under S-deficiency, while glutathione levels were comparatively maintained. This contrasts with earlier reports, in which only a moderate (~20%) reduction in cysteine was observed, together with a pronounced decline in GSH (Dietzen et al., 2020). Additionally, Col-0 did not show uniform induction of some canonical sulfur starvation marker genes, differing from the typical response described previously (Dietzen et al., 2020). These observations point to a divergence between metabolic and transcriptional responses, which may be influenced by the experimental context. In our study, plants were grown in a sand-based system and analyzed at a later developmental stage, whereas most previous studies have relied on controlled nutrient media and early response time points. Importantly, our results highlight an underexplored dimension of sulfur metabolism, showing that both developmental stage and growth conditions can substantially modulate sulfur deficiency responses. Similar context-dependent discrepancies between controlled and more natural growth conditions have been reported in *Arabidopsis*, where field experiments revealed limited correspondence with laboratory-derived phenotypes across traits such as fitness, flowering time,

and photosynthesis (Koehl et al., 2015). Such insights into sulfur metabolite dynamics can guide the development of crops with improved nutrient efficiency and enhanced tolerance to nutrient fluctuations commonly encountered in agricultural soils.

5.2 Group-specific coordination of nutrient and metabolic responses to sulfur deficiency

Many studies have shown strong interactions between nitrate and sulfate assimilation (Koprivova et al., 2000; Takahashi & Saito., 1996; Sarda et al., 2014; Shah et al., 2022), and nitrate uptake and reduction are known to be suppressed under S deficiency (Dubousset et al., 2009; Sarda et al., 2014; Lee et al., 2016). The opposite pattern is also well reported: at the transcriptional level, N limitation downregulates APR activity and the expression of genes involved in sulfate assimilation (Yamaguchi et al., 1999; Koprivova et al., 2000; Luo et al., 2020). Cysteine acts as the convergence point for three major pathways of primary metabolism, i.e., carbon, nitrogen, and sulfate assimilation, pointing out again probable N-S crosstalk (Jobe et al., 2019). Similarly, sulfur and phosphate signaling are tightly interconnected, with leaf phosphate often positively correlated with sulfate levels (Ristova et al., 2019; Soda et al., 2019; Rouached et al., 2011). Consistent with these interactions, we hypothesized that sulfur deficiency would affect nitrogen and phosphate accumulation across accessions, and that variation in basal sulfur content may influence the extent to which these nutrient interactions are modulated. Our data revealed pronounced, group-specific alterations in nitrate and phosphate accumulation under sulfur limitation, indicating that variation in basal sulfur content does shape the coordination of nitrogen and phosphate homeostasis. Across all groups, sulfur deficiency reduced shoot nitrate levels, consistent with previous reports showing that sulfur limitation constrains nitrate uptake and assimilation (Fig. 13A) (Kaur et al., 2011; Li et al., 2020). However, a decline in shoot nitrate was particularly pronounced in the low-S group, followed by mid-S accessions, and was accompanied by higher root nitrate accumulation in the low-S group, whereas the mid-S and high-S groups exhibited levels similar to the control under S deficiency (Fig. 13A & B). This pattern indicated that sulfur limitation can uncouple nitrate uptake from nitrate accumulation in shoots of the low-S group by stimulating nitrate reduction and utilization, thereby altering root-to-shoot nitrate partitioning (Kaiser et al., 2002; Wang et al., 2018).

Hence, to check whether this is true at the regulatory level, we measured the relative expression of nitrate assimilation genes in these accessions. Indeed, nitrate assimilation was enhanced in low-S group as upregulation of *NIA1*, *NIA2* and slight induction of *NiR1*, was observed for shoots of low-S accessions specifically App1-16 (Fig 14). Gene *NIA1, and NIA2* encodes nitrate reductase (NR) that catalyzes the first and rate-limiting step of nitrate assimilation. Gene *NiR1* encodes nitrite reductase, which converts nitrite to ammonium (NH_4^+) in the plastids, hence catalyzing the second step of N-assimilation (Stitt, 1999; Stitt & Scheible, 1999). Besides, we also observed upregulation of *HRS1* in shoots of low-S accession In-0 under S-deficiency (Fig. 14). *HRS1 (NIGT1)* is a GARP-family transcription factor that integrates nutrient signals and modulates nitrate-related transcriptional networks, including coordination

with phosphate signaling in *Arabidopsis* (Medici et al., 2015). Hence, induction of this gene in shoots indicates active integration of nitrogen and phosphate signaling pathways, suggesting that sulfur deficiency triggers broader nutrient reprogramming in this genotype. Such a nitrate response in the low-S group is consistent with the study by Stitt et al. (2002), in which nitrate depletion was linked to strong activation of nitrate reduction. In addition, increased NR activity due to *NIA1* upregulation has previously been linked to improved acclimation to stress, as *NIA1* is a key component of NR-mediated nitric oxide (NO) production in *Arabidopsis* (Zhao et al., 2009). NO acts as a signaling molecule and serves an important role in different abiotic stress tolerance, including drought, salt stress, heat, and metal toxicity in plants (Mata & Lamattina, 2001; Zhao et al., 2007; Song et al., 2006; Rodríguez-Serrano et al., 2006; Tian et al., 2007). Further, the activation of nitrate reduction can also be attributed to increased demand for reduced nitrogen to support cysteine biosynthesis, as cysteine is a common link between N-S signaling, thereby lowering steady-state nitrate levels in shoots, as we saw in the low-S group (Kopriva & Koprivova, 2014; Tobe et al., 2019). Together, these responses indicate that low-S accessions might actively redirect nitrate toward assimilation and metabolic integration rather than storage, thereby improving adaptation to long-term S-deficiency stress.

In contrast, while the mid-S group responded similarly to the low-S group, high-S accessions, especially Hod, showed repression of *NIA1* in roots along with downregulation of *NiR1* and *NRT1;1* in shoots. The downregulation of these genes despite nitrate depletion suggests active restriction of nitrogen assimilation under sulfur limitation (Fig. 14). In Hod, the loss-of-function of *APR2* may hence trigger feedback regulation that downregulates nitrate assimilation to maintain stoichiometric balance between nitrogen and sulfur metabolism. Such a response aligns well with the study by Kaur et al. (2011), in which sulfur deprivation not only alters sulfur metabolism but also suppresses components of nitrate assimilation, including nitrate reductase activity and transcript abundance, reflecting coordinated nutrient regulation. Also, downregulation of *NIA1* has been previously linked to reducing NO synthesis, leading to insensitive stomata that fail to close under abscisic acid treatment, as observed in the *nia1nia2* double mutant in *Arabidopsis* (Zhao et al., 2016). Thus, downregulation of nitrate assimilation genes can be another piece of evidence for the sensitivity of the high-S group under S-limitation, even though they have higher foliar S-content. Further, our data also revealed that supplementation with sulfate (SP treatment) restored the shoot nitrate levels back to control values in low-S and high-S accessions, indicating nitrate homeostasis is highly sensitive to transient sulfur availability (Fig. 13A). However, the lack of recovery in mid-S accessions suggests their reduced capacity to rapidly integrate fluctuating sulfur signals into nitrate transport and assimilation responses (Fig. 13A).

Additionally, our data showed a positive correlation between cysteine biosynthetic and nitrate assimilation genes, further supporting coordinated regulation of nitrogen and sulfur metabolism at the transcriptional level. Such co-regulation has been described in multiple systems and is thought to ensure stoichiometric balance between nitrogen and sulfur (Hesse et al., 2004; Reuveny et al., 1980; Prosser et al., 2001). Such a balance is important to maintain the amino acid levels in plants, which are further

used for protein synthesis (Carfagna et al., 2011). Given the differential responses of S-related metabolites and nitrate among these groups, we then examined the global metabolomic profile in 35-day-old leaves of these accessions under S deficiency (Fig. 15). Metabolic changes under S deficiency have been well reported in several studies, as S limitation causes systemic internal rebalancing of plant metabolism (Nikiforova et al., 2006). Such rebalancing can cause either an increase or a decrease in levels of distinct metabolites, thereby revealing the plants' priorities aimed at economizing resources for survival and, eventually, seed production (Zenzen et al., 2024; Nikiforova et al., 2006; Nikiforova et al., 2003). In our study, we observed that S-deficiency induces broad metabolic reprogramming; however, the extent of this reorganization differed among groups and was highly genotype-dependent. Consistent with previous reports, most accessions showed a significant accumulation of several amino acids under sulfur deficiency, with Kro-0 and Hod exhibiting a stronger response (Blake-Kalff et al., 1998; Hirai et al., 2004) (Fig. 15). This accumulation is likely a consequence of reduced metabolic flux through the sulfur assimilation pathway, we have previously reported in Hod. As expected from our previous results, where low-S group performed better under S-deficiency, this group also showed modest changes to amino acid accumulation. While surprisingly Col-0, the reference genotypes, also behaved similarly to the low-S group, contrary to previously mentioned studies, this could be due to different developmental stages and growth systems used in our experiments. Interestingly, in the low-S accession App1-16, we observed an accumulation of glutamate, glycine, and serine, consistent with the cysteine-nitrate and redox patterns described above (Figs. 8, 10, 13, 31). This combination of amino acids suggests active nitrogen assimilation and enhanced photorespiratory flux, a pathway often stimulated under nutrient and redox stress to support carbon-nitrogen redistribution and maintain redox balance (Foyer et al., 2009). Such a pattern is consistent with a strong decline in shoot nitrate, accompanied by the induction of nitrate assimilation genes, as described before, further validating enhanced nitrate turnover rather than reduced uptake (Figs. 14 and 31). While in high-S accession Hod, accumulation of glutamate alongside asparagine and aspartate is indicative of nitrogen retention and stress-driven metabolic reprogramming, with asparagine serving as a low-cost storage and transport form of nitrogen when growth and anabolic investment are constrained (Fig. 15) (Lam et al., 1996). This could also be linked to strong sulfur-starvation signaling, together with repression of nitrate assimilation genes, as observed in our earlier dataset, accompanied by pronounced depletion of sulfate and glutathione and elevated oxidative stress (Fig. 31).

Sulfur starvation also affected the accumulation of several sugars and organic acids among the group. The increased accumulation of sucrose observed in both high-S accessions and Kro-0 is consistent with a shift toward carbon storage under nutrient limitation, which might further affect photosynthesis and growth in plants (Fig. 15) (Yan et al., 2022; Lemoine et al., 2013). Such accumulation of sugar levels can also be linked to increased flux of carbon towards starch content as seen in *Spirodela polyrhiza* (Duckweed). S-deficiency led to an increase in starch content in Duckweed, which was 42% and 73% higher under nitrogen and phosphorus limitation, respectively (Sun et al., 2022). While an increase in

raffinose in both low-S accessions under S-deficiency can be linked to their role described previously in regulating abiotic stress tolerance (Yan et al., 2022). Accumulation of one of the organic acids, α-ketoglutarate, in both high-S accessions indicates an imbalance between carbon availability and nitrogen assimilation, suggesting restricted incorporation of carbon skeletons into amino acid biosynthesis under sulfur deficiency (Fig. 15) (Doucette et al., 2011). In high-S accessions, elevated levels of other metabolites, such as phosphorylated hexoses and glycerol, suggest enhanced glycolytic flux and osmotic adjustment, which are commonly associated with stress-induced metabolic reprogramming (Fig. 15) (Obata & Fernie, 2012). By contrast, the more limited metabolic changes in low-S accessions point to a strategy of maintaining metabolic balance rather than undergoing large-scale reorganization. Together, these results indicate that sulfur deficiency alters how natural accessions coordinate nutrient cross-talk and metabolic networks. Low-S accessions appear to prioritize flexible redistribution of nitrate and sulfur resources and limit global metabolic disruption, whereas high-S accessions and one of the mid-S accessions, Kro-0, undergo extensive transcriptional and metabolic reprogramming that reflects higher physiological stress. Thus, variation in sulfur status shapes not only sulfur metabolism itself but also the broader coordination of nitrogen, phosphorus, and carbon metabolism, ultimately defining distinct adaptive strategies under sulfur-limited conditions.

The pronounced relative decline in shoot phosphate in low-S accessions highlights their reliance on S-P signalling interactions (Rouached, 2011; Ristova et al., 2022) and may represent part of their conservative adjustment strategy, in which both nitrogen and phosphate metabolism are reprogrammed to maintain sulfur homeostasis under deficiency (Fig. 13C). Our data showed that, although low-S accessions accumulated higher shoot phosphate under control conditions, consistent with our previous findings (Jager et al., 2023), they also exhibited the greatest relative decline under sulfur deficiency, even at a late developmental stage (Fig. 13C). This behaviour is consistent with the well-documented coordination between sulfate and phosphate signalling, in which sulfur limitation suppresses phosphate accumulation through shared regulatory components, such as *PHR1* and SPX-domain proteins (Rouached et al., 2011; Mangalakkadan et al., 2026). The absence of a phosphate decline in high-S accessions likely reflects already low basal phosphate levels, suggesting limited dynamic range rather than enhanced buffering capacity. Moreover, the inability of short-pulse sulfate supply to restore phosphate levels in the low-S and mid-S groups highlights that phosphate homeostasis responds more slowly to sulfur availability than nitrate, in agreement with reports that phosphate signalling integrates longer-term nutrient status rather than short-term fluctuations (Fig. 13C) (Ares et al., 2022).

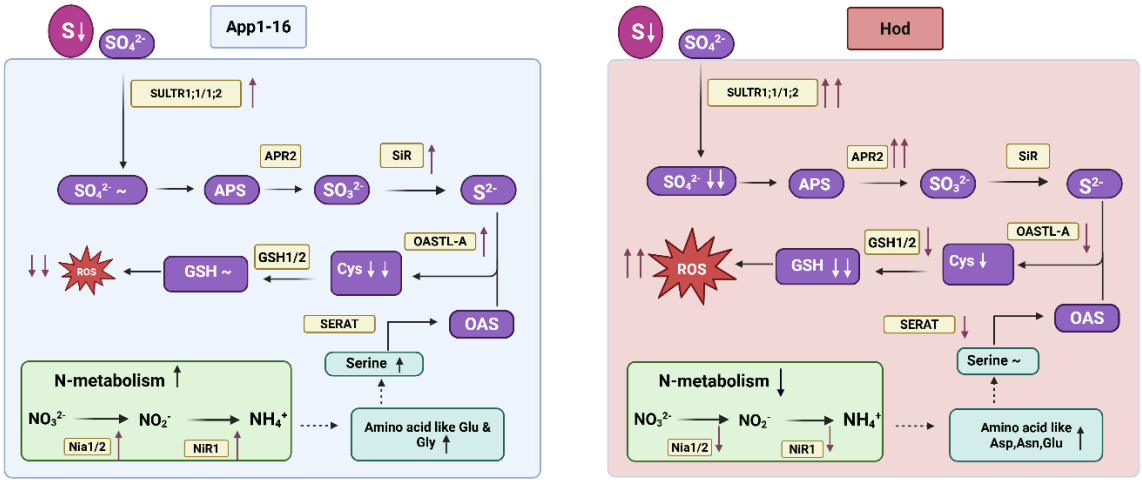

Figure 31: Conceptual model illustrating contrasting sulfur-nitrogen signalling and metabolic strategies in low-S (App1-16) and high-S (Hod) *Arabidopsis thaliana* accessions under sulfur deficiency. Purple arrows indicate transcriptional or regulatory responses, with upward arrows denoting induction and downward arrows indicating repression. Arrows within metabolite boxes represent relative changes in metabolite abundance, where upward arrows indicate accumulation and downward arrows indicate depletion and symbol (~) indicates levels being unchanged.

5.3 Life history strategies and inter-generational outcome of S-availability

Sulfur is an essential nutrient playing a pivotal role in plant physiology and development, largely because of its central role in metabolism (Kopriva et al., 2004). Several studies have reported that sulfur deficiency reduces protein synthesis, due to limitations in amino acid biosynthesis, and inhibits photosynthesis, ultimately leading to retarded growth (Klapheck et al., 1982; Cilbert et al., 1997). Given its importance, we then wanted to examine how S-availability can shape life-history adaptation in our *Arabidopsis* accessions that differ in intrinsic sulfur status. Our metabolic data from earlier chapters revealed that S-limitation is negatively related to the size of pre-existing S-pools; we wanted to assess whether this also holds true for developmental traits. Indeed, that was the case, as high-S accessions experienced disproportionate penalties in vegetative growth, flowering regulation, and reproductive output, whereas low-S accessions exhibited comparatively stable performance despite limited sulfur availability, with mid-S accessions showing an intermediate response. The pronounced reduction in rosette diameter observed in both high-S and mid-S accessions under sulfur deficiency indicates their greater dependence on a sustained sulfur supply to maintain vegetative growth (Fig. 16Ai-ii). Hence, this indicates that high-S accessions, which accumulate higher sulfur pools under control conditions, likely operate at a higher metabolic baseline and therefore experience stronger metabolic constraints when sulfur becomes limiting. Decline in their growth even under the short-pulse treatment further supports this interpretation, suggesting that brief sulfur availability is insufficient to meet ongoing sulfur demand in these accessions (Fig. 16Ai). In contrast, low-S accessions displayed stable growth patterns even under control condition consistent with the fact that almost all accessions selected randomly were

late flowering, as many of the accessions in our panel originate from Northern and Central Europe (e.g. Sweden and the Czech Republic), regions enriched for winter-annual *Arabidopsis* genotypes adapted to extended vegetative growth and delayed flowering (Stinchcombe et al., 2004; Johanson et al., 2000). However, irrespective of sulfur regime, they exhibited a consistent growth strategy even under S-deficiency, without any reductions being reported, indicating a conservation adaptation strategy (Fig. 16Ai). Such strategies have been described in nutrient-limited environments, where slower growth rates minimize nutrient demand and enhance tolerance to resource scarcity as one of the stress-tolerance strategies (Chapin, 1980; Grime, 2001). The absence of a strong additional growth penalty under sulfur deficiency in low-S accessions suggests that these genotypes are pre-adapted to operate at low sulfur availability, relying on internal reallocation and tight metabolic control rather than high uptake capacity.

Flowering time further revealed distinct, group-specific developmental strategies in response to fluctuating sulfur supply (Fig. 16B). We observed that low-S accessions maintained flowering-time ratios close to unity under both sulfur-deficient and short-pulse treatments, with minimal within-group variability (Fig. 16B). Thus, low-S accessions not only maintained stable growth patterns but also didn't exhibit plasticity in flowering time under fluctuating S-supply. Mid-S accessions showed consistently elevated flowering time ratios under sulfur deficiency with less intragroup variability, indicating these accessions show a delay in flowering time under S-deficiency. This was quite different from the previous literature where accelerated flowering has been reported for the low-S group (Nikiforova et al., 2006). One possible explanation is the prioritization of other physiological processes for immediate survival in these accessions, as flowering can be energy-intensive and metabolically demanding, and they respond normally to a short pulse treatment (Fig. 16B) (Baek et al., 2026). However, this can also be linked to altered flower morphology in this group, as sulfur deficiency is known for a drastic reduction in the number of open flowers, thus causing retarded floral transition, although we didn't test the accessions for this since it was beyond the scope of this study (Ausma et al., 2021). In contrast, high-S accessions exhibited accelerated flowering time under both S-deficiency and short-pulse treatments, reinforcing the interpretation of enhanced phenological plasticity in this group (Supplementary Fig. 5A; Fig. 16B). Such stress-induced acceleration of flowering has been previously reported in *Arabidopsis* under severe sulfur limitation and is commonly interpreted as a stress-escape strategy (Nikiforova et al., 2005; Kazan & Lyons, 2016). Such a response can also be linked to impaired sulfate transport, as observed previously in the *sultr2;1* mutant, where impaired sulfate transport resulted in earlier bolting compared with wild-type Col-0 (Soudthedlath et al., 2024). Additionally, this may be due to inefficient redox buffering, as glutathione limitation can hasten flowering time, as reported earlier: treatment with L-buthionine sulfoximine (BSO), which depletes GSH, accelerates flowering unless GSH is supplemented (Ogawa et al., 2001). Our data on decreased translocation and significant reduction of GSH in high-S accessions can further validate these findings (Fig. 7 & 8).

As known previously, sulfur plays a crucial role in reproductive development, including seed filling and embryo development, through its involvement in protein synthesis and antioxidant defense (Zuber et al.,

2010; Kopriva et al., 2019). In *Arabidopsis*, it has been reported that under sulfur deficiency, *SDI1* is strongly induced during seed development, where it represses sulfur-rich compounds such as glucosinolates and S-rich seed storage proteins, thereby reallocating sulfur resources (Aarabi et al., 2021). Additionally, in several cereals, S-deficiency has been shown to reduce both yield and grain quality, thereby affecting nutritional value (MacGrath et al., 1996; Etienne et al., 2018; Sharma et al., 2024). Supplementation with sulfur, by contrast, can increase productivity; for example, in wheat, average grain yield increased from 0.20 to 0.29 $kg\,m^{-2}$ following S-fertilization (Yu et al., 2021). Consistent to prior studies, we observed sulfur deficiency led to a significant reduction in seed weight across all groups (Supplementary Fig. 5B). Indeed, not only the quantity of seed but also the quality of seed was affected as seen in our ionomics dataset on these seeds, where total-S content was also significantly reduced under S-deficiency indicating overall role of sulfur in controlling reproductive fitness in plants (Fig. 16D). However, while all previous studies could document the impact of sulfur deficiency on plant growth and seed development. To our knowledge, our study is the first to define how natural variation in intrinsic sulfur status shapes reproductive allocation strategies under sulfur limitation. By linking sulfur content to the trade-off between seed number and seed provisioning, we could show a genotype-dependent framework that connects nutrient status to fitness outcomes. We observed that low-S accessions maintained relatively stable silique numbers but exhibited reduced seed weight and total-S content, suggesting that these genotypes prioritize seed quantity over seed quality under sulfur limitation. Mid-S accessions, in contrast, showed reduced silique number with only minor effects on seed weight, indicating a partial shift toward maintaining seed provisioning at the expense of reproductive output, although reduced seed sulfur content suggests that sulfur allocation to seeds was still constrained. High-S accessions were the most reproductively sensitive, showing reductions in both silique number and seed weight, as well as lower seed total-S content. This indicates an inability to sustain neither seed quantity, nor seed quality under sulfur deficiency. Altogether, these patterns indicate that reproductive responses to sulfur deficiency are not solely determined by the external nutrient environment but are strongly shaped by the genotype's intrinsic sulfur status. Basal sulfur content thus appears to predefine how plants allocate resources to reproduction under stress, influencing the balance between seed number and seed provisioning.

As already discussed, prolonged S-deficiency leads to transcriptional reprogramming towards accelerated flowering (Nikiforova et al., 2005) and also affects the quality of seeds (Muttucumaru et al., 2006; Zörb et al., 2009). However, how the genetically induced (accession) and environmentally induced (S-deficiency) variation in S-content affect the performance of the next generation has never been addressed. Emerging evidence suggests that epigenetic mechanisms are involved in sulfur-deficiency responses, as sulfur limitation can influence genome-wide DNA methylation in plants (Huang et al, 2019). This is likely linked to the fact that S-adenosylmethionine (SAM), the universal methyl donor for DNA methylation, is synthesized from cysteine in the primary sulfate assimilation pathway (Huang et al., 2019). In line with this, methylation changes have been associated with the gene *MSA1*

(More Sulfur Accumulation 1; previously annotated as *SHM7*), where mutations lead to altered DNA methylation patterns in several sulfur-deficiency-responsive genes (Huang et al., 2016). Similarly, Global Transcription Factor Group E proteins, GTE7 and GTE2, along with the chromatin remodelling factor INO80 Subunit 2B (IES2B) have been associated in modulating dynamic DNA methylation at the *SULTR1;1* promoter in *Arabidopsis* (Luo et al., 2025). Parallel studies have shown that other nutrient stresses, such as phosphate, nitrate and zinc deficiencies, lead to altered global DNA methylation at the whole-genome level (Secco et al., 2015; Chen et al., 2018). Based on this, we hypothesized that sulfur deficiency in the parental generation could influence seed traits and thereby affect metabolism and functional performance in the offspring, potentially improving their response to sulfur limitation. Our transgenerational analysis revealed that sulfur availability can influence offspring traits but, in a genotype-specific manner, highlighting a potential link between sulfur metabolism and epigenetic regulation (Fig. 17). A clear example was observed in the high-S accession Hod, where progeny from sulfur-deficient parents maintained lower sulfate levels even when grown under control conditions (Fig. 17A). This was quite contradictory to the high-S phenotype seen in this accession. One reason behind it could be the maternal effect on seed sulfur provisioning, likely caused by altered sulfur allocation during seed development, which is also consistent with the reduced total-S content of seeds observed in this genotype (Fig 16D). Another explanation for such a phenotype can also be triggered by DNA-methylation due to reduced sulfur availability in the parental generation, which may affect methylation-related processes during seed formation. Such a transfer of methylation patterns into the progeny due environmental stresses like nutrient deficiency, salt, jasmonic acid, or salicyclic acid treatment have been described for genetically identical apomictic dandelions (*Taraxacum officinale*) (Heard et al., 2014). Flowering time responses showed a similar pattern for two accessions, App1-16 and Zu-1, from low-S and high-S group respectively (Fig. 17C). In App1-16, parental sulfur deficiency increased the delay in flowering under S-limitation, whereas in Zu-1 it promoted earlier flowering, consistent with a stress-escape response. These contrasting responses suggest that parental sulfur status can influence developmental sensitivity in a genotype-dependent manner, possibly through changes in seed nutrient status or epigenetic regulation during seed development. Such transgenerational modulation in flowering time has been reported in *Arabidopsis thaliana*, where parental effect on mild heat triggered flowering in genotypes adapted to dry summers (Groot et al., 2017). A similar response has been observed in other plant species, such as *Brassica rapa.* Plants grown from seeds collected after natural drought stress flowered earlier than those from seeds collected before the drought (Franks, 2011). Additionally, while flowering time and sulfate content showed transgenerational effects, most other traits, including nitrate, phosphate, thiol levels, and silique number, were primarily determined by the sulfur conditions experienced by the offspring rather than the parental environment (Supplementary Fig. 7 & 8). However, this does not imply that sulfur deficiency is not involved in epigenetic regulation; rather, such effects may require multiple generations to influence transcriptional plasticity. This is consistent with findings in *Arabidopsis thaliana,* where Suter and Widmer (2013) reported no parental

or transgenerational effects after two generations of mild salt stress in Col-0. In contrast, exposure over three generations, particularly when combined with the Sha-0 genotype, resulted in improved growth under salt stress. Moreover, transgenerational effects are often context-dependent and strongly influenced by the environment experienced by the offspring (Groot et al., 2016). This may partly explain why we did not observe consistent parental effects across most traits, as our soil-based growth system differs from the controlled conditions typically used in studies of epigenetic regulation under sulfur deficiency. Nevertheless, our results demonstrate that parental sulfur status can influence offspring performance, although in a genotype-dependent manner.

5.4 S-content variation shapes the magnitude and architecture of transcriptional acclimation under sulfur deficiency

Sulfur (S) deficiency is known to trigger a coordinated transcriptional reprogramming aimed at maintaining sulfur homeostasis, reallocating internal sulfur pools, and minimizing growth penalties under nutrient stress (Yoshimoto et al., 2002; Takahashi et al., 2007; Maruyama-Nakashita et al., 2017). Apart from *Arabidopsis*, a large number of genes responsive to sulfate deficiency have been identified through transcriptomic studies, primarily in rice, *Setaria virdis*, tomato, and wheat (Zenzen et al., 2024; Canales et al., 2020; Dai et al., 2015). These studies motivated us to test the hypothesis that natural variation in basal sulfur content preconditions the transcriptional state of accessions, thereby shaping the magnitude and coordination of their responses to sulfur limitation. Given that previous transcriptomic analyses of sulfur deficiency have largely been conducted at early developmental stages in *Arabidopsis,* we performed RNA-Seq at 18 days to capture the primary transcriptional response to sulfur limitation and facilitate direct comparison with existing datasets. Under this hypothesis, low-S accessions would be expected to rely on a more selective and efficient regulatory adjustment, whereas high-S accessions would require broader transcriptional reprogramming because their metabolic and physiological strategy is less suited to sustained sulfur shortage, as seen broadly in previous chapters. The root transcriptomic data strongly support this view, as high-S accessions showed by far the largest number of DEGs under sulfur deficiency, while low-S accessions displayed much fewer transcriptional changes (Fig. 19). Such stronger transcriptional reprogramming was also followed by stronger induction of S-marker genes in the high-S group, even in early developmental stages. Such enhanced transcriptional reactivity likely reflects increased sensitivity to sulfur limitation, consistent with SLIM1-mediated responses scaling with sulfur status rather than stress tolerance (Brumbarova & Ivanov, 2019; Nakashita et al., 2006). At the same time, we found core 55 DEGs that were shared across all six accessions, including well-known regulators of the sulfate starvation response, such as *SDI1, SDI2, LSU1, APR2, SHM7*, and *GGCT2;1* (Hubberten et al., 2012; Maruyama-Nakashita et al., 2006) (Fig. 20). These findings confirm that core sulfur-transcriptional modules are widely shared, irrespective of accession background. However, the core set represents ~1.7% of the total transcriptional response, indicating that most of the response is shaped by genetic background, as we observed in our PCA, where

the treatment effect was subsided by genotypic effects (Fig. 19A). Hence, despite extensive evidence for conserved sulfur starvation signalling components, i.e., SLIM1-mediated regulation of *SDI* and *LSU* genes (Ristova et al., 2022; Maruyama-Nakashita et al., 2006), our data indicate that these accessions share distinct downstream transcriptional output. Such a response has also been previously described for monocots under S-deficiency, where a large number of DEGs were species-specific, i.e., rice and *Setaria viridis*, with only a small proportion (58) of DEGs shared between them. This indicates that similar physiological phenotypes could result from distinct regulatory mechanisms or indicates expression level polymorphism. This was seen previously in *Arabidopsis*, where strong cis-acting polymorphisms, many of which are likely to be structural variations, were responsible for the genetic regulation of global gene expression diversity in the leaf of natural *A. thaliana* accessions (Zan et al., 2016). Additionally, it was also seen that using smaller collections of natural *A. thaliana* accessions, large expression variation has been observed both at individual gene (Richards et al. 2012; Gan et al., 2011) and gene-network (Kliebenstein et al. 2006; van Leeuwen et al., 2007) response levels. Together, these findings support the notion that phenotypic convergence under sulfur deficiency does not require conserved transcriptional responses but can instead be achieved through multiple, accession-specific regulatory solutions.

It was particularly notable, that, in addition to the expected GO categories related to sulfur starvation, several enriched terms were not directly associated with sulfur homeostasis, including circadian clock components such as *CCA1, LHY*, and *RVE/LCL5* (Fig. 20C; Supplementary Fig. 10). These genes were not only present within the core set of 55 DEGs but were also enriched among group-specific DEGs across all three sulfur-content classes. Sulfur metabolism has long been linked to diurnal and circadian regulation, with previous studies demonstrating that OAS-dependent sulfur signaling is tightly integrated with clock function, mediated in part by transcription factors such as *RVE1* and *RVE8,* which are predicted to regulate OAS cluster genes (Ran et al., 2020). Collectively, these observations indicate that sulfur-deficiency responses are not solely nutrient-driven but are embedded within circadian regulatory networks. Another GO category was flavonoid biosynthetic and metabolic process involving genes *CHIL, FLSI,* and *F3'H*, upregulated in all three groups. These genes are involved in flavonoid biosynthesis, which might indicate accumulation of flavonoids under S-deficiency as has been reported previously (Nikiforova et al., 2003). Such response can be traced to the antioxidant properties of flavonoids, which help counteract excessive ROS production and repair damage caused by environmental stresses such as drought, salinity, and toxic metal stress (Shomali et al., 2022; Hatier et al., 2008). Hence, this could indicate shared response to S-deficiency in the groups by enhancing flavonoid production to maintain cellular redox homeostasis.

Beyond this conserved core, our data reveal distinct transcriptional responses across sulfur-content groups under S-deficiency. Group-specific DEGs in low-S accessions indicate that, in addition to sulfur assimilation pathways, they also reinforce photoprotective and chloroplast-associated processes by upregulating genes such as *SIG5* and *SOUL-1* (Fig. 24). Gene *SIG5*, involved in transcription of plastid

genes within chloroplast, is induced under multiple stress conditions and enhances PSII repair, thereby supporting photosynthetic efficiency (Nagashima et al., 2004). While *SOUL-1* is a heme-binding protein that can bind tetrapyrroles, it functions in heme transport and degradation, contributing to intracellular ROS homeostasis, and its overexpression has been linked to enhanced oxidative stress tolerance (Huang et al., 2025; Sun et al., 2025). Accordingly, increased expression of these genes in low-S accessions likely contributes to their improved performance under S-deficiency by maintaining photosynthetic function and limiting ROS accumulation, consistent with their lower H_2O_2 and superoxide levels (Fig. 10). In parallel, low-S accessions showed repression of carbohydrate remobilization, as evidenced by downregulation of genes involved in sugar and starch metabolism (*TPPE, ISA3, BXL2*). The relatively stable sugar levels in low-S accessions observed in our metabolite data, together with the downregulation of these genes, suggests a restrained carbon turnover, indicative of a strategy to preserve metabolic stability under sulfur deficiency (Fig. 29). A similar strategy has been reported in *Spirodela polyrhiza*, where young fronds under sulfur deficiency reduce PSII light absorption, maintain redox balance, and redirect carbon toward starch and anthocyanin accumulation (Peršić et al., 2025). Consistent with this, low-S group showed upregulation of *UGT78D2*, which catalyzes the glucosylation of flavonols and anthocyanidins, suggesting that low-S accessions may channel their carbon into flavonoid-based protective pathways (Lee et al., 2005). At the same time, low-S accessions showed repression of glucosinolates and defense-related compounds, including camalexin and other indole phytoalexins. Such responses have been widely documented in *Arabidopsis* and are linked to reduced GSH, as it serves as a precursor to sulfur-containing secondary metabolites, such as camalexin (Aarabi et al., 2020; Falk et al., 2007). However, as low-S accessions maintained GSH levels better than other groups, this may also reflect a sulfur-saving strategy in which sulfur is redirected from defense compounds toward essential metabolic functions (Sugiyama et al., 2021). Overall, low-S accessions exhibit a tightly coordinated transcriptional strategy that links chloroplast protection, carbon economy, and sulfur reallocation to sustain metabolic and redox stability under sulfur limitation.

In addition to the common sulfur-starvation programme, DEGs unique to mid-S accessions showed compensatory strategy centered on antioxidant buffering and secondary metabolic adjustment (Fig. 25). The KEGG pathway showed enrichment for flavonoid and sesquiterpenoid biosynthesis. Terpenoid biosynthesis has not been directly linked to S-deficiency before, but they have been reported to mitigate oxidative stress by scavenging reactive oxygen species (ROS) and modulating antioxidant enzyme systems under abiotic stress (Shan et al., 2025). Consistently, upregulated DEGs also included genes involved in detoxification, such as *GSTL1* and *AER*. *AER* has been shown to alleviate oxidative stress by detoxifying reactive carbonyl species under nutrient limitation, while GST-related enzymes contribute to ROS scavenging and stress tolerance (Shan et al., 2025; Chan et al., 2014). Despite this, mid-S accessions were unable to fully prevent oxidative stress relative to low-S accessions, as observed in our data, indicating that this strategy is less effective. For example, repression of *GLY14*, involved in methylglyoxal (MG) detoxification, may contribute to enhanced oxidative damage, as MG accumulates

under abiotic stress and disrupts cellular redox balance (Zheng et al., 2024). This interpretation is further supported by enrichment of "response to cadmium (Cd) ion" among upregulated DEGs and our shoot ionomic data showing higher Cd accumulation under sulfur deficiency in this group (Supplementary Fig. 16). Given that glutathione (GSH) is central to Cd detoxification through sequestration and immobilization mediated by *LSU1* and *LSU2*, increased Cd levels suggest a reduced capacity to maintain redox and metal homeostasis (Li et al., 2023). In addition, mid-S accessions uniquely showed repression of oxygen-responsive signalling, with "response to hypoxia" enriched among downregulated DEGs. Similar patterns have been reported in the *eil1* mutant, a key regulator of ethylene signaling, suggesting attenuated ethylene-mediated stress responses under sulfur deficiency in the group (Dietzen et al., 2020). Collectively, these findings indicate that mid-S accessions rely on a reactive, redox-centered compensatory strategy involving detoxification and secondary metabolism; however, limited coordination of these processes may result in reduced ability to control oxidative stress relative to low-S accessions.

In contrast, high-S accessions, apart from activation of sulfur starvation pathways, revealed a broader and more complex response involving photosynthetic electron transport, carbohydrate metabolism, and also circadian rhythm (Fig. 26). The group showed enhanced transcriptional regulation of electron transport toward photosystem I (PSI), as genes associated with its proper functioning, including *PGR5, PDE329*, and *CFBP1*, were upregulated (Yamamoto et al., 2018; Strand et al., 2017). As PSI is involved in cyclic electron flow, which is responsible for producing ATP without reducing $NADP^+$, thus increased electron flow to the system indicates that high-S accessions prioritize ATP production under S-deficiency (Walker et al., 2014). Such an imbalance in photosynthetic function has also been reported in rice under S-deficiency; however, no direct link of these mechanisms has been studied in *Arabidopsis* yet, further explaining the broader impact of S-deficiency in plants (Lunde et al., 2008). The group also responded to S-deficiency by upregulating genes like *SUS3, GoLSI* involved in carbohydrate metabolism. While increased *SUS* transcript levels are linked with meeting the increased glycolytic demand during environmental stress (Ricard et al., 1998; Déjardin et al., 1999), gene *GoLSI* is linked with osmoprotectant function by maintaining ROS levels against heavy metal stress (Ranjan et al., 2025). Hence, this indicates that the high-S group prioritizes photosynthetic energy balance while reallocating carbon toward stress-protective metabolites under S-deficiency. This response was further accompanied by repression of detoxification-related genes, particularly glutathione S-transferases (*GSTF, GSTU*), as well as downregulation of glucosinolate and indole metabolism. As GSTs are involved in the conjugation of GSH to toxic compounds, and are usually upregulated under S-starvation, their repression in this group suggests GSH-independent detoxification. Some studies have reported that several GSTs are involved in regulating the binding and transport of defence-related compounds e.g. indole-derived compounds (Dixon et al., 2011). Hence, the co-clustering of indole-containing biosynthetic pathways with *GST* genes for downregulated DEGs further validate this fact. Another notable feature was the low overlap of DEGs between Zu-1 and Hod, with several genes showing

opposite regulation. These included pathways related to cell wall organization, developmental signalling, and protein regulation, indicating divergent regulatory strategies despite similar sulfur status. The contrasting behaviour of *MGL* further supports this divergence. *MGL* catalyzes methionine degradation and contributes to sulfur recycling via methanethiol (Goyer et al., 2007), and is typically induced under sulfur deficiency (Dietzen et al., 2020). Its induction in Zu-1 but repression in Hod suggests that Zu-1 retains greater capacity for internal sulfur remobilization, consistent with maintained cysteine levels, whereas Hod appears more constrained under S-deficiency. Collectively, these findings indicate that high-S accessions mount a strong but heterogeneous response characterized by enhanced energy reprogramming yet limited detoxification and recycling capacity, reflecting a less coordinated and less efficient acclimation to sulfur deficiency.

Transcriptomic data under control conditions further demonstrated that natural variation in sulfur content is underpinned by distinct baseline transcriptional programs that likely precondition subsequent stress responses (Fig. 27). Surprisingly, low-S accessions did not show clear functional enrichment despite a large number of DEGs, suggesting a more distributed and flexible transcriptional organization rather than reliance on specific pathways. This was consistent with correlation analysis between DEGs and S-content, where genes associated with diverse biological processes were identified; for example, *IAA34,* involved in auxin signalling and apical hook formation, and *APX2*, which functions in H_2O_2 detoxification via the ascorbate-GSH cycle (Caverzan et al., 2012; Wang et al., 2024) (Fig. 28). In contrast, mid-S accessions showed enrichment of cysteine and methionine metabolism, with genes such as *NS2* and *ACC2* involved in SAM biosynthesis (Roje et al., 2006). This group also exhibited enrichment of quinone biosynthesis pathways, including *DHNAT-2,* involved in redox-active phylloquinone synthesis, indicating coordinated regulation of sulfur assimilation and redox cofactors consistent with their intermediate stress response (Lohmann et al., 2006). High-S accessions, however, were enriched for sulfation processes mediated by sulfotransferases such as *ATST4A, ATST4C*, and *ATST2B,* indicating preferential allocation of sulfur toward secondary metabolism, including glucosinolates (Koprivova et al., 2016) (Supplementray Fig. 15B). Sulfation reactions consume activated sulfate (PAPS), and in Hod, which carries a loss-of-function mutation in *APR2*, a key enzyme in sulfate reduction, this likely restricts flux into reduced sulfur pools (cysteine and glutathione) while allowing continued accumulation and utilization of sulfate for sulfation. This is consistent with our previous study (Jager et al., 2023), where high-S accessions showed higher indolic glucosinolate content and increased expression of *SOT17.* This may explain the paradox of high sulfate content despite limited assimilation capacity, as sulfur is stored or diverted into sulfated compounds rather than incorporated into primary metabolism. Such a shift results in apparent sulfur accumulation but reduced metabolic availability, consistent with the impaired physiological performance of high-S accessions specially Hod under sulfur deficiency. Additionally, high-S accessions showed enhanced expression of genes such as *SPPL1* and *SAR2,* associated with protein turnover and vesicular trafficking, suggesting elevated basal activity of cellular processing and transport systems that may facilitate sulfate storage or

compartmentalization (Han et al., 2009; Tripathy et al., 2020). Collectively, these findings indicate that high sulfur content does not reflect enhanced assimilation capacity but rather altered sulfur partitioning, where limited reduction capacity (e.g., *APR2* constraint), combined with active sulfation and storage processes, leads to sulfate accumulation and shapes distinct adaptive strategies under sulfur deficiency.

5.5 Coordinated transcriptional and metabolic reprogramming under sulfur deficiency during early development

To further corroborate the transcriptional response observed in our data, we performed global metabolic profiling of 18-day-old roots and shoots of these genotypes for direct comparison of the two traits and to explore whether transcriptional and metabolic reprogramming are coordinated in response to S-deficiency (Fig. 29 & 30). Consistent with previous finding by Nikiforova et al. (2006), we also observed a strong link between these two datasets, but we were also surprised to find striking differences in the metabolites of early- and late-developing shoots (mentioned in earlier chapter) of the same genotypes. Such age related metabolic and transcriptomics changes have been previously reported in *Arabidopsis* (Buchanan-Wollaston et al., 2003; Breeze et al., 2011; Woo et al., 2018). For example, the contents of some metabolite like choline and amino acids like alanine and glutamine were high in four-week-old *Arabidopsis* plants and less abundant in six-week-old plants along with γ-aminobutyric acid (GABA) present only in four-week-old plants (Jafari et al., 2017). Additionally, our data also revealed that sulfur deficiency induced markedly stronger metabolic changes in shoots than in roots, consistent with role of shoots as the primary site of sulfate reduction and assimilation (Fig. 29) (Kopriva et al., 2015). This tissue bias is well documented at the transcriptional level (Dietzen et al., 2020; Nikiforova et al., 2003; Hirai et al., 2004) and is here reflected at the metabolic level, indicating that sulfur-responsive gene expression is rapidly translated into metabolic adjustments during early growth. Our findings revealed accumulation of branched-chain amino acids (BCAAs) in shoots across all genotypes (Fig. 29). Despite this, RNA-Seq analysis showed enrichment of downregulated genes associated with the BCAA metabolic process, suggesting that reduced metabolic turnover may contribute to their accumulation. However, this was much pronounced in mid-S and high-S groups. This may indicate a shift in the metabolic pathway from Aspartic (Asp) through the branch-point homoserine toward accumulating BCAAs, such as threonine and isoleucine, in these groups (Blake Kalff et al., 1998). It can also be due to the reduced metabolic flow along sulfur assimilation pathway (Blake kalff et al., 1998; Hirai et al., 2004). Alternatively, the accumulation of BCAAs may result from enhanced protein degradation under stress conditions, a process regulated by ABA signaling that increases the availability of free amino acids (Huang et al., 2017). In contrast, the general decline in amino acid levels in roots indicates reduced biosynthetic activity and supports the view that roots primarily function as sulfur-acquisition and transport organs rather than as sites of metabolic buffering. Changes in organic acid and sugar metabolism in shoots further indicate a reorganization of central carbon metabolism under sulfur limitation (Fig. 29). Reduced levels of organic acid and TCA cycle intermediates, particularly in low-S

and mid-S are consistent with earlier reports that sulfur deficiency may affect mitochondrial function and, consequently, respiration in these genotypes, highlighting that natural sulfur variation modulates not only sulfur metabolism itself but also the plant's broader energetic state (Nikiforova et al., 2005). Hence, when interpreted together with group-specific DEGs marked by induction of photoprotective and chloroplast-associated genes and repression of carbon remobilization, this suggests a coordinated strategy in the low-S group in which carbon flux is restricted while maintaining photosynthetic stability and redox balance. The reduction in organic acids, together with enrichment of redox-related pathways such as ubiquinone biosynthesis, indicates a disruption of central carbon metabolism in mid-S accessions, accompanied by compensatory activation of electron transport and redox buffering mechanisms to maintain cellular homeostasis.

Importantly, the integrative correlation analysis directly links these metabolic adjustments to sulfur-responsive transcriptional programs (Fig. 30). Positive associations between sulfur uptake and assimilation genes (e.g. *SULTR1;2, SHM7*) and metabolites related to carbon and amino acid metabolism support the concept of coordinated sulfur-carbon-nitrogen regulation, a hallmark of sulfur starvation responses (Hesse et al., 2004; Jobe et al., 2019). Conversely, negative correlations between sulfur deficiency markers such as *SDI1* and BCAAs reinforce the regulatory role of *SDI1* as a central hub that reallocates sulfur away from secondary and growth-associated metabolism toward essential processes (Blake kalff et al., 1998; Hirai et al., 2004). The presence of both positive and negative gene-metabolite correlations, particularly in shoots, indicates that sulfur deficiency does not induce a uniform metabolic shutdown but rather a selective reprogramming of pathways depending on sulfur status and genotype. Roots exhibited fewer, more gene-specific correlations, consistent with a more constrained metabolic role and tighter transcriptional control, particularly linking sulfur signaling to nitrogen metabolism and stress responses. Overall, these results demonstrate that sulfur deficiency elicits an integrated transcriptional-metabolic response already during early development, and that natural sulfur variation shapes the balance between metabolic conservation and flexibility. Low-S accessions preferentially downregulate central metabolism, whereas mid-S and high-S accessions display broader metabolic plasticity. This early divergence in metabolic strategy likely underpins the distinct physiological and fitness outcomes observed later in development, reinforcing sulfur homeostasis as a systems-level trait emerging from coordinated gene-metabolite networks.

5.6 Conclusion and future perspective

Our work demonstrates that effective adaptation to sulfur limitation depends not on the magnitude of sulfate reserves, but on the coordinated integration of uptake, assimilation, allocation, redox buffering, and life-history regulation (Nikiforova et al., 2005; Kopriva & Koprivova, 2014; Jobe et al., 2019). Contrary to our initial hypothesis, accessions with lower basal sulfur content (low-S) consistently performed better under sulfur deficiency. These genotypes maintained sulfur pools through enhanced

uptake and translocation, while efficiently channeling sulfur flux toward glutathione via coordinated regulation of cysteine and nitrate pathways. This was further supported by their higher basal expression of stress- and redox-associated genes and a restrained, targeted transcriptional response under sulfur limitation, involving photoprotective adjustments and reduced carbon remobilization. Together, these features define a highly plastic, assimilation-centered strategy that supports metabolic stability and stress tolerance.

In contrast, high-S accessions exhibited a storage-oriented strategy that was already evident under control conditions, as indicated by enrichment of sulfation-related pathways mediated by sulfotransferases. In the case of Hod, loss-of-function of *APR2* likely restricts sulfate reduction, reinforcing sulfur allocation toward sulfated metabolites and contributing to sulfate accumulation without effective assimilation. Under sulfur deficiency, these accessions displayed strong transcriptional reprogramming, including induction of sulfur-starvation pathways, photosynthetic electron transport, and carbohydrate metabolism. However, this response was poorly coordinated with metabolic demand, resulting in depletion of reduced sulfur pools, increased oxidative stress, and fitness penalties. Divergence within this group, particularly in sulfur recycling via *MGL*, further highlights distinct regulatory routes, with repression of *MGL* in Hod likely contributing to its higher sensitivity due to limited sulfur remobilization. Developmental traits further indicated that high-S accessions are more susceptible to sulfur deficiency, as they exhibited reduced rosette diameter and accelerated flowering and reproductive penalties. Mid-S accessions occupied an intermediate position, showing activation of canonical sulfur-starvation responses along with additional detoxification and secondary metabolic pathways, including flavonoid, terpenoid, and glutathione-associated metabolism. Despite this compensatory response, they exhibited elevated oxidative stress and incomplete physiological adjustment, indicating a less efficient adaptive strategy than that of low-S accessions. Our study further shows that effective sulfur stress tolerance arises not from maximal activation of starvation signaling, but from coordinated and efficient integration of metabolic, redox, and developmental responses. Accordingly, future work should focus on elucidating post-transcriptional and post-translational regulation of sulfur pathways, linking sulfur-use strategies to ecological and evolutionary contexts, and testing plant responses under combined nutrient stresses, particularly nitrate and phosphate, which more closely reflect natural and agricultural environments.

Importantly, our study provides novel insights by integrating early and late developmental stages within a sand–soil system that better reflects natural environmental heterogeneity. The discrepancies observed relative to previous studies, particularly in Col-0 responses, highlight the strong context dependency of sulfur-deficiency responses. Furthermore, our work is among the first to demonstrate genotype-dependent parental effects of sulfur status on offspring traits such as flowering time and sulfate content. Our findings also extend sulfur biology into reproductive outcomes, showing that sulfur deficiency not only reduced vegetative sulfur pools but also lowered total sulfur content in seeds and reduced seed weight across all genotypes, indicating that sulfur-use strategies directly influence seed provisioning and

reproductive quality. Importantly, our data reveal that sulfur variation extends beyond sulfur metabolism itself, reshaping nutrient crosstalk and metabolic coordination, particularly with nitrogen, phosphorus, and carbon metabolism. At the molecular level, the limited overlap of DEGs among accessions underscores extensive regulatory divergence, suggesting that similar physiological outcomes can arise through distinct transcriptional architectures. In this context, expression genome-wide association studies (eGWAS) represent a valuable approach to identify regulatory loci underlying expression variation. Moreover, our study identifies novel pathways, including flavonoid and sesquiterpenoid metabolism and photosynthetic adjustments, as well as candidate genes not previously associated with sulfur deficiency, thereby expanding the known regulatory landscape of sulfur responses. In addition, the pronounced differences between root and shoot metabolic profiles highlight the importance of tissue-specific regulation, and reciprocal grafting experiments would provide a powerful approach to disentangle root- versus shoot-driven control of sulfur uptake, long-distance signaling, and allocation strategies under deficiency.

From an applied perspective, our work challenges the assumption that higher nutrient content confers greater resilience. Instead, it highlights that lower sulfur content, when coupled with efficient assimilation and allocation, represents a promising trait for improving nutrient-use efficiency and stress tolerance in crops. Rather than selecting for high nutrient accumulation, breeding strategies should focus on optimizing the coordination between uptake, assimilation, and metabolic demand. Overall, this study establishes sulfur-use efficiency as an emergent property of integrated gene–metabolite networks shaped by natural variation, providing a conceptual framework for linking nutrient metabolism with plant adaptation and agricultural improvement.

6. REFERENCES

Aarabi, F., Kusajima, M., Tohge, T., Konishi, T., Gigolashvili, T., Takamune, M., ... & Maruyama-Nakashita, A. (2016). Sulfur deficiency–induced repressor proteins optimize glucosinolate biosynthesis in plants. *Science Advances*, *2*(10), e1601087.

Aarabi, F., Naake, T., Fernie, A. R., & Hoefgen, R. (2020). Coordinating Sulfur Pools under Sulfate Deprivation. Trends in Plant Science, 25(12), 1227-1239. https://doi.org/10.1016/j.tplants.2020.07.007

Aarabi, F., Rakpenthai, A., Barahimipour, R., Gorka, M., Alseekh, S., Zhang, Y., Salem, M. A., Brückner, F., Omranian, N., Watanabe, M., Nikoloski, Z., Giavalisco, P., Tohge, T., Graf, A., Fernie, A. R., & Hoefgen, R. (2021). Sulfur deficiency-induced genes affect seed protein accumulation and composition under sulfate deprivation. *Plant Physiology*, *187*(4), 2419-2434. https://doi.org/10.1093/plphys/kiab386

Ahmad A, Abdin MZ (2000a) Interactive effect of sulphur and nitrogen on the oil and protein contents and on the fatty acid profiles of oil in the seeds of rapeseed (*Brassica campestris* L.) and mustard (*Brassica juncea* L. Czern. and Coss.). J Agron Crop Sci 185:49–54. https://doi.org/10.1046/j.1439-037X.2000.00401.x

Ahmad S, Fazli IS, Jamal A, Iqbal M, Abdin MZ (2007) Interactive effect of sulfur and nitrogen on nitrate reductase and ATP-sulfurylase activities in relation to seed yield from *Psoralea corylifolia* L. J Plant Biol 50:351–357.

Ali MM, Mian MS, Islam A, Begum JA, Ferdous AKM (2004) Interaction effects of sulphur and phosphorus on wetland rice. Asian J Plant Sci 5:597–601

Almario J, Jeena G, Wunder J, Langen G, Zuccaro A, Coupland G, Bucher M. Root-associated fungal microbiota of nonmycorrhizal Arabis alpina and its contribution to plant phosphorus nutrition. Proc Natl Acad Sci U S A. 2017;114(44):E9403–12.

Al-Shehbaz I O'Kane S Jr (2002) Taxonomy and phylogeny of Arabidopsis (Brassicaceae). The Arabidopsis Book 1: 1–22, doi/10.1199/tab.001

Apodiakou, A., & Hoefgen, R. (2023). New insights into the regulation of plant metabolism by O-acetylserine: Sulfate and beyond. *Journal of Experimental Botany*, *74*(11), 3361-3378. https://doi.org/10.1093/jxb/erad124

Astolfi S., Celletti S., Vigani G., Mimmo T., Cesco S. Interaction between sulfur and iron in plants. Front. Plant Sci. 2021;12:670308. doi: 10.3389/fpls.2021.670308.

Atwell, S., Huang, Y. S., Vilhjálmsson, B. J., Willems, G., Horton, M., Li, Y., ... & Nordborg, M. (2010). Genome-wide association study of 107 phenotypes in Arabidopsis thaliana inbred lines. *Nature*, *465*(7298), 627-631.

Aubry, S., Smith-Unna, R. D., Boursnell, C. M., Kopriva, S., & Hibberd, J. M. (2014). Transcript residency on ribosomes reveals a key role for the A rabidopsis thaliana bundle sheath in sulfur and glucosinolate metabolism. The Plant Journal, 78(4), 659-673.

Ausma, T., Bansal, V., Kraaij, M., Verloop, A. C., Gasperl, A., Müller, M., Kopriva, S., De Kok, L. J., & Van der Kooi, C. J. (2021). Floral displays suffer from sulphur deprivation. *Environmental and Experimental Botany*, *192*, 104656. https://doi.org/10.1016/j.envexpbot.2021.104656

Authier, A., Cerdán, P., & Auge, G. (2023). Non-stressful temperature changes affect transgenerational phenotypic plasticity across the life cycle of Arabidopsis thaliana plants. *Annals of Botany*, *132*(7), 1259. https://doi.org/10.1093/aob/mcad171

Baek, G., Yoon, J., Shin, N. H., Choi, J., Park, Y. J., Chin, J. H., & Cho, L. H. (2026). Coordinating nutrient supply and flowering time for sustainable agriculture. *Journal of Experimental Botany*, *77*(4), 969-984. https://doi.org/10.1093/jxb/eraf492

Ball L, Accotto GP, Bechtold U, Creissen G, Funck D, Jimenez A, Kular B, Leyland N, Mejia-Carranza J, Reynolds H, Karpinski S, Mullineaux PM. Evidence for a direct link between glutathione

biosynthesis and stress defense gene expression in Arabidopsis. Plant Cell. 2004 Sep;16(9):2448-62. doi: 10.1105/tpc.104.022608. Epub 2004 Aug 12. PMID: 15308753; PMCID: PMC520945.

BaoShengjie, AnLijun, SuSha, ZhouZhongjing, and GanYinbo. 2011. Expression patterns of nitrate, phosphate, and sulfate transporters in *Arabidopsis* roots exposed to different nutritional regimes. *Botany*. **89**(9): 647-653. https://doi.org/10.1139/b11-053

Baránek, M., Fragkostefanakis, S., Sauvage, C., Maury, S., Kaiserli, E., Testillano, P. S., & Verdier, J. (2025). Maternal environmental effects and climate-smart seeds: Unlocking epigenetic inheritance for crop innovation in the seed industry. *The Plant Journal*, *123*(3), e70407. https://doi.org/10.1111/tpj.70407

Baxter, I., M. Ouzzani, S. Orcun, B. Kennedy, S. S. Jandhyala et al., 2007 Purdue ionomics information management system. An integrated functional genomics platform. Plant Physiol 143: 600-611.

Baxter, I., Muthukumar, B., Park, H. C., Buchner, P., Lahner, B., Danku, J., Zhao, K., Lee, J., Hawkesford, M. J., Guerinot, M. L.and Salt, D. E. (2008). Variation in molybdenum content across broadly distributed populations of Arabidopsis thaliana is controlled by a mitochondrial molybdenum transporter (MOT1). PLoS Genet, 4**,** pp. e1000004. doi:https://doi.org/10.1371/journal.pgen.1000004.

Bednarek, P., Pislewska-Bednarek, M., Svatoš, A., Schneider, B., Doubsky, J., Mansurova, M., ... & Schulze-Lefert, P. (2009). A glucosinolate metabolism pathway in living plant cells mediates broad-spectrum antifungal defense. *Science*, *323*(5910), 101-106.

Bick, J. A., Setterdahl, A. T., Knaff, D. B., Chen, Y., Pitcher, L. H., Zilinskas, B. A., & Leustek, T. (2001). Regulation of the Plant-type 5‘-Adenylyl Sulfate Reductase by Oxidative Stress. *Biochemistry*, 40(30), 9040-9048.

Bielecka, M., Watanabe, M., Morcuende, R., Scheible, W. R., Hawkesford, M. J., Hesse, H., & Hoefgen, R. (2015). Transcriptome and metabolome analysis of plant sulfate starvation and resupply provides novel information on transcriptional regulation of metabolism associated with sulfur, nitrogen and phosphorus nutritional responses in Arabidopsis. Frontiers in Plant Science, 5, 805. https://doi.org/10.3389/fpls.2014.00805

Blake-Kalff MM, Harrison KR, Hawkesford MJ, Zhao FJ, McGrath SP.. 1998. Distribution of sulfur within oilseed rape leaves in response to sulfur deficiency during vegetative growth. Plant Physiology 118, 1337–1344.

Bolger AM, Lohse M, Usadel B. Trimmomatic: a flexible trimmer for Illumina sequence data. Bioinformatics. 2014;30(15):2114–20.

Bouranis DL, Malagoli M, Avice JC, Bloem E.. 2020. Advances in plant sulfur research. Plants (Basel) 9, 256. [DOI] [PMC free article] [PubMed] [Google Scholar]

Brachi B, Meyer CG, Villoutreix R, Platt A, Morton TC, Roux F, Bergelson J.. 2015. Coselected genes determine adaptive variation in herbivore resistance throughout the native range of *Arabidopsis thaliana*. Proceedings of the National Academy of Sciences USA 112, 4032–4037.

Breeze E, Harrison E, McHattie S, et al. 2011. High-resolution temporal profiling of transcripts during Arabidopsis leaf senescence reveals a distinct chronology of processes and regulation. The Plant cell 23, 873–894.

Brumbarova, T., & Ivanov, R. (2019). The Nutrient Response Transcriptional Regulome of Arabidopsis. *IScience*, *19*, 358.https://doi.org/10.1016/j.isci.2019.07.045

Brunold C, Landolt W, Lavanchy P (1983) SO2 and assimilatory sulfate reduction in beech leaves. Physiol Plant 59:313–318. https://doi.org/10.1111/j.1399-3054.1983.tb04207.x

Buchanan-Wollaston V, Earl S, Harrison E, Mathas E, Navabpour S, Page T, Pink D. 2003. The molecular analysis of leaf senescence—a genomics approach. Plant Biotechnology Journal 1, 3–22.

Burow M, Halkier BA.. 2017. How does a plant orchestrate defense in time and space? Using GSLs in Arabidopsis as case study. Current Opinion in Plant Biology 38, 142–147.

Bustos, R., Castrillo, G., Linhares, F., Puga, M. I., Rubio, V., Pérez-Pérez, J., ... & Paz-Ares, J. (2010). A central regulatory system largely controls transcriptional activation and repression responses to phosphate starvation in Arabidopsis. *PLoS genetics*, *6*(9), e1001102.

Calderwood A., Kopriva S. (2014). Hydrogen sulfide in plants: from dissipation of excess sulfur to signaling molecule. *Nitric Oxide* 41 72–78. 10.1016/j.niox.2014.02.005

Campos, A., W. F. A. van Dijk, P. Ramakrishna, T. Giles, P. Korte et al., 2021 1,135 ionomes reveal the global pattern of leaf and seed mineral nutrient and trace element diversity in Arabidopsis thaliana. Plant J 106: 536-554.

Canales J, Uribe F, Henriquez-Valencia C, Lovazzano C, Medina J, Vidal EA. Transcriptomic analysis at organ and time scale reveals gene regulatory networks controlling the sulfate starvation response of Solanum lycopersicum. BMC Plant Biol. 2020;20(1):385.

Carfagna, S., Vona, V., Di Martino, V., Esposito, S., & Rigano, C. (2011). Nitrogen assimilation and cysteine biosynthesis in barley: Evidence for root sulphur assimilation upon recovery from N deprivation. *Environmental and Experimental Botany*, *71*(1), 18-24. https://doi.org/10.1016/j.envexpbot.2010.10.008

Caverzan, A., Passaia, G., Rosa, S. B., Ribeiro, C. W., Lazzarotto, F., & Margis-Pinheiro, M. (2012). Plant responses to stresses: Role of ascorbate peroxidase in the antioxidant protection. *Genetics and Molecular Biology*, *35*(4 Suppl), 1011. https://doi.org/10.1590/s1415-47572012000600016

Champigny, M.J., Sung, W.W., Catana, V. et al. RNA-Seq effectively monitors gene expression in Eutrema salsugineum plants growing in an extreme natural habitat and in controlled growth cabinet conditions. BMC Genomics 14, 578 (2013). https://doi.org/10.1186/1471-2164-14-578

Chan EK, Rowe HC, Kliebenstein DJ.. 2010. Understanding the evolution of defense metabolites in *Arabidopsis thaliana* using genome-wide association mapping. Genetics 185, 991–1007.

Chan, C., & Lam, H. M. (2014). A Putative Lambda Class Glutathione S-Transferase Enhances Plant Survival under Salinity Stress. *Plant and Cell Physiology*, *55*(3), 570-579. https://doi.org/10.1093/pcp/pct201

Chang C Bowman JL DeJohn AW Lander ES Meyerowitz EM (1988) Restriction fragment length polymorphism linkage map for Arabidopsis thaliana . Proc Natl Acad Sci USA 85: 6856–6860

Chao DY, Baraniecka P, Danku J, Koprivova A, Lahner B, Luo H, Yakubova E, Dilkes B, Kopriva S, Salt DE (2014). Variation in sulfur and selenium accumulation is controlled by naturally occurring isoforms of the key sulfur assimilation enzyme ADENOSINE 5'-PHOSPHOSULFATE REDUCTASE2 across the Arabidopsis species range. Plant Physiol. 166:1593-1608.

Chao, D. Y., Silva, A., Baxter, I., Huang, Y. S., Nordborg, M., Danku, J., Lahner, B., Yakubova, E.and Salt, D. E. (2012). Genome-wide association studies identify heavy metal ATPase3 as the primary determinant of natural variation in leaf cadmium in Arabidopsis thaliana. PLoS Genet, 8**,** pp. e1002923. doi:https://doi.org/10.1371/journal.pgen.1002923.

Chapin F S. The mineral nutrition of wild plants.Annu. Rev. Ecol. Syst. 11:233-60. 1980. [Institute of Arctic Biology, University ofAlaska. Fairbanks. AKI

Chapman JM, Muhlemann JK, Gayomba SR, Muday GK. RBOH-Dependent ROS Synthesis and ROS Scavenging by Plant Specialized Metabolites To Modulate Plant Development and Stress

Responses. Chem Res Toxicol. 2019 Mar 18;32(3):370-396. doi: 10.1021/acs.chemrestox.9b00028. Epub 2019 Mar 11. PMID: 30781949; PMCID: PMC6857786.

Chardon, F., Barthélémy, J., Daniel-Vedele, F., & Masclaux-Daubresse, C. (2010). Natural variation of nitrate uptake and nitrogen use efficiency in Arabidopsis thaliana cultivated with limiting and ample nitrogen supply. *Journal of Experimental Botany*, *61*(9), 2293-2302. https://doi.org/10.1093/jxb/erq059

Chen, X., Schönberger, B., Menz, J., & Ludewig, U. (2018). Plasticity of DNA methylation and gene expression under zinc deficiency in Arabidopsis roots. *Plant and Cell Physiology*, *59*(9), 1790-1802. https://doi.org/10.1093/pcp/pcy100

Cilbert, S.M., Clarkson, D.T., Cambridge, M.L., Lambers, H., & Hawkesford, M.J. (1997). SO42-Deprivation Has an Early Effect on the Content of Ribulose-1,5-Bisphosphate Carboxylase/Oxygenase and Photosynthesis in Young Leaves of Wheat. *Plant Physiology*.

Corinna Heeg, Cordula Kruse, Ricarda Jost, Michael Gutensohn, Thomas Ruppert, Markus Wirtz, Rüdiger Hell, Analysis of the *Arabidopsis O*-Acetylserine(thiol)lyase Gene Family Demonstrates Compartment-Specific Differences in the Regulation of Cysteine Synthesis, *The Plant Cell*, Volume 20, Issue 1, January 2008, Pages 168–185, https://doi.org/10.1105/tpc.107.056747

Dai Z, Plessis A, Vincent J, Duchateau N, Besson A, Dardevet M, Prodhomme D, Gibon Y, Hilbert G, Pailloux M, Ravel C, Martre P. Transcriptional and metabolic alternations rebalance wheat grain storage protein accumulation under variable nitrogen and sulfur supply. Plant J. 2015 Jul;83(2):326-43. doi: 10.1111/tpj.12881. Epub 2015 Jun 8. PMID: 25996785.

Daudi, A., Cheng, Z., O'Brien, J. A., Mammarella, N., Khan, S., Ausubel, F. M., & Bolwell, G. P. (2012). The apoplastic oxidative burst peroxidase in Arabidopsis is a major component of pattern-triggered immunity. The Plant Cell, 24(1), 275–287. https://doi.org/10.1105/tpc.111.093039

David Secco, Chuang Wang, Huixia Shou, Matthew D Schultz, Serge Chiarenza, Laurent Nussaume, Joseph R Ecker, James Whelan, Ryan Lister, (2015) .Stress induced gene expression drives transient DNA methylation changes at adjacent repetitive elements . eLife 4:e09343. https://doi.org/10.7554/eLife.09343

Davidian, J., & Kopriva, S. (2010). Regulation of Sulfate Uptake and Assimilation—The Same or Not the Same? Molecular Plant, 3(2), 314-325. https://doi.org/10.1093/mp/ssq001

de Bang, T.C., Husted, S., Laursen, K.H., Persson, D.P. and Schjoerring, J.K. (2021), The molecular–physiological functions of mineral macronutrients and their consequences for deficiency symptoms in plants. New Phytol, 229: 2446-2469. https://doi.org/10.1111/nph.17074

de Kok LJ, Stahl K, Rennenberg H (1989) Fluxes of atmospheric hydrogen sulphide to plant shoots. New Phytol 112:533–542. https://doi.org/10.1111/j.1469-8137.1989.tb00348.x

DéjardinA, Sokolov L, Kleczkowski L.1999. Sugar/osmoticum levels modulate differential abscisic acid-independent expression of two stress-responsive sucrose synthase genes in Arabidopsis. Biochemical Journal344,503–509.

Del Carmen Martinez-Ballesta M, Moreno DA, Carvajal M.. 2013. The physiological importance of GSLs on plant response to abiotic stress in Brassica. International Journal of Molecular Sciences 14, 11607–11625.

Dietzen C, Koprivova A, Whitcomb SJ, Langen G, Jobe TO, Hoefgen R, Kopriva S (2020). The transcription factor EIL1 participates in the regulation of sulfur deficiency response in Arabidopsis. Plant Physiol 184:2120-2136.

Dixon David P, Jonathan D. Sellars, Robert Edwards; The *Arabidopsis* phi class glutathione transferase *At*GSTF2: binding and regulation by biologically active heterocyclic

ligands. *Biochem J* 15 August 2011; 438 (1): 63–70. doi: https://doi.org/10.1042/BJ20101884

Doucette CD, Schwab DJ, Wingreen NS, Rabinowitz JD. α-Ketoglutarate coordinates carbon and nitrogen utilization via enzyme I inhibition. Nat Chem Biol. 2011 Oct 16;7(12):894-901. doi: 10.1038/nchembio.685. PMID: 22002719; PMCID: PMC3218208.

Dubousset L, Abdallah M, Desfeux AS, Etienne P, Meuriot F, Hawkesford MJ, Avice JC (2009) Remobilization of leaf S compounds and senescence in response to restricted sulphate supply during the vegetative stage of oilseed rape are affected by mineral N availability. J Exp Bot 60:3239–3253.

Dubreuil-Maurizi C, Poinssot B. Role of glutathione in plant signaling under biotic stress. Plant Signal Behav. 2012 Feb;7(2):210-2. doi: 10.4161/psb.18831. Epub 2012 Feb 1. PMID: 22353869; PMCID: PMC3405692.

Dubreuil-Maurizi, C., Vitecek, J., Marty, L., Branciard, L., Frettinger, P., Wendehenne, D., Meyer, A. J., Mauch, F., & Poinssot, B. (2011). Glutathione Deficiency of the Arabidopsis Mutant pad2-1 Affects Oxidative Stress-Related Events, Defense Gene Expression, and the Hypersensitive Response. Plant Physiology, 157(4), 2000-2012. https://doi.org/10.1104/pp.111.182667

Duke, S. H., & Reisenauer, H. M. (1986). Roles and requirements of sulfur in plant nutrition. Sulfur in agriculture, 27, 123-168.

Elmore, J., Dodson, A., Muttucumaru, N., Halford, N., Parry, M., & Mottram, D. (2010). Effects of sulphur nutrition during potato cultivation on the formation of acrylamide and aroma compounds during cooking. *Food Chemistry*, *122*(3), 753-760. https://doi.org/10.1016/j.foodchem.2010.03.049

El-Soda M, Neris Moreira C, Goredema-Matongera N, Jamar D, Koornneef M, Aarts MGM. QTL and candidate genes associated with leaf anion concentrations in response to phosphate supply in Arabidopsis thaliana. BMC Plant Biol. 2019 Sep 18;19(1):410. doi: 10.1186/s12870-019-1996-3. PMID: 31533608; PMCID: PMC6751748.

Etienne P, Sorin E, Maillard A, Gallardo K, Arkoun M, Guerrand J, Cruz F, Yvin JC, Ourry A. Assessment of sulfur deficiency under field conditions by single measurements of sulfur, chloride and phosphorus in mature leaves. Plants. 2018;7(2):37. doi:10.3390/plants7020037.

Ewels P, Magnusson M, Lundin S, Käller M. MultiQC: summarize analysis results for multiple tools and samples in a single report. Bioinformatics. 2016;32(19):3047–8.

F S Chapin III,, E Schulze, H A Mooney. 1990. The Ecology and Economics of Storage in Plants. *Annual Review Ecology, Evolution, and Systematics*. 21:423-447. https://doi.org/10.1146/annurev.es.21.110190.002231

Falk K.L., Tokuhisa J.G., Gershenzon J. The effect of sulfur nutrition on plant glucosinolate content: Physiology and molecular mechanisms. Plant Biol. 2007;9:573–581. doi: 10.1055/s-2007-965431.

Fayezeh Aarabi, Thomas Naake, Alisdair R. Fernie, Rainer Hoefgen, Coordinating Sulfur Pools under Sulfate Deprivation. Trends in Plant Science, Volume 25, Issue 12, 2020, Pages 1227-1239, ISSN 1360-1385, https://doi.org/10.1016/j.tplants.2020.07.007

Fiehn, O., Kopka, J., Dörmann, P., Altmann, T., Trethewey, R.N., Willmitzer, L., 2000. Metabolite profiling for plant funckonal genomics. Nat Biotechnol 18, 1157–1161. https://doi.org/10.1038/81137

Forieri I, Sticht C, Reichelt M, Grerz N, Hawkesford MJ, Malagoli M, Wirtz M, Hell R. 2017. System analysis of metabolism and the transcriptome in *Arabidopsis thaliana* roots reveals differential co-regulation upon iron, sulfur and potassium deficiency. *Plant, Cell & Environment* 40: 95–107.

Foyer CH, Bloom AJ, Queval G, Noctor G. Photorespiratory metabolism: genes, mutants, energetics, and redox signaling. Annu Rev Plant Biol. 2009;60:455-84. doi: 10.1146/annurev.arplant.043008.091948. PMID: 19575589.

Foyer, C.H. and Noctor, G. (2005) Oxidant and Antioxidant Signalling in Plants: A Reevaluation of the Concept of Oxidative Stress in a Physiological Context. Plant Cell and Environment, 28, 1056-1071. https://doi.org/10.1111/j.1365-3040.2005.01327.x

Franks SJ. 2011. Plasticity and evolution in drought avoidance and escape in the annual plant Brassica rapa.New Phytologist190, 249–257.

G. Liang, H. He, D. Yu. Identification of nitrogen starvation-responsive microRNAs in Arabidopsis thaliana. PLoS One, 7 (2012). p. e48951, 10.1371/journal.pone.0048951

Gan X, Stegle O, Behr J, Steffen J G, Drewe Pet al. , 2011 Multiple reference genomes and transcriptomes for Arabidopsis thaliana. Nature 477(7365): 419–423.

Ghani, A., R. G. McLaren and R. S. Swift, 1990 Seasonal fluctuations of sulfate and soil microbial biomass-S in the surface of a Wakanui soil. New Zealand Journal of Agricultural Research 33: 467-472.

Girondé, A., Dubousset, L., Trouverie, J., Etienne, P., & Avice, J. C. (2014). The impact of sulfate restriction on seed yield and quality of winter oilseed rape depends on the ability to remobilize sulfate from vegetative tissues to reproductive organs. *Frontiers in Plant Science*, *5*, 124668. https://doi.org/10.3389/fpls.2014.00695

Goyer A, Collakova E, Shachar-Hill Y, Hanson AD (2007) Functional characterization of a methionine gamma-lyase in Arabidopsis and its implication in an alternative to the reverse trans-sulfuration pathway. Plant Cell Physiol 48: 232-242

Grime, J.P. (2001) Plant Strategies, Vegetation Processes, and Ecosystem Properties. 2nd Edition, John Wiley & Sons, Chichester.

Groot, M. P., Kooke, R., Knoben, N., Vergeer, P., B. Keurentjes, J. J., Ouborg, N. J., & F. Verhoeven, K. J. (2016). Effects of Multi-Generational Stress Exposure and Offspring Environment on the Expression and Persistence of Transgenerational Effects in Arabidopsis thaliana. *PLOS ONE*, *11*(3), e0151566. https://doi.org/10.1371/journal.pone.0151566

Groot, M. P., Kubisch, A., Ouborg, N. J., Pagel, J., Schmid, K. J., Vergeer, P., & Lampei, C. (2017). Transgenerational effects of mild heat in Arabidopsis thaliana show strong genotype specificity that is explained by climate at origin. *New Phytologist*, *215*(3), 1221-1234. https://doi.org/10.1111/nph.14642

Gullner, G., Komives, T., Király, L., & Schröder, P. (2018). Glutathione S-Transferase Enzymes in Plant-Pathogen Interactions. *Frontiers in Plant Science*, *9*, 427485. https://doi.org/10.3389/fpls.2018.01836

Gupta, D., Regon, P., Mai, H. J., Patel, M., Raje, R. S., Bauer, P., & Panda, S. K. (2025). Transcriptional regulation reveals potent drought tolerance mechanisms in contrasting genotypes of Cajanus cajan (L.) Millspaugh. *BMC Plant Biology*, *25*, 1287. https://doi.org/10.1186/s12870-025-07174-6

H. Fontanetto, O. Keller, R. Inwinkelried, N. Citroni, F. García. Phosphorus and sulfur fertilization of corn in the northern Pampas. Better Crops International, 14 (1) (2000), p. 3

Haas F.H., Heeg C, Queiroz R, Bauer A, Wirtz M, Hell R. (2008). Mitochondrial serine acetyltransferase functions as a pacemaker of cysteine synthesis in plant cells.*Plant Physiol.*1481055–1067. 10.1104/pp.108.125237

Haider, I., Yunmeng, Z., White, F., Li, C., Incitti, R., Alam, I., Gojobori, T., Ruyter-Spira, C., Al-Babili, S., & Bouwmeester, H. J. (2023). Transcriptome analysis of the phosphate starvation response sheds light on strigolactone biosynthesis in rice. *The Plant Journal*, *114*(2), 355-370. https://doi.org/10.1111/tpj.16140

Halkier, B. A., & Gershenzon, J. (2006). Biology and biochemistry of glucosinolates. *Annu. Rev. Plant Biol.*, *57*, 303-333.

Han, S., Green, L., & Schnell, D. J. (2009). The Signal Peptide Peptidase Is Required for Pollen Function in Arabidopsis. *Plant Physiology*, *149*(3), 1289. https://doi.org/10.1104/pp.108.130252

Hartmann, T., Hönicke, P., Wirtz, M., Hell, R., Rennenberg, H. and Kopriva, S. (2004) Sulfate assimilation in poplars (*Populus tremula* x *P. alba*) overexpressing γ-glutamylcysteine synthetase in the cytosol. *J. Exp. Bot.* **55**, 837–845.

Hasan MM, Chowdhury MAH, Saha BK, Islam MR (2013) Major nutrient contents and their uptake by brinjal as influenced by phosphorus and sulphur. J Bangladesh Agri Univ 11:41–46. https://doi.org/10.22004/ag.econ.209744

Hasanuzzaman M, Nahar K, Anee TI, Fujita M. Glutathione in plants: biosynthesis and physiological role in environmental stress tolerance. Physiol Mol Biol Plants. 2017 Apr;23(2):249-268. doi: 10.1007/s12298-017-0422-2. Epub 2017 Mar 10. PMID: 28461715; PMCID: PMC5391355.

Hasanuzzaman, M., Nahar, K., Anee, T. I., & Fujita, M. (2017). Glutathione in plants: Biosynthesis and physiological role in environmental stress tolerance. *Physiology and Molecular Biology of Plants*, *23*(2), 249. https://doi.org/10.1007/s12298-017-0422-2

Hatier, J.H.B.; Gould, K.S. Foliar anthocyanins as modulators of stress signals. J. Theor. Biol. 2008, 253, 625–627.

Hawkesford MJ. Plant responses to sulphur deficiency and the genetic manipulation of sulphate transporters to improve S-utilization efficiency. J Exp Bot. 2000 Jan;51(342):131-8. PMID: 10938804.

HAWKESFORD, M. J., & DE KOK, L. J. (2006). Managing sulphur metabolism in plants. *Plant, Cell & Environment*, *29*(3), 382-395. https://doi.org/10.1111/j.1365-3040.2005.01470.x

HeardE.MartienssenR. A. (2014). Transgenerational epigenetic inheritance: myths and mechanisms.*Cell*15795–109. 10.1016/j.cell.2014.02.045

Hell R. & Bergmann L. (1990) γ−Glutamylcysteine synthetase in higher plants: catalytic properties and subcellular localization. Planta 180, 603–612.

Hell, R., & Wirtz, M. (2011). Molecular biology, biochemistry and cellular physiology of cysteine metabolism in Arabidopsis thaliana. The Arabidopsis book/American Society of Plant Biologists, 9, e0154.

Herms, D. A., & Mattson, W. J. (1992). The Dilemma of Plants: To Grow or Defend. The Quarterly Review of Biology. https://doi.org/10.1086/417659

Herrmann, J., Ravilious, G. E., McKinney, S. E., Westfall, C. S., Lee, S. G., Baraniecka, P., ... & Jez, J. M. (2014). Structure and mechanism of soybean ATP sulfurylase and the committed step in plant sulfur assimilation. Journal of Biological Chemistry, 289(15), 10919-10929.

Hesse, H., Nikiforova, V., Gakière, B., & Hoefgen, R. (2004). Molecular analysis and control of cysteine biosynthesis: Integration of nitrogen and sulphur metabolism. Journal of Experimental Botany, 55(401), 1283-1292. https://doi.org/10.1093/jxb/erh136

Hesse, H., Trachsel, N., Suter, M., Kopriva, S., von Ballmoos, P., Rennenberg, H., & Brunold, C. (2003). Effect of glucose on assimilatory sulphate reduction in Arabidopsis thaliana roots. *Journal of Experimental Botany*, *54*(388), 1701-1709.

Hewitt, E. J. (1952). Sand and Water Culture Methods Used in the Study of Plant Nutrition. Common-wealth Agricultural Bureaux.

Higashi Y, Hirai MY, Fujiwara T, Naito S, Noji M, Saito K (2006) Proteomic and transcriptomic analysis of Arabidopsis seeds: molecular evidence for successive processing of seed proteins and its implication in the stress response to sulfur nutrition. Plant J 48: 557–571

Hirai, M. Y., Fujiwara, T., Awazuhara, M., Kimura, T., Noji, M., & Saito, K. (2003). Global expression profiling of sulfur-starved Arabidopsis by DNA macroarray reveals the role of O-acetyl-l-

serine as a general regulator of gene expression in response to sulfur nutrition. *The Plant Journal*, *33*(4), 651-663.

Hirai, M. Y., Yano, M., Goodenowe, D. B., Kanaya, S., Kimura, T., Awazuhara, M., ... & Saito, K. (2004). Integration of transcriptomics and metabolomics for understanding of global responses to nutritional stresses in Arabidopsis thaliana. *Proceedings of the National Academy of Sciences*, 101(27), 10205-10210.

Hoefgen, R., & Nikiforova, V. J. (2008). Metabolomics integrated with transcriptomics: assessing systems response to sulfur-deficiency stress. *Physiologia Plantarum*, *132*(2), 190-198.

Huang T, Jander G. Abscisic acid-regulated protein degradation causes osmotic stress-induced accumulation of branched-chain amino acids in Arabidopsis thaliana. Planta. 2017;246(4):737–747. doi: 10.1007/s00425-017-2727-3

Huang T, Jander G. Abscisic acid-regulated protein degradation causes osmotic stress-induced accumulation of branched-chain amino acids in Arabidopsis thaliana. Planta. 2017 Oct;246(4):737-747. doi: 10.1007/s00425-017-2727-3. Epub 2017 Jul 1. PMID: 28668976.

Huang XY, Li M, Luo R, Zhao FJ, Salt DE. Epigenetic regulation of sulfur homeostasis in plants. J Exp Bot. 2019 Aug 19;70(16):4171-4182. doi: 10.1093/jxb/erz218. PMID: 31087073.

Huang, C. Y., Shirley, N., Genc, Y., Shi, B., & Langridge, P. (2011). Phosphate Utilization Efficiency Correlates with Expression of Low-Affinity Phosphate Transporters and Noncoding RNA, IPS1, in Barley. *Plant Physiology*, *156*(3), 1217. https://doi.org/10.1104/pp.111.178459

Huang, H., Zhang, C., Wang, H., Wu, F., & Fang, Q. (2025). A rice SOUL family heme-binding protein REAC1 enhances the antioxidative capacity of C. Elegans through modulation of ROS-related gene expression. *Scientific Reports*, *15*(1), 10379. https://doi.org/10.1038/s41598-025-95254-w

Huang, X. Y., D. Y. Chao, A. Koprivova, J. Danku, M. Wirtz et al., 2016 Nuclear Localised MORE SULFUR ACCUMULATION1 Epigenetically Regulates Sulfur Homeostasis in Arabidopsis thaliana. PLoS Genet 12: e1006298.

Huang, X. Y., Li, M., Luo, R., Zhao, F. J., & Salt, D. E. (2019). Epigenetic regulation of sulfur homeostasis in plants. *Journal of Experimental Botany*, *70*(16), 4171-4182. https://doi.org/10.1093/jxb/erz218

Huang, X., & Han, B. (2014). Natural variations and genome-wide association studies in crop plants. *Annual review of plant biology*, *65*, 531-551.

Hubberten, H. M., Klie, S., Caldana, C., Degenkolbe, T., Willmitzer, L., & Hoefgen, R. (2012). Additional role of O-acetylserine as a sulfur status-independent regulator during plant growth. *The Plant Journal*, *70*(4), 666-677.

Ikram S, Bedu M, Daniel-Vedele F, Chaillou S, Chardon F.. 2012. Natural variation of Arabidopsis response to nitrogen availability. Journal of Experimental Botany 63, 91–105.

Inal, A. Günes, M. Alpaslan, M. Sait Adak, S. Taban, F. Eraslan.Diagnosis of sulfur deficiency and effects of sulfur on yield and yield components of wheat grown in Central Anatolia, Turkey. J. Plant Nutr., 26 (7) (2003), pp. 1483-1498

J.R. Stinchcombe, C. Weinig, M. Ungerer, K.M. Olsen, C. Mays, S.S. Halldorsdottir, M.D. Purugganan, & J. Schmitt, A latitudinal cline in flowering time in Arabidopsis thaliana modulated by the flowering time gene FRIGIDA, Proc. Natl. Acad. Sci. U.S.A. 101 (13) 4712-4717, https://doi.org/10.1073/pnas.0306401101 (2004).

Jafari, T., Durian, G., Rahikainen, M., Kortesniemi, M., Kangasjärvi, S., & Sinkkonen, J. (2017). NMR study of age dependent metabolic adjustments in wild type and pp2a-b'γ mutant Arabidopsis thaliana. Phytochemistry Letters, 22, 13-20. https://doi.org/10.1016/j.phytol.2017.07.015

Jamal, A., Fazli, I. S., Ahmad, S., Kim, K. T., Oh, D. G., & Abdin, M. Z. (2006). Effect of sulfur on nitrate reductase and ATP-sulfurylase activities in groundnut (Arachis hypogaea L.). Journal of Plant Biology, 49(6), 513–517.

Jan Kolář, Jana Seňková. Reduction of mineral nutrient availability accelerates flowering of Arabidopsis thaliana, Journal of Plant Physiology, Volume 165, Issue 15, 2008, Pages 1601-1609, ISSN 0176-1617, https://doi.org/10.1016/j.jplph.2007.11.010.

Jimenez-Gomez JM Corwin JA Joseph B Maloof JN Kliebenstein DJ (2011) Genomic analysis of QTLs and genes altering natural variation in stochastic noise. PLoS Genet 7: e1002295

Jimenez-Gomez JM, Corwin JA, Joseph B, Maloof JN, Kliebenstein DJ.. 2011. Genomic analysis of QTLs and genes altering natural variation in stochastic noise. PLoS Genetics 7, e1002295.

Jobe TO, Zenzen I, Rahimzadeh Karvansara P, S.. 2019. Integration of sulfate assimilation with carbon and nitrogen metabolism in transition from C3 to C4 photosynthesis. Journal of Experimental Botany 70, 4211–4221.

Johanson U, West J, Lister C, Michaels S, Amasino R, Dean C. Molecular analysis of FRIGIDA, a major determinant of natural variation in Arabidopsis flowering time. Science. 2000 Oct 13;290(5490):344-7. doi: 10.1126/science.290.5490.344. PMID: 11030654.

Jones-Rhoades, M. W., & Bartel, D. P. (2004). Computational identification of plant microRNAs and their targets, including a stress-induced miRNA. Molecular cell, 14(6), 787-799.

Jost, R., Altschmied, L., Bloem, E., Bogs, J., Gershenzon, J., Hähnel, U., ... & Hell, R. (2005). Expression profiling of metabolic genes in response to methyl jasmonate reveals regulation of genes of primary and secondary sulfur-related pathways in Arabidopsis thaliana. *Photosynthesis Research*, *86*(3), 491-508.

Kaiser WM, Huber SC. Post-translational regulation of nitrate reductase: mechanism, physiological relevance and environmental triggers. J Exp Bot. 2001 Oct;52(363):1981-9. doi: 10.1093/jexbot/52.363.1981. PMID: 11559733.

Kant S, Kant P, Raveh E, Barak S. Evidence that differential gene expression between the halophyte, Thellungiella halophila, and Arabidopsis thaliana is responsible for higher levels of the compatible osmolyte proline and tight control of Na+ uptake in T. halophila. Plant Cell Environ. 2006 Jul;29(7):1220-34. doi: 10.1111/j.1365-3040.2006.01502.x. PMID: 17080945.

Kataoka, T., Watanabe-Takahashi, A., Hayashi, N., Ohnishi, M., Mimura, T., Buchner, P., Hawkesford, M. J., Yamaya, T., & Takahashi, H. (2004). Vacuolar Sulfate Transporters Are Essential Determinants Controlling Internal Distribution of Sulfate in Arabidopsis. *The Plant Cell*, *16*(10), 2693. https://doi.org/10.1105/tpc.104.023960

Katz E, Li JJ, Jaegle B, Ashkenazy H, Abrahams SR, Bagaza C, Holden S, Pires CJ, Angelovici R, Kliebenstein DJ.. 2021. Genetic variation, environment and demography intersect to shape Arabidopsis defense metabolite variation across Europe. eLife 10, e67784.

Kaur, G., Chandna, R., Pandey, R. et al. Sulfur starvation and restoration affect nitrate uptake and assimilation in rapeseed. Protoplasma 248, 299–311 (2011). https://doi.org/10.1007/s00709-010-0171-3

Kawashima, C. G., Matthewman, C. A., Huang, S., Lee, B. R., Yoshimoto, N., Koprivova, A., Rubio-Somoza, I., Todesco, M., Rathjen, T., Saito, K., Takahashi, H., Dalmay, T., & Kopriva, S. (2011). Interplay of SLIM1 and miR395 in the regulation of sulfate assimilation in Arabidopsis. The Plant Journal, 66(5), 863-876. https://doi.org/10.1111/j.1365-313X.2011.04547.x

Kazan, K., & Lyons, R. (2015). The link between flowering time and stress tolerance. *Journal of Experimental Botany*, *67*(1), 47-60. https://doi.org/10.1093/jxb/erv441

Ken'ichi Ogawa, Yasushi Tasaka, Masanobu Mino, Yoshikazu Tanaka, Masaki Iwabuchi, Association of Glutathione with Flowering in Arabidopsis thaliana, Plant and Cell Physiology, Volume 42, Issue 5, 15 May 2001, Pages 524–530, https://doi.org/10.1093/pcp/pce065

Kertesz, M. A., and P. Mirleau, 2004 The role of soil microbes in plant sulfur nutrition. J Exp Bot 55: 1939-1945.

Khamsalath Soudthedlath, Toshiki Nakamura, Tsukasa Ushiwatari, Jutarou Fukazawa, Keishi Osakabe, Yuriko Osakabe, Akiko Maruyama-Nakashita, SULTR2;1 Adjusts the Bolting Timing by Transporting Sulfate from Rosette Leaves to the Primary Stem, Plant and Cell Physiology, Volume 65, Issue 5, May 2024, Pages 770–780, https://doi.org/10.1093/pcp/pcae020

Khan M. S, Haas F H, Samami A A, Gholami A, Bauer A. Fellenberg K.et al (2010). Sulfite reductase defines a newly discovered bottleneck for assimilatory sulfate reduction and is essential for growth and development in Arabidopsis thaliana.Plant Cell221216–1231. 10.1105/tpc.110.074088

Kim D, Paggi JM, Park C, Bennett C, Salzberg SL. Graph-based genome alignment and genotyping with HISAT2 and HISAT-genotype. Nat Biotechnol. 2019;37(8):907–15.

Klapheck, S., Grosse, W., & Bergmann, L. (1982). Effect of Sulfur Deficiency on Protein Synthesis and Amino Acid Accumulation in Cell Suspension Cultures of Nicotiana tabacum. *Zeitschrift für Pflanzenphysiologie*, *108*(3), 235-245. https://doi.org/10.1016/S0044-328X(82)80123-2

Kliebenstein D J, West M A, Van Leeuwen H, Kim K, Doerge Ret al. , 2006 Genomic survey of gene expression diversity in Arabidopsis thaliana. Genetics 172(2): 1179–1189

Koehl, K.I. and Laitinen, R.A.E. (2015). From the Greenhouse to the Real World – Arabidopsis Field Trials and Applications. In Molecular Mechanisms in Plant Adaptation, R.A.E. Laitinen (Ed.). https://doi.org/10.1002/9781118860526.ch9

Kopriva S**.** (2015) Plant sulfur nutrition: from Sachs to Big Data. Plant Signal. Behav. 10, e1055436

Kopriva S., Koprivova A. (2004) Plant adenosine 5'phosphosulfate reductase - the past, the present, and the future. J. Exp. Bot. 55, 1775-1783.

Kopriva, S., & Rennenberg, H. (2004). Control of sulphate assimilation and glutathione synthesis: Interaction with N and C metabolism. *Journal of Experimental Botany*, *55*(404), 1831-1842. https://doi.org/10.1093/jxb/erh203

Kopriva, S., Mugford, S. G., Baraniecka, P., Lee, B. R., Matthewman, C. A., & Koprivova, A. (2012). Control of sulfur partitioning between primary and secondary metabolism in Arabidopsis. Frontiers in Plant Science, 3, 30360. https://doi.org/10.3389/fpls.2012.00163

Kopriva, S., Muheim, R., Koprivova, A., Trachsel, N., Catalano, C., Suter, M., & Brunold, C. (1999). Light regulation of assimilatory sulphate reduction in Arabidopsis thaliana. *The Plant Journal*, *20*(1), 37-44.

Koprivova A, Giovannetti M, Baraniecka P, Lee B-R, Grondin C, Loudet O, Kopriva S (2013). Plant Physiol. 163:1133-1141. Natural Variation in ATPS1 Isoform of ATP Sulfurylase Contributes to Control of Sulfate Levels in Arabidopsis. Natural variation for sulfate content in Arabidopsis is highly controlled by adenosine 5'-phosphosulfate reductase.

Koprivova A, Kopriva S. Sulfation pathways in plants. Chem Biol Interact. 2016 Nov 25;259(Pt A):23-30. doi: 10.1016/j.cbi.2016.05.021. Epub 2016 May 17. PMID: 27206694.

Koprivova A., Elkatmis B., Gerlich S.C., Trick M., Harper A.L., Bancroft I., Kopriva **S.** (2023) Natural Variation in OASC Gene for Mitochondrial O-Acetylserine Thiollyase Affects Sulfate Levels in Arabidopsis. Plants 12, 35.

Koprivova, A., & Kopriva, S. (2014). Molecular mechanisms of regulation of sulfate assimilation: First steps on a long road. *Frontiers in Plant Science*, *5*, 116492. https://doi.org/10.3389/fpls.2014.00589

Koprivova, A., Suter, M., Brunold, C., & Kopriva, S. (2000). Regulation of Sulfate Assimilation by Nitrogen in Arabidopsis. *Plant Physiology*, *122*(3), 737. https://doi.org/10.1104/pp.122.3.737

Koprivova, A., Suter, M., Den Camp, R. O., Brunold, C., & Kopriva, S. (2000). Regulation of Sulfate Assimilation by Nitrogen in Arabidopsis. *Plant Physiology*, *122*(3), 737-746. https://doi.org/10.1104/pp.122.3.737

Kopylova E, Noé L, Touzet H. SortMeRNA: fast and accurate filtering of ribosomal RNAs in metatranscriptomic data. Bioinformatics. 2012;28(24):3211–7

Krueger, S., Niehl, A., Lopez Martin, M. C., Steinhauser, D., Donath, A., Hildebrandt, T., ... & Hesse, H. (2009). Analysis of cytosolic and plastidic serine acetyltransferase mutants and subcellular metabolite distributions suggests interplay of the cellular compartments for cysteine biosynthesis in Arabidopsis. Plant, Cell & Environment, 32(4), 349-367.

Kumar, D., Yusuf, M. A., Singh, P., Sardar, M. and Sarin, N. B. (2014). Histochemical Detection of Superoxide and H_2O_2 Accumulation in *Brassica juncea* Seedlings. *Bio-protocol* 4(8): e1108. DOI: 10.21769/BioProtoc.1108.

Kuzuhara Y, Isobe A, Awazuhara M, Fujiwara T, Hayashi H. 2000. GSH levels in phloem sap of rice plants under sulfur deficient conditions. Soil Science and Plant Nutrition 46, 265–270.

L. Aula, J.S. Dhillon, P. Omara, G.B. Wehmeyer, K.W. Freeman, W.R. Raun. World sulfur use efficiency for cereal crops. Agron. J., 111 (5) (2019), pp. 2485-2492

L.C. Hsieh, S.I. Lin, A.C. Shih, J.W. Chen, W.Y. Lin, C.Y. Tseng, W.H. Li, T.J. Chiou. Uncovering small RNA-mediated responses to phosphate deficiency in Arabidopsis by deep sequencing. Plant Physiol., 151 (2009), pp. 2120-2132, 10.1104/pp.109.147280

Lahner B, Gong J, Mahmoudian M, Smith EL, Abid KB, et al. Genomic scale profiling of nutrient and trace elements in Arabidopsis thaliana . Nat Biotechnol. 2003;21:1215–1221. doi: 10.1038/nbt865.

Lam HM, Coschigano KT, Oliveira IC, Melo-Oliveira R, Coruzzi GM. THE MOLECULAR-GENETICS OF NITROGEN ASSIMILATION INTO AMINO ACIDS IN HIGHER PLANTS. Annu Rev Plant Physiol Plant Mol Biol. 1996 Jun;47:569-593. doi: 10.1146/annurev.arplant.47.1.569. PMID: 15012301.

Lasky JR, Des Marais DL, Lowry DB, Povolotskaya I, McKay JK, Richards JH, Keitt TH, Juenger TE. Natural variation in abiotic stress responsive gene expression and local adaptation to climate in Arabidopsis thaliana. Mol Biol Evol. 2014 Sep;31(9):2283-96. doi: 10.1093/molbev/msu170. Epub 2014 May 21. PMID: 24850899; PMCID: PMC4137704.

Lee BR, Zaman R, Avice JC, Ourry A, Kim TH (2016) Sulfur use efficiency is a significant determinant of drought stress tolerance in relation to photosynthetic activity in *Brassica napus* cultivars. Front Plant Sci 7:459.

Lee, Y., Yoon, H.R., Paik, Y.S. *et al.* Reciprocal regulation of*Arabidopsis* UGT78D2 and BANYULS is critical for regulation of the metabolic flux of anthocyanidins to condensed tannins in developing seed coats. *J. Plant Biol.* **48**, 356–370 (2005). https://doi.org/10.1007/BF03030577

Lefebvre, V., Kiani, S. P., & Durand-Tardif, M. (2009). A Focus on Natural Variation for Abiotic Constraints Response in the Model Species Arabidopsis thaliana. *International Journal of Molecular Sciences*, *10*(8), 3547-3582. https://doi.org/10.3390/ijms10083547

Lemoine, R., Camera, S. L., Atanassova, R., Dédaldéchamp, F., Allario, T., Pourtau, N., Bonnemain, J. L., Laloi, M., Coutos-Thévenot, P., Maurousset, L., Faucher, M., Girousse, C., Lemonnier, P., Parrilla, J., & Durand, M. (2013). Source-to-sink transport of sugar and regulation by environmental factors. Frontiers in Plant Science, 4, 272. https://doi.org/10.3389/fpls.2013.00272

Leustek T, Martin MN, Bick JA, Davies JP. 2000. Pathways and regulation of sulfur metabolism revealed through molecular and genetic studies. Annual Review of Plant Physiology and Plant Molecular Biology 51, 141–165.

Lewandowska, M., & Sirko, A. (2008). Recent advances in understanding plant response to sulfur-deficiency stress. *Acta Biochimica Polonica*, *55*(3), 457–471.

Li, Legong et al. Functional Cloning and Characterization of a Plant Efflux Carrier for Multidrug and Heavy Metal Detoxification * Journal of Biological Chemistry, Volume 277, Issue 7, 5360 - 5368

Li, Q., Gao, Y., & Yang, A. (2019). Sulfur Homeostasis in Plants. International Journal of Molecular Sciences, 21(23), 8926. https://doi.org/10.3390/ijms21238926

Li, R., Zhou, Z., Zhang, T., Su, H., & Li, J. (2023). Overexpression of LSU1 and LSU2 confers cadmium tolerance by manipulating sulfur metabolism in Arabidopsis. *Chemosphere*, *334*, 139046. https://doi.org/10.1016/j.chemosphere.2023.139046

Liao Y, Smyth GK, Shi W. featureCounts: an efficient general purpose program for assigning sequence reads to genomic features. Bioinformatics. 2014;30(7):923–30.

Likens GE, Butler TJ, Buso DC.. 2001. Long- and short-term changes in sulfate deposition: effects of the 1990 Clean Air Act Amendments. Biogeochemistry 52, 1–11.

Liu, X., Hu, B., & Chu, C. (2022). Nitrogen assimilation in plants: Current status and future prospects. *Journal of Genetics and Genomics*, *49*(5), 394-404. https://doi.org/10.1016/j.jgg.2021.12.006

Liu, Z., Liu, D., Fu, X., Du, X., Zhang, Y., Zhen, W., Li, S., Yang, H., He, S., & Li, R. (2022). Integrated transcriptomic and metabolomic analyses revealed the regulatory mechanism of sulfur application in grain yield and protein content in wheat (Triticum aestivum L.). *Frontiers in Plant Science*, *13*, 935516. https://doi.org/10.3389/fpls.2022.935516

Lohmann A, Schöttler M, Bréhélin C ...Deficiency in Phylloquinone (Vitamin K1) Methylation Affects Prenyl Quinone Distribution, Photosystem I Abundance, and Anthocyanin Accumulation in the Arabidopsis AtmenG Mutant *Journal of Biological Chemistry, 2006; 281, 40461-40472

Loudet, O., Saliba-Colombani, V., Camilleri, C., Calenge, F., Gaudon, V., Koprivova, A., North, K. A., Kopriva, S., & Daniel-Vedele, F. (2007). Natural variation for sulfate content in Arabidopsis thaliana is highly controlled by APR2. *Nature Genetics*, *39*(7), 896-900. https://doi.org/10.1038/ng2050

Love MI, Huber W, Anders S. Moderated estimation of fold change and dispersion for RNA-seq data with DESeq2. Genome Biol. 2014;15(12):550.

Lu, G., Harper, A. L., Trick, M., Morgan, C., Fraser, F., O'Neill, C., & Bancroft, I. (2014). Associative transcriptomics study dissects the genetic architecture of seed glucosinolate content in Brassica napus. *DNA research*, *21*(6), 613-625.

Lu, Y. (2018). Assembly and transfer of iron–sulfur clusters in the plastid. Frontiers in plant science, 9, 336.

Lunde, C., Zygadlo, A., Simonsen, H.T., Nielsen, P.L., Blennow, A. and Haldrup, A. (2008), Sulfur starvation in rice: the effect on photosynthesis, carbohydrate metabolism, and oxidative stress protective pathways. Physiologia Plantarum, 134: 508-521. https://doi.org/10.1111/j.1399-3054.2008.01159.x

Luo, J., Havé, M., Clément, G., Tellier, F., Balliau, T., Launay-Avon, A., Guérard, F., Zivy, M., & Masclaux-Daubresse, C. (2020). Integrating multiple omics to identify common and specific molecular changes occurring in Arabidopsis under chronic nitrate and sulfate limitations. *Journal of Experimental Botany*, *71*(20), 6471-6490. https://doi.org/10.1093/jxb/eraa337

Luo, R. J., Zhuo, C. J., Liang, M., Liu, H., Gu, X., Zhao, F. J., & Huang, X. Y. (2025). The GTE7-IES2B-GTE2 complex epigenetically regulates sulfur homeostasis in Arabidopsis thaliana. *New Phytologist*, *248*(1), 211-230. https://doi.org/10.1111/nph.70398

M. Koornneef, C. Alonso-Blanco, D. Vreugdenhil. Naturally occurring genetic variation in Arabidopsis thaliana. Annu. Rev. Plant Biol., 55 (2004), pp. 141-172

Madhu, Sharma, A., Kaur, A., Tyagi, S., & Upadhyay, S. K. (2023). Glutathione peroxidases in plants: Innumerable role in abiotic stress tolerance and plant development. Journal of Plant Growth Regulation, 42, 598–613.

Mangalakkadan, A., Roychowdhury, A., Chennakesavulu, K., & Kumar, R. Phosphate starvation response 1 (PHR1): A versatile master regulator shaping plant resilience beyond phosphate deprivation. *Journal of Experimental Botany*. https://doi.org/10.1093/jxb/erag002

Maruyama-Nakashita A, Nakamura Y, Yamaya T, Takahashi H (2004) Regulation of high-affinity sulphate transporters in plants: towards systematic analysis of sulphur signalling and regulation. J Exp Bot 55:1843–1849. https://doi.org/10.1093/jxb/erh175

Maruyama-Nakashita, A. (2017). Metabolic changes sustain the plant life in low-sulfur environments. Current Opinion in Plant Biology, 39, 144-151. https://doi.org/10.1016/j.pbi.2017.06.015

Maruyama-Nakashita, A., Nakamura, Y., Tohge, T., Saito, K., & Takahashi, H. (2006). Arabidopsis SLIM1 is a central transcriptional regulator of plant sulfur response and metabolism. The Plant Cell, 18(11), 3235-3251.

Mata CG, Lamattina L (2001) Nitric oxide induces stomatal closure and enhances the adaptive plant responses against drought stress. Plant Physiol 126: 1196–1204

May M.J. & Leaver C.J. (1994) *Arabidopsis thaliana* γ–glutamylcysteine synthetase is structurally unrelated to mammalian, yeast and *Escherichia coli* homologs. *Proceedings of the National Academy of Sciences of the United States of America* **91**, 10059–10063.

McGrath SP, Zhao FJ, Withers PJA. Development of sulphur deficiency in crops and its treatment. Proceedings-Fertiliser Society (United Kingdom).1996.

Medici A, Marshall-Colon A, Ronzier E, Szponarski W, Wang R, Gojon A, Crawford NM, Ruffel S, Coruzzi GM, Krouk G (2015) AtNIGT1/HRS1 integrates nitrate and phosphate signals at the Arabidopsis root tip. Nat Commun 6: 6274

Meyer, Y., Siala, W., Bashandy, T., Riondet, C., Vignols, F., & Reichheld, J. P. (2008). Glutaredoxins and thioredoxins in plants. *Biochimica et Biophysica Acta (BBA)-Molecular Cell Research*, *1783*(4), 589-600.

Mishra SV, Maurya D, Gupta G (2010) Effect of phosphorus and sulphur and their interaction on mustard crop. Asian Sci 5:79–84

Mugford, S. G., Yoshimoto, N., Reichelt, M., Wirtz, M., Hill, L., Mugford, S. T., ... & Kopriva, S. (2009). Disruption of adenosine-5′-phosphosulfate kinase in Arabidopsis reduces levels of sulfated secondary metabolites. The Plant Cell, 21(3), 910-927.

Murillo, M., & Leustek, T. (1995). Adenosine-5′-Triphosphate-Sulfurylase fromArabidopsis thalianaandEscherichia coliAre Functionally Equivalent but Structurally and Kinetically Divergent: Nucleotide Sequence of Two Adenosine-5′-Triphosphate-Sulfurylase cDNAs fromArabidopsis thalianaand Analysis of a Recombinant Enzyme. Archives of Biochemistry and Biophysics, 323(1), 195-204. https://doi.org/10.1006/abbi.1995.0026

Muttucumaru, N., N. G. Halford, J. S. Elmore, A. T. Dodson, M. Parry et al., 2006. Formation of high levels of acrylamide during the processing of flour derived from sulfate-deprived wheat. J Agric Food Chem 54: 8951-8955.

Nagashima, A., Hanaoka, M., Shikanai, T., Fujiwara, M., Kanamaru, K., Takahashi, H., & Tanaka, K. (2004). The Multiple-Stress Responsive Plastid Sigma Factor, SIG5, Directs Activation of the psbD Blue Light-Responsive Promoter (BLRP) in Arabidopsis thaliana. *Plant and Cell Physiology*, *45*(4), 357-368. https://doi.org/10.1093/pcp/pch050

Nam HG Giraudat J Den Boer B Moonan F Loos WD Hauge BM Goodman HM (1989) Restriction fragment length polymorphism linkage map of Arabidopsis thaliana . Plant Cell 1: 699–705

Nanthakumar S, Panneerselvam P, Krishnakumar S (2014) Effect of phosphorus and sulphur on growth, yield and quality parameters of hybrid maize. Int J Adv Life Sci 7:85–92

Narayan OP, Kumar P, Yadav B, Dua M, Johri AK. Sulfur nutrition and its role in plant growth and development. Plant Signal Behav. 2023 Dec 31;18(1):2030082. doi: 10.1080/15592324.2022.2030082. Epub 2022 Feb 7. PMID: 35129079; PMCID: PMC10730164.

Nicholas de Jager, Varsa Shukla, Anna Koprivova, Martin Lyčka, Lorina Bilalli, Yanrong You, Jürgen Zeier, Stanislav Kopriva, Daniela Ristova (2023). Traits linked to natural variation of sulfur

content in Arabidopsis thaliana.. Journal of Experimental Botany, Volume 75, Issue 3, 2 February 2024, Pages 1036–1050, https://doi.org/10.1093/jxb/erad401

Nikiforova V, Freitag J, Kempa S, Adamik M, Hesse H, Hoefgen R. Transcriptome analysis of sulfur depletion in Arabidopsis thaliana: interlacing of biosynthetic pathways provides response specificity. Plant J. 2003;33(4):633–50.

Nikiforova VJ, Kopka J, Tolstikov V, Fiehn O, Hopkins L, Hawkesford MJ, Hesse H, Hoefgen R. 2005. Systems rebalancing of metabolism in response to sulfur deprivation, as revealed by metabolome analysis of Arabidopsis plants. Plant Physiology 138, 304–318.

Nikiforova, V. J., Gakière, B., Kempa, S., Adamik, M., Willmitzer, L., Hesse, H., & Hoefgen, R. (2004). Towards dissecting nutrient metabolism in plants: A systems biology case study on sulphur metabolism. Journal of Experimental Botany, 55(404), 1861-1870. https://doi.org/10.1093/jxb/erh177

Noctor, G., & Foyer, C. H. (2016). Redox homeostasis and antioxidant metabolism in plants. Plant, Cell & Environment, 39, 951–964.

Noctor, g., Mhamdi, a., Chaouch, s., Han, y., Neukermans, j., Marquez-garcia, b., queval, g., & foyer, c. h. (2012). Glutathione in plants: An integrated overview. Plant, Cell & Environment, 35(2), 454-484. https://doi.org/10.1111/j.1365-3040.2011.02400.x

Obata, T., & Fernie, A. R. (2012). The use of metabolomics to dissect plant responses to abiotic stresses. *Cellular and Molecular Life Sciences: CMLS*, *69*(19), 3225. https://doi.org/10.1007/s00018-012-1091-5

P.J. Randall, J.R. Freney, K. Spencer. Diagnosing sulfur deficiency in rice by grain analysis. Nutrient Cycl. Agroecosyst., 65 (3) (2003), pp. 211-219

Parashar A, Tripathi L (2020) Effect of phosphorus and sulphur on the growth and yield of black gram (*Vigna mungo* L.). J Pharmacogn Phytochem 9:2585–2588

Paulose, B., Chhikara, S., Coomey, J., Jung, H. I., Vatamaniuk, O., & Dhankher, O. P. (2013). A γ-glutamyl cyclotransferase protects Arabidopsis plants from heavy metal toxicity by recycling glutamate to maintain glutathione homeostasis. *The Plant Cell*, *25*(11), 4580-4595.

Paz-Ares, J., Puga, M. I., Rojas-Triana, M., Martinez-Hevia, I., Diaz, S., Poza-Carrión, C., Miñambres, M., & Leyva, A. (2022). Plant adaptation to low phosphorus availability: Core signaling, crosstalks, and applied implications. Molecular Plant, 15(1), 104-124. https://doi.org/10.1016/j.molp.2021.12.005

Peršić, V., Melnjak, A., Domjan, L., Zellnig, G., & Dunić, J. A. (2025). Age-Specific Physiological Adjustments of Spirodela polyrhiza to Sulfur Deficiency. *Plants*, *14*(13). https://doi.org/10.3390/plants14131907

Pilon-Smits E A, Hwang S, Mel Lytle C, Zhu Y, Tai J C, Bravo R. C.et al (1999). Overexpression of ATP sulfurylase in indian mustard leads to increased selenate uptake, reduction, and tolerance.Plant Physiol.119123–132. 10.1104/pp.119.1.123

Pivato M, Fabrega-Prats M, Masi A. 2014. Low-molecular-weight thiols in plants: functional and analytical implications. Archives of Biochemistry and Biophysics 560, 83–99.

ProsserIM, Purves JV, Saker LR, Clarkson DT.2001. Rapid disruption of nitrogen metabolism and nitrate transport in spinach plants deprived of sulphate. Journal of Experimental Botany52,113–121.

Quirino, B.F., Reiter, WD. & Amasino, R.D. One of two tandem Arabidopsis genes homologous to monosaccharide transporters is senescence-associated. Plant Mol Biol 46, 447–457 (2001). https://doi.org/10.1023/A:1010639015959

Rai, G. K., Kumar, P., Choudhary, S. M., Singh, H., Adab, K., Kosser, R., Magotra, I., Kumar, R. R., Singh, M., Sharma, R., Corrado, G., & Rouphael, Y. (2022). Antioxidant Potential of Glutathione and Crosstalk with Phytohormones in Enhancing Abiotic Stress Tolerance in Crop Plants. Plants, 12(5), 1133. https://doi.org/10.3390/plants12051133

Ran, X., Zhao, F., Wang, Y., Liu, J., Zhuang, Y., Ye, L., Qi M., Cheng J. & Zhang, Y. (2020). Plant Regulomics: a data-driven interface for retrieving upstream regulators from plant multi-omics data. The Plant Journal, 101(1), 237-248.

Ranjan, A., Gautam, S., Michael, R., & Trivedi, P. K. (2025). Galactinol synthase 1, AtGolS1, affects arsenate tolerance by modulating phosphate homeostasis in sensitive ecotype Slavi-1 of Arabidopsis. *Journal of Hazardous Materials*, *499*, 140114. https://doi.org/10.1016/j.jhazmat.2025.140114

Rennenberg H, Schneider S, Weber P (1996) Analysis of uptake and allocation of nitrogen and sulphur compounds by trees in the field. J Exp Bot 47:1491–1498. https://doi.org/10.1093/jxb/47.10.1491

ReuvenyZ, Dougall D, Trinity P.1980. Regulatory coupling of nitrate and sulfate assimilation pathways in cultured tobacco cells. Proceedings of the National Academy of Sciences, USA77,6670–6672.

RicardB, Toai TV, Chourey P, Saglio P.1998. Evidence for the critical role of sucrose synthase for anoxic tolerance of maize roots using a double mutant. Plant Physiology116,1323–1331.

Richards C L, Rosas U, Banta J, Bhambhra N, Purugganan M D, 2012 Genome-wide patterns of Arabidopsis gene expression in nature. PLoS Genet. 8(4): e1002662.

Ristova D, Kopriva S. 2022. Sulfur signaling and starvation response in Arabidopsis. iScience 25, 104242.

Ristova, D., & Kopriva, S. (2022). Sulfur signaling and starvation response in Arabidopsis. IScience, 25(5), 104242. https://doi.org/10.1016/j.isci.2022.104242

Ritchie ME, Phipson B, Wu D, Hu Y, Law CW, Shi W, Smyth GK. limma powers differential expression analyses for RNA-sequencing and microarray studies. Nucleic Acids Res. 2015;43(7):e47.

Rodríguez-Serrano M, Romero-Puertas MC, Zabalza A, Corpas FJ, Gómez M, Delrío LA, Sandalio LM (2006) Cadmium effect on oxidative metabolism of pea (Pisum sativum L.) roots: imaging of reactive oxygen species and nitric oxide accumulation in vivo. Plant Cell Environ 29: 1532–1544

Roje, S. (2006). S-Adenosyl-l-methionine: Beyond the universal methyl group donor. Phytochemistry, 67(15), 1686-1698. https://doi.org/10.1016/j.phytochem.2006.04.019

Rotte, C., & Leustek, T. (2000). Differential Subcellular Localization and Expression of ATP Sulfurylase and 5′-Adenylylsulfate Reductase during Ontogenesis of Arabidopsis Leaves Indicates That Cytosolic and Plastid Forms of ATP Sulfurylase May Have Specialized Functions. Plant Physiology, 124(2), 715-724. https://doi.org/10.1104/pp.124.2.715

Rouached H, Secco D, Arpat B, Poirier Y. 2011. The transcription factor PHR1 plays a key role in the regulation of sulfate shoot-to-root flux upon phosphate starvation in Arabidopsis. BMC Plant Biology 11, 19.

Rus, A; Baxter, I; Muthukumar, B; Gustin, J; Lahner, B; Yakubova, E; Salt, DE. Natural variants of AtHKT1 enhance Na(+) accumulation in two wild populations of Arabidopsis. PLoS Genet 2006, 2, e210.

Salt DE. Update on plant ionomics. Plant Physiol. 2004;136:2451–2456. doi: 10.1104/pp.104.047753.

Sarda X, Diquelou S, Abdallah M, Nesi N, Cantat O, Le Gouée P, Ourry A (2014) Assessment of sulphur deficiency in commercial oilseed rape crops from plant analysis. J Agric Sci 152:616–633

SCHNAUBELT D., SCHULZ P., HANNAH M.A., YOCGO R.E., & FOYER C.H. (2013) Perturbations in cellular GSH homeostasis influence shoot and root development but have no negative effects on abiotic stress tolerance in Arabidopsis thaliana. Frontiers in Plant Physiology. doi:10.3389/fpls.2013.00416.

Schnug E, Haneklaus S. 2005. Sulphur deficiency symptoms in oilseed rape (*Brassica napus* L.) - The aesthetics of starvation. *Phyton Annales Rei Botanicae* **45**: 79–95.

Shah, S.H., Islam, S. & Mohammad, F. Sulphur as a dynamic mineral element for plants: a review. J Soil Sci Plant Nutr 22, 2118–2143 (2022). https://doi.org/10.1007/s42729-022-00798-9

Shan, Y., & Jin, S. (2025). Biosynthetic Machinery to Abiotic Stress-Driven Emission: Decoding Multilayer Regulation of Volatile Terpenoids in Plants. *Antioxidants*, *14*(6). https://doi.org/10.3390/antiox14060673

Shibagaki, N., & Grossman, A. R. (2010). Binding of cysteine synthase to the STAS domain of sulfate transporter and its regulatory consequences. *Journal of Biological Chemistry*, *285*(32), 25094-25102.

Shijuan Yan, Qing Liu, Wenyan Li, Jianbing Yan & Alisdair R. Fernie(2022) Raffinose Family Oligosaccharides: Crucial Regulators of Plant Developmentand Stress Responses, Critical Reviews in Plant Sciences, 41:4, 286-303, DOI:10.1080/07352689.2022.2111756

Shomali, A., Das, S., Arif, N., Sarraf, M., Zahra, N., Yadav, V., Aliniaeifard, S., Chauhan, D. K., & Hasanuzzaman, M. (2022). Diverse Physiological Roles of Flavonoids in Plant Environmental Stress Responses and Tolerance. *Plants*, *11*(22). https://doi.org/10.3390/plants11223158

Sirko, A., Wawrzyńska, A., Rodríguez, M. C., & Sęktas, P. (2015). The family of LSU-like proteins. *Frontiers in plant science*, *5*, 774.

Skipsey M., Cummins I., Andrews C.J., Jepson I. & Edwards R. (2005b) Manipulation of plant tolerance to herbicides through co-ordinated metabolic engineering of a detoxifying glutathione transferase and thiol cosubstrate. *Plant Biotechnology Journal* **3**, 409–420.

Song LL, Ding W, Zhao MG, Sun BT, Zhang LX (2006) Nitric oxide protects against oxidative stress under heat stress in the calluses from two ecotypes of reed. Plant Sci 171: 449–458

Stitt M. Nitrate regulation of metabolism and growth. Curr Opin Plant Biol. 1999 Jun;2(3):178-86. doi: 10.1016/S1369-5266(99)80033-8. PMID: 10375569.

Stitt, M., & Scheible, W. (1999). Nitrate acts as a signal to control gene expression, metabolism and biomass allocation.

Stitt, M., Müller, C., Matt, P., Gibon, Y., Carillo, P., Morcuende, R., Scheible, W., & Krapp, A. (2002). Steps towards an integrated view of nitrogen metabolism. Journal of Experimental Botany, 53(370), 959-970. https://doi.org/10.1093/jexbot/53.370.959

Strand, D. D., Fisher, N., & Kramer, D. M. (2017). The higher plant plastid NAD(P)H dehydrogenase-like complex (NDH) is a high efficiency proton pump that increases ATP production by cyclic electron flow. *The Journal of Biological Chemistry*, *292*(28), 11850. https://doi.org/10.1074/jbc.M116.770792

Sugimura, N., Sakuraba, Y., Usuda, K., Ohtsuki, N., Monda, K., Iba, K., & Yanagisawa, S. (2025). Natural variation in potassium deficiency responses among Arabidopsis thaliana accessions. *Plant and Cell Physiology*, *66*(6), 956. https://doi.org/10.1093/pcp/pcaf041

Sugiyama, R., Li, R., Kuwahara, A., Nakabayashi, R., Sotta, N., Mori, T., Ito, T., Ohkama-Ohtsu, N., Fujiwara, T., Saito, K., Nakano, R. T., Bednarek, P., & Hirai, M. Y. (2021). Retrograde sulfur flow from glucosinolates to cysteine in Arabidopsis thaliana. Proceedings of the National Academy of Sciences, 118(22), e2017890118. https://doi.org/10.1073/pnas.2017890118

Sun, S. K., Ahmad, N., Callenius, H., Rajab, H., Uslu, V. V., Cruz Cruz, J. R., Zhao, F. J., Wirtz, M., & Hell, R. (2025). The plastid cysteine synthase complex regulates ABA biosynthesis and stomatal closure in Arabidopsis. *Nature Communications*, *16*(1), 8960. https://doi.org/10.1038/s41467-025-64705-3

Sun, Z., Guo, W., Zhao, X., Chen, Y., Yang, J., Xu, S., & Hou, H. (2022). Sulfur limitation boosts more starch accumulation than nitrogen or phosphorus limitation in duckweed (Spirodela polyrhiza). *Industrial Crops and Products*, *185*, 115098. https://doi.org/10.1016/j.indcrop.2022.115098

Suter, L., & Widmer, A. (2013). Environmental Heat and Salt Stress Induce Transgenerational Phenotypic Changes in Arabidopsis thaliana. *PLOS ONE*, *8*(4), e60364. https://doi.org/10.1371/journal.pone.0060364

Takahashi H, Saito K. Subcellular localization of spinach cysteine synthase isoforms and regulation of their gene expression by nitrogen and sulfur. Plant Physiol. 1996;112:273–280. doi: 10.1104/pp.112.1.273.

Takahashi H., Kopriva S., Giordano M., Saito K., Hell R. (2011) Sulfur Assimilation in Photosynthetic Organisms: Molecular Functions and Regulations of Transporters and Assimilatory Enzymes. Annu. Rev. Plant Biol. 62, 157-184.

Takahashi, H. (2023). Sulfur metabolism: Actions for plant resilience and adaptation. Journal of Experimental Botany, 74(11), 3271–3285. https://doi.org/10.1093/jxb/erad189

Takahashi, H., Watanabe-Takahashi, A., Smith, F. W., Blake-Kalff, M., Hawkesford, M. J., & Saito, K. (2000). The roles of three functional sulphate transporters involved in uptake and translocation of sulphate in Arabidopsis thaliana. The Plant Journal, 23(2), 171-182. https://doi.org/10.1046/j.1365-313x.2000.00768.x

Tandon, H. L. S. (1984). Sulphur research and agricultural production in India. New Delhi, India: Fertiliser Development and Consultation Organisation.

Teotla US, Mehta VS, Ghosh D, Srivastava PC (2000) Phosphorus-sulphur interaction in moongbean (*Vigna radiata* L. Wilczek): I. Yield, phosphorus and sulphur contents. Legume Res Inter J 23:106–109

Tian QY, Sun DH, Zhao MG, Zhang WH (2007) Inhibition of nitric oxide synthase (NOS) underlines aluminum-induced inhibition of root elongation in Hibiscus moscheutos. New Phytol 174 322–331

Tripathy, M. K., Deswal, R., & Sopory, S. K. (2020). Plant RABs: Role in Development and in Abiotic and Biotic Stress Responses. *Current Genomics*, *22*(1), 26. https://doi.org/10.2174/1389202922666210114102743

Van Leeuwen H, Kliebenstein D J, West M A, Kim K, van Poecke Ret al. , 2007 Natural variation among Arabidopsis thaliana accessions for transcriptome response to exogenous salicylic acid. Plant Cell 19(7): 2099–2110.

Vauclare, P., Kopriva, S., Fell, D., Suter, M., Sticher, L., Ballmoos, P. V., Krähenbühl, U., Den Camp, R. O., & Brunold, C. (2002). Flux control of sulphate assimilation in Arabidopsis thaliana: Adenosine 5′-phosphosulphate reductase is more susceptible than ATP sulphurylase to negative control by thiols. The Plant Journal, 31(6), 729-740. https://doi.org/10.1046/j.1365-313X.2002.01391.x

Verhoeven, K. J., Jansen, J. J., van Dijk, P. J., & Biere, A. (2010). Stress-induced DNA methylation changes and their heritability in asexual dandelions. *New Phytologist, 185*, 1108–1118.

Walker, B. J., Strand, D. D., Kramer, D. M., & Cousins, A. B. (2014). The Response of Cyclic Electron Flow around Photosystem I to Changes in Photorespiration and Nitrate Assimilation. *Plant Physiology*, *165*(1), 453-462. https://doi.org/10.1104/pp.114.238238

Wang YY, Cheng YH, Chen KE, Tsay YF. Nitrate Transport, Signaling, and Use Efficiency. Annu Rev Plant Biol. 2018 Apr 29;69:85-122. doi: 10.1146/annurev-arplant-042817-040056. Epub 2018 Mar 23. PMID: 29570365.

Wang, CL., Oliver, D.J. Cloning of the cDNA and genomic clones for glutathione synthetase from *Arabidopsis thaliana* and complementation of a*gsh2* mutant in fission yeast. *Plant Mol Biol* **31**, 1093–1104 (1996). https://doi.org/10.1007/BF00040827

Wang, J. L., Wang, M., Zhang, L., Li, Y. X., Li, J. J., Li, Y. Y., Pu, Z. X., Li, D. Y., Liu, X. N., Guo, W., Di, D. W., Li, X. F., Guo, G. Q., & Wu, L. (2024). WAV E3 ubiquitin ligases mediate degradation of IAA32/34 in the TMK1-mediated auxin signaling pathway during apical hook

development. *Proceedings of the National Academy of Sciences*, *121*(17), e2314353121. https://doi.org/10.1073/pnas.2314353121

Wangeline A. L, Burkhead J L, Hale K. L, Lindblom S. D, Terry N, Pilon M.et al (2004). Overexpression of ATP sulfurylase in Indian mustard: effects on tolerance and accumulation of twelve metals.J. Environ. Qual.3354–60. 10.2134/jeq2004.5400

Watanabe M, Hubberten HM, Saito K, Hoefgen R. General regulatory patterns of plant mineral nutrient depletion as revealed by serat quadruple mutants disturbed in cysteine synthesis. Mol Plant. 2010 Mar;3(2):438-66. doi: 10.1093/mp/ssq009. PMID: 20339158.

Watanabe, M., Kusano, M., Oikawa, A., Fukushima, A., Noji, M., and Saito, K. (2008a). Physiological roles of the beta-substituted alanine synthase gene family in Arabidopsis. *Plant Physiol.* 146, 310–320.

Watanabe, M., Mochida, K., Kato, T., Tabata, S., Yoshimoto, N., Noji, M., & Saito, K. (2008b). Comparative genomics and reverse genetics analysis reveal indispensable functions of the serine acetyltransferase gene family in Arabidopsis. *The Plant Cell*, *20*(9), 2484-2496.

Wawrzyńska, A., Piotrowska, J., Apodiakou, A., Brückner, F., Hoefgen, R., & Sirko, A. (2022). The SLIM1 transcription factor affects sugar signaling during sulfur deficiency in Arabidopsis. *Journal of Experimental Botany*, *73*(22), 7362-7379. https://doi.org/10.1093/jxb/erac371

Weigel, D. (2012). Natural Variation in Arabidopsis: From Molecular Genetics to Ecological Genomics. *Plant Physiology*, *158*(1), 2-22. https://doi.org/10.1104/pp.111.189845

Wong CE, et al. (2006) Transcriptional profiling implicates novel interactions between abiotic stress and hormonal responses in Thellungiella, a close relative of Arabidopsis. Plant Physiol 140:1437–1450.

Woo HR, Masclaux-Daubresse C, Lim PO. 2018. Plant senescence: how plants know when and how to die. Journal of Experimental Botany 65, 715–718.

Yamaguchi Y, Nakamura T, Harada E, Koizumi N, Sano H.1999. Differential accumulation of transcripts encoding sulfur assimilation enzymes upon sulfur and/or nitrogen deprivation in Arabidopsis thaliana. Bioscience, Biotechnology and Biochemistry63,762–766.

Yamamoto, H., & Shikanai, T. (2019). PGR5-Dependent Cyclic Electron Flow Protects Photosystem I under Fluctuating Light at Donor and Acceptor Sides. *Plant Physiology*, *179*(2), 588-600. https://doi.org/10.1104/pp.18.01343

Yang ZL, Kunert G, Sporer T, Kornig J, Beran F.. 2020. Glucosinolate abundance and composition in brassicaceae influence sequestration in a specialist flea beetle. Journal of Chemical Ecology 46, 186–197.

Yong-Villalobos, L., González-Morales, S. I., Wrobel, K., Gutiérrez-Alanis, D., Cervantes-Peréz, S. A., Hayano-Kanashiro, C., Oropeza-Aburto, A., Cruz-Ramírez, A., Martínez, O., & Herrera-Estrella, L. (2015). Methylome analysis reveals an important role for epigenetic changes in the regulation of the Arabidopsis response to phosphate starvation. *Proceedings of the National Academy of Sciences*, *112*(52), E7293-E7302. https://doi.org/10.1073/pnas.1522301112

Yoshimoto, N., Inoue, E., Watanabe-Takahashi, A., Saito, K., & Takahashi, H. (2007). Posttranscriptional Regulation of High-Affinity Sulfate Transporters in Arabidopsis by Sulfur Nutrition. Plant Physiology, 145(2), 378. https://doi.org/10.1104/pp.107.105742

Yoshimoto, N., Takahashi, H., Smith, F. W., Yamaya, T., & Saito, K. (2002). Two distinct high-affinity sulfate transporters with different inducibilities mediate uptake of sulfate in Arabidopsis roots. *The Plant Journal*, 29(4), 465-473.

Yu Z, She M, Zheng T, Diepeveen D, Islam S, Zhao Y, Zhang Y, Tang G, Zhang Y, Zhang J, et al. Impact and mechanism of sulphur-deficiency on modern wheat farming nitrogen-related sustainability and gliadin content. Comm Bio. 2021;4(1):1–6. doi: 10.1038/s42003-021-02458-7.

Yu, B., Xu, C., & Benning, C. (2002). Arabidopsis disrupted in SQD2 encoding sulfolipid synthase is impaired in phosphate-limited growth. *Proceedings of the National Academy of Sciences*, *99*(8), 5732-5737.

Yu, X., Sukumaran, S., & Márton, L. (1998). Differential Expression of the Arabidopsis Nia1 and Nia2 Genes : Cytokinin-Induced Nitrate Reductase Activity Is Correlated With Increased Nia1 Transcription and mRNA Levels. Plant Physiology, 116(3), 1091. https://doi.org/10.1104/pp.116.3.1091

Yu, Y., Zhong, Z., Ma, L., Xiang, C., Chen, J., Huang, X. Y., Xu, P., & Xiong, Y. (2022). Sulfate-TOR signaling controls transcriptional reprogramming for shoot apex activation. *New Phytologist*, *236*(4), 1326-1338. https://doi.org/10.1111/nph.18441

Zan, Y., Shen, X., Forsberg, S. K., & Carlborg, Ö. (2016). Genetic Regulation of Transcriptional Variation in Natural Arabidopsis thaliana Accessions. *G3 Genes|Genomes|Genetics*, *6*(8), 2319-2328. https://doi.org/10.1534/g3.116.030874

Zenzen, I., Cassol, D., Westhoff, P. *et al.* Transcriptional and metabolic profiling of sulfur starvation response in two monocots. *BMC Plant Biol* **24**, 257 (2024). https://doi.org/10.1186/s12870-024-04948-2

Zhao F, Evans EJ, Bilsborrow PE, Syers JK (1993) Influence of sulphur and nitrogen on seed yield and quality of low glucosinolate oilseed rape (*Brassica napus* L). J Sci Food Agric 63:29–37. https://doi.org/10.1002/jsfa.2740630106

Zhao MG, Tian QY, Zhang WH (2007) Nitric oxide synthase-dependent nitric oxide production is associated with salt tolerance in Arabidopsis. Plant Physiol 144: 206–217

Zhao, C., Cai, S., Wang, Y., & Chen, Z. H. (2016). Loss of nitrate reductases NIA1 and NIA2 impairs stomatal closure by altering genes of core ABA signaling components in Arabidopsis. *Plant Signaling & Behavior*, *11*(6), e1183088. https://doi.org/10.1080/15592324.2016.1183088

Zhao, M. G., Chen, L., Zhang, L. L., & Zhang, W. H. (2009). Nitric Reductase-Dependent Nitric Oxide Production Is Involved in Cold Acclimation and Freezing Tolerance in Arabidopsis. *Plant Physiology*, *151*(2), 755-767. https://doi.org/10.1104/pp.109.140996

Zheng, Q., Xin, J., Zhao, C. et al. Role of methylglyoxal and glyoxalase in the regulation of plant response to heavy metal stress. Plant Cell Rep 43, 103 (2024). https://doi.org/10.1007/s00299-024-03186-y

Zhou J, Zhang H, Huang Y, Jiao S, Zheng X, Lu W, Jiang W, Bai X. Impact of Sulfur Deficiency and Excess on the Growth and Development of Soybean Seedlings. Int J Mol Sci. 2024 Oct 19;25(20):11253. doi: 10.3390/ijms252011253. PMID: 39457037; PMCID: PMC11508489.

Zörb C, Steinfurth D, Seling S, Langenkämper G, Koehler P, Wieser H, Lindhauer MG, Mühling KH. Quantitative protein composition and baking quality of winter wheat as affected by late sulfur fertilization. J Agric Food Chem. 2009 May 13;57(9):3877-85. doi: 10.1021/jf8038988. PMID: 19326868.

Zuber, H., Davidian, J. C., Wirtz, M., Hell, R., Belghazi, M., Thompson, R., & Gallardo, K. (2010). Sultr4;1 mutant seeds of Arabidopsis have an enhanced sulphate content and modified proteome suggesting metabolic adaptations to altered sulphate compartmentalization. *BMC Plant Biology*, *10*, 78. https://doi.org/10.1186/1471-2229-10-78

7. SUPPLEMENTARY FIGURES

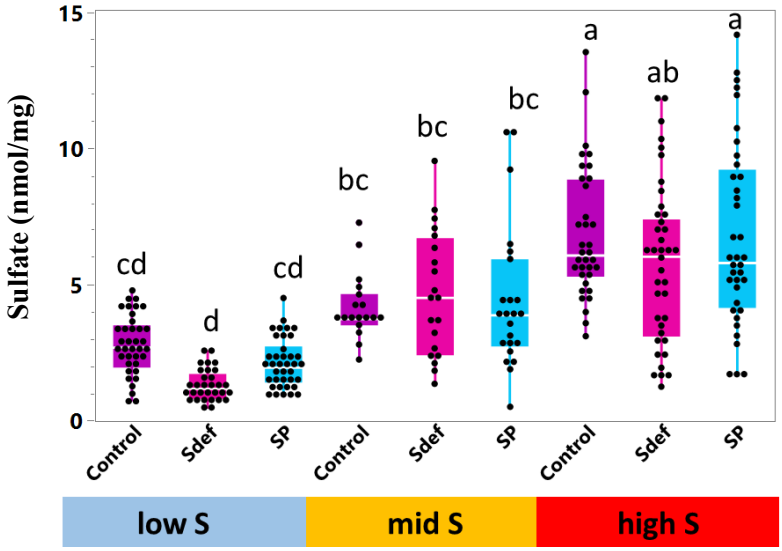

Supplementary Figure 1: Shoot Sulfate content (nmol/ mg^{-1}) measured at 4th week in low-S (blue), mid-S (orange), and high-S (red) accessions grown under control (750 µM sulfate), sulfur-deficient (0 µM), or short-pulse (SP; intermittent supply) conditions. Plants were grown in a 9:1 sand: soil mix and fertilized twice weekly with the indicated S regimes. At week 4, the 7th–8th leaves were harvested (n = 8 per accession). Data were analyzed using mixed models followed by Tukey's HSD; different letters indicate significant differences ($P < 0.05$). Boxplots show means ± SE.

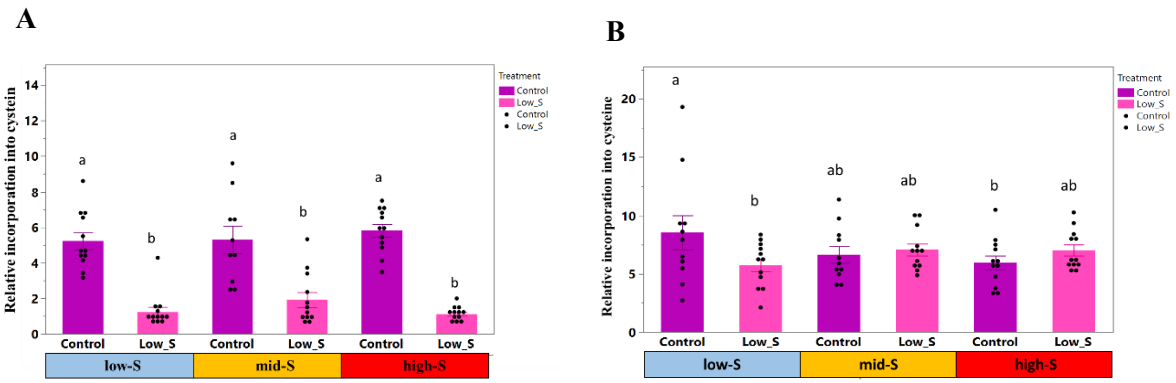

Supplementary Figure 2: (A) [^{35}S] incorporation into cysteine [%] in shoots among group **(B)** [^{35}S] incorporation into cysteine [%] in roots among group. *Arabidopsis* plants (25 seedlings) fed with either 750 µM SO_4^{2-} (Control) or 15 µM SO_4^{2-} (S-def) were grown on a nylon net in hydroculture for 14 d and, after incubation with [35S] sulfate for 3 hours, shoots and roots were harvested separately and measured via HPLC with a radiodetector or after elution from DEAE-Sephadex by scintillation counting. Statistical analysis was performed using two-way ANOVA followed by Tukey's post hoc test for multiple comparisons for treatment and genotype. Lowercase letters indicate significant differences ($p < 0.05$) between the genotypes and the treatments. Values are means ± s.e.m. (n=4-6).

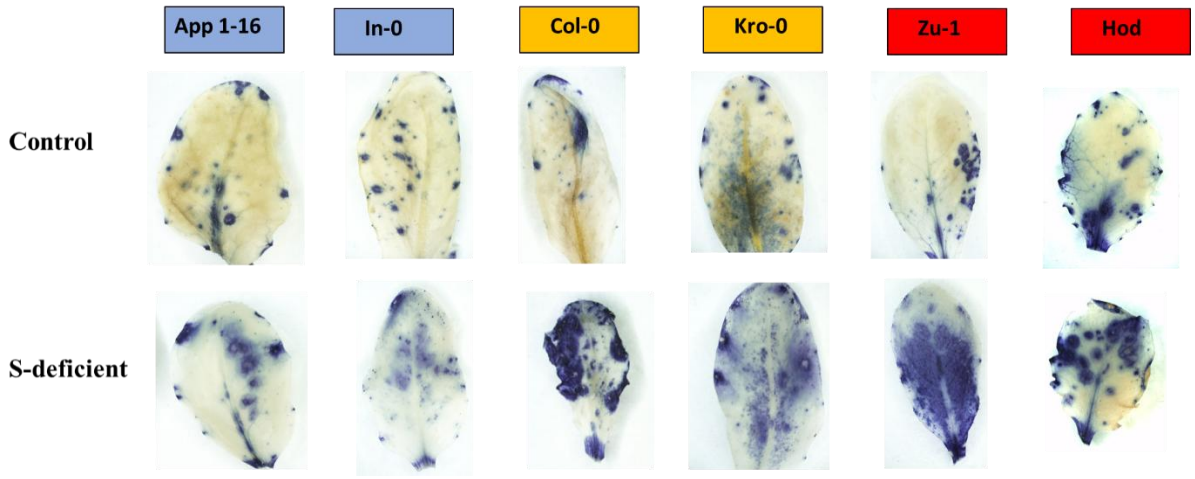

Supplementary Figure 3: Pictures of NBT stained 35 days old seedlings of *A. thaliana* accessions. i.e. App1-16 (low-S), In-0 (low-S), Col-0 (mid-S), Kro-0 (mid-S), Zu-1 (high-S) and Hod (high-S) under control and S-def conditions.

A

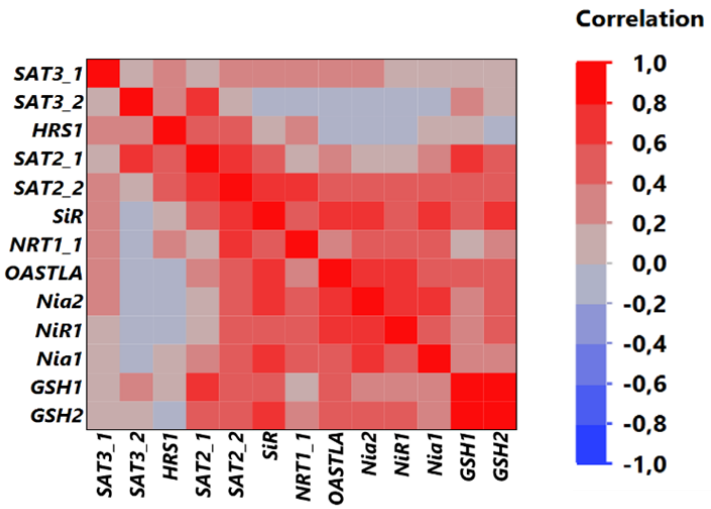

	SAT3_1	SAT3_2	SAT2_1	SAT2_2	SiR	OASTLA	NRT1_1	Nia1	Nia2	NiR1	HRS1	GSH1	GSH2
SAT3_1	<,0001	0,9265	0,1534	0,0036	0,1150	0,0010	0,0114	0,1480	0,0622	0,4003	0,0714	0,7420	0,2687
SAT3_2	0,9265	<,0001	<,0001	0,5971	0,9753	0,5353	0,3331	0,7893	0,1903	0,9237	0,0047	0,0559	0,2724
SAT2_1	0,1534	<,0001	<,0001	<,0001	0,0001	0,0288	0,2698	0,0479	0,4085	0,3064	<,0001	<,0001	0,0002
SAT2_2	0,0036	0,5971	<,0001	<,0001	<,0001	0,0004	<,0001	<,0001	<,0001	0,0006	0,0006	<,0001	<,0001
SiR	0,1150	0,9753	0,0001	<,0001	<,0001	<,0001	<,0001	<,0001	<,0001	<,0001	0,1740	<,0001	<,0001
OASTLA	0,0010	0,5353	0,0288	0,0004	<,0001	<,0001	0,0042	<,0001	<,0001	<,0001	0,9550	0,0002	<,0001
NRT1_1	0,0114	0,3331	0,2698	<,0001	<,0001	0,0042	<,0001	0,0003	0,0001	<,0001	0,0448	0,2865	0,0029
Nia1	0,1480	0,7893	0,0479	<,0001	<,0001	<,0001	0,0003	<,0001	<,0001	0,0002	0,3280	0,0590	0,0640
Nia2	0,0622	0,1903	0,4085	<,0001	<,0001	<,0001	0,0001	<,0001	<,0001	<,0001	0,7361	0,0051	<,0001
NiR1	0,4003	0,9237	0,3064	0,0006	<,0001	<,0001	<,0001	0,0002	<,0001	<,0001	0,8705	0,0149	<,0001
HRS1	0,0714	0,0047	<,0001	0,0006	0,1740	0,9550	0,0448	0,3280	0,7361	0,8705	<,0001	0,6113	0,8965
GSH1	0,7420	0,0559	<,0001	<,0001	<,0001	0,0002	0,2865	0,0590	0,0051	0,0149	0,6113	<,0001	<,0001
GSH2	0,2687	0,2724	0,0002	<,0001	<,0001	<,0001	0,0029	0,0640	<,0001	<,0001	0,8965	<,0001	<,0001

B

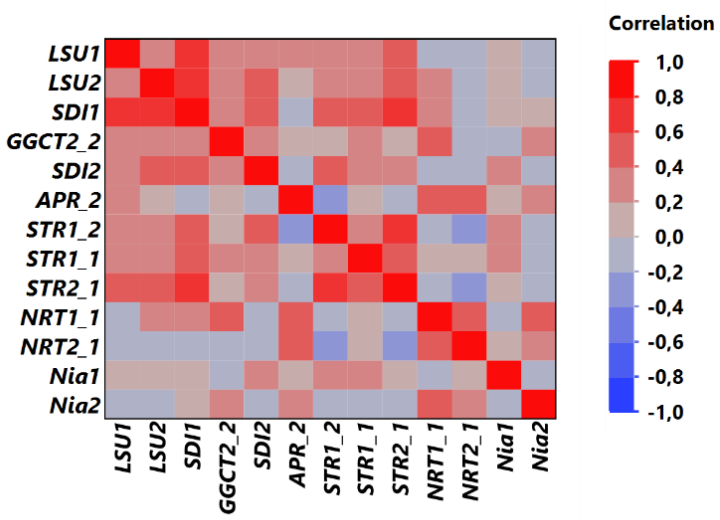

	LSU1	LSU2	SDI1	GGCT2_2	SDI2	APR_2	STR1_2	STR1_1	STR2_1	NRT1_1	NRT2_1	Nia1	Nia2
LSU1	<,0001	0,0038	<,0001	0,0624	0,0068	0,0696	0,0589	0,0064	<,0001	0,7030	0,8886	0,5037	0,3047
LSU2	0,0038	<,0001	<,0001	0,0066	<,0001	0,2441	0,0062	0,0049	0,0002	0,0064	0,4347	0,2789	0,5507
SDI1	<,0001	<,0001	<,0001	0,0174	<,0001	0,9640	0,0001	0,0003	<,0001	0,1043	0,1824	0,8768	0,7591
GGCT2_2	0,0624	0,0066	0,0174	<,0001	0,0026	0,1674	0,2145	0,0981	0,7411	<,0001	0,2019	0,8589	0,0789
SDI2	0,0068	<,0001	<,0001	0,0026	<,0001	0,3098	<,0001	0,0049	0,0110	0,7838	0,3328	0,0079	0,2045
APR_2	0,0696	0,2441	0,9640	0,1674	0,3098	<,0001	0,0079	0,4030	0,2380	<,0001	0,0003	0,2850	0,0782
STR1_2	0,0589	0,0062	0,0001	0,2145	<,0001	0,0079	<,0001	0,0094	<,0001	0,4782	0,1116	0,0421	0,4484
STR1_1	0,0064	0,0049	0,0003	0,0981	0,0049	0,4030	0,0094	<,0001	0,0001	0,1339	0,6510	0,0391	0,5170
STR2_1	<,0001	0,0002	<,0001	0,7411	0,0110	0,2380	<,0001	0,0001	<,0001	0,5712	0,0656	0,4504	0,3055
NRT1_1	0,7030	0,0064	0,1043	<,0001	0,7838	<,0001	0,4782	0,1339	0,5712	<,0001	0,0002	0,2354	<,0001
NRT2_1	0,8886	0,4347	0,1824	0,2019	0,3328	0,0003	0,1116	0,6510	0,0656	0,0002	<,0001	0,2393	0,0093
Nia1	0,5037	0,2789	0,8768	0,8589	0,0079	0,2850	0,0421	0,0391	0,4504	0,2354	0,2393	<,0001	0,6280
Nia2	0,3047	0,5507	0,7591	0,0789	0,2045	0,0782	0,4484	0,5170	0,3055	<,0001	0,0093	0,6280	<,0001

Supplementary Figure 4: (A) Correlation matrix along with correlation probability between relative expression cysteine biosynthesis and nitrate assimilation genes in shoots of *A. thaliana* acessions **(B)** Correlation matrix along with correlation probability between relative expression sulfate and nitrate assimilation genes in roots of *A. thaliana* acessions

A B

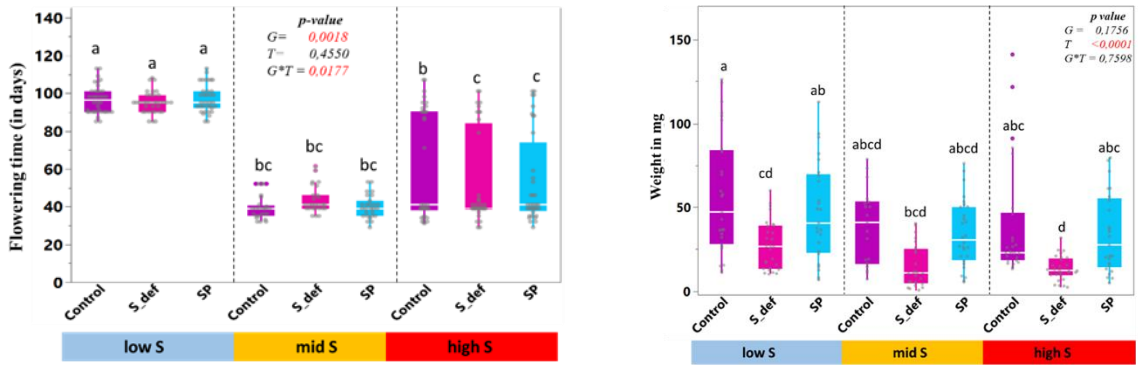

Supplementary Figure 5: (A) Flowering time in days **(B)** Weight of seeds (in mg) in low-S (blue), mid-S (orange), and high-S (red) accessions grown under control (750 µM sulfate), sulfur-deficient (0 µM) or short-pulse (SP; intermittent supply) conditions. Data were analyzed using mixed models followed by Tukey's HSD; different letters indicate significant differences ($P < 0.05$). Boxplots show means ± SE with (n=8 per accessions). Plants were grown in a 9:1 sand: soil mix and fertilized twice weekly with the indicated S regimes.

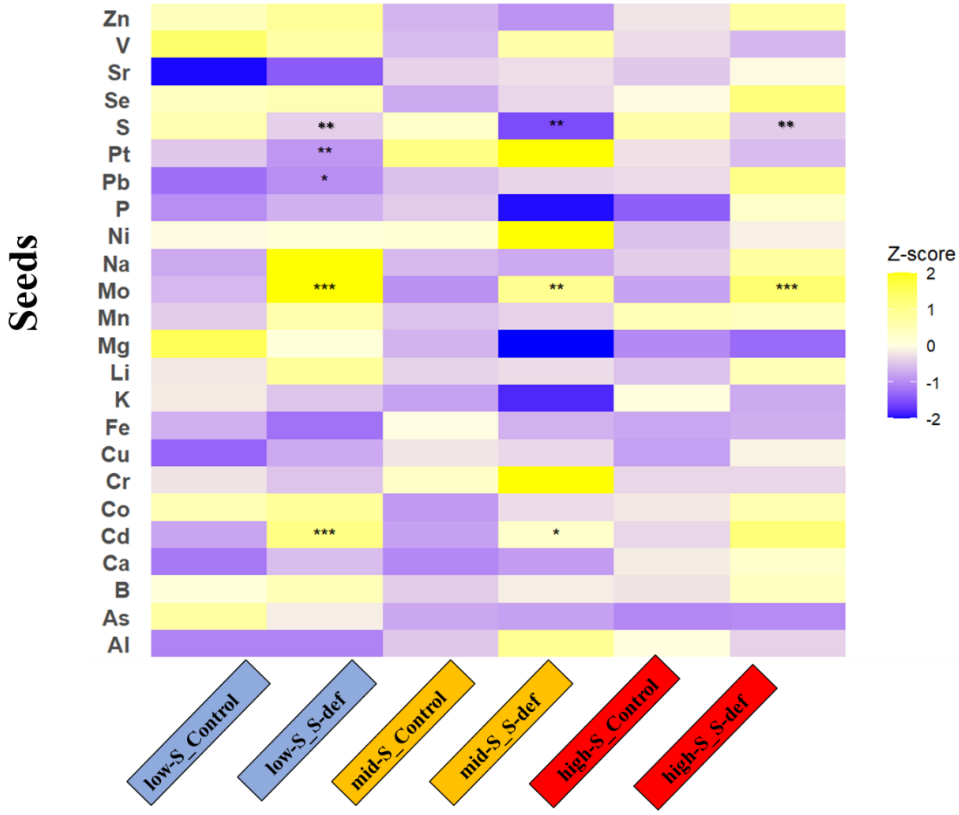

Supplementary Figure 6: Heatmap representing elemental composition in seeds of low-S (blue), mid-S (orange), and high-S (red) accessions grown under control (750 µM sulfate), sulfur-deficient conditions. Data were analyzed using post-hoc test; different letters indicate significant differences (* p

< 0.05, ** p < 0.01, *** p < 0.001). Boxplots show means ± SE with (n=8 per accessions). Plants were grown in a 9:1 sand: soil mix and fertilized twice weekly with the indicated S regimes.

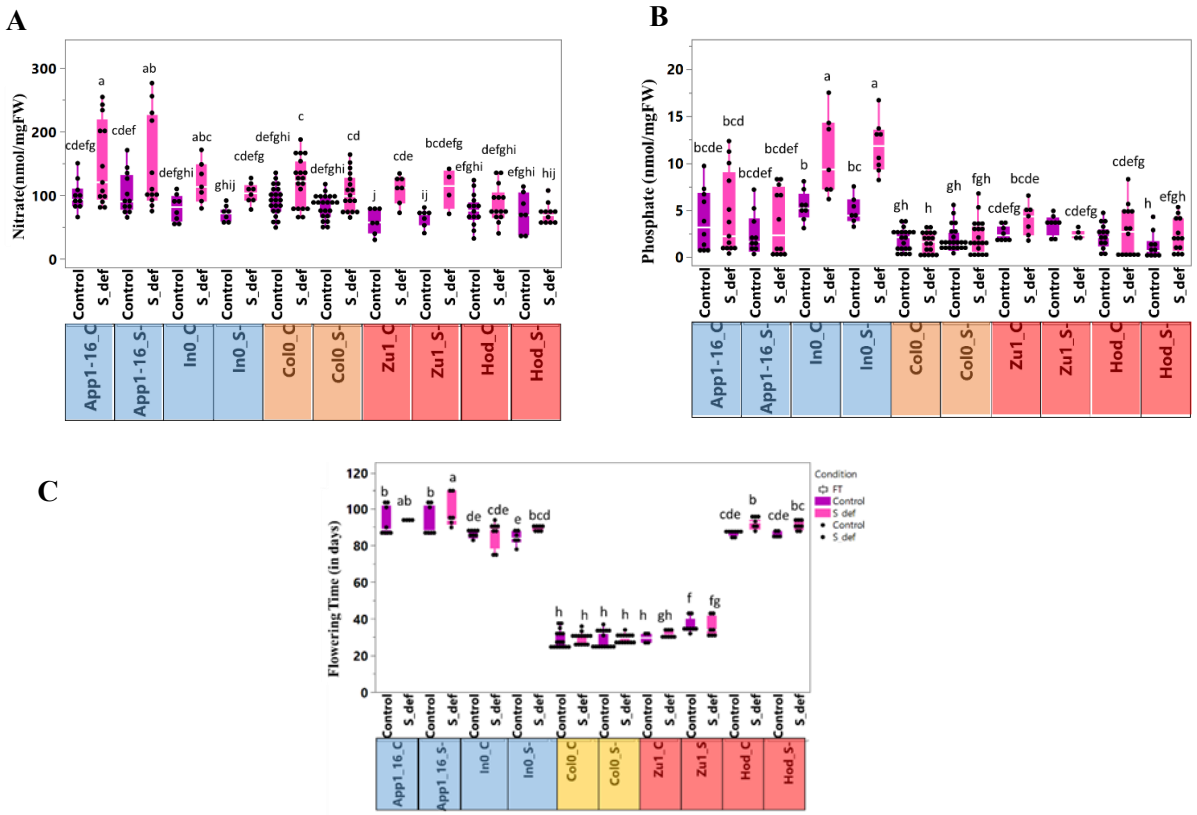

Supplementary Figure 7: (A) Shoot nitrate content (nmol mg^{-1} FW), **(B)** Shoot phosphate content (nmol mg^{-1} FW) **(C)** Flowering time in days in App1-16 and In-0 (low-S group; blue), Col-0 (mid-S group; orange), and Zu-1 and Hod (high-S group; red) accessions. Plants were grown in a 9:1 sand: soil mixture and fertilized twice weekly with either control nutrient solution containing 750 µM sulfate or sulfur-deficient solution (0 µM sulfate). For the next-generation experiment, seeds derived from parental plants grown under control (C) or sulfur-deficient (S-) conditions were germinated and cultivated under the same two sulfur regimes. At week 5, the 7th–8th rosette leaves were harvested for analysis (n = 8 per accession per treatment). Data were analyzed using two-way ANOVA followed by post hoc tests. Different letters indicate statistically significant differences among genotypes and treatments (P < 0.05). Boxplots represent means ± SE.

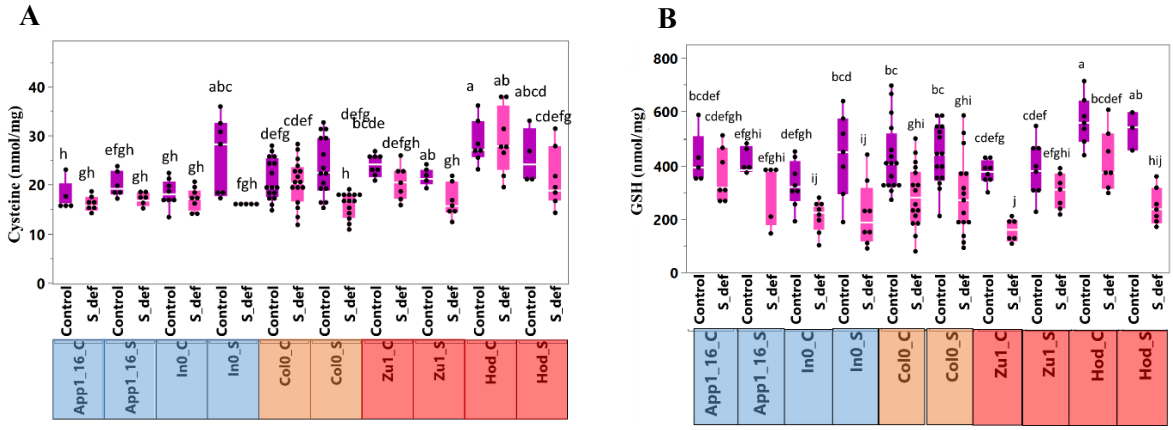

Supplementary Figure 8: (A) Shoot cysteine content (nmol mg^{-1} FW), **(B)** Shoot GSH content (nmol mg^{-1} FW) in App1-16 and In-0 (low-S group; blue), Col-0 (mid-S group; orange), and Zu-1 and Hod (high-S group; red) accessions. Plants were grown in a 9:1 sand: soil mixture and fertilized twice weekly with either control nutrient solution containing 750 µM sulfate or sulfur-deficient solution (0 µM sulfate). For the next-generation experiment, seeds derived from parental plants grown under control (C) or sulfur-deficient (S-) conditions were germinated and cultivated under the same two sulfur regimes. At week 5, the 7th–8th rosette leaves were harvested for analysis (n = 8 per accession per treatment). Data were analyzed using two-way ANOVA followed by post hoc tests. Different letters indicate statistically significant differences among genotypes and treatments ($P < 0.05$). Boxplots represent means ± SE.

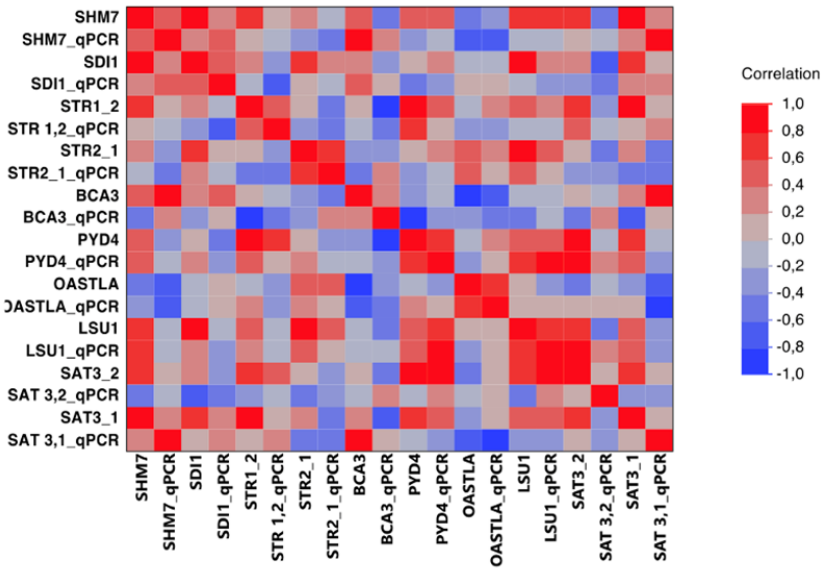

Supplementary Figure 9: Heatmap representing correlation analysis between relative expression of genes studied using q-PCR (for example Gene_qPCR) and RNA-Seq dataset. Colors represent log_2 (low S / control) ratios, with blue indicating negative correlation and red positive correlation.

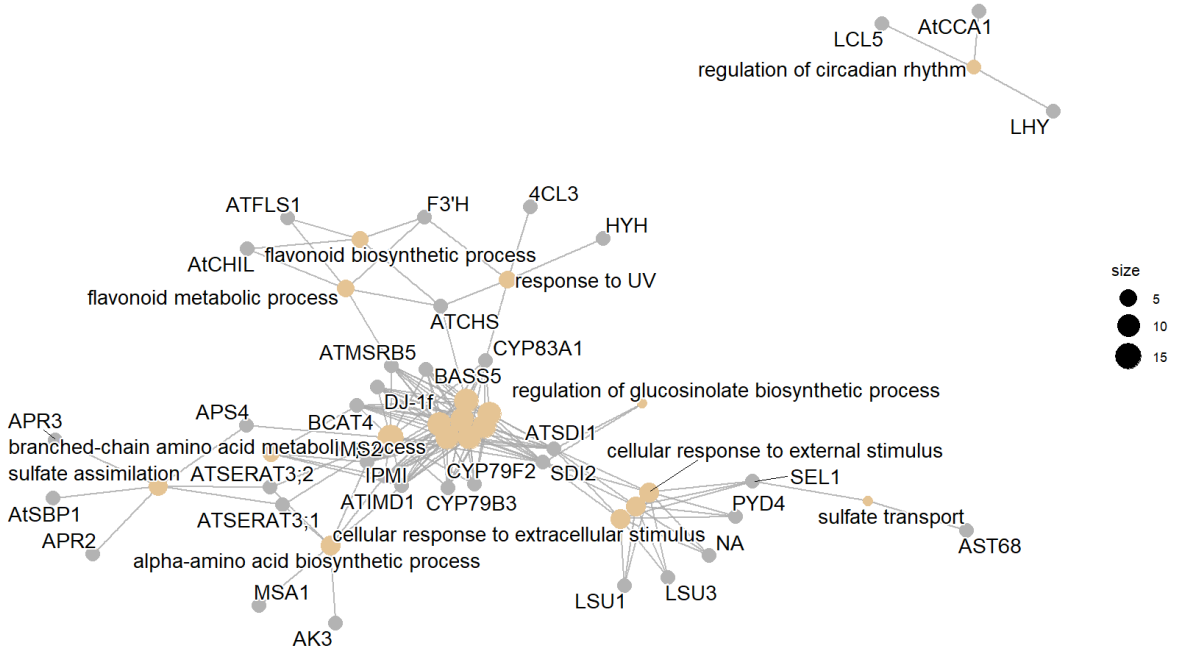

Supplementary Figure 10: Network visualization of enriched Gene Ontology (GO) biological processes identified from the set of 55 core differentially expressed genes in response to S-deficiency. Orange nodes represent significantly enriched GO terms, while gray nodes represent genes associated with these terms. Edges indicate functional associations between genes and GO categories. Node size reflects the number of genes associated with each GO term.

A

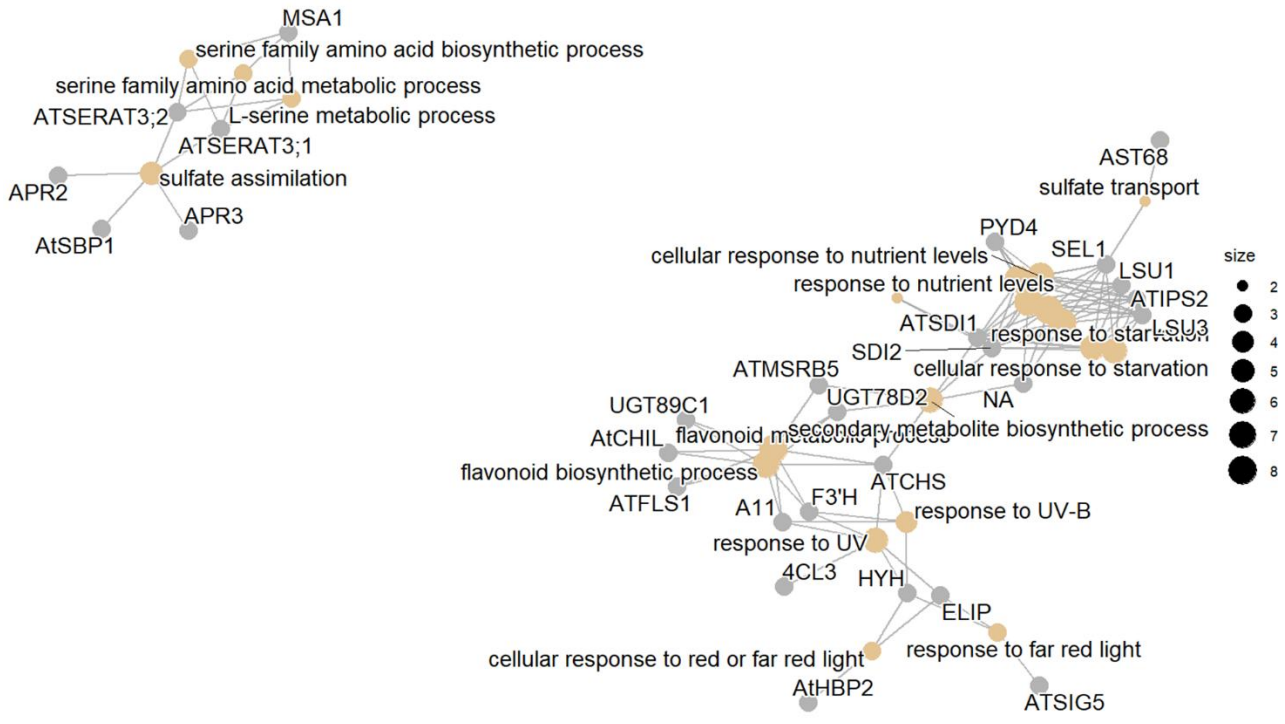

B

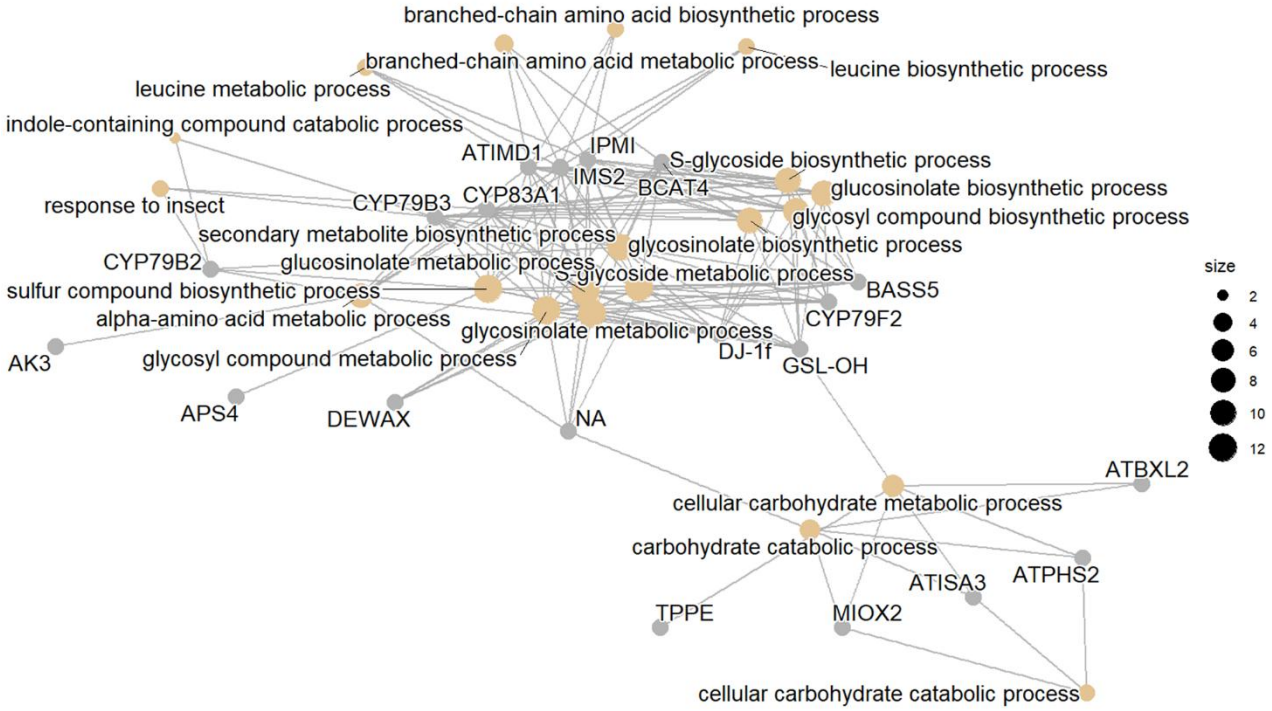

Supplementary Figure 11: Network visualization of enriched Gene Ontology (GO) biological processes identified from the set of **(A)** Upregulated DEGs **(B)** Downregulated DEGs shared among low-S accessions in response to S-deficiency. Orange nodes represent significantly enriched GO terms, while gray nodes represent genes associated with these terms. Edges indicate functional associations between genes and GO categories. Node size reflects the number of genes associated with each GO term.

A

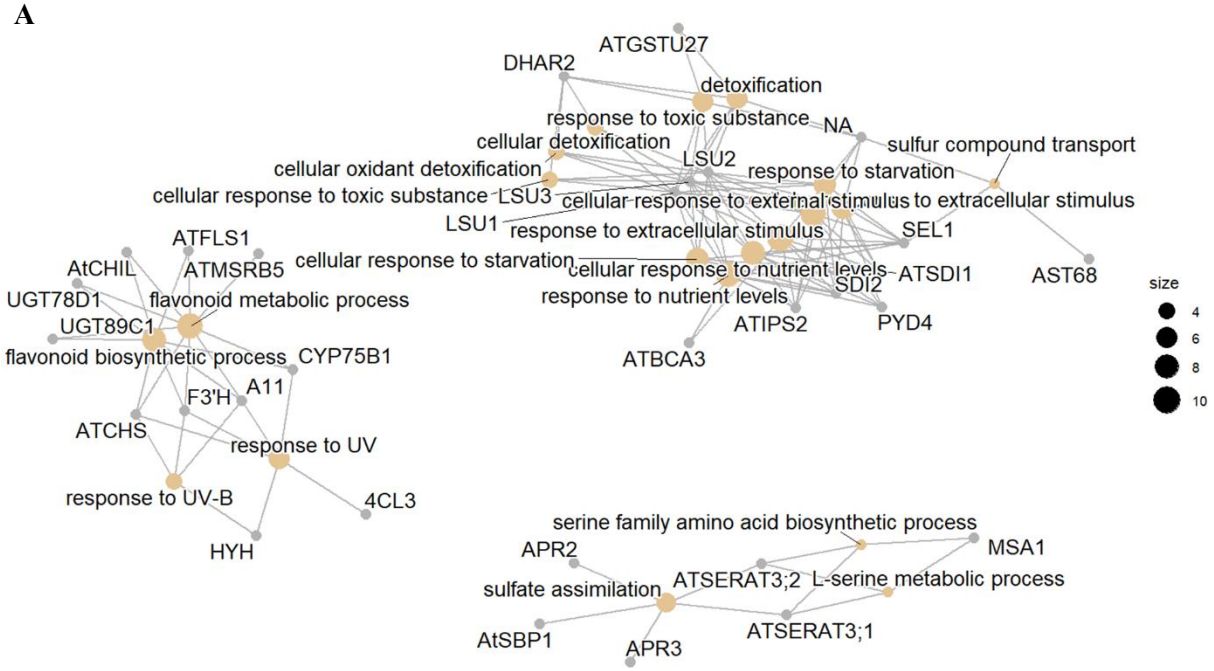

B

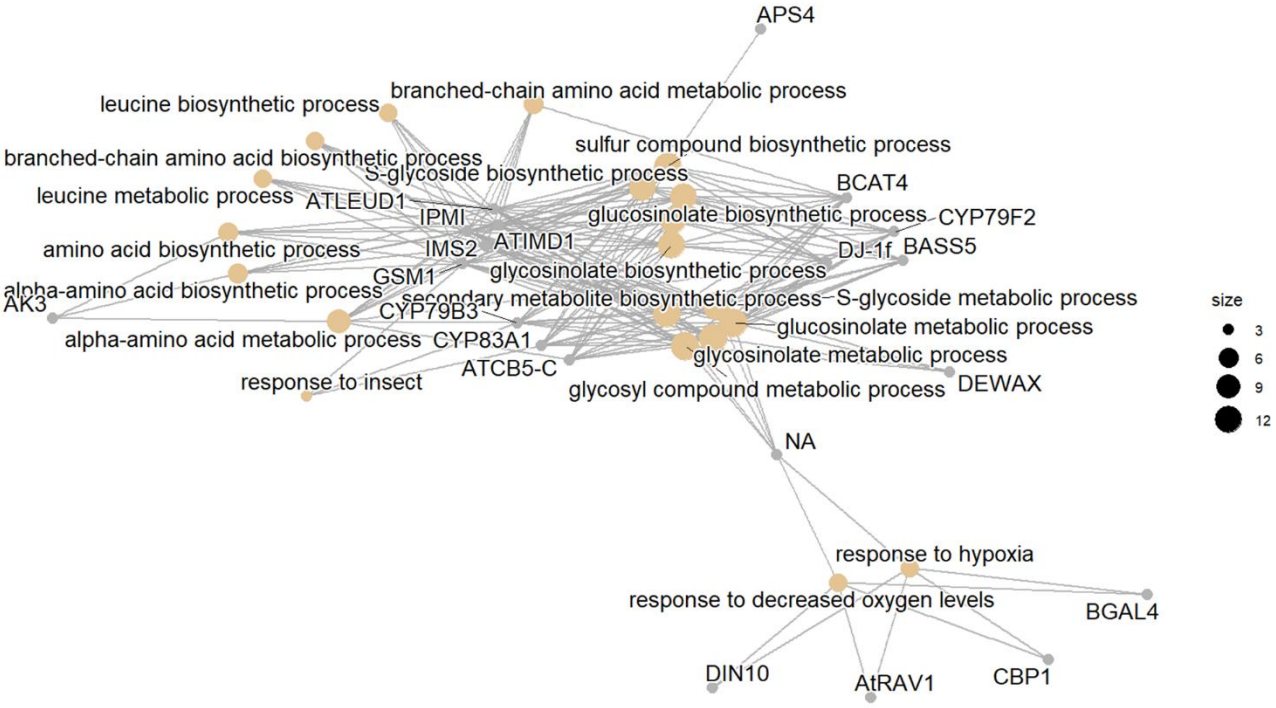

Supplementary Figure 12: Network visualization of enriched Gene Ontology (GO) biological processes identified from the set of **(A)** Upregulated DEGs **(B)** Downregulated DEGs shared among mid-S accessions in response to S-deficiency. Orange nodes represent significantly enriched GO terms, while gray nodes represent genes associated with these terms. Edges indicate functional associations between genes and GO categories. Node size reflects the number of genes associated with each GO term.

A

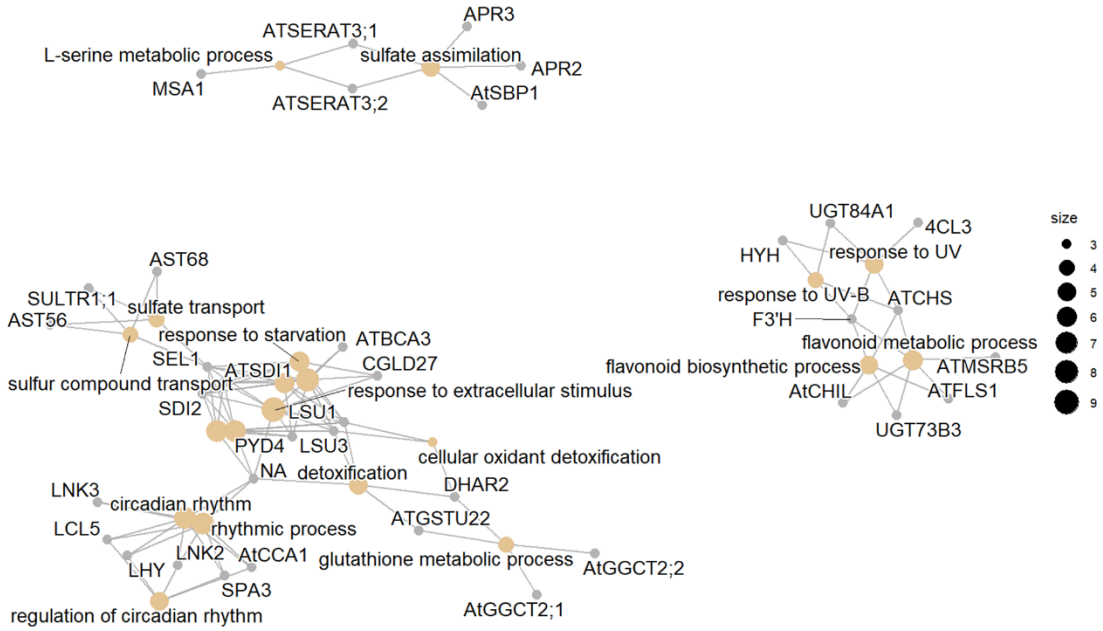

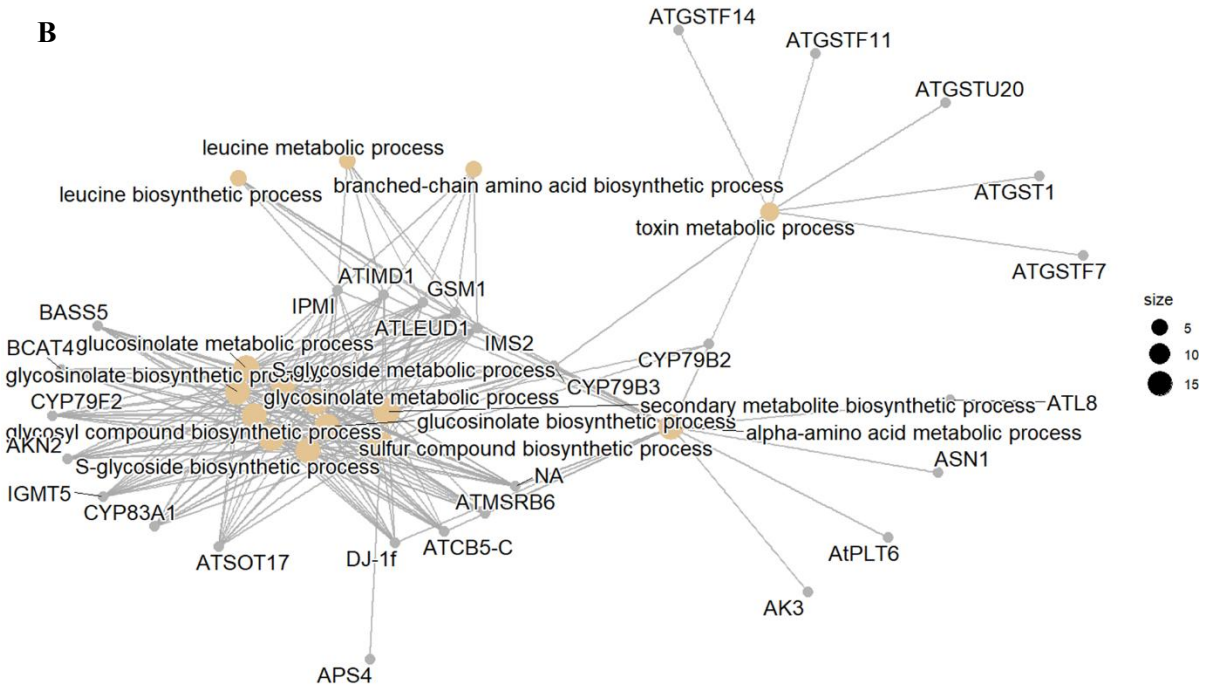

Supplementary Figure 13: Network visualization of enriched Gene Ontology (GO) biological processes identified from the set of **(A)** Upregulated DEGs **(B)** Downregulated DEGs shared among high-S accessions in response to S-deficiency. Orange nodes represent significantly enriched GO terms, while gray nodes represent genes associated with these terms. Edges indicate functional associations between genes and GO categories. Node size reflects the number of genes associated with each GO term.

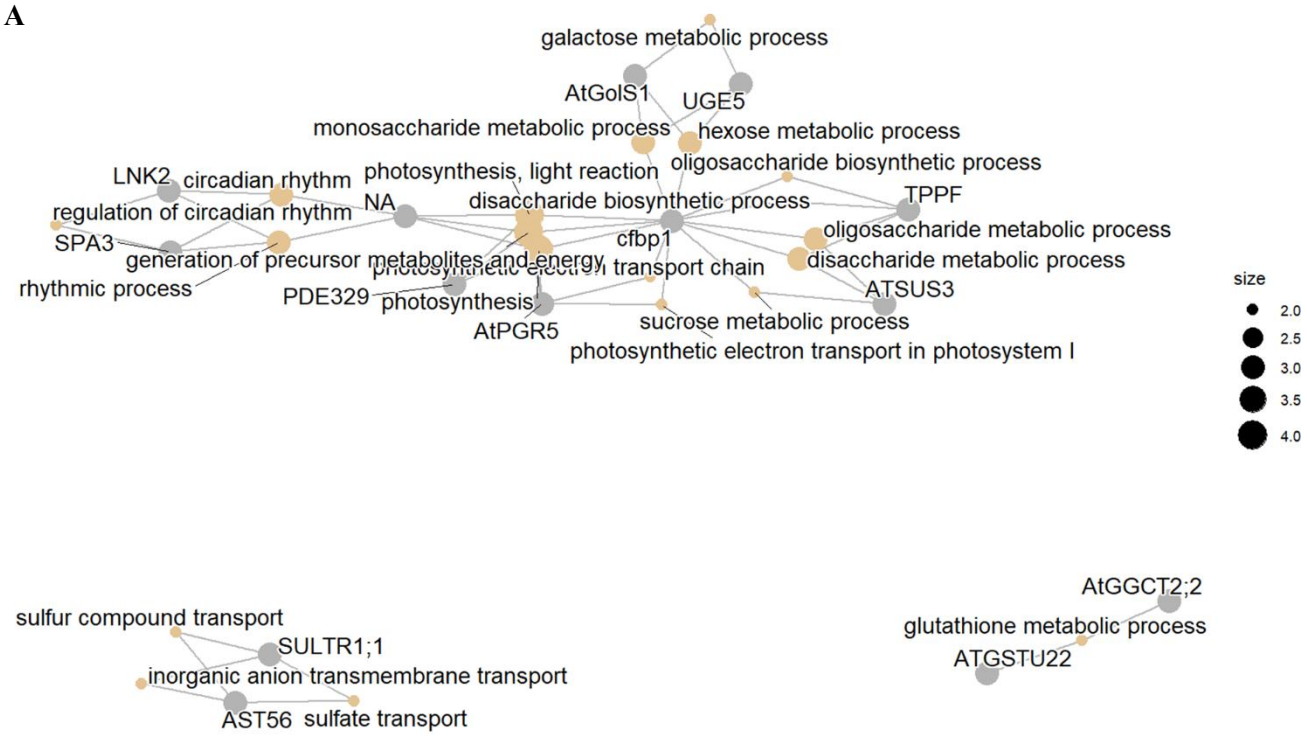

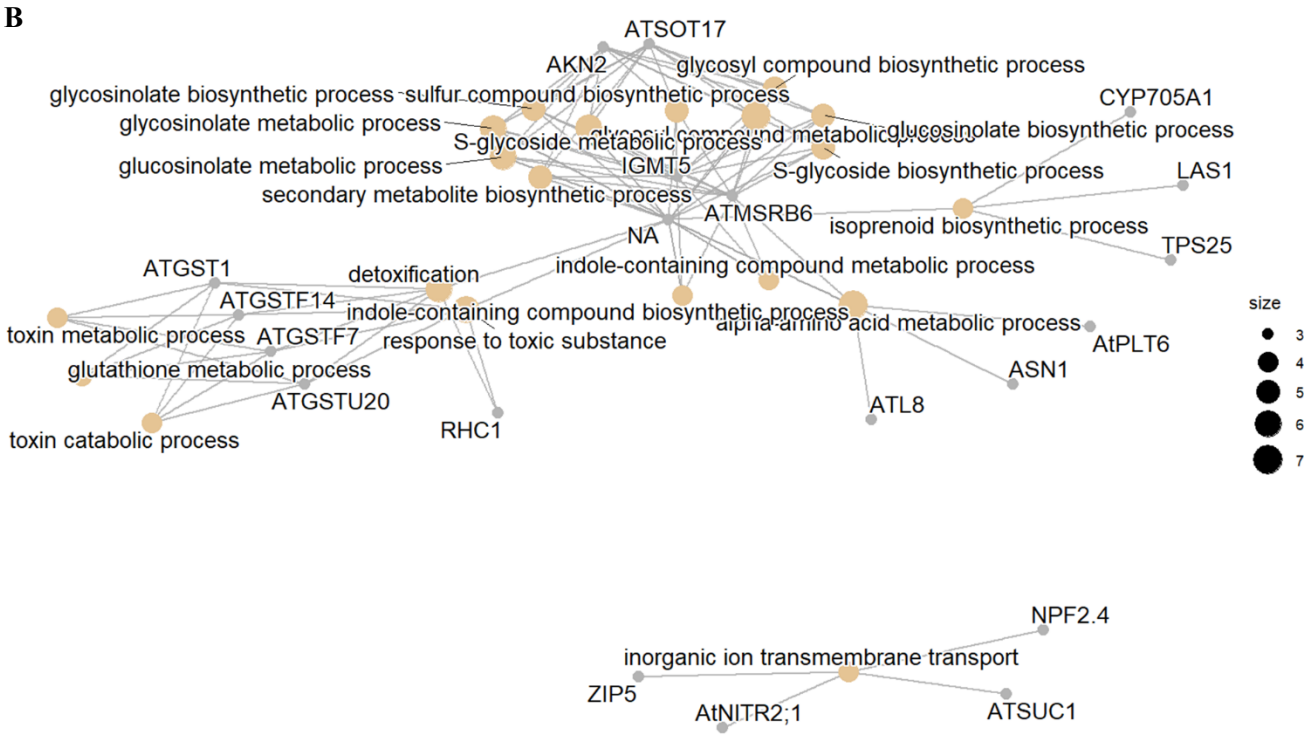

Supplementary Figure 14: Network visualization of enriched Gene Ontology (GO) biological processes identified from the set of **(A)** Upregulated DEGs **(B)** Downregulated DEGs unique to high-S group in response to S-deficiency. Orange nodes represent significantly enriched GO terms, while gray nodes represent genes associated with these terms. Edges indicate functional associations between genes and GO categories. Node size reflects the number of genes associated with each GO term.

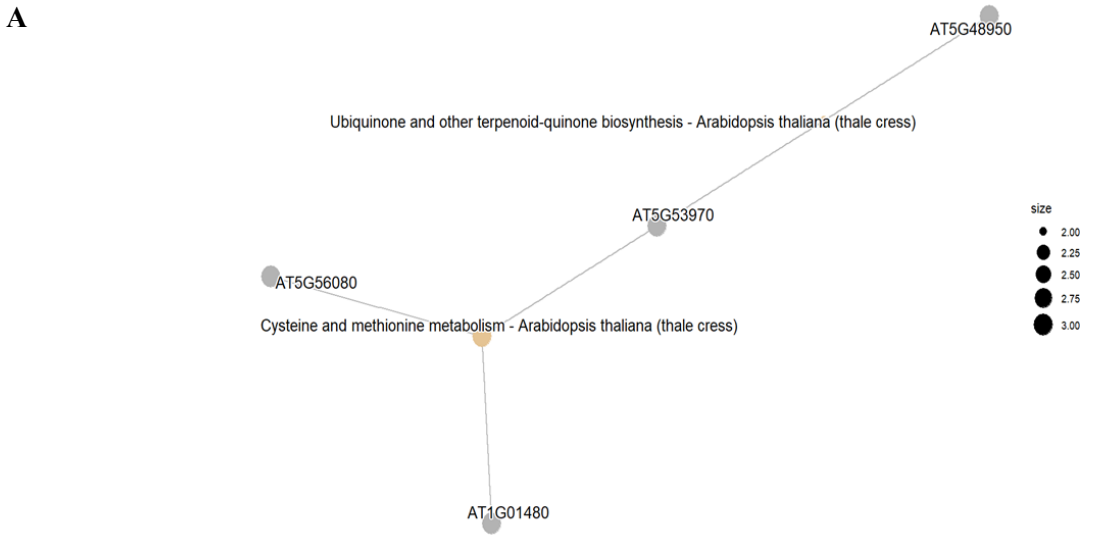

B

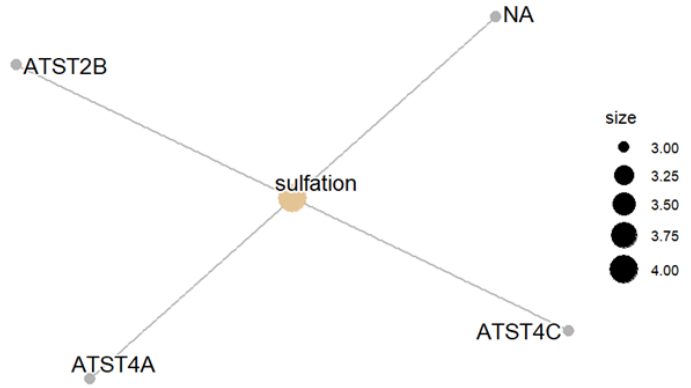

Supplementary Figure 15: Network visualization of enriched Gene Ontology (GO) biological processes identified from the **(A)** DEGs unique to mid-S group **(B)** DEGs unique to high-S group under control condition. Orange nodes represent significantly enriched GO terms, while gray nodes represent genes associated with these terms. Edges indicate functional associations between genes and GO categories. Node size reflects the number of genes associated with each GO term.

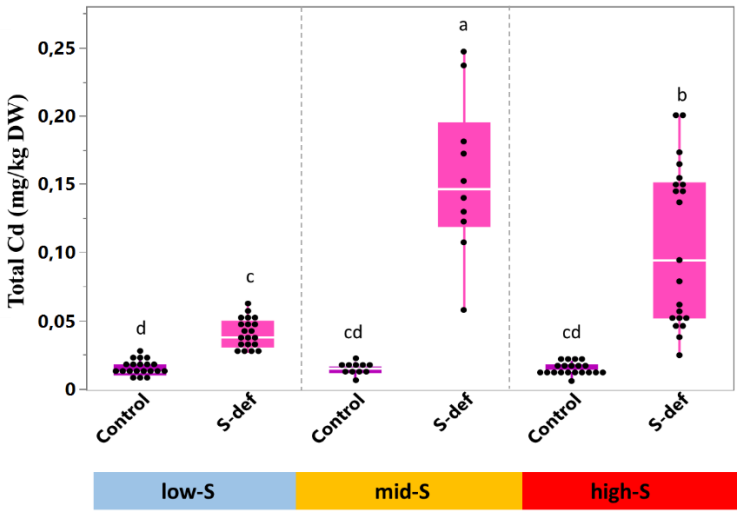

Supplementary Figure 16: Total Cadmium (Cd) content (nmol/ mg^{-1}) in shoot in low-S (blue), mid-S (orange), and high-S (red) accessions grown under control (750 µM sulfate), sulfur-deficient (0 µM), conditions. Data were analyzed using mixed models followed by Tukey's HSD; different letters indicate significant differences ($P < 0.05$). Boxplots show means ± SE.

A

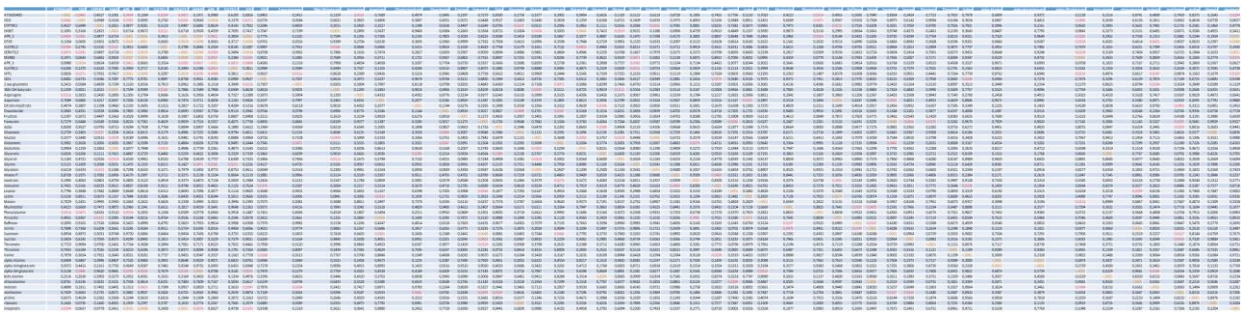

B

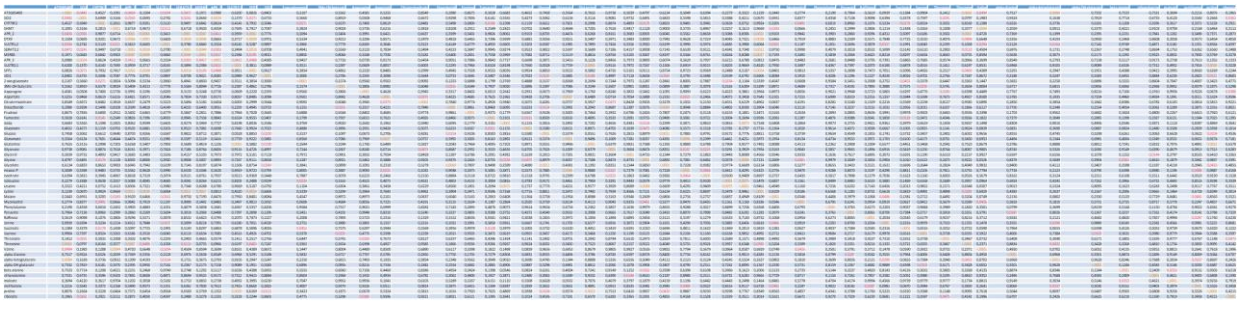

Supplementary Figure 17: Correlation probability of sulfur-responsive genes and metabolites in **(A)** shoots and **(B)** roots as described in Figure 30. P-values < 0.05 representing significant correlation.

TABLE OF FIGURES

TABLE OF TABLES

ACKNOWLEDMENTS

I would first like to extend my deepest gratitude to Prof. Stanislav Kopriva for trusting me with this project and for allowing me to conduct and experience science in his lab. Thank you for all your scientific guidance and support throughout my PhD journey. I would also like to thank Dr. Daniela Ristova for being my daily supervisor and guiding me mentally and professionally. I did learn a lot from your experiences and wisdom.

Thanks to my TAC members, Prof. Maria von Korff, for her valuable insights into the project, and Dr. Akansha Singh for her time and support. I would also like to thank Prof. Tatjana Hildebrandt for accepting to be a second reviewer in my thesis. Also, thanks to Prof. Guenter Schwarz for accepting being a chair in my thesis defense. I would like to thank Babis, coordinator of TRR341, for addressing my problems with patience.

A huge thanks to all my student helpers, Maliha and Pooja, without them this project wouldn't have been possible. I would also like to thank my students and guests, Maryam, Severin, and Niloofar, for being a part of this project and helping me get some interesting data. I have learned a lot from you guys.

I want to thank all technicians of AG Kopriva, especially Sabine and Bastian, for all their help with the project and also in the lab. I am also thankful to Dr. Anna Koprivova for welcoming me in lab and sharing her knowledge whenever I had queries. I am also thankful to Renate for assisting me with all the paperwork. I would also like to thank Philipp from CEPLAS for running the Metabolomics for me.

My deepest gratitude goes to some amazing colleagues I met along the way, especially Raissa, who made sure the thesis looked as nice as it could, and Büsra, for all the support and fun throughout these 3.5 years. I will miss working with you guys, but anyway, I'm happy to have you as friends for life.

I would also like to thank colleagues from the TRR341 graduate school, Renan, Lina, Sandy, Yuna, and Abdul. It was always fun to attend all the retreats with you guys.

I'm also thankful to my family, especially my Father, who believed in my dreams and always supported me in my career. Without your support, I would not be who I am today. I am also grateful to my mother, my cute elder sister, and my brother for being there for me. I am also fortunate to have a second family with two supporting elder brothers, an elder sister, and a second father (father-in-law), and I would like to thank them for always caring for me. Also, thanks to Gudrun for making my first experience in Germany memorable.

Last but not least, I would like to thank my husband, Dr. Shriram Saraf, for being my biggest cheerleader in this journey. Without your love and support, I would not have been able to achieve this milestone.